SYNTHETIC AND BIOLOGICAL STUDIES ON AMICETIN AND ITS ANALOGUES TOWARDS THE DEVELOPMENT OF NEW ANTIMYCOBACTERIAL AGENTS

by

Catherine Mojica Serrano

A dissertation submitted to the faculty of
The University of Utah
in partial fulfillment of the requirements for the degree of

Doctor of Philosophy

Department of Chemistry

The University of Utah

December 2015

The University of Utah Graduate School

STATEMENT OF DISSERTATION APPROVAL

The following faculty members served as the supervisory committee chair and members for the dissertation of Catherine Mojica Serrano. Dates at right indicate the members' approval of the dissertation.

Ryan E. Looper, Chair	4/17/2015 Date Approved
Cynthia J. Burrows, Member	4/17/2015 Date Approved
Gary E. Keck, Member	4/17/2015 Date Approved
John C. Conboy, Member	4/17/2015 Date Approved
Darrell R. Davis, Member	4/17/2015 Date Approved

The dissertation has also been approved by Cynthia J. Burrows

Chair of the Department/School/College of Chemistry

and by David B. Kieda, Dean of The Graduate School.

ABSTRACT

Tuberculosis (TB) remains one of the world's deadliest infectious diseases, second only to Human Immunodeficiency Virus (HIV). The alarming global statistics on TB has prompted a renewed interest in the discovery and development of antitubercular drugs in the scientific community. As part of the growing efforts toward the development of new TB drugs, we have identified amicetin as a viable candidate for antitubercular drug discovery. A recent natural product library screening has identified amicetin, a ribosomal antibiotic isolated from *Streptomyces vinaceusdrappus* in 1953, to be active against TB, relatively noncytotoxic, and compatible with current antiretroviral therapy (ART). Here we present synthetic and biological studies on amicetin and its analogues.

A modular synthetic route towards the formation of cytimidine, a derivative of amicetin, as well as some analogues *via* a one-pot copper catalyzed *N*-aryl amidations is described. This route allows the efficient and rapid diversification of the cytimidine core by exploiting the regioselective coupling of a 4-iodobenzamide with a 2-halopyrimidine affording the union of three fragments in a single synthetic manipulation. Synthetic efforts toward the synthesis of the disaccharide moiety using the Noyori-Achmatowicz reaction sequence were also presented.

In line with our efforts, amicetin was expressed, isolated, and purified from *Streptomyces vinaceusdrappus* and was co-crystallized with the 70S subunit of *Thermus thermophilus* ribosome at 3.5 Å. From our crystallographic data, amicetin

forms a Watson-Crick base pair through its cytosine moeity with G2262 (*T. thermophilus* numbering). Its aminosugar moeity forms cation-π interactions with the A2450 while its *p*-aminobenzoyl group π-stacks with A2613. Its α-methylserine moeity forms a hydrogen bond with the R18 of the ribosomal protein L16. Amicetin displaces the penultimate cytosine of the conserved CCA 3' end of the P-site tRNA, trapping the P-site tRNA in a nonproductive conformation, thereby inhibiting protein synthesis.

Additionally, a number of synthesized analogues were found to exhibit good antimycobacterial property, the most potent of which, analogue 3, has an IC_{50} of 0.98 μM against *M. tuberculosis* H37Ra and selective cytotoxicity of $IC_{50} > 100$ μM against CEM-TART cell line. These active analogues were found to inhibit bacterial protein synthesis using luciferase assay. All amicetin analogues were found to exhibit a narrow spectrum of antibacterial activity and selective cytotoxicity against mammalian cells regardless of their antimycobacterial potency. Crystal structures of analogues 1 and 5 bound to the 70S subunit of the *T. thermophilus* ribosome were obtained at 3.1 Å. Both analogues were observed occupying the same binding site as amicetin. Analogue 1, the more potent of the two, however, exhibited a closer binding motif to amicetin, exhibiting all key interactions aforementioned while analogue 5 lacks the cation-π interaction with A2450.

These discoveries provide modular routes to amicetin analogues as well as key insights into their biological activity. Current and future efforts are being directed towards the development of more potent amicetin antimycobacterial agents.

To my loving family, whom I love and miss

TABLE OF CONTENTS

LIST OF FIGURES

LIST OF TABLES

LIST OF ABBREVIATIONS

A	adenine
α	alpha
Ac	acetyl
$[\alpha]^{20}_{D}$	specific rotation at wavelength of sodium D line
A_{570}	absorbance at 570 nm
A site	aminoacyl site
AIDS	acquired immune deficiency syndrome
AMK	amikacin
Ar	aryl
ATP	adenosine triphosphate
AZ	Astra Zeneca
ß	beta
BCG	Bacille Calmette-Guérin
BIKAKEN	Institute of Microbial Chemistry, Japan
Bn	benzyl
BnOH	benzyl alcohol
Boc	tert-butyloxycarbonyl
2,2'-bipy	2,2'-bipyridine
Bs	broad singlet
^{t}Bu	tert-Butyl

c	concentration for specific rotation measurements
C	cytosine
°C	degrees Celsius
CAMPs	cationic antimicrobial peptides
Cbz	carbobenzyloxy
CDC	Center for Disease Control
CD4	cluster of differentiation antigen 4
CD_{50}	half maximal cytotoxic dose
CM	capreomycin
CFX	ciprofloxacin
CYP	cytochrome p450
CYP2C9	cytochrome p450 isoform 2C9
CYP34A	cytochrome p450 isoform 34A
d	doublet
DCS	D-cycloserine
dd	doublet of doublet
DEPT	Distortionless Enhancement by Polarization Transfer
ddd	doublet of double of doublet
dq	doublet of quartet
DMAP	4-dimethylaminopyridine
dmeda	*N,N'*-Dimethylethylenediamine
DMF	*N,N*-dimethylformamide
DMSO	dimethyl sulfoxide
DNA	deoxyribonucleic acid
EC_{50}	50% effective concentration

EMA	European Medicines Association
EMB	ethambutol
equiv	equivalent
ESI	electrospray ionization
Et_3N	triethylamine
Et_2O	diethylether
ETO	ethionamide
EtOAc	ethyl acetate
EtOH	ethanol
FDA	Food and Drug Administration
G	guanine
g	gram(s)
GSK	Glaxo-Smith-Kline
h	hour(s)
HAART	highly active antiretroviral therapy
HIV	human immunodeficiency virus
Hm	*Haloarcula marismortuii*
hq	8-hydroxyquinoline;
HRMS	high-resolution mass spectroscopy
Hz	hertz
IC_{50}	half maximal inhibitory concentration
IDRI	Infectious Disease Research Institute
iM4TB	Innovative Medicines for TB
IMM	Institute of Materia Medica
INH	isoniazid

IR	infrared spectroscopy
J	coupling constant
KB	ß-keratin
KM	kanamycin
KM-R	kanamycin resistant
L	liter
LD_{50}	half maximal lethal dosage
Leu	leucine
LHMDS	lithium hexamethyldisilazide
LTBI	latent TB infection
LXF	levofloxacin
m	multiplet or milli
µ	micro
M	molar
Me	methyl
MeI	methyl iodide
MEC	minimum effective concentration
MHz	megahertz
MDR-TB	multi-drug resistant TB
MIC	minimum inhibitory concentration
min	minute(s)
mol	mole(s)
mp	melting point
Mtb	*Mycobacterium tuberculosis*
m/z	mass to charge ratio

n	nano
NBS	*N*-bromosuccinimide
NBSH	2-Nitrobenzenesulfonylhydrazide
NIAID	National Institute for Infectious Diseases and Allergy
NM-R	neomycin resistant
NMM	*N*-methylmorpholine
NMR	nuclear magnetic resonance
NNRTI	non-nucleotide reverse transcriptase inhibitors
NRTI	nucleoside reverse transcriptase inhibitors
NtRTI	nucleotide reverse transcriptase inhibitors
OD_{600}	optical density at 600 nm
OBz	benzoate
p	para
PAS	*p*-aminosalicylic acid
PC-R	penicillin G resistant
$Pd_2(dba)_3$	Tris(dibenzylideneacetone)dipalladium
P-gp	P-glycoprotein
Ph	phenyl
pH	hydrogen ion concentration in aqueous solution
Phe	phenylalanine
phen	phenanthroline
PhH	benzene
PI	protease inhibitor
PPh_3	triphenyl phospine
ppm	parts per million

p-site	peptidyl site
PTC	peptidyl transeferace center
pyr	pyridine
PZA	pyrazinamide
q	quartet
RMP	rifampicin
RNA	ribonucleic acid
rt	room temperature
Rf	retention factor
RF1	release factor 1
RF2	release factor 2
RNS	reactive nitrogen species
ROS	reactive oxygen species
S	Svedberg, sedimentation unit
s	singlet or strong
SAR	structure activity relationship
smFRET	single-molecule Förster resonance energy transfer
SM-R	streptomycin resistant
STAND	Shortening Treatments by Advancing Novel Drugs
STM	Streptomycin
t	triplet
TB	tuberculosis
TC-R	tetracycline resistant
TDR-TB	totally drug-resistant TB
THF	tetrahydrofuran

TMS	trimethylsilyl
THZ	thioacetanone
TNF	tumor necrosis factor
TRD	terizidone
tRNA	transfer RNA
TsOH	p-toluenesulfonyl acid
Tth	*Thermus thermophilus*
UIC	University of Illinois, Chicago
UPenn	University of Pennsylvania
UV	ultra-violet
VIM	viomycin
WHO	World Health Organization
XDR-TB	extensively drug-resistant TB
XXDR-TB	extremely drub-resistant TB

ACKNOWLEDGEMENTS

The completion of this dissertation would not be possible without the support and love I have received from many people – family and friends from back home in Manila, here in Salt Lake City, and from several cities around the globe. I would like to thank you all.

First and foremost, to my adviser, Prof. Ryan E. Looper, thank you for taking a chance with me. Thank you for your guidance and patience, most especially the latter. Thank you for recognizing my strengths and affirming them to me. Thank you for being honest with my weaknesses, it will only help me to improve more as a scientist. Thank you for "putting a fire under me", which prompted me to focus and finish. I would not be writing this very sentence had you not been there to say, "just do it!" Again, thank you.

To my labmates, past and present members of the Looper Group, thank you. I wish I could enumerate all of you here and highlight all the ways you have been part of my graduate school career, but that would make this acknowledgement section too long. Thank you for being part of my academic journey, especially during the tough moments when everything seems so bleak, and the end is nowhere in sight. Thank you for all the favors you have bestowed upon me. From biggest favors, including editing this very manuscript, to the smallest act of kindness like helping me get a bottle of chemical on the top shelf. Thank you for all the years filled with laughter, witty banters, sarcasm, and occasional encouragements here and there. We

somehow love and hate each other at the same time. We are our own cheerleaders and hard critiques. We are more than just co-workers. We are one weird family.

To my committee members: Professors Cynthia Burrows, Gary Keck, John Conboy, and Darrell Davis, thank you for your wisdom and guidance, especially during my candidacy exams. Thank you for your invaluable insight into my project and research proposal. I could honestly say that you all have been firm but kind to me in all of my examinations. Thank you.

To my collaborators, Dr. Michael Koch, Dr. Lou Barrows, Dr. Daniel Eiler, and Dr. Thomas Steitz, thank you for your help in the biological assays and biophysical experiments. Thank you for giving me the opportunity to learn valuable techniques outside of organic chemistry.

To all my professors in graduate school, from whom I have gleaned knowledge especially during my 1st year, thank you. Thank you for passing to me your knowledge in physical organic chemistry, synthesis, organometallics, spectroscopy, and biochemistry. These courses have not only helped me directly in my research but also helped me developed an analytical and critical mind.

To all the students from the Organic Chemistry Division, including past and present members of the Keck, Sigman, Rainier, Louie, Poulter and Burrows research groups (back when they were still our neighbors), thank you. Thank you for all your help throughout these years.

To all the chemistry and non-chemistry people who have indirectly helped me finish my thesis by keeping me sane, thank you. This includes my Filipino friends here in Salt Lake City; all former and present graduate students of the University of Utah and many countrymen and women that I have been blessed to meet. Thank you being my family here. Thank you for all the birthdays, holidays,

and Pacquiao fight parties that we spent together. In this group of people, I would like to especially thank Elen Ramirez for being my "mom" here. Thank you for giving me the encouragement during hard times. Thank you for inspiring me to continuously strive for progress and excellence. Thank you for being there when I am sick or even just homesick.

Next, to my friends from K2 the Church, including my present bible study group, thank you. Thank you for all the encouragement, prayer and support, even though I have absent lately. To Susie Nelson, thank you for being such a great comfort during hard and confusing times. To Dr. Tricia Shepherd and her husband Troy thank you for encouraging and challenging me in every aspect of my life.

To one of my closest friends, Dr. Mark Mabanglo, thank you for your friendship, love, encouragement and support. Even though you are a chemistry person too, our friendship extends beyond the brick walls of Henry Eyring. Thank you for being a fun roommate. Thank you being my cheerleader. Thank you for believing in me. *Auf wiedersehen.*

To one of my longest known friends, someone who has been there from the start, Dr. Patricia Ignacio-de Leon, thank you. You have been there for me since college. Thank you for standing beside me through ups and downs. Thank you for being there for me even in spite of the distance. Thank you for the daily prayers and words of encouragement especially during thesis writing.

To my loving family, thank you. I would not be here without your love, faith, and support. Thank you Mama and Papa for allowing me to pursue my dreams. Thank you for telling me that you always have my back. Thank you for your unwavering love and support all these years. Thank you for all the prayers and words of encouragement. Thank you James and Alyssa, my siblings, for believing in

your “Ate”. [1] Thank you for being such a wonderful family. I love you all.

Last but not the least, even though this could sound as cliché as a rapper or a pop star accepting his Grammy, or a country star receiving his CMAs, I would like to thank God for everything. Thank you for my talents. Thank you for this great opportunity to study in the US. Thank you for strength to carry on. Thank you for the grace that I have received from you. *Soli Deo gloria.*

[1] Ate = *n. (pr. uh-teh)* Honorific pertaining to an older sister or a title of respect given to an older woman.

CHAPTER 1

INTRODUCTION

1.1 Tuberculosis: A Brief History of an Ancient Disease

Tuberculosis (TB) has plagued the human race throughout history and may be responsible for the overall highest mortality rate caused by a single pathogen.[1] The earliest known account of TB comes from 4000-5000 year old Egyptian mummies with characteristic Pott's deformities associated with skeletal tuberculosis.[2] TB was well recorded in ancient Greece, but known by a different name, phthisis.[1] In 400 BC, in his book *Of the Epidemics*, Hippocrates described phthisis as a fatal disease with symptoms such as coughing, chest pain, and bloody sputum. This is the earliest recorded diagnosis of the disease known today as TB.[3]

During the 19th century, incidence of TB or consumption, as it was known back then, was at its peak, especially in Europe with approximately one-quarter of the population infected at that time.[4] It was not until the 19th century when modern understanding of the disease started, beginning with the pioneering work of René Théophile Hyacinthe Laennec, who invented the stethoscope and published treaties on autopsies of TB patients.[5] His work contributed greatly to the diagnosis and understanding of the pathology of the disease, from which we still benefit to this day. Following the work of Laennec, Jean-Antoine Villemin demonstrated the transmissibility of TB through the inoculation of a rabbit with liquid from

tuberculous cavities– enlarged air spaces formed from extensive necrosis of lung tissues.[6] A greater understanding of the etiology of TB was attributed to Hermann Heinrich Robert Koch. In his famous presentation to the Berlin Physiological Society, *Die Aetiologie der Tuberculose,* he reported the isolation of *Mycobacterium tuberculosis* (*Mtb*) from both animal and human specimens and the replication of the disease in guinea pigs.[7, 8] His work enabled the proper diagnosis of the most lethal disease in human history and won him a Noble Prize in Medicine or Physiology in 1905. Koch also isolated tuberculin from the tubercle bacilli, which he believed at the time to be a valuable for therapy, but was later found to be more useful for diagnostic purposes. In 1909, Clemens Freiherr von Pirquet followed up on Koch's work and developed a diagnostic protocol known today as the tuberculin skin test.[9, 10]

With improved diagnostics, as well as proper sanitation in hospital and specialized TB sanatariums, TB mortality decreased towards the end of the 19th century. The discovery of the Bacille Calmette-Guérin (BCG) vaccine by Albert Calmette and his associate Camille Guérin in 1921 led to extensive vaccination, especially among children.[11, 12] Introduction of TB chemotherapy culminated the modern era of TB management, beginning with the discovery of *p*-amino salicylic acid (PAS) by Jorgen Lehmann in 1943[13, 14] While PAS was found to be only bacteriostatic, it was the first therapeutic agent with any efficacy used in the treatment of tuberculosis. Not long after in 1944, Albert Schatz, Elizabeth Bugie and Selman Waksman isolated and reported streptomycin as the first bactericidal effective against *Mtb.*[15] Introduction of oral mycobacterial drugs, such as isoniazid in 1952, pyrazinamide and rifamycin in 1957,[16] allowed for home treatment, diminishing the need for sanatoriums.[17] Implementation of short-course

combination therapy in the 1970s then increased treatment success rates to 95%.[18]

In the mid-1980's the treatment success rates declined largely due to the emergence of drug-resistant mycobacteria and AIDS.[3] First reports of multidrug-resistant strains of TB (MDR-TB) were reported during this decade. In 2006, a TB epidemic in rural South Africa exposed a new, more deadly strain of TB, which has since been labeled as extensively drug-resistant TB (XDR-TB).[19] Deadlier strains have been reported in the past decade. In 2007, totally drug-resistant strains (TDR-TB) were first reported.[20]

TB is an ancient disease with a long history that continues to afflict humanity to this day. With the occurrence of TB outbreaks on the rise, the World Health Organization (WHO) seeks to address and eradicate this global health problem.[21]

1.2 TB: A Global Problem

TB is caused by *Mycobacterium tuberculosis* (*Mtb*), an acid-fast rod-shaped bacillus primarily transmitted *via* the respiratory route.[7, 8] The bacilli most commonly attack the pulmonary system (pulmonary TB or more simply TB), but can also affect the genitourinary, vertebral, and nervous system (extra-pulmonary TB).[22] Symptoms of pulmonary TB often include chronic cough, chest pains, sputum production, weakness, fatigue, appetite loss, weight loss, fever, chills, night sweats, and hemoptysis— the expectoration of blood or blood stained sputum.[23]

TB is an airborne disease– the tubercle bacilli can be easily spread through a simple exhale, sneeze or cough of an infected person. A single sneeze for example, can release up to 40,000 aerosolized droplets.[24] Each droplet, containing as few as 1-3 bacilli, is capable of infection.[25, 26] With such ease of transmission, it is estimated

that one-third of the world's population, about 2 billion people, are infected with TB.[27, 28]

TB remains to be the world's most prevalent infectious disease second only to Human Immunodeficiency Virus (HIV), with over 9 million newly reported cases and 1.5 million TB-related deaths in 2013.[27] The subsequent silent transmission of the bacilli from untreated patients makes this infectious disease a pressing global health problem. In 2013 alone, an estimated 3 million people with TB were either undiagnosed or missed by the national notification systems, leaving these people to potentially infect others.[27] For every year a single infected individual is left untreated, he or she can infect as many as 10-15 other people.[29] When left undiagnosed and untreated, TB has a mortality rate of about 70% within 10 years.[30] With so many undocumented cases, it is not surprising that annual surveillance reports show no significant drop in the number of new cases of TB or TB mortality despite years of efforts.[31, 32]

The majority of newly reported TB incidents are from poverty-stricken regions where deficient public health funding limits access to health care; including, but not limited to, proper diagnostic assays, vaccination and chemotherapy. Inadequate public health infrastructure has been a major factor in the rapid spread and high mortality of the disease. Poor patient compliance in developing countries also presents major obstacles in the complete eradication of TB. About 56% of newly reported cases in 2013 occurred in Asia, with populous countries like India and China having the greatest burden of the disease at 24% and 11%, respectively. Around 82% of the world's TB cases are concentrated in 22 high-burden countries, with India, China, Nigeria, Pakistan, Indonesia, and South Africa hardest hit.[27]

The fewest cases have been reported in developed and high-income regions

including the Eastern Mediterranean region at 8%, the European region at 4% and the Americas at 3%. Canada, United States of America, Japan, Australia, New Zealand, and countries of Western Europe reported the lowest incidence rates, with less than 10-50 cases per 100,000 people.[27] The highest numbers of reported cases in these regions are among foreign-born residents and recent immigrants from countries where TB is endemic.[33, 34, 35]

With current medical advances on diagnosis and chemotherapy, TB is now considered a curable disease. However, the resurgence of drug resistant pathogens and subsequent rise in related morbidity and mortality across the globe presents an imposing threat.[36] Recent reports on the rise of drug-resistant tuberculosis are particularly alarming, and what was considered an ancient scourge has emerged as a dangerous threat, especially to developing parts of the world. The World Health Organization (WHO) 2014 Survey reported about 480,000 new cases[27] of MDR-TB—a form of TB caused by *Mtb* exhibiting resistance to first-line drugs isoniazid and rifampin.[37] The number of people diagnosed with MDR-TB tripled between 2009 and 2013. About 210,000 MDR-TB related deaths were reported in 2013 alone.[27]

XDR-TB is a form of TB caused by *Mtb* that are not only resistant to first-line drugs, but also resistant to fluoroquinolones and second line injectable polypeptides or aminoglycosides.[38] It has been estimated that the current average percentage of MDR-TB cases that are also XDR-TB is about 9.6%. In 2013, at least one incidence of XDR-TB was reported in 100 countries, up from 92 countries in 2012; this number includes developed nations such as the United States where TB is not endemic.[27]

The ominous progression in the evolution of deadlier strains of *Mtb* has been documented in at least three countries. In 2007, Migliori and co-workers reported two cases of extremely drug-resistant TB (XXDR-TB) in Italy.[20] Not long after in

2009, the term totally drug resistant-TB (TDR-TB) was first used to describe the clinical isolates from 15 patients in Iran that are resistant to all first-line and second-line drugs.[39] While the terminology TDR-TB has not yet been officially endorsed by the WHO, a published article on TDR-TB cases in India in 2012[40] documenting *Mtb* isolates exhibiting resistance to all drugs has nevertheless captured international attention. The official classification of such reported cases remain under the XDR-TB classification in spite of their clinical differences and manifestations; specifically, their drug-susceptibility test results differ from cases that strictly follow the official definition of XDR-TB.

Compounding the problem of TB is its co-infection with HIV. A huge upsurge in TB cases has been observed since the HIV epidemic in the 1980s. In 2014, the WHO estimated that at least one-third of the 35.3 million people living with HIV are co-infected with TB.[41] In 2013, there were 1.1 million new cases of TB among HIV-positive people. TB remains to be the leading cause of death among people with HIV infection; in 2013 about 360,000 HIV-associated TB deaths were reported in that year alone.[27]

TB has once been considered an ancient scourge, a disease of the past. In the present-day era of advanced therapeutics and antibiotics, epidemiological studies have shown, however, that this infectious disease has resurfaced and is now a modern-day global problem. Overall, global statistics for both occurrence and related mortality for drug resistant TB have remained considerably unchanged since 2007.[27-32] Efforts from the medical and scientific community, governing bodies and funding agencies are all needed in combating this disease.

1.3 TB Drugs and Treatment Regimen

Currently, there are more than twenty anti-TB drugs that are used for the treatment of TB.[42] They are classified into two main groups based on efficacy, potency, disease strain, and experience of use. First-line drugs have the greatest activity against *Mtb* and are the first compounds administered to new patients with active TB. The basic TB drugs include isoniazid, rifampin, pyrazinamide, and ethambutol (Table 1.1).

Second-line drugs are usually reserved for drug-resistant cases (Table 1.2). Compounds in this class are comprised of injectable aminoglycosides, injectable

Table 1.1 First-line TB drugs[43]

Drug (Abbreviation)	Structure	Target and Effect
Isoniazid (INH)	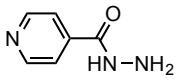	Enoyl-[acyl-carrier-protein] reductase; Inhibits mycolic acid synthesis
Rifampicin (RMP)	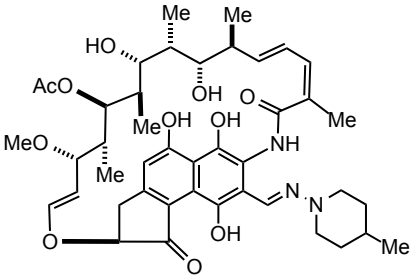	RNA polymerase; Inhibits transcription
Pyrazinamide (PZA)	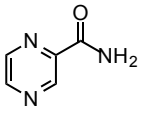	S1 component of 30S ribosomal subunit; Inhibits translation and *trans*-translation, acidifies cytoplasm
Ethambutol (EMB)	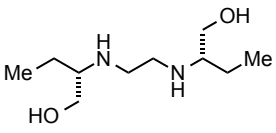	Arabinoyl transferases; Inhibits arabinogalactan biosynthesis

Table 1.2 Second-line TB drugs[43]

Drug (Abbreviation)	Structure	Target and Effect
Streptomycin (STM)	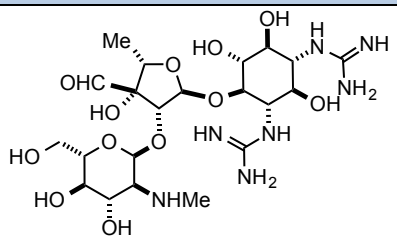	S12 and 16S rRNA components of the 30S ribosomal subunit; Inhibits protein synthesis
Kanamycin (KM)	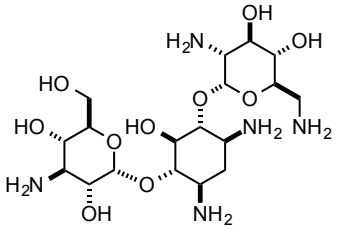	30S ribosomal subunit; Inhibits protein synthesis
Amikacin (AMK)	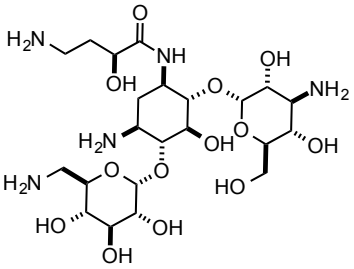	30S ribosomal subunit; Inhibits protein synthesis
Capreomycin (CM)	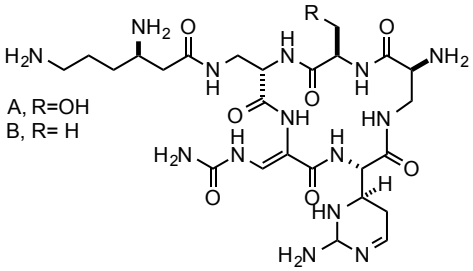	Interbridge B2a between 30S and 50S ribosomal subunits; Inhibits protein synthesis
Viomycin (VIM)	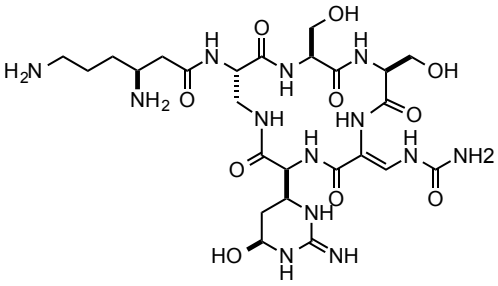	Interbridge B2a between 30S and 50S ribosomal subunits; Inhibits protein synthesis

Table 1.2 (continued...)[43]

Drug (Abbreviation)	Structure	Target and Effect
Ciprofloxacin (CFX)	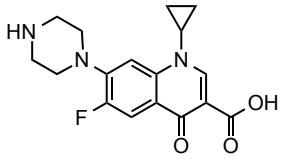	DNA gyrase; Inhibits DNA replication
Levofloxacin (LFX)	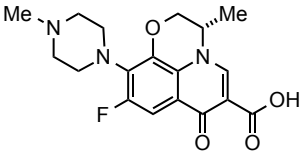	DNA gyrase; Inhibits DNA replication
p-Amino-salicylic acid (PAS)	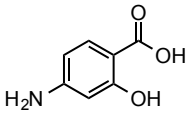	Dihydropteroate synthase; Inhibits folate biosynthesis
Cycloserine (DCS)	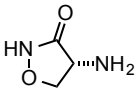	D-alanine racemase and ligase ; Inhibits peptidoglycan synthesis
Terizidone (TRD)	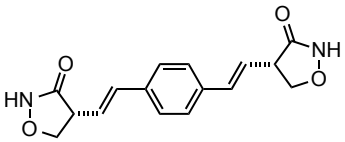	D-alanine racemase and ligase ; Inibits peptidoglycan synthesis
Ethionamide (ETO)	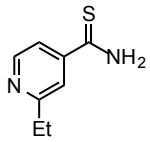	Enoyl-[acyl-carrier-protein] reductase; Inhibits mycolic acid synthesis
Thiocetazone (THZ)	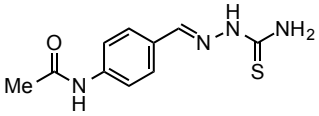	Cyclopropane mycolic acid synthases; Inhibits cyclopropa-nation of cell wall mycolic acids

polypeptide, oral and injectable fluoroquinolones, and various other orally administered compounds. A third group of TB drugs, third-line drugs, have undefined roles and efficacy but are used in very special cases of drug-resistant TB such as XDR-TB and TDR-TB. Third-line anti-TB drugs are more expensive and have more side effects than first-line and second-line drugs, and are only administered as a last resort.[42]

TB treatment requires at least six months of two-phase short-course regimen, administered under direct observed therapy (DOT). The first phase is a 2-month long intensive dosage of four drugs: isoniazid (INH), rifampicin (RMP), pyrazinamide (PZA) and ethambutol (EMB). It is followed by a 4-month course of isoniazid and rifampicin.[42] Globally, the success rate of short course treatment is about 87% recovery.[44]

Combination therapy for the basic treatment of drug-susceptible TB (DS-TB) was introduced in the 1970's and has been used for over fifty years.[18] Regimens are only adjusted in cases of drug-resistant TB. The rationale for combination therapy is based on lowering the probability of resistance though spontaneous mutation. For example, the frequency of spontaneous mutations conferring resistance for first line drugs ranges from 10^{-6} to 10^{-10} – about 10^{-5} for PZA, 10^{-7} for EMB, 10^{-8} INH, and 10^{-10} for RMP.[45] Because these mutations are independent of each other, in theory, the probability of developing bacillary resistance to a four-drug regimen consisting of INH, RMP, PZA, and EMB becomes 10^{-30}. The probability of simultaneous resistance to three anti-TB drugs would be virtually nonexistent and treatment success rate is increased.

Additionally, *Mtb* is a complex pathogen that exists in different populations of varying growth rates and persistence during infection. In a single infected

individual, there would be rapidly growing bacilli alongside with slowly growing, as well as sporadically replicating populations.[46] INH and STM both exhibit good bactericidal properties and therefore can address the rapidly growing populations.[43] However, these agents are not suitable for clearing persistent and sporadically multiplying population of *Mtb.* PZA, a sterilizing antibiotic, effectively kills these persistent populations.[43] Combination therapy affords access to drugs with different modes of action, thereby effectively addressing problems in treating TB infection.

1.4 TB Pathogenesis

TB infection begins when droplet nuclei containing the mycobacteria are inhaled and enter the lungs (Figure 1.1). Most of the tubercle bacilli will remain in the lungs; however, a small amount of tubercle bacilli may enter the bloodstream and spread to other parts of the body, such as in the case of extra-pulmonary TB. In the lungs, the bacilli travel to the alveoli, where macrophages engulf them by phagocytosis.[47] Inside the macrophage, the bacilli replicate exponentially before reaching a plateau.[48] In addition to macrophages, lymphocytes and dendritic cells are recruited to the primary site of infection.[49] The immune cells, macrophages and fibroblasts aggregate and eventually form nodules and lesions called granulomas, the hallmark of TB.[50] Granulomas act as a form of physical barrier preventing further dissemination of the mycobacterium to the remainder of the lung and other organs. Additionally, they act as a local communication site for the dendritic cells and the local lymph nodes.

Upon containment in granulomas, the progression of tuberculosis is largely influenced by the host's immune system. Under optimal circumstances, the human body's immune response is robust enough to contain and eliminate the bacilli. Acti-

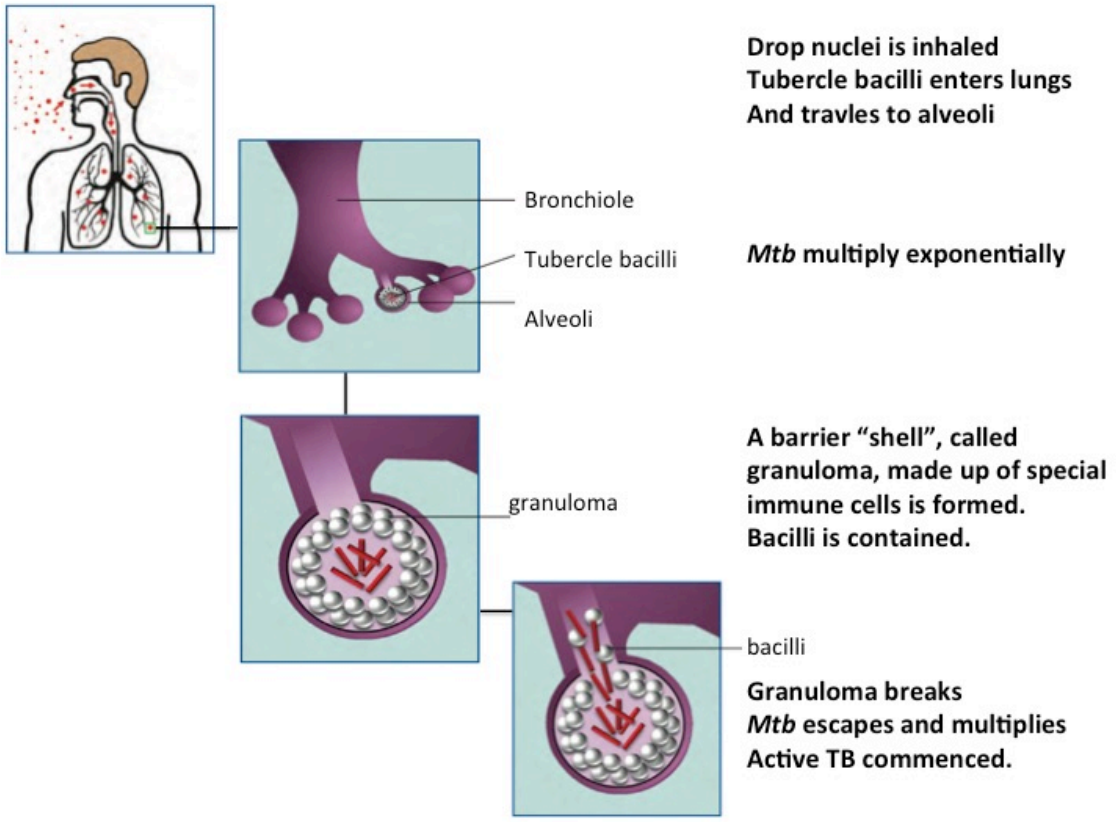

Figure 1.1 Pathogenesis of TB[51]

vation and maturation of macrophages to phagolysosomes– a cytoplasmic body formed by the fusion of the phagosome with a lysosome, subsequently elicits an arsenal of host defense mechanisms against the bacilli.[52] Increase in acidity in the phagosomal environment has been observed, simultaneously facilitating the enzymatic degradation of bacterial lipids arresting microbial metabolism.[53] Production of reactive oxygen and nitrogen species (ROS and RNS) by phagosomal enzymes are responsible for further damage of primary bacterial metabolites.[54, 55] Lymphatic T cells (CD4 and CD8) are also primed as part of the body's innate and adaptive immune response to TB infection.[56] T-lymphocytes secrete cytolytic proteins such as perforin and granulysin that directly kill the infected cells.[57, 58] Interferon gamma (IFNγ), a cytokine secreted by T lymphocytes, is known to play a

critical role in suppressing bacterial burden and inflammation by inducing autophagy,[59] a catabolic mechanism wherein unnecessary or dysfunctional cellular components are degraded through lysosomal processes for cell survival. In the case of TB, autophagy also facilitates the maturation of phagosomes to phagolysosomes, and suppresses mycobacterial growth and damaging inflammation responses.[59] Ultimate clearance of the bacilli requires this maturation process.[60] Phagolysosomes release hydrolytic enzymes and cationic antimicrobial peptides (CAMPs), such as defensins, which permeabilize the bacillus' cell membrane, making it more susceptible to complete degradation.[61]

While macrophages act as the primary effector cell for bacterial clearance, they also provide a habitat for mycobacteria to persist and develop host-defense mechanisms to counter every immune response. For example, reactive oxidative species are known to modify bacterial proteins leading to eventual bacterial death; *Mtb* has developed *in vitro* tolerance to ROS and RNS.[62, 63] *Mtb* has developed the ability to arrest phagosomal maturation, averting the bacilli's destruction causing infection.[64] To avoid detection and degradation, *Mtb* can translocate from inside the phagolysosome to the cytosol.[65] Propagation of infection can also happen through host macrophage necrosis, characterized by disruption of the host surface membrane, allowing the escape of *Mtb* to the surrounding tissue.[66]

The interplay between bacterial persistence and host-immune response determines whether a primary infection will progress into active TB or not. If the immune system is incapable of containing and clearing the bacilli, and they disseminate and multiply, then active TB infection has begun. If the bacilli is contained but not eradicated, latent TB infection (LTBI) is established in the patient, who may or may not develop active TB at some point in their lifetime.

While TB pathogenesis has been studied for decades, it is impossible to predict, upon primary infection, which course will it take.

1.5 Latency and Biofilm Formation

Statistically speaking, primary infection often does not progress to active TB.[67] More than 90% of people infected with TB are asymptomatic, and are clinically categorized as having the latent form of TB infection (LTBI) [68]. During this dormant state, patients are noninfectious but remain a reservoir for potential transmission.[69] Latent infection arises from the mycobacteria's innate ability to enter a state of dormancy and subclinical persistence within the host as a mechanism of survival. This is a direct result of host's immune response to primary infection to quarantine the bacteria.

Formation of granuloma is the primary mechanism by which the host isolates the bacilli from the rest of the lung tissue and the body. In latent TB, granulomas sequester the bacteria for a long period of time, forcing the bacteria to enter a dormant and noninfective state.[3] Solid granulomas formed during latency are encircled by a fibrotic wall, which limits resources by separating them from the surrounding tissues. Low nutrient and oxygen supply inside the granuloma triggers a global down regulation of metabolic genes, causing *Mtb* to transition to a low-metabolic, non- or low-replicating, but persistent state.[70] Such bacilli are found to be resistant to TB drugs.[71] This drug resistance is exclusively a physiologic state resulting from the down-regulation of *Mtb* growth functions during dormancy, and is independent from genetic mutations.[72]

A new school of thought on TB pathogenesis suggests that *Mtb's* persistence is not only due to its ability to enter latency but also due to its ability to form

biofilms. Clinical features and mechanisms involved in the persistence of the tubercle bacilli bear similarities to biofilm-associated infections.[73] Several species of mycobacteria, including *Mtb,* are known to form biofilms *in vitro*.[74, 75, 76] A pathological study on the surviving population of bacilli in a post-treated guinea pig infection model has shown evidence of microcolonies of bacteria concentrated around the acellular rim in the granulomas.[77] A protein similar to pilin, a fibrous protein involved in cell adhesion mechanism, is found in *Mtb's* genetic code, and expressed *in vivo*.[78] The protein binds strongly to the eukaryotic extracellular matrix; supporting the idea that pathogen's surface could be actively engaged in surface attachment. In another study, nonreplicating *Mtb* accumulated an extracellular matrix that is, in part, composed of carbohydrates and free mycolic acid, characteristic of biofilm formation in bacterial survival.[79] Drug tolerance is also observed during pellicle-biofilm formation of drug-hypersensitive *mycobacteria* strains.[80] The observed conferred resistance was reversible upon the addition of agents that disrupt *Mtb* biofilm formation in conjunction with conventional antibiotics.

Whether as independent or cooperative mechanisms of survival, both latency and biofilm formation in *Mycobacterium tuberculosis* elicit antibiotic recalcitrance. This conferred phenotypic resistance is one reason for prolonged chemotherapy and one of the major hurdles to overcome in TB therapy.

1.6 Latent TB Progression

While most cases of TB are asymptomatic, LTBI cases have a significant risk for disease development within a finite time frame. Within a period of 1 to 2 years, 5-10% of patients with latent infections will develop an active form of the disease.[67]

Progression of latent to active TB varies greatly from patient to patient and is dictated by the individual's immune system.[81]

Cytokine imbalance can cause the latent bacilli to be released from solid granulomas, triggering disease activation.[82] Therapeutic neutralization of tumor necrosis factor (TNF) in treating autoimmune diseases can also account for LTBI activation.[83] Upon TNF neutralization, decreased macrophage activity, macrophage death, and granulysin-containing T-cells depletion have been observed.[84, 85]

Immunocompromised patients such as those infected with HIV have a much higher risk of developing active TB.[86, 87] The depletion in CD4 T-cells, lymphatic cells involved in tubercle clearance during primary and latent infection, accounts for activation of TB among HIV patients.[88] HIV also preferentially targets and depletes *Mtb* specific CD4 T-cells.[89] Overall, the activation of dormant *Mtb* is controlled by the increase in HIV viral load and its subsequent effect on T cells and cytokine production.[90, 91] HIV increases the probability of not only contracting a primary infection but also activating latent TB.[92, 93]

1.7 Recurrent TB

TB recurrence after a full or partial treatment is a pervasive problem.[94] Overall, the risk of reactivation is estimated to be about 10% within a patient's lifetime.[95] People who have contracted TB once are at a greater risk of developing TB than those who never had the disease in the first place.[96] Both HIV-positive and HIV-negative hosts are subject to relapse and re-infection, the two main causes of recurrent TB.[97] By definition, relapse of TB infection is the recurrence of the disease with the same endogenous *Mtb* strain, while re-infection is caused by a new exogenous strain.[98]

Re-infection is associated with a weakened immune system as HIV-positive patients are more prone to reinfection than HIV-negative patients.[99] Most cases of TB relapse, on the clinical level, are attributed to poor and inadequate therapy.[97] On the cellular level, it is suggested that *Mtb's* ability to form biofilms can also account for the relapse of previously treated TB,[100] as reactivation of the disease was found to occur in residual necrotic cells harboring live bacilli.[101]

Recurrence creates setbacks for clinicians formulating therapies. Recurrent tuberculosis necessitates another cycle of treatment that is usually more toxic, takes longer to complete, and is largely unavailable in most parts of the world.[97] Additionally, recurrent TB poses the threat of drug resistance.[102]

1.8 Mechanisms of TB Drug Resistance

Mycobacterium tuberculosis has acquired and intrinsic mechanisms for drug resistance as an evolutionary measure of survival. Acquired resistance is said to occur when a particular strain of *Mtb* obtains the ability to resist a particular antibiotic to which they were previously susceptible. Intrinsic resistance is *Mtb's* endowed ability to actively neutralize the actions of certain antibiotics.

Like other microorganisms, *Mtb* has acquired the ability to undergo spontaneous chromosomal mutations resulting in genetic drug-resistance, which happens at a frequency of 10^{-6} to 10^{-8} mycobacterial replications.[103] Horizontal gene transfer *via* plasmids and transposons does not mediate drug resistance in *Mtb* unlike other microorganisms.[104] All known acquired resistance to anti-TB drugs is the result of spontaneous mutations (Table 1.3).

In theory, the probability of simultaneous resistance to three anti-TB drugs would be virtually nonexistent, about 10^{-18} to 10^{-20}, a probability that is contrary to

Table 1.3 Mechanisms of drug resistance in *Mtb*[105]

Drug	Resistant gene(s)	Gene function	Mutation frequency (%)
Isoniazid	*kat*G	Catalase-peroxidae	50-95
	*inh*A	Enoyl ACP reductase	8-43
Rifampin	*rpo*B	ß subunit of RBA polymerase	95
Pyrazinamide	*pnc*A	Nicotinamidase/pyrazinamidase	72-97
Ethambutol	*emb*B	Arabinoyl transaferase	47-65
Streptomycin	*rps*L	S12 ribosomal protein	52-59
	rrs	16S rRNA	8-21
Amikacin	*rrs*	16S rRNA	76
Quinolones	*gyr*A	DNA gyrase subunit A	75-94
	*gyr*B	DNA gyrase subunit B	
Ethionamide	eta*A*	Flavin monooxygenase	37
	*inh*A		56
PAS	*thy*A	Thymidylate synthase	36

the global presence of drug-resistant TB today. Selection of resistant mutants is amplified by the human errors in the clinical practice of TB treatment. Extensive drug use due to increasing infection rates lengthy regimens creates a positive pressure on the selective evolution of progressively resistant strains.[106] Exposure to sub-lethal levels of bactericidal antibiotics has been implicated in inducing mutagenesis though the production of reactive oxygen species (ROS).[107]

Aside from acquired resistance, *Mtb* is known to have an intrinsic passive drug resistance attributed to its thick cell wall, composed of arabinogalactan, mycolic acid, and a periplasm-like interlayer similar to that of gram-negative bacteria, which limits the permeability of antibiotics.[106] For instance, *Mtb's* multilayered cell wall hinders ß-lactam antibiotic diffusion by two orders of magnitude in mycobacteria.[108]

Mtb has also developed other specialized active intrinsic mechanisms. Enzyme-mediated chemical modification and degradation of antibiotics confers resistance in *Mtb*. Acetylation by acetyltransferases prevents aminoglycoside to bind

to ribosomes.[109] Expression of hydrolases mainly account for *Mtb's* intrinsic resistance to ß-lactam antibiotics.[110] Target modification, i.e., methylation of ribosomes, prevents efficient binding macrolides and lincosamide antibiotics.[111, 112] Target mimicry, i.e., formation of DNA-mimics, sequesters the inhibitory action of fluoroquinolones on DNA replication.[113] Efflux pumps allow *Mtb* to expel antibiotics.[114] These are few examples of *Mtb's* specialized mechanisms for drug resistance.

1.9 TB-HIV Co-infection and Highly Active Antiretroviral Treatment

TB and HIV, the top infectious diseases in the world today, overlap not only in their epidemiology but also in their bi-directional interaction on pathogenesis, progression and drug treatment interaction. The current standard treatment of HIV, highly active antiretroviral therapy (HAART), is composed of a triple-drug therapy: two nucleoside or nucleotide reverse transcriptase inhibitors (NRTI/NtRTI) alongside with a non-nucleoside reverse transcriptase inhibitor (NNRTI) or protease inhibitor (PI).[115] HIV's triple-drug combination along with the cocktail of drugs used for the treatment of TB, presents the problem of opposing pharmacokinetic interactions, as with any multidrug therapy. Interactions between rifampin (RMP), a key first-line TB drug, and PIs and NNRTIs are largely responsible for the challenges encountered during HAART.[116]

Antiretrovirals such as PIs and NNRTIs are metabolized through the cytochrome P450 (CYP) enzymes, primarily through its 3A4 and 2C9 isoforms.[117] RMP activates and induces the expression of hepatic cytochromes CYP3A4 rendering the plasma levels of the antiretrovirals subtherapeutic. Rifampin reduces

the plasma levels of NNRTIs efavirenz and nevirapine by 22-26% and 31%, respectively.[118, 119] RMP reduces PIs' plasma concentration significantly by 35-92% and induces the activity of the efflux multidrug transporter P-glycoprotein (P-gp), subsequently decreasing the cellular concentration of PIs.[120, 121] The anatoginstic effects of co-treating a patient with HAART and rifamycins has been correlated with HIV treatment failure[116]

1.10 TB Drug Development

Most of the current TB drugs were developed and approved for use as part of combination therapy several decades ago. The research and development of new TB drugs has been dormant for nearly fifty years, but there has been a resurgence of interest in the scientific community that began nearly ten years ago[122] With support from WHO's Stop TB campaign, investment from funding agencies, and research efforts by scientists, a number of new drug candidates have entered the pipeline (Table 1.4, Figure 1.2).[123, 124] Most compounds are currently in the hit-to-lead and lead optimization stages, while some of the candidates are in Phase II and Phase III clinical trials.

A number of these compounds are repurposed antibiotics previously developed and used for treating other infectious diseases and have been approved for the treatment of special cases of drug-resistant TB.[122] Fluoroquinolones such as gatifloxacin and moxifloxacin, have been approved as second-line drugs for the treatment of MDR-TB.[125] These compounds are now being tested against DS-TB. Rifapentine, a member of the rifamycin family of antibiotics, has a longer half-life than rifampicin and is being developed, together with isoniazid, as part of a three-month regimen for LTBI.[126] Oxazolidinones linezolid, sutezolid, and AZD5847 are

Table 1.4 Current global pipeline of new TB drugs[122-124]

Lead Identification	Lead Optimization	Pre-Clinical Development	Phase 1	Phase 2	Phase 3
ATP Synthesis Inhibitors *Calibir*	Cyclopeptides Macrolides, Ureas *Sanofi*	CPZEN-45 *BIKAKEN, Lilly, NIAID, IDRI*	TBA-354 *Univ. of Auckland / UIC / TB Alliance*	Sutezolid *Sequella*	Bedaquiline *Janssen*
Whole-Cell Hit-to-Lead Program *GSK / Sanofi*	Diarylquinolines *Janssen / Univ. of Auckland / UIC*	Q203 *Qurient*		SQ109 *Sequella*	Delamanid (OPC-67683) *Otsuka*
RNA Polymerase Inhibitors *Rutgers U.*	Indazole, Pyrazinamides *GSK*	SQ609, SQ641 *Sequella*		Rifapentine (DS-TB) *CDC, Sanofi*	Rifapentine (LTBI) *CDC, Sanofi*
Energy Metabolism Inhibitors *AZ / UPenn*	Thiophene Carboxamides *Calibir*	TBI-166 *IMM*		AZD5847 *AZ*	Pretomanid – Moxifloxacin – Pyrazinamide *TB Alliance*
POA Prodrug *Yonsei*		PBTZ169 *iM4TB*		Bedaquiline – Pretomanid – Pyrazinamide *TB Alliance*	
Hit ID Program *Takeda / Sanofi / Daiichi Sankyo / Shionogi*		DC-159a *Japan Anti-TB Assoc.*			

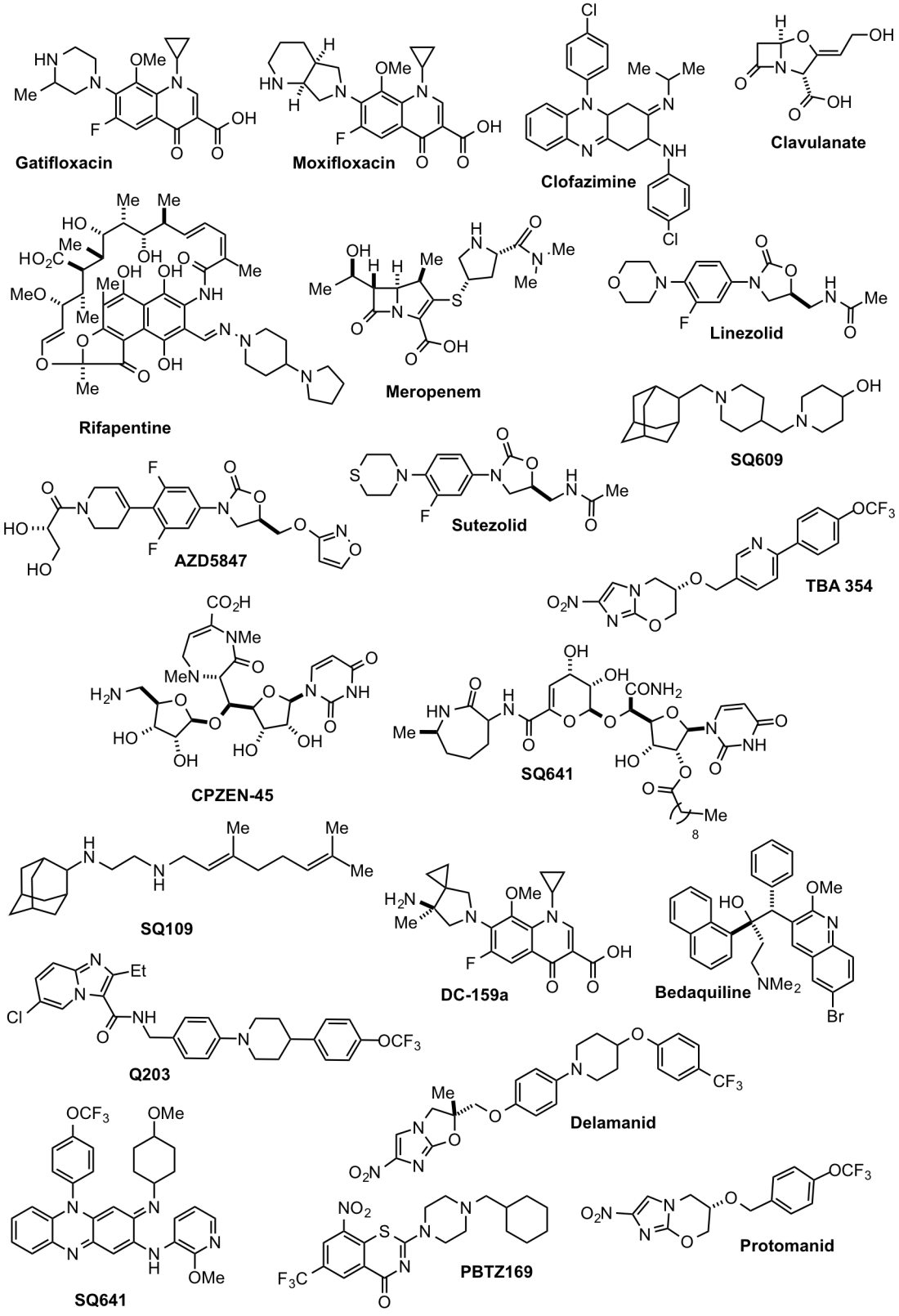

Figure 1.2 TB drugs in the pipeline[122-124]

currently employed in a randomized clinical trial in patients with XDR-TB.[127] The efficacy of clavulanic acid-meropenem combination therapy for XDR-TB is also currently under investigation.[128]

New chemical entities (NCEs) as TB drugs have also been discovered in the past decade. [122, 129] Bedaquiline (Sirturo) is a diarylquinoline that inhibits ATP synthase, decreasing intracellular ATP levels.[130] In December 2012, through a fast-track approval process, bedaquiline was approved by the Food and Drug Administration (FDA) for the treatment of MDR-TB. [131] It is the first TB drug to be approved in forty years,[132] and is currently in Phase 3 clinical trials for DS-TB. Otsuka's delamanid (Deltyba), a nitro-dihydro-imidazooxazole that inhibits mycolic acid biosynthesis, [133] was approved by European Medicines Agency (EMA) in November 2013 and is currently under FDA and WHO pre-qualification status.[134] Another mycolic acid synthesis inhibitor, Q109 is an ethylenediamine developed by Suquella.[135] Pre-clinical candidate PBTZ169, is a benzothiazinone antibiotic that inhibits decaprenylphosphoryl-beta-D-ribose 2'-epimerase (DprE1), an enzyme involved in the synthesis of key mycobacterial cell wall components.[136] These novel and repurposed TB drugs have been integrated into multidrug regimens in clinical trials.

1.11 Amicetin as a Potential Lead for Antitubercular Drug Discovery

The alarming global statistics on TB along with the inadequacy of current treatments has prompted a recent interest in the discovery and development of drugs. While most big pharmaceutical companies have yet to actively re-engage in the research and development of new compounds, the scientific community at large,

particularly academic and research institutions are spearheading the resurgence in TB drug discovery. After almost half a century of research hiatus, a promising pipeline for new antitubercular drugs has emerged through a multifaceted approach; including but not limited to, the discovery of new compounds, the repurposing of existing drugs, and the re-evaluation and re-engineering of existing antibacterial compounds.[137]

Over the past half-century, a myriad of natural products with antibiotic activity have been discovered.[138, 139] Most of the antibiotics used in clinical treatment today are either natural products, derivatives, or analogues of a compound expressed by bacteria.[140] It can be argued that compounds produced by bacteria have been, and could still be, the best source for potent antibiotic scaffolds. This rationale has inspired a number of research laboratories, including the Looper group and the Barrows group at the University of Utah, to start re-evaluating existing natural product libraries. Through this approach amicetin (Figure 1.3) was re-identified as a viable candidate for antitubercular drug discovery. Initial compound screening identified amicetin to be active against TB, selective against prokaryotic cells, and compatible with highly active antiretroviral therapy (HAART). Research efforts and collaborative work from the Steitz, Barrows, and Looper research groups have been aimed towards the synthesis, re-isolation, analogue design and development, and biological evaluation of amicetin analogues.

1.11.1 Amicetin: Isolation and Biological Activity

Amicetin (Figure 1.3), also known as allomycin and sacromycin, is an aminohexopyranose nucleoside antibiotic isolated from *Streptomyces vinaceusdrappus*[141, 142] and *Streptomyces fasciculatis*[143] in 1953. The antibiotic has

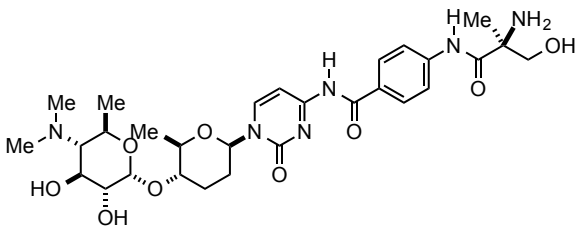

Figure 1.3 Amicetin

been isolated by other research groups from other *Streptomyces* species.[144, 145, 146] The chemical structure of amicetin was proposed, initially, through classical pre-NMR techniques of chemical degradation and derivatization (Scheme 2.1).[147, 148, 149] Its gross chemical structure was obtained through hydrolysis reactions, specific configuration and stereochemistry of the sugar components were established by synthesis and NMR studies on amicetin derivatives and degradation products.[150, 151, 152] The crystal structure of amicetin was published later, affirming the results of the seminal works.[153]

Amicetin has antimicrobial activity against a number of acid-fast gram positive bacteria (Table 1.5), including *Staphylococcus aureus* (FDA-209), with a minium inhibitory concentration (MIC) of 2.0 μg/mL, and *Mycobacterium tuberculosis* (H37Rv), with an MIC of 0.5 μg/mL.[141] It is also found to be active against *Mycobacterium smegmatis,* with an MIC of 8 μg/mL.[154] Amicetin is ineffective against gram-negative species, except for mutant species of *Eschericia coli*.[155] It is about ten-fold less active against *E. coli* with a half maximal inhibitory concentration (IC_{50}) of 0.3 μM compared to *Enterococcus faecalis* where it exhibits an IC_{50} of 0.02 μM.[156] In a disk diffusion assay, mutant strain *E. coli* H135 is found to be sensitive to amicetin at 50 μg/disk concentration. Amicetin is active *in vivo* against *M. tuberculosis* H37Rv in mouse infection models. When tested against the

Table 1.5 Antibacterial spectrum of amicetin compared with streptomycin[157]

Test organisms*	MIC (μg/mL)	
	Amicetin	Streptomycin
Staphylococcus aureus FDA-209	0.2	2.0
Mycobacterium tuberculosis H37Rv	0.5	1.0
Mycobacterium tuberculosis ATCC-607	1.0	1.0
Bacillus subtilis I11	4.0	0.1
Klebseilla pneumoniae PCI-602	>20	0.2
Escherichia coli ATCC-26	>20	1.0
Bodenheimer's coco-bacillus PCI-3	>20	1.0

same species, amicetin is found to be less effective than streptomycin sulfate on a weight basis. [158]

Amicetin also exhibits *in vitro* antiviral activity, measured as the number of plaque forming units (PFU) per 0.5 mL after 24 hours of incubation, against deoxyribonucleic acid viruses herpes, vaccinia, and pseudorabies.[159] The replication of herpes virus in chick embroyo monolayers is inhibited by about four log units using a 100 μg/ml concentration of amicetin. At 160 μM, it inhibits the replication of vaccinia and pseudorabies by one log unit and two and a half log units, respectively, compared to the control.

The potency-toxicity ratio of amicetin is favorable compared to other antibiotics. Cytotoxicity of amicetin towards mammalian cells is lower than other antibiotics of its class.[159] It has an intermediate activity against KB strain of human epidermoid carcinoma cells, with a reported IC_{50} of 7 μg/mL,[160] and has been reported to prolong the survival time of mice with leukemia-82.[161] Another clinical study showed that amicetin was inactive against acute leukemia in children who had previously developed resistance to chemotherapy.[162] Interestingly, amicetin's toxicity across test species varies significantly.[141] Its acute intravenous LD_{50} is 90 mg/kg for mice and 200 mg/kg for rats. Subcutaneous LD_{50} values for mice and

rats are approximately 600-700 mg/kg and 600 mg/kg, respectively. When administered subcutaneously in guinea pigs, amicetin is forty times more toxic than streptomycin, but only one-tenth as toxic as penicillin. When tested for ototoxicity, unlike streptomycin, amicetin was found to not cause eighth nerve damage, an adverse effect common to aminoglycoside antibiotics.[141, 163, 164]

Early biochemical studies have shown amicetin to be a protein synthesis inhibitor.[165] Since other cytosine nucleoside antibiotics are known to be peptidyl tranferase inhibitors, it has been suggested that perhaps amicetin has the same mode of action as well. The exact process through which amicetin inhibits the transpeptidation process has been extensively studied and will be discussed in the following chapters.

1.12 Natural Products Related to Amicetin: Pyrimidine Nucleoside Antibiotics Type I

In the past 50 years a number of pyrimidine nucleoside antibiotics have been isolated and studied. Most of these compounds are produced by the *Streptomyces* species. Among them, are a number of antibiotics that are structurally similar to amicetin, featuring a cytosine group, a sugar moeity, and two basic centers. For the purpose of this review, these compounds will be referred to as type-I pyrimidine nucleoside antibiotics. Some compounds are almost identical in structure to amicetin, while some others have been co-isolated with amicetin suggesting a shared biosynthetic pathway. Type-I compounds are generally active against gram-positive bacteria and are less toxic than other pyrimidine nucleoside antibiotics.

1.12.1 Bamicetin

Bamicetin (Figure 1.4) was co-isolated with amicetin in 1958 by Haskell from *Streptomyces plicatus*.[166] It was isolated as both the free base and the hydrochloride salt. Preliminary proposals on the structure of bamicetin were based on data from initial degradation studies. Results from the acid hydrolysis of bamicetin identified cytimidine as one of the fragments, indicating that both amicetin and bamicetin have the same aglycone component. Glycosidic fragments obtained from the aforementioned antibiotics, however, differ on the number of carbons. Amicetin yielded a 14-carbon aminosugar, while bamicetin yielded a 13-carbon aminosugar. Respective periodate oxidation of the sugars gave a mixture of formic acid, glyoxal and methylamine for bamicetin, and dimethylamine for amicetin, suggesting that amicetin's structure differs from bamicetin by one methyl group.[167]

Bamicetin is also reported to be active against *M. tuberculosis* H37Rv (data not shown).[166] Bamicetin is twice as active as amicetin against *E. coli* P-D 04863.[166] Bmicetin exhibited an MIC of 16 µg/mL against *Mycobacterium smegmatis*, only half as active as amicetin.[154] Translational studies done by Lovett and co-workers reported inhibition of peptidyl transferase activity of *B. subtilis* and *E. coli* 70S ribosomes to be nearly twice as strong as amicetin's,[166, 168] Cerna and co-workers

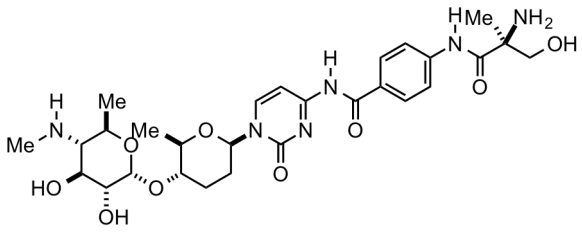

Figure 1.4 Bamicetin

have previously noted that with respect to the inhibition of specific steps in the peptidyl transferase, bamicetin has a similar inhibitory property as that exhibited by amicetin.[169] For both bamicetin and amicetin, complete inhibition of Ac-Phe transfer to puromycin was achieved at millimolar concentrations of the antibiotics. Lovett's report also presented the selective inhibition of translation on prokaryotic ribosomes of *B. subtilis* and *E. coli,* over eukaryotic ribosomes *Saccaromyces cerevisiae* and archaic ribosomes *Haloferax volcani*.[168]

1.12.2 Oxamicetin

Oxamicetin (Figure 1.5) is an antibiotic isolated from the fermentation broth of *Arthrobacter oxamicetus* sp. nov. from a soil sample collected at Kominato, Chiba, Japan by Konishi and co-workers in 1973.[170] Structural elucidation of oxamicetin was achieved through a combination of degradation studies and spectroscopic methods.[171]

Not surprisingly, oxamicetin exhibited an antibacterial spectrum comparable to amicetin (Table 1.6). It is less active than amicetin with respect to activity against Gram-positive species like *Staphylococcus,* as well as acid-fast species like*Mycobacterium*, but is slightly more active against Gram-negative bacteria like *Escherichia*. When tested *in vivo* on mouse infection models *S. aureus* Smith and mg/kg respectively. On the other hand, oral administration of the antibiotic did not produce any valuable *in vivo* activity. In mouse models, oxamicetin exhibited lower acute toxicity relative to amicetin, with an intravenous LD_{50} of about 200 mg/kg compared to the latter's 68-90 mg/kg. It was also reported to be nontoxic at 400 mg/kg when administered subcutaneously.

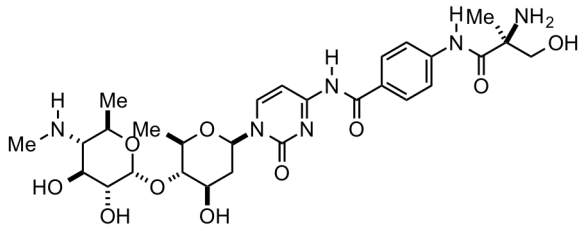

Figure 1.5 Oxamicetin

Table 1.6 Antibacterial spectrum of oxamicetin in comparison to amicetin[172]

Test organisms*	MIC (μg/mL)	
	Oxamicetin	Amicetin
Micrococcus flavus	1.6	3.1
Sarcina lutea PCI 1001	1.6	1.6
Staphylococcus aureus Terajima	1.6	0.8
Mycobacterium 607 (KM-R/SM-R)	3.1	1.6
Mycobacterium phlei	3.1	0.8
Salmonella typhosa Yale	3.1	3.1
Escherichia coli A 15169	6.3	6.3
Bacillus subtilis PCI-219	6.3	12.5
Streptococcus pyogenes S-23	6.3	3.1
Mycobacterium 607	12.5	3.1
Mycobacterium 607 (KM-R)	12.5	3.1
Mycobacterium ranae	12.5	3.1
Staphylococcus aureus # 193 (PC-R/TC-R)	12.5	6.3
Staphylococcus aureus Russell (PC-R)	12.5	6.3
Staphylococcus aureus Smith	12.5	6.3
Bacillus anthracis 115	25	12.5
Diplococcus pneumonia Type 2	25	3.1
Escherichia coli NIHJ	25	50
Escherichia coli A 20365 (KM-R/NM-R/SM-R)	25	50
Proteus vulgaris A 9526	25	100
Streptococcus pyogenes Digonet	25	3.1
Klebsiella pneumonia D11	50	100
Proteus morganii A 20031	50	>100
Proteus vulgaris A 9436	50	50
Shigella sonnei Yale	50	100
Salmonella enteritidis A 9531	50	100
Escherichia coli Juh1	100	>100
Shigella flexneri A 9684	100	100
Streptococcus pyogenes Dick	100	50
Proteus mirabilis A 9554	>100	>100
Pseudomonas aeruginosa D15	>100	> 100

1.12.3 SF2457

SF2457 (Figure 1.6) is a closely related aminohexopyranose nucleoside isolated by Itoh and Miyadoh in 1992.[173] Unlike other antibiotics in the amicetin family produced by *Streptomyces* and *Arthrobacter* species, SF2457 was isolated from the fermentation broth of *Nocardia brasiliensis* SF2457, from the soil sample collected at Toba City, Mie Prefecture, Japan. SF2457 was isolated and purified as a free base, and was described as a water soluble, colorless and amorphous powder. The structure of SF2457 was determined from spectroscopic analysis of the molecule itself, as well as from its degradation products. These experiments identified SF2457 as a close analogue of oxamicetin, containing a D-alanine rather than an α-methylserine moiety.

Similar to other analogues, it exhibited strong activity against Gram-positive bacteria such as subspecies of *Staphylococcus aureus* and some species of *Salmonella* (Table 1.7). However, the antibiotic was also found to be inactive against Gram-negative bacteria. Aside from the initial report on its isolation, there have been no other published studies on SF2457.

1.12.4 Cytosaminomycins

Haneda and co-workers isolated four active compounds from the fermentation broth of *Streptomyces amakusaensis* KO-8119 and designated the isolates as cytosaminomycins A, B, C and D (Figure 1.7).[174] Cytosaminomycin A and B were reported as a pale yellow powder and crystal, respectively, while cytosaminomycin C and D were reported as white powders.

The structures of the cytosaminomycins were determined by both one and two-dimensional NMR studies and high resolution fast atom bombardment mass

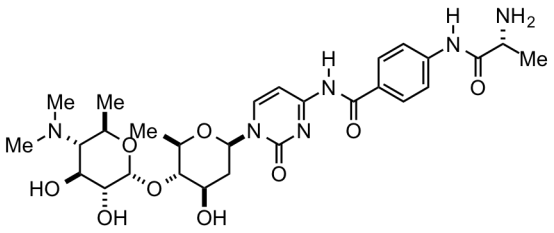

Figure 1.6 SP2457

Table 1.7 Antibacterial spectrum of SF2457[175]

Test organisms	MIC (μg/mL)
Staphylococcus aureus 209P JC-1	1.56
Staphylococcus aureus Smith S-424	1.56
Staphylococcus aureus No. 26	1.56
Staphylococcus epidermidis ATCC 14990	1.56
Staphylococcus epidermidis 109	1.56
Bacillus anthracis No. 119	1.56
Salmonella typhi O-901-W	1.56
Salmonella enteritidis No. 11	1.56
Enterococcus faecium ATCC 8043	12.5
Shigella sonnei EW33 Type I	25
Proteus vulgaris OX19	50
Salmonella sp. D-0001	50
Salmonella typhimurium LT-2	50
Escherichia coli JR66/W677	50
Escherichia coli JC-2	100
Escherichia coli No. 29	100
Escherichia coli W3630 RGN823	100
Morganella morganii Konno	100
Kleibsiella pneumoniae PCI602	100
Kleibsiella pneumoniae 22#3038	100
Serratia marcanscens MB-3848	100
Citrobacter freundii GN346	>100
Proteus mirabilis GN310	>100
Providencia rettgeri J-0026	>100
Pseudomonas aeruginosa MB-3829	> 100
Pseudomonas cepacia M-0527	> 100
Xanthomonas maltophilia M-0627	> 100

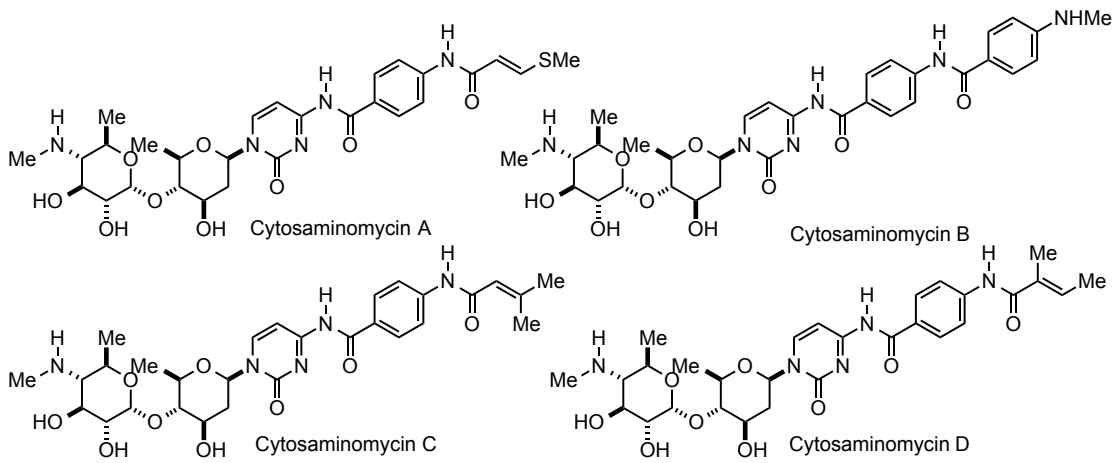

Figure 1.7 Cytosaminomycins

spectrometry.[176] Cytosaminomycins were shown to be related to oxyplicacetin[186] and contain the same hydroxycytosamine nucleoside fragment but differ at the N6-acylation of the cytosine moiety. The acyl groups contained were (*E*)-3-(methylthio)acrylic acid, 4-methylaminobenzoic acid, 3-methylcrotonic acid, and tiglic acid for cytosaminomycins A, B, C, and E respectively.

Coccidiosis is a parasitic disease common in poultry and is caused by a group of protozoans including *Eimeria tenella*. It is common practice in the poultry business to use polyether ionophores such as monensin,[177] salinomycin,[178] and lasalocid in combatting coccidiosis.[179] Recent reports have stated that such ionophores have become progressively ineffective due to resistant *Eimeria* sp.[180] The cytosaminomycins were tested primarily for their anticoccidial activity against monensin-resistant *E. tenella* using an *in vitro* assay that employs primary chicken embryonic cells and BHK-21 cells as hosts (Table 1.8). Anticoccidial activity was measured using minimum effective concentrations; determining the lowest concentration at which no schizont formation was observed. Cytosaminomycin A was found to be the most active, followed by cytosaminomycins B and C, and lastly

Table 1.8 Anticoccidial activity of cytosaminomycins[181]

Compound	MEC (μg/mL)			
	Chicken embryonic cells		BHK-21 cells	
	Anticoccidial activity	Cytotoxicity	Anticoccidial activity	Cytotoxicity
Cytosaminomycin A	0.31	10	0.16	0.31
Cytosaminomycin B	0.62	5	1.25	2.5
Cytosaminomycin C	0.62	5	1.25	5.0
Cytosaminomycin D	2.5	10	10	> 10
Monensin	---	0.03	---	0.03

by cytosaminomycin D. The observed cytotoxicity of cytosaminomycins B, C, and D against the host cells was about the same. Cytosaminomycin A, on the other hand, showed the highest selectivity index in the chicken embryonic cell assay with respect to minimum effective dose for cytotoxicity versus anticoccidial activity among its co-isolates. Additionally, the antimicrobial activity of cytosaminomycins was tested using disk diffusion assay (Table 1.9) at a concentration of 5 mg on a 6 mm paper disk cytosaminomycins showed antibacterial activity against gram-positive, gram-negative and wall-less bacteria. Cytosaminomycin A and C exhibited better biological activities than cytosaminomycins B and D. At these specific concentrations none of compounds exhibited activity against *Candida albicans*, *Saccharomyces sake*, *Aspergillus niger* and *Mucor racemosus*.

Table 1.9 Antimicrobial activity of cytosaminomycins A-D[182]

Organism	Inhibition Zone Diameter (mm)			
	A	B	C	D
Micrococcus luteus PCI1001	20	14	21	10
Escherichia coli NIHJ	14	7	14	0
Xanthomonas oryzae	14	0	17	16
Acholeplasma laidlawi PG-8	24	14	24	11
Bacteroides fragilis	10	0	12	0

1.12.5 Streptcytosines

Streptcytosines A–E (Figure 1.8) were isolated from a culture broth of Streptomyces sp. TPU1236A collected in Okinawa, Japan by Bu and co-workers in 2014.[154] Streptcytosine A closely resemble amicetin's structure, while streptcytosines B–E where close deoxy-analogues of cytosaminomycins A, C, and D. Streptcytosine A inhibited the growth of *Mycobacterium smegmatis* (MIC = 32 µg/mL), while streptcytosine B-E were not active at 50 µg/disc. It is less active than bamicetin and amicetin, with MICs of 16 µg/mL and 8 µg/mL, respectively. To date, no further studies on the streptocytocines have been made.

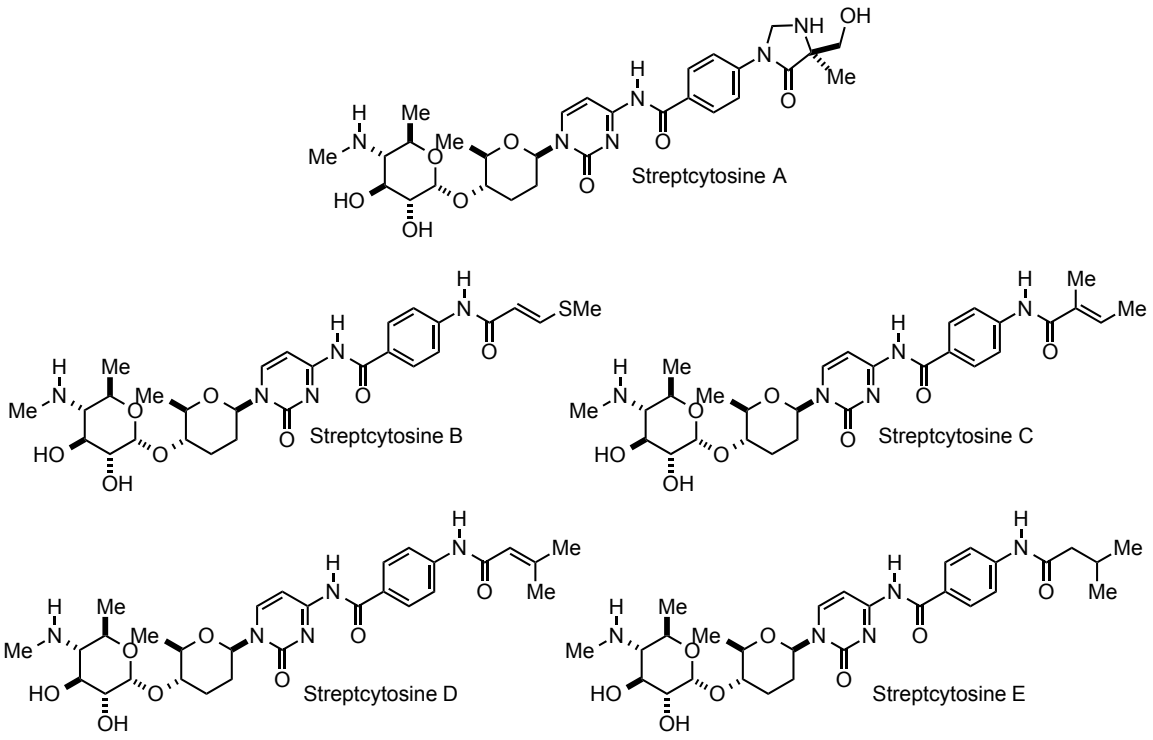

Figure 1.8 Streptcytocines

1.12.6 Plicacetin

Haskell and co-workers reported a third antibiotic isolated from the same culture filtrates of *Streptomyces plicatus* that produced amicetin and bamecin, and named the compound plicacetin (Figure 1.9).[145] The same antibiotic was independently reported by Sensi and co-workers a few months earlier in 1957 and was named "amicetin B". It was isolated from an actinomycete species arbitrarily designated as *Streptomyces* sp. 285.[183] Like amicetin and bamicetin, plicacetin's structure was determined through degradation studies.[167] It was concluded that plicacetin had the same overall structure as amicetin minus its amino acid moeity, and is probably a biosynthetic precursor of amicetin.[145]

Initial studies reported plicacetin's biological activity against *M. tuberculosis* H37Rv, both *in vitro* and *in vivo,* to be much lower than that of amicetin and bamicetin, and thus were not investigated further at the time.[145] Two decades later this observation was supported by studies on plicacetin's effect on the peptidyl transferase reaction of *E. coli* B 70S ribosome*s.*[169] Plicacetin does not inhibit peptidyl transferase even at concentrations wherein amicetin and bamicetin showed complete inhibition. For example, with respect to its inhibitory effect on puromycin reaction with either AcPhe-tRNA or poly-Lys-tRNA as donor substrates, plicacetin displayed only about 1% of the activity exhibited by amicetin and bamicetin at millimolar concentrations. When comparing concentrations at 50% inhibition of

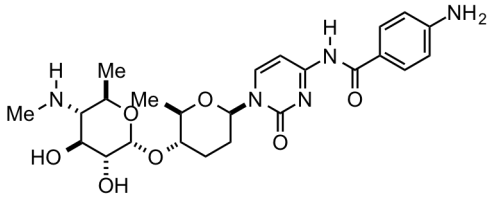

Figure 1.9 Plicacetin

puromycin reaction with CACCA-Leu-Ac as a donor substrate, plicacetin is ten times less active than amicetin. It also does not inhibit the binding of donor and acceptor substrates to the peptidyl transferase center of the ribosome.[169, 184] Examining plicacetin's structural features and biological activity, strongly indicates that an aminoacyl moiety, a D-a-methylserine in the case of amicetin and bamicetin, is essential for intercepting ribosomal transpeptidation reactions.

1.12.7 Norplicacetin

In 1977, Evans and Weare reported a fourth antibiotic isolated from *Streptomyces plicatus* from fermentation cultures of a soil sample obtained from Ghana.[185] The antibiotic was described as white needles that exhibited an identical UV spectrum with known compound, plicacetin. Additional spectroscopic data obtained from mass spectrometry and NMR spectroscopy further suggested that its structure is closely related to plicacetin, minus a methyl group on the latter's aminosugar moiety. The compound was named norplicacetin (Figure 1.10) and was assigned as the mono-methyl analogue of plicacetin and possible precursor to bamicetin. The antibiotic spectrum and activity of norplicacetin (Table 1.10) resem bles the activity of plicacetin. It is moderately active against Gram–positive bacteria and acid-fast mycobacteria.

1.12.8 Oxyplicacetin

Oxyplicacetin (Figure 1.11) was isolated from the fermentation cultures of *Streptomyces ramulosus* Tu-34 by Yongle and co-workers in 1985.[186] Little is known about this compound except for studies done by Haneda and co-workers in 1994. Oxyplicacetin exhibited some antimicrobial activity (Table 1.11) at 5 μg/i.d,

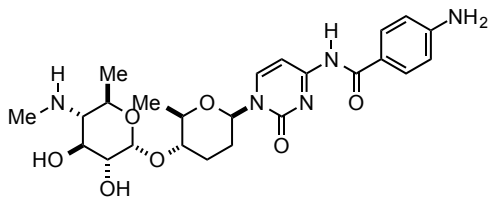

Figure 1.10 Norplicacetin

Table 1.10 Antibacterial spectrum of norplicacetin[187]

Test organisms	MIC (μg/mL)
Mycobacterium bovis BCG 1077	0.5
Mycobacterium bovis BCG 1173	0.5
Staphylococcus aureus Glaxo 618	4
Streptococcus pneumoniae	4
Haemophilus influenzae Glaxo 1184E	8
Escherichia coli Glaxo 573	16
Staphylococcus aureus Glaxo 663 and 853-E	31
Mycobacterium smegmatis ATCC 607	62
Mycobacterium smegmatis NCTC 8158	62
Escherichia coli 1161	>500
Klebsiella aerogenes Glaxo 1082E	>500
Pseudomonas aeruginosa Glaxo 1371E	>500
Candida albicans Glaxo C316	>500

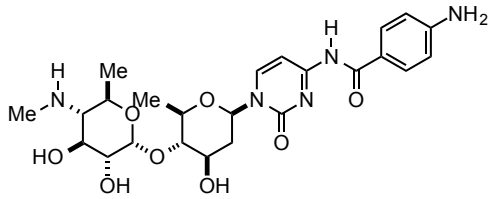

Figure 1.11 Oxyplicacetin

Table 1.11 Antimicrobial activity of oxyplicacetin[188]

Organism	Inhibition Zone Diameter (mm)
Micrococcus luteus PCI1001	18
Escherichia coli NIHJ	12
Xanthomonas oryzae	16
Acholeplasma laidlawi PG-8	17

using 6 mm paper disk in disk diffusion assays. Oxyplicacetin also showed anticoccidial activity against *Eimeria tenella*, with MEC values of 5.0 and 1.25 μg/mL for chicken embryonic cells and BHK-21 cells. The same study reported complete cytotoxicity against BHK-21 at 5.0 μg/mL but no apparent cytotoxicity against chicken embryonic cells at 10 μg/mL for oxyplicacetin.

1.13 Natural Products Related to Amicetin: Pyrimidine Nucleoside Antibiotics Type II

The second type of pyrimidine nucleoside antibiotics have only one basic terminal group, either an amino group or an aminoacyl moeity, attached to a sugar moeity that is bound to the cytosine group. Most of these antibiotics closely resemble the structure of blasticidin S (Figure 1.12), the first discovered antibiotic of its type and the most explored member of this group. For the purposes of this section, the following compounds are classified as Type-II or blasticidin-type pyrimidine nucleoside antibiotics. Not only do these compounds share the same bonding arrangement with blasticidin S, but also exhibit similar antimicrobial and toxicity properties. These compounds typically have broad but modest antibacterial activity, and are generally more toxic than Type-I pyrimidine nucleoside antibiotics.

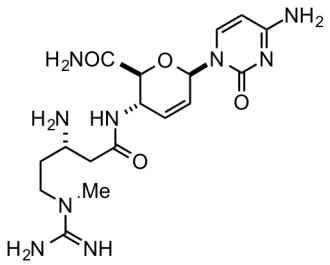

Figure 1.12 Blasticidin S

1.13.1 Blasticidin S

Blasticidin S (Figure 1.12, *vide infra*) was isolated from the fermentation broth of *Streptomyces griseochromogenes* by Takeuchi and co-workers in 1958.[189] Its discovery was part of the screening initiative at the National Institute of Agricultural Science, Tokyo, in search of compounds that were active against *Piricularia oryzae*, the cause of rice blast disease, hence the parent name blasticidin. The compound is, however, not structurally related to blasticidin A, B, and C.[189, 190, 191]

The biological activity profile of blasticidin S was examined by agar streak dilution method and broth dilution methods against a number of microorganisms. Blasticidin S was found to be moderately active against a number of bacteria including species of *Mycobacterium tuberculosis* and *Pseudomonas fluorescens* (Table 1.12). It is also reported to be active against a number of pytopathogens with MICs ranging from 5-50 μg/ml, (Table 1.13). At 5 μg/ml. (MIC) it displays the most activity against *Bacterium aroideae*, *Bacterium citri*, *Pseudomonas tobaci*, and *Piricularia oryzae*. The modest activity demonstrated by blasticidin S against gram-negative bacteria is over shadowed by animal toxicity; when injected intravenously to mice, it was found to have an LD_{50} of 2.82 mg/kg.[189]

It has antitumor activity against transplantable animal tumor.[192] Blasticidin S displayed 30-68% tumor growth inhibition against Walker adenocarcinoma 256 in rats, about 60-70% inhibition in Ehrlich carcinoma inhibition and 40% sarcoma 180 in mice through intraperitoneal injection of 1.5 to 3 mg, twice daily over two weeks. It is also worth noting that none of the animals died of toxicity during the course of the experiment.

Subsequent biological studies on the mechanism of action of blasticidin S

Table 1.12 Antimicrobial spectrum of blasticidin S[193]

Test organisms	MIC (μg/mL)
Pseudomonas fluorescens	5
Mycobacterium tuberculosis H37RA	10
Mycobacterium tuberculosis ATCC 607	50
Mycobacterium phlei	50
Micrococcus pyogenes var. *aureus* 209 P	50
Bacillus subtilis	50
Sacrina lutea	50
Escherichia coli	50
Penicillium notatum	>100
Penicillium chrysogenum Q176	>100
Aspergillus oryzae	>100
Trichophytone purpureum	>100
Candida albicans	>100
Pseudosaccharomyces samtacruxensis	>100
Saccharomyces cerevisiae	>100
Torula albia	>100
Torula utilis	>100

Table 1.13 Antipytopathogenic spectrum of blasticidin S[194]

Test organisms	MIC (μg/mL)
Bacterium citri	5
Bacterium aroideae	5
Pseudomonas tobaci	5
Piricularia oryzae	5-10
Sclerotinia mali	10
Alternaria kikuchiana	50
Erwinia aroidae	50
Gloeosporium kaki	50
Gloeosporium lacticolor	50
Pseudomonas solanacearum	50
Xanthomonas citri	50

reported interesting observations. Kinetic studies have shown blasticidin S both enhancing P-site binding and inhibiting the A-site binding of aminoacyl-CACCA.[195, 196] It doesn't promote the premature release of peptides from the ribo somes unlike puromycin, an A-site inhibitor, suggesting a different mechanism of action. Blasticidin S, however, was later reported to compete with A-site binding antibiotic puromycin and sparsomycin.[197, 198] It was further suggested that its mode of action may involve binding to the A site based on results from resistance studies wherein strains resistant to sparsomycin and puromycin are found to be co-resistant to blasticidin S and vice versa.[199]

The crystal structure of blasticidin S bound to the 50S ribosome subunit of *Haloarcula marismortui* (Figure 1.13) has been solved by Steitz and published in 2003,[200] and shows two copies of blasticidin S bound to the P site of the ribosome. Both copies interact with the highly conserved P loop of the ribosome but with different affinities. The stronger site (Figure 1.13A) shows both the cytosine and the sugar moeity of blasticidin S perfectly aligns with the corresponding cytidine, C74, of a P-site substrate. The cytosine of blasticidin forms a Watson-Crick base pair with G2251 (*E. coli* numbering), while its pyranose ring superimposes with the corresponding ribose of C74. The guanidinium tail was originally described as forming hydrophobic interactions with A2439, although stronger forces such as cationic-π interactions would have played a greater role. The guanidinium tail also hydrogen bonds with the phosphates of A2439 and A2600. In the weaker site (Figure 1.13B), blasticidin base pairs with G2252, in place of C75 of the P-site substrate but without the superimposing of its sugar to its ribose equivalent. Both guanines, G2251 and G2252, are critical to the proper positioning of the conserved CCA terminus of the P-site bound tRNA. Overall, the data suggests that

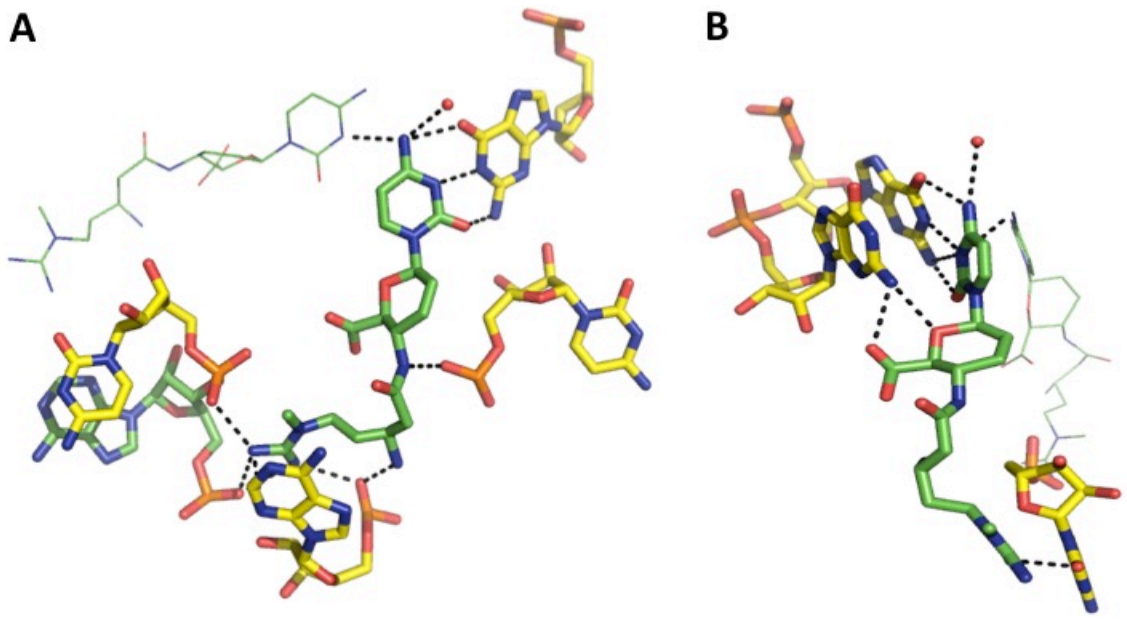

Figure 1.13 Blasticidin S binding to 50S ribosome subunit of *H. marismortuii* A) Stronger binding site and B) Weaker binding site: blasticidin S (green), ribosome residues (yellow), water (red), second blasticidin S molecule (green, line).

blasticidin S competes with the P-site substrate binding, thereby inhibiting protein synthesis.

The work provided insight, at the molecular level, as to how cytosine nucleo side antibiotics possibly elicit their biological activity. However, it neither provides a detailed mechanism by which it inhibit the peptidyl transferase reaction, nor does it provide an explanation to the previously reported nuances and apparent contradictory observations in its mechanism of action, i.e., its co-resistance and competition with known A-site antibiotics and stabilization of the binding of P-site substrates.

Korostelev and co-workers sought to answer this conundrum using biological assays, X-ray crystallography, and single-molecule Förster resonance energy transfer (smFRET).[201] In their published work, Korostelev re-examined how blasticidin S stabilizes the binding of P-site substrates. Monitoring the binding of

N-formyl-methionyl-tRNA to the P-site of *E. coli* 70S ribosomes pre-incubated with varying concentrations of blasticidin, he showed that it only interferes with P-site substrate [^{35}S]-fMet-tRNA^{fMet} binding at high millimolar concentrations (IC_{50} ~20 mM). This exceeds the inhibition constant for peptidyl transfer up to five orders of magnitude, which is about 200-400 nM,[202, 203] and is is also about four orders of magnitude higher than the concentration needed to inhibit bacterial growth. It is proposed that the observed competition with the P-site substrate is only effected by blasticidin S binding to the second low-affinity site as observed in the crystal structure of *H. marismortui* co-crystallized with millimolar concentrations of the antibiotic.[189] Blasticidin is therefore not an effective P-site inhibitor despite binding to the P-site. It was then suggested that perhaps it affects another facet of protein synthesis.

Single molecule FRET experiments were employed to monitor the inter-subunit dynamics of the ribosomal complex during the translocation process.[204] Fluorophores were attached to proteins S6 and L9 of the 30S and 50s subunit respectively to monitor. How blasticidin affects the affinity of tRNA to the 50S P-site is monitored by measuring the fluctuations between conformations of the ribosomal units. In the absence of the antibiotic, the ribosomes maintained its rotated hybrid state 70% of the time. Upon addition of blasticidin, 80% of the ribosomes remained in the nonrotated conformation. Blasticidin was found to slow down the counterclockwise rotation of the 30S subunit during the translocation process by up to five-fold. It is suggested that blasticidin stabilizes the acceptor end of the P-site tRNA preventing the rotation of the 30S subunit and the shifting of the deacylated tRNA into the hybrid states, corresponding to previous reports on blasticidin's stabilization P-site substrates.[169, 196, 201]

Blasticidin is also found to inhibit peptide release and peptidyl transfer during termination and elongation steps, respectively, supporting the seminal works on its biological activity.[195, 196, 201] Peptide release during the termination step is catalyzed by release factors 1 and 2 (RF1 and 2), proteins that bind to the A-site and facilitate the peptidyl-tRNA hydrolysis. Blasticidin inhibits RF1-mediated release of [^{35}S]-fMet release from P-site bound [^{35}S]-fMet-tRNA^{fMet}. The apparent inhibition constant (K_i) is 32 ± 18 nM for the RF1-mediated release. For the inhibition of peptidyl transfer of [^{35}S]-fMet to puromycin, the values are much higher at 182 ± 39 nM. Blasticidin has been cited as a peptidyl transaferase inhibitor but its strong inhibition of the termination step is particularly noteworthy since no specific inhibitors for this step have been previously identified.[205]

Korostelev also presented a 3.4 Å crystal structure of blasticidin S bound to the 70S *Thermus thermophilus* ribosome complex (Figure 1.14).[201] Compared to the previous work of Steitz, wherein two molecules of blasticidin S were bound to the vacant 50S subunit, only one copy is found in the 70S-tRNA complex. The conformation and the binding site of blasticidin S in the more recent published crystallographical data, however, is very similar to that described for the higher affinity site, with an all-atom rms difference of 0.57 Å, which is within the boundary of acceptable coordinate error for a 3.4 Å resolution. The guanidinium group of blasticidin stacks with A2439, possibly forming cation-π interactions with the adenine. A hydrogen bond network formed with the guanidine tail and the phosphate groups of A2439, A2600, and C2601 further stabilizes the structure. The cytosine moeity base pairs with G2251, replacing the pairing between G2251 and C75 in antibiotic-free 70S-tRNA complexes. It also intercalates between C74 and A76 of the CCA terminus of the P-site tRNA. These interactions displaces the CCA

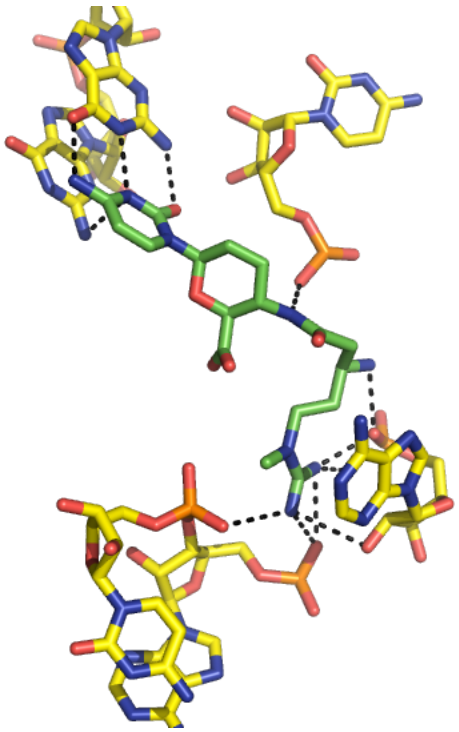

Figure 1.14 Blasticidin S bound to the 70S *T. thermophilus* ribosome complex

terminus of the P-site tRNA toward the A-site dramatically, by about 7Å. This observed shift of P-site tRNA towards the A-site explains the reported effect of blasticidin on A-site substrates.[195 201] The protrusion of the CCA end may have also led to steric interference with the highly conserved GGQ region known to bind release factors, mediating the premature release of peptide described earlier. In addition, the distortion may also result in the poor positioning of substrates for nucleophilic attack during peptidyl transfer.

1.13.2 Gougerotin

Gougerotin (Figure 1.15) is an antibiotic that was isolated from *Streptomyces gougerotii* No. 21544 by Kanzaki and co-workers in 1962.[206] It has been isolated independently by another research group from other species of *Streptomyces* and

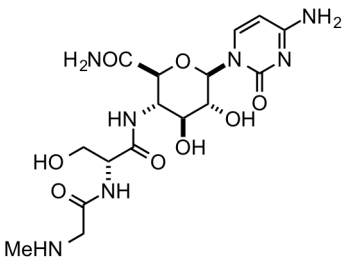

Figure 1.15 Gougerotin

also has been assigned a different name, yungumycin.[207, 208] The initial structure of gougerotin was proposed by Iwasaki from a series of classical chemical studies,[209] but was reinvestigated and revised by Fox and co-workers in 1965 through derivitization and synthetic studies.[210, 211]

Gougerotin is active against a number of gram-positive, gram-negative bacteria and mycobacteria (Table 1.14).[206] It was also reported to reduce the growth of rice seedlings by 60% and 100% at 0.1 mM and 0.3 mM respectively.[207] Gougerotin is known to be toxic to mammalian systems, with an LD_{50} of 57 mg/kg for mice *via* intravenous injection. However, the toxicity of the compound is delayed.

Gougerotin belongs to the cytosine nucleoside family of antibiotics known to inhibit protein synthesis.[212] Initial experiments have shown gougerotin inhibits the amino acid transfer in the polyuridylic acid-dependent synthesis of polyphenylalanine in cell-free *E. coli* systems. It was also shown that gougerotin inhibits protein synthesis by inhibiting the transfer reaction of amino acids from aminoacyl-tRNA to the nascent peptide. Gougerotin inhibits the transfer reaction in both cell-free systems obtained from murine liver samples and rabbit reticulocytes.[213, 214, 215] It was originally proposed that gougerotin and puromycin may have the same mechanism of action based on their structural similarities.

Subsequently, it was shown that gougerotin's specific mode of action to be

Table 1.14 Antimicrobial spectrum of gougerotin[216]

Test organisms	MIC (μg/mL)
Micrococcus flavus	40
Mycobacterium tuberculosis H37Rv	100
Escherichia coli	200
Brevibacillus brevis	200
Staphylococcus aureus 209 P	400
Bacillus subtilis PCI 219	400
Alternaria kikuchiana	>500
Candida albicans	>500
Colleto lagernarium	>500
Gibberella fujikuroi	>500
Glomerella cingulate	>500
Penicillium chrysogenum Q 176	>500
Phytophytophora infestans	>500
Piricularia oryzae	>500
Saccaromyces cerevisiae	>500
Mycobacterium avium	800
Mycobacterium avium Streptomycin-fast	800
Mycobacterium 607	800
Pseudomonas aeruginosa	800
Sarcina lutea	800
Brevibacillus cereus	>800
Mycobacterium smegmatis	>800

different from that of puromycin. Gougerotin does not compete with the binding of the aminoacyl-tRNA in the ribosome complex, nor does it act as an aminoacyl-tRNA analogue that terminates the peptide elongation process like puromycin.[215, 214] To date, the detailed mechanism of action has not been completely and specifically elucidated for gougerotin. Much of what is known is based on the aforementioned seminal work in the 1960s. However, its mechanism of action can be inferred from studies done on other closely related cytidine antibiotics such as blasticidin S.

1.13.3 Anthelmycin/Hikizimycin

Anthelmycin (Figure 1.16) was isolated from *Streptomyces longissimus* ATCC-14562 from soil samples collected in Indiana, U.S.A by Hamill and Hoehn in

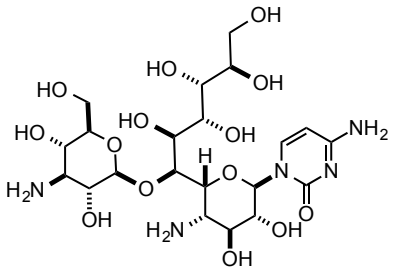

Figure 1.16 Anthelmycin/Hikizimycin

1964.[217] Its hydrochloride salt was obtained as white crystals that are stable in solution from pH 1 to 10 at and 25 °C. Like other related cytosine antibiotics, it does not exhibit a distinct melting point but decomposes above 200 °C. It is reported to be very soluble in water, acidic aqueous solutions, in methanol, but is practically insoluble in other organic solvents.

The cytosine antibiotic hikizimycin was independently isolated from the fermentation broth of *Streptomyces* sp. strain A-5, found in the soil sample collected at the Hikizi river-side, Kanagawa Prefecture, Japan by Uchida and co-workers in 1971.[218] It was obtained as obtained as a colorless hydrobromide crystalline salt exhibiting similar physical properties to that of anthelmycin. Initial studies on the structure of the two antibiotics reported that both contained cytosine and 3-amino-3-deoxy-D-glucose.[219, 220, 221] Common physical properties and structural features lead to the re-examination of the identities of both antibiotics and have confirmed the intimation that anthelmycin and hikizimycin are the same antibiotics.

Anthelmycin exhibited a broad but weak antimicrobial activity profile (Table 1.15).[217] While hikizimycin exhibited moderate activity against certain species of *Pseudomonas* and *Xanthomonas*, it is notably active against phytopathogenic fungi (Table 1.16).[218] The reported antibacterial and antifungal

Table 1.15 Antimicrobial spectrum of anthelmycin/hizikimycin[222]

Test organisms	MIC (μg/mL)
Pseudomonas syringae	2
Pseudomonas fluorescens	10
Alternaria solani	12.5
Ceratostomella ulmi	12.5
Helminthosporium sativum	25
Mycobacterium avium	25
Pseudomonas tabaci	40
Aerobacter aerogenes	50
Klebsiella pneumonia	50
Mycobacterium tuberculosis ATCC 607	50
Pseudomonas solanacearum	50
Shigella paradysenteriae	50
Xanthomonas oryzae	50
Xanthomonas phaseoli	50
Agrobacterium tumefaciens	55
Penicillium chrysogenum	80
Aspergillus niger	100
Bacillus subtilis	100
Colletotrichum pisi	100
Endoconidiopora fagacearum	100
Erwinia amylovora	100
Penicillium expansum	100
Pseudomonas aeruginosa	100
Salmonella enteritidis	100
Pullularia sp.	100
Aspergillus oryzae	150
Trichophyton rubrum	150
Escherichia coli	200
Corynebacterium michiganese	200
Proteus vulgaris	200
Staphylococcus aureus	200
Xanthomonas campestri	200
Candida albicans	>200
Candida utilis	>200
Saccharomyces cerevisiae	>200

Table 1.16 Antipytopathogenic spectrum of Anthelmycin/Hikizimycin[223]

Test organisms	MIC (μg/mL)
Alternaria kikuchiana	1
Alternaria tenius	2
Ascochyta sojaecola	2
Curvularia lunata	2
Sclerotium bataticola	2
Stemphylium lotii	5
Botrytis tulipae	10
Carvularia geniculate	10
Helminthosporium sativum	10
Helminthosporium oryzae	10
Rhizoctonia solani	10
Botrytis cinerae	20
Sclerotium rolfisii	20
Colletotrichum linicolum	20
Piricularia oryzae	100
Fusarium oxysporium	>200
Trichoderma viridi	>200

properties were closely similar to that of blasticidin S. Anthelmycin also exhibited antiviral activity by protecting HeLa cells from herpes simplex and inhibiting production of encephalomyocarditis (EMC) virus.[224, 225]

When tested for its *in vivo* activity, anthelmycin was found to be an effective anthelmintic agent against a number of parasites such as pinworms, roundworms, whipworms, and strongyles. Oral administration of anthelmycin at a dosage of 12 g per ton of normal swine ration eliminated 100% of the total population of *Oesopagostumum* sp. (nodular worms), 100% of *Trichuris suis* (whipworms), and 80% of *Ascaris suis* (roundworms). In addition, anthelmycin also exhibited housefly larvacidal activity[217] and notable toxicity towards green peach aphids.[226] The acute toxicity (LD_{50}) of anthelmycin in mouse models, was about 5 mg/kg and 150 mg/kg *via* intravenous administration and oral administration, respectively.

Seminal studies on the biological activity of anthelmycin have reported it to

be a protein synthesis inhibitor, specifically the peptidyl transferase reaction, in both prokaryotic and eukaryotic ribosomes.[227] However, while being structurally similar to amicetin and blasticidin S, anthelmycin lacked the aminoacyl moeity other members of the cytosine nucleoside family of antibiotics possess. Footprinting studies showed that anthelmycin inhibits the peptide bond formation by binding to the same ribosomal receptor site as blasticidin S and possibly other structurally related inhibitors.[228]

1.13.4 Mildiomycin

Mildiomycin (Figure 1.17) was isolated from *Streptoverticillium rimofaciens* B-98891 found in a soil sample collected in Papua New Guinea, as part of the agricultural antibiotic screening program of Takeda Chemical Industries.[229] It was isolated as a white formate salt and was immediately identified as structurally similar to blasticidin S and gougerotin. Initial physico-chemical studies done on the antibiotic determined it to be a new compound with a novel 5-hydroxymethyl cytosine, which has never been reported within its class of nucleoside antibiotics. The structure of mildiomycin was established by spectroscopic studies on its free base and x-ray crystallography on its benzoate derivative.[230, 231]

Mildiomycin showed activity against acid-fast bacteria *Mycobacterium phlei*

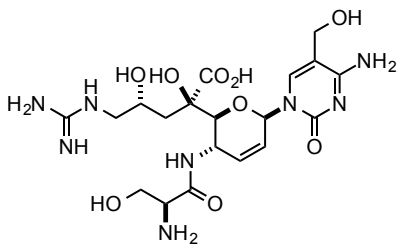

Figure 1.17 Mildiomycin

and fungus *Rhodotorula rubra*, a form of powdery mildew that causes extensive damage to a number of essential agricultural crops. Similar to gougerotin and blasticidin S, it exhibited weak antimicrobial activity on gram-positive, gram-negative bacteria, and fungi (Table 1.17).

Compared to blasticidin S, mildiomycin is relatively nontoxic. The acute mammalian toxicity of mildiomycin in female mice (LD_{50}) was determined to be 599 mg/kg by intravenous administration, which is 200-fold less toxic than blasticidin S.[232] The LD_{50} values for the same species measured *via* subcutaneous, intraperitoneal, and oral routes were 1150 mg/kg, 1050 mg/kg and 5250 mg/kg, respectively. In female rats the LD_{50} values were measured as 684 mg/kg, 70 mg/kg, 842 mg/kg, and 4120 mg/kg *via* subcutanoues, intravenous, interperitoneal and oral routes respectively, which are all at least 100-fold less toxic than related cytosine nucleoside antibiotics.[232]

Table 1.17 Antimicrobial spectrum of mildiomycin[233]

Test organisms	MIC (μg/mL)
Rhodotorula rubra IFO 0870	50
Mycobacterium phlei IFO 3158	50
Guignardia laricina IFO 7888	100
Alternaria kikuchiana IFO 8414	250
Botrytis cinerea TFK 12	250
Cochliobolus miyabeanus IFO 5277	250
Mycobacterium smegatis ATCC 607	250
Escherichia coli IFO 12734	500
Pseudomonas aeruginosa IFO 3449	500
Sclerotinia sclerotiorum IFO 9395	500
Trichopython mentagrophytes IFO 5809	500
Bacillus brevis IFO 3331	>500
Bacillus cereus IFO 3466	>500
Bacillus subtilis IFO 3513	>500
Proteus vulgaris IFO 3045	>500
Sarcinia lutea IFO 3232	>500
Staphylococcus aureus IFO 3061	>500

Adverse allergic effects of mildiomycin were also tested on rabbit skin and cornea.[232] No irritation was observed during a dosing period of 10 days, at 1,000 ppm concentration. No significant effect was observed in a toxicity test using killifish, water fleas and carps at a dosage of 20 ppm for 7 days. Chronic toxicity of mildiomycin was also measured over a period of 30 days. Daily dosing of 200 mg/kg in mice or rats produced no adverse effects. The study was extended over a three-month period and no significant adverse effects were observed, leading to the conclusion that mildiomycin is considered to have low toxicity.[229]

When the mechanism of action was probed, mildiomycin was found to be a selective protein synthesis inhibitor in human HeLa cells (Table 1.18).[234] It was found to be more potent and selective inhibitor of mammalian protein synthesis than blasticidin S, gougerotin and anthelmycin. The activity, however, is reversed with respect to bacterial and fungal protein synthesis. It was also found to be less active in the inhibition of RNA or DNA synthesis.[234] Nucleoside antibiotics like mildiomycin are molecules across the cellular membrane, owed to their very hydrophilic nature. However, when paired with animal viruses that permeabilize cell membranes the antibiotic can cross the membrane.[235] An increase in potency was observed when HeLa cells are transfected with encephalomyocarditis virus.

Table 1.18 Effect of mildiomycin and other antibiotics on protein synthesis[236]

Antibiotic (Concentration)	% Control		
	Yeast	HeLa	*E. coli*
None	100	100	100
Mildiomycin (50 μM)	19	0	0
Mildiomycin (20 μM)	86	0	53
Mildiomycin (10 μM)	92	0	90
Anthelmycin (10 μM)	109	103	25
Gougerotin (10 μM)	64	84	24
Blasticidin S (10 μM)	5	20	6

In vitro experiments on the direct effect of mildiomycin in the protein synthesis machinery, using S-30 rabbit reticulocyte lysate, determined the IC_{50} to be 0.5 μM. Mildiomycin has no effect on the binding of Phe-tRNA (P-site substrate) and *N*-Ac-Phe-tRNA (A-site substrate) to the ribosome in a poly-(U) system. Similar to blasticidin S, mildiomycin inhibits the peptidyl transferase reaction of ^{3}H]-puromycin using yeast polysomes.[234, 237] It exhibited 43% inhibition of the puromycin reaction at a concentration of 100 μM, which is considerably lower than anisomycin's (90% inhibition) and trichodermin's (80% inhibition) activities at the same antibiotic concentration.[234]

1.13.5 Ezomycins A_1 and A_2

Ezomycins A_1 and A_2 (Figure 1.18) were isolated by Sakata and co-workers in 1974 from the fermentation broths of *Streptomyces* found in samples collected in Hokkaido.[238] Ezomycin A_1 was isolated as a white amorphous powder, while Ezomycin A_2 was obtained as a crystalline solid. Ezomycin A_1 is highly soluble in water while ezomycin A_2 is partially soluble in water, but easily soluble in acidic and basic conditions. Both antibiotics are practically insoluble in most organic solvents.[238]

The structures of ezomycins A_1 and A_2 were determined by degredative

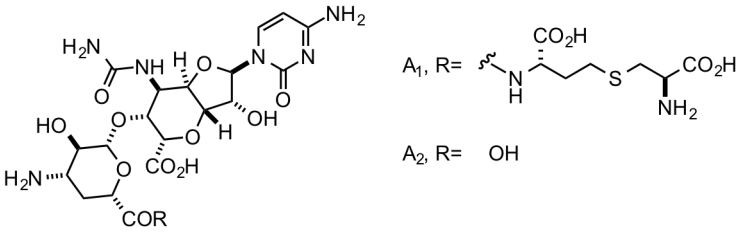

Figure 1.18 Ezomycins A_1 and A_2

experiments [239, 240, 241] and spectrometric studies.[242, 243] Their structures feature aunique octosyl cytosine nucleoside, a deoxyglycoside (ezoaminuroic acid) and an *N*-linked pseudopeptide (L-cystathionine) for ezomycin A_1. Other ezomycins have been co-isolated with A_1 and A_2 such as ezomycins B_1 and B_2, which are uracil analogues of A_1 and A_2 respectively. Ezomycin A_1 was found to be inactive against most microbes except for *Sclerotina* and *Botrytis* (Table 1.19). On the other hand, ezomycin A_2, lacking the L-cystathioninyl, was devoid of any significant antimicrobial activity.[238] To date no additional study has been done on ezomycins.

Table 1.19 Antimicrobial spectrum of Ezomycin A_1 [244]

Test organisms	MIC (μg/mL)
Sclerotinia sclerotiorum	6.3
Botrytis cinerea	6.3
Sclerotinia libertiana	50
Botrytis alli	50
Bacillus subtilis PCI 219	>100
Blastomyces brasiliensis OUT 4210	>100
Candida albicans YU 1200	>100
Candida tropicalis IAM 4862	>100
Cornyebacterium xerosis	>100
Escherichia coli NIHJ JC-2	>100
Gloesporum kaki #KYU: 438	>100
Klebsiella pneumoniae PCI 602	>100
Mycobacterium smegmatis ATCC 607	>100
Proteus vulgaris OX-19	>100
Pseudomonas aeruginosa IAM 1095	>100
Saccharomyces cervisiae ATCC 9736	>100
Sarcina lutea PCI 1001	>100
Trichophyton mentagrophytes	>100
Trichophyton interdigiate	>100

1.14 References

1. Daniel, T. M. History of tuberculosis. *Resp. Med.* **2006**, *100*, 1862-1870.

2. Cave, A. J. E. The evidence for the incidence of tuberculosis in ancient Egypt. *Br. J. Tuberc.* **1939**, *33*, 142-52.

3. Jardao, L. Vieira, O. V. Tuberculosis: New aspects of an old disease. *Int. J. Cell. Bio.* **2011**, *2011*, 1-13.

4. Krause, A. K. Tuberculosis and public health. *Am. Rev. Tuberc.* **1928**, *18*, 271-322.

5. Daniel, T. M. René Theophile Hyacinthe Laennec and the founding of pulmonary medicine. *Int. J. Tuberc. Lung. Dis.* **2004**, *8,* 517-8.

6. Cambau E.; Drancourt, M. Steps towards the discovery of *Mycobacterium tuberculosis* by Robert Koch, 1882. *Clin. Microbiol. Infect.* **2014,** *20*, 196-201.

7. Koch, R. Die aetiologie der tuberculose. *Berl. Klin. Wochenschr.* **1882,** *19*, 221-230.

8. Koch, R.; Brock, T. D.; Fred, E. B. The etiology of tuberculosis. *Rev. Infect. Dis.* **1982**, *4,* 1270-1274.

9. Koch, R. Weitere mitteilungen uber ein heilmittel gegen tuberculose. *Dtsch. Med. Wschr.* **1891**, *17*, 101-2.

10. von Pirquet, C. Frequency of tuberculosis in childhood. *J. Am. Med. Assoc.* **1909**, *52*, 675-8.

11. Sakula, A. BCG: Who were Calmette and Guérin? *Thorax* **1983**, *38*, 806-12.

12. Calmette A. On preventive vaccination of the new-born against tuberculosis by B.C.G. *Br. J. Tuberc.* **1928**, *22*, 161-165.

13. Lehmann, J. Para-aminosalicylic acid in the treatment of tuberculosis. *Lancet* **1946,** *5*, 15.

14. O' Connor, J. A. Para-aminosalicylic acid in the treat of tuberculosis. *Postgrad. Med. J.* **1948**, *24*, 455-462.

15. Schatz, A.; Bugie, E.; Waksman, S. A. Streptomycin, a substance exhibiting antibiotic activity against gram-positive and gram-negative bacteria. *Proc. Exp. Biol. Med.* **1944**, *55*, 66-9.

16. Maggi, N.; Pasqualucci, C. R.; Ballota, R.; Sensi, P. Rifampicin: an orally active rifamycin. *Chemotherapy* **1966**, *11*, 285-292.

17. Saltini, C. Chemotherapy and diagnosis of tuberculosis. *Respir. Med.* **2006**,

100, 2085-2097.

18. Iseman, M. D. Tuberculosis therapy: past, present and future. *Eur. Respir. J.* **2002, *20*, 87s-94s.**

19. Gandhi, N. R.; Moll, A.; Sturm, A. W.; Pawinski, R.; Govender, T. Lalloo, U.; Zeller, K.; Andrews, J.; Friedland, G. Extensively drug-resistant tuberculosis as a cause of death in patients co-infected with tuberculosis and HIV in a rural area of South Africa. *Lancet* **2006**, *368*, 1575-1580.

20. Migliori, G. B.; De Iaco, G.; Besozzi, G.; Centis, R.; Cirillo, D. M. First tuberculosis cases in Italy resistant to all tested drugs. *Eurosurveillance* **2007**, *12*, 3194.

21. World Health Organization End TB Strategy http://www.who.int/tb/post2015_strategy/en/ (accessed February 28, 2015).

22. Golden P. M.; Vikram, R. H. Extrapulmonary tuberculosis: an overview. *Am. Fam. Physician* **2005**, *72*, 1761-1768.

23. Lawn, S. D. Zumla, A. I. Tuberculosis. *Lancet* **2011**, *378*, 57-72.

24. Cole, E. C.; Cook, C. E. Characterization of infectious aerosols in health care facilities: an aid to effective engineering controls and preventative strategies. *Am. J. Infect. Control* **1998**, *26*, 453-464.

25. Nicas, M.; Nazaroff, W.; Hubbard A. Toward understanding the risk of secondary airborne infection. *J. Occup. Environ. Hyg.* **2005**, *2*, 143-154.

26. Riley, R. L.; Mills, C. C.; O'Grady, F.; Sultan, L.; Wittstadt, F. Shivpuri, D. N. Infectiousness of air from a tuberculosis ward. Ultraviolet irradiation of infected air: comparative infectiousness of different patients. *Am. Rev. Respir. Dis.* **1962**, *85*, 511-525.

27. World Health Organization Global Tuberculosis Report 2014. http://www.who.int/tb/publications/global_report/en/ (accessed March 7, 2015).

28. World Health Organization Global Tuberculosis Report 2013. http://www.who.int/tb/publications/global_report/en/ (accessed March 2, 2014).

29. Médecins Sans Frontières Factsheet on Tuberculosis. http://www.msfaccess.org/content/msf-factsheet-tuberculosis (accessed March 2, 2014).

30. Tiermersma, E. W.; van der Werf, M. J.; Borgdorff, M. W.; Williams B. G.; Nagelkerke N. J. D. Natural history of tuberculosis: duration and fatality of untreated pulmonary tuberculosis in HIV-negative patients: a systematic review. *PLoS One* **2011**, *6*, e17601.

31. World Health Organization Global Tuberculosis Report 2012.

http://www.who.int/tb/publications/global_report/en/ (accessed January 15, 2013).

32. World Health Organization Global Tuberculosis Report 2011. http://www.who.int/tb/publications/global_report/2011/en/ (accessed March 2, 2014).

33. Hill, A. N.; Becerra, J.; Castro, K. G. Modelling tuberculosis trends in the USA. *Epideiol. Infect.* **2012**, *140*, 1862-1872.

34. Surveillance Report: Tuberculosis Surveillance and Monitoring in Europe 2012 Geneva: World Health Organization http://ecdc.europa.eu/en/publications/Publications/1203-Annual-TB-Report.pdf (accessed March 22, 2014).

35. Abubakar, I.; Lipman, M.; Anderson, C.; Davies, P.; Zumla, A. Tuberculosis in the UK— time to regain control. *Brit. Med. J.* **2011**, *343*, d4281.

36. World Health Organization Antimicrobial Resistance Report 2013 http://www.who.int/mediacentre/factsheets/fs194/en/ (accessed March 2, 2014).

37. World Health Organization Multidrug-resistant TB 2013 Update. http://www.who.int/tb/publications/factsheets/en/ (accessed March 2, 2014).

38. World Health Organization 2006 Press Release: "WHO Global Task Force outlines measures to combat XDR-TB worldwide" http://www.who.int/mediacentre/news/notes/2006/np29/en/ (accessed March 22, 2014).

39. Velayati, A.; Masjedi, M. R.; Farnia, P.; Tabarsi, P.; Ghanavi, J.; Ziazarifi, A. H.; Hoffner, S. E. Emergence of new forms of totally drug-Rresistant tuberculosis bacilli. Super extensively drug-resistant tuberculosis or totally drug-resistant strains in Iran. *Chest* **2009**, *136*, 420.

40. Udwadia, Z. F.; Amala, R. A.; Ajbani, K. K.; Rodrigues, C. Totally drug-resistant tuberculosis in India. *Clin. Infect. Dis.* **2012**, *54*, 579.

41. World Health Organization HIV-Associated TB Facts 2014 http://www.who.int/tb/challenges/hiv (accessed March 2, 2015).

42. World Health Organization. Treatment of tuberculosis guidelines 4th Ed. (WHO, 2010). http://www.who.int/tb/publications/2010/9789241547833/en/ (accessed March 7, 2015).

43. Old and new TB drugs: mechanisms of action and resistance http://cdn.intechopen.com/pdfs-wm/28840.pdf (accessed March 10, 2015).

44. Countdown to 2015, World Health Organization Global Tuberculosis Report 2013 Supplement. http://www.who.int/tb/publications/global_report/en/ (accessed March 2, 2014).

45. David, H. L. Probability distribution of drug-resistant mutants in unselected populations of *Mycobacterium tuberculosis*. *Applied Microbiol.* **1970**, *20*, 810-814.

46. Jain, S. K.; Lamichhane, G.; Nimmagadda, S.; Pomper, M. G.; Bishai, W. R. Antibiotic treatment of tuberculosis: old problems, new solutions. *Microbe* **2008**, *3*, 285-292.

47. Houben, E. N.; Nguyen, L.; Pieters, J. Interaction of pathogenic mycobacteria with the host immune system. *Curr. Opin. Microbiol.* **2006**, *9*, 76-85.

48. Lazarevic. V.; Nolt, D.; Flynn, J. L. Long term control of *Mycobacterium tuberculosis* infection is mediated by dynamic immune responses. *J. Immunol.* **2005**, *175*, 1107-1117.

49. Kumar, V.; Abbas, A. K.; Fausto, N.; Mitchell, R. N. *Robbins Basic Pathology*, 8th Edition; Saunders Elsevier: Philadelphia, PA, 2007; 516-522.

50. Gengenbacher, M.; Kaufman, S. H. E. *Mycobacterium tuberculosis*: success through dormancy. *FEMS Microbiol. Rev.* **2012**, *514-532.*

51. Transmission and Pathogenesis of Tuberculosis. Figure adapted from http://www.cdc.gov/tb/education/corecurr/pdf/chapter2.pdf (accessed March 4, 2015).

52 Vergne, I.; Singh, S.; Roberts, E.; Kyei, G.; Master, S.; Harris, J.; de Haro, S.; Naylor, J.; Davis, A.; Delgado, M.; Deretic, V. Autophagy in immune defense against *Mycobacterium tuberculosis. Autophagy.* **2006**, *2*, 175-8.

53. Huynh, K. K.; Grinstein, S. Regulation of vacuolar pH and its modulation by some microbial species. *Microbiol. Mol. Biol. Rev.* **2007**, *71*, 452-462.

54. Fang, F. C. Antimicrobial reactive oxygen and nitrogen species: concepts and controversies. *Nat. Rev. Microbiol.* **2004**, 2, 820-832.

55. Jordao, L.; Bleck, C. K.; Mayorga, L.; Griffiths, G.; Anes, E. On the killing of mycobacteria by macrophages. *Cell. Microbiol.* **2008**, *10*, 529-548.

56. Ehlers, S.; Schaible, U. E. The granuloma in tuberculosis: dynamics of a host-pathogen collusion. *Front. Immunol.* **2013**, *3*, 411.

57. Stenger, S.; Hanson, A.; Teitelbaum, R.; Dewan, P.; Niazi, K. R.; Froelich, C. J.; Ganz, T.; Thoma-Uszynski, T.; Melian, A.; Bogdan, C.; Porcelli, S. A.; Bloom, B. R.; Krensky, A. M.; Modlin, R. L. An antimicrobial activity of cytolytic T Cells mediated by granulysin. *Science* **1988**, *282*, 121-125.

58. Woodworth, J. S.; Wu, Y.; Behar, S. M. *Mycobacterium tuberculosis*-specific CD8 T cells require perforin to kill target cells and provide protection *in vivo*. *J. Immunol.* **2008**, *181*, 8595-8603.

59. Castillo, E. F.; Dekonenko, A.; Arko-Mensah, J.; Mandell, M. A.; Dupont, N.; Jiang, S. Delgado-Vargas, M.; Timmins, G. S.; Bhattacharya, D.; Yang, H.; Hutt, J. Lyons, C. R.; Dobos, K. M.; Deretic, V. Autophagy protects against active tuberculosis by suppressing bacterial burden and inflammation. *Proc. Nat. Acad. Sci.* **2012**, *109*, E3168-E3176.

60. Purdy, G. E.; Russell, D. G. Lysosomal ubiquitin and the demise of *Mycobacterium tuberculosis*. *Cell Microbiol.* **2007**, *9*, 2768-2774.

61. Russell, D. G.; Mwandumba, H. C.; Rhoades, E. E. *Mycobacterium* and the coat of many lipids. *J. Cell Biol.* **2002,** *158*, 421-426.

62. Manca, C.; Paul, S.; Barry, C. E.; Freedman, V. H.; Kaplan, G. *Mycobacterium tuberculosis* catalase and peroxidase activities and resistance to oxidative killing in human monocytes in vitro. *Infect. Immun.* **1999**, *67*, 74-79.

63. Yu, K.; Mitchell, C.; Xing, Y.; Magliozzo, R. S.; Bloom, B. R.; Chan, J. Toxicity of nitrogen oxides and related oxidants on mycobacteria: *M. tuberculosis* is resistant to peroxynitrite anion. *Tubercle Lung Dis.* **1999**, *79*, 191-198.

64. Vergne, I.; Chua, J.; Singh, S. B.; Deretic, V. Cell biology of *Mycobacterium tuberculosis* phagosome, *Ann. Rev. Cell Dev. Biol.* **2004**, *20,* 367-394.

65. van der Wel, N.; Hava, D.; Houben D.; Fluitsma, D.; van Zon, M.; Pierson, J.; Brenner, M.; Peters, P. J. *M. tuberculosis* and *M. leprae* translocate from the phagolysosome to the cytosol in myeloid cells. *Cell* **2007**, *129*, 1287-1298.

66. Chen, M.; Gan, H.; Remold, H. G. A mechanism of virulence: virulent *Mycobacterium tuberculosis* strain H37Rv, but not attenuated H37Ra, causes significant mitochondrial inner membrane disruption in macrophages leading to necrosis. *J. Immunol.* **2006**, *176*, 3707-3716.

67. Flynn, J. L.; Chan, J. Tuberculosis: latency and reactivation. *Infect. Immun.* **2001**, *69*, 4195-4201.

68. Zumla, A.; Raviglione, M.; Hafner, R.; von Reyn, C. F. Tuberculosis. *N. Engl. J. Med.* **2013**, *368*, 745-755.

69. Lin P. L.; Flynn, J. L. Understanding latent tuberculosis: a moving target. *J. Immunol.* **2010**, *185*, 15-22.

70. Betts, J. C.; , Lukey, P. T.; Robb, L. C.; McAdam, R. A.; Duncan, K. Evaluation of a nutrient starvation model of *Mycobacterium tuberculosis* persistence by gene and protein expression profiling. *Mol. Microbiol.* **2002**, *43*, 717-731.

71. Xie, Z.; Siddiqi, N.; Rubin, E. J. Differential antibiotic susceptibilities of starved *Mycobacterium tuberculosis* isolates. *Antimicrob. Agents Chemother.* **2005**, *49,* 4778-4780.

72. Gengenbacher, M.; Kaufmann, S. H. E. *Mycobacterium tuberculosis*: success

through dormancy. *FEMS Microbiol. Rev.* **2012**, *36*, 514-532.

73. Islam, M. S.; Richards, J. P.; Ojha, A. K. Targeting drug tolerance in mycobacteria: a perspective from mycobacterial biofilms. *Expert Rev. Anti Infect. Ther.* **2012**, *10*, 1055-1066.

74. Hall-Stoodley, L.; Brun, O. S.; Polshyna, G.; Barker, L. P. *Mycobacterium marinum* biofilm formation reveals cording morphology. *FEMS Microbiol. Lett.* **2006**, *257*, 43-49.

75. Recht, J.; Kolter, R. Glycopeptidolipid acetylation affects sliding motility and biofilm formation in *Mycobacterium smegmatis*. *J. Bacteriol.* **2001,** *183*, 5718-5724.

76. Ojha, A. K.; Baughn, A. D.; Sambandan, D.; Hsu, T.; Trivelli, X.; Guerardel, Y.; Alahari, A.; Kremer, L.; Jacobs, W. R. Jr.; Hatfull, G. F. Growth of *Mycobacterium tuberculosis* biofilms containing free mycolic acids and harbouring drug-tolerant bacteria. *Mol Microbiol.* **2008**, *69*, 164-174.

77. Lenaerts, A. J.; Hoff, D.; Aly, S.; Andries, K.; Cantarero, L.; Andries, K.; Orme, I. M.; Basaraba, R. J. Location of persisting mycobacteria in a Guinea pig model of tuberculosis revealed by r207910. *Antimicrob. Agents. Chemother.* **2007**, *51*, 3338-3345.

78. Alteri, C. J.; Xicohténcatl-Cortes, J.; Hess, S.; Caballero-Olín, G.; Girón, J. A.; Friedman, R. L. *Mycobacterium tuberculosis* produces pili during human infection. *Proc. Nat. Acad. Sci.* **2007**, *104*, 5145-5150.

79. Bacon, J.; Alderwick, L. J.; Allnutt, J. A.; Gabasova, E.; Watson, R.; Hatch, K. A; Clark, S. O.; Jeeves, R. E.; Marriott, A.; Rayner, E.; Tolley, H.; Pearson, G.; Hall, G.; Besra, G. S.; Wernisch, L.; Williams, A.; Marsh, P. D. Nonreplicating *Mycobacterium tuberculosis* elicits a reduced infectivity profile with corresponding modifications to the cell wall and extracellular matrix *PLoS ONE* 2014, *9*, e87329.

80. Sambandan, D.; N. Dao, D. N.; Weinrick, B. C.; Vilchèze, C.; Gurcha, S. S.; Ojha, A.; Kremer, L.; Besra, G. S.; Hatfull, G. F.; Jacobs, W. R. Keto-mycolic acid-dependent pellicle formation confers tolerance to drug-sensitive *Mycobacterium tuberculosis*. *MBio.* **2013**, *4*, e00213-e00222.

81. Ewer, K.; Millington, K. A.; Deeks, J. J.; Alvarez, L.; Bryant, G.; Lalvani, A. Dynamic antigen-specific T cell responses after point source exposure to *Mycobacterium tuberculosis*. *Am. J. Respir. Crit. Care Med.* **2006**, *174*, 831-839.

82. Russell, D. G. *Mycobacterium tuberculosis*: here today, and here tomorrow. *Nat. Rev. Mol. Cell Biol.* ***2001,*** *2*, 569-577.

83. Harris, J.; Keane, J. How tumor necrosis factor blockers interfere with tuberculosis immunity. *Clin. Exp. Immunol.* 2010, *161*, 1-9.

84. Clay, H.; Volkman, H. E.; Ramakrishnan, L. Tumor necrosis factor signaling mediates resistance to mycobacteria by inhibiting bacterial growth and macrophage death. *Immunity* 2008, *29*, 283-294.

85. Bruns, H.; Meinken, C.; Schauenberg, P.; Härter, G.; Kern, P.; Modlin, R. L.; Antoni, C.; Stenger, S. Anti-TNF immunotherapy reduces $CD8^+$ T cell-mediated antimicrobial activity against *Mycobacterium tuberculosis* in humans. *J. Clin. Invest.* 2009, *119*, 1167-1177.

86. Barry, C. L.; Boshoff, H. I.; Dartois, V.; Dick, T.; Ehrt, S.; Flynn, Schnappinger, D.; Wilkinson, R. J.; Young, D. The spectrum of latent tuberculosis: rethinking the biology and intervention strategies. *Nat. Rev. Microbiol.* **2009**, *7*, 845-855.

87. Selwyn, P. A.; Alcabes, P.; Hartel, D.; Buono, D., Schoenbaum, E. E.; Klein, R. S.; Davenny, K.; Friedland, G. Clinical manifestations and predictors of disease progression in drug users with human immunodefficiency virus infection. *N. Engl. J. Med.* **2009**, *327*, 1697-1703.

88. Kwan, C. K.; Ernst, J. D. HIV and tuberculosis: a deadly human syndemic. *Clin. Microbiol. Rev.* **2011**, *24*, 351-376.

89. Geldmacher, C.; Ngwenyama, N.; Schuetz, A.; Petrovas, C.; Reither, K.; Heeregrave, E. J.; Casazza, J. P.; Ambrozak, D. R.; Louder, M.; Ampofo, W.; Pollakis, G.; Hill, B.; Sanga, E.; Saathoff, E.; Maboko, L.; Roederer, M.; Paxton, W. A.; Hoelscher, M.; Koup, R. A. Preferential infection and depletion of *Mycobacterium tuberculosis*-specific CD4 T cells after HIV-1 infection. *J. Exp. Med.* **2010**, *207*, 2869-2881.

90. Serbina, N. V.; Lazarevic, V.; Flynn, J. L. CD4+ T cells are required for the development of cytotoxic CD8+ T cells during *M. tuberculosis* infection. *J. Immunol.* **2001**, *167*,6991-7000.

91. Cowley, S. C.; Elkins, K. L. CD4+ T cells mediate IFN-γ indepen dent control of *Mycobacterium tuberculosis* infection both *in vitro* and *in vivo*. *J. Immunol.* **2003**, *171*, 4689-4699.

92. Daley, C. L.; Small, P. M.; Schecter, G. F. Schoolnik, G, K.; McAdam, R. A.; Jacobs, W. R. Jr.; Hopewell, P. C. An outbreak of tuberculosis with accelerated progression among persons infected with human immunodeficiency virus. An analysis using restriction fragment-length polymorphism. *N. Engl. J. Med.* **1992**, *326*, 231-235.

93. Wolday, D.; Hailu, B.; Girma, M.; Hailu, E.; Sanders, E.; Fontanet, A. L. Low CD4+ T-cell count and high HIV viral load precede the development of tuberculosis disease in a cohort of HIV-positive Ethiopians. *Int. J. Tuberc. Lung. Dis.* **2003**, *7*, 110-116.

94. Corbett, E. L.; Bandason, T,; Cheung, Y. B.; Makamure, B.; Dauya, E.; Munyati, S. S.; Churchyard, G. J.; Williams, B. G.; Butterworth, A. E.;

Mungofa, S.; Hayes, R. J.; Mason, P. R. Prevalent infectious tuberculosis in Harare, Zimbabwe: burden, risk factors and implications for control. *Int. J. Tuberc. Lung. Dis.* **2009**, *13*, 1231-1237.

95. Andrews. J. R. Noubary. F.; Walensky, R. P.; Cerda, R.; Losina, E.; Horsburgh, C. R. Risk of progression to active tuberculosis following reinfection with *Mycobacterium tuberculosis*. *Clin. Infect. Dis.* **2012**, *54*, 784-191.

96. Verver, S. Robin M. Warren, Nulda Beyers, Madalene Richardson, Gian D. van der Spuy, Martien W. Borgdorff, Donald A. Enarson, Marcel A. Behr, Paul D. van Helden. Rate of reinfection of tuberculosis after successful treatment is higher than rate of new tuberculosis. *Am. J. Respir. Crit. Care Med.* **2005** *171*, 1430-1435.

97. Chaisson, R. E.; Churchyard, G. J. Recurrent tuberculosis: relapse, reinfection, and HIV. *J. Infect. Dis.* **2010**, *201*, 653-655.

98. de Steenwinkela, J. E. M.; de Knegta, G. J.; ten Kate, M. T.; Verbrugha, H. A.; Hernandez-Pandob, R.; Leenen, P. J. M.; Bakker-Woudenberga, I. A. J. M. Relapse of tuberculosis versus primary tuberculosis; course, pathogenesis and therapy in mice. *Tuberculosis* **2013**, *93*, 213-221.

99. Crampin, A.C.; Mwaungulu, J. N.; Mwaungulu, F. D.; Mwafulirwa, D. T.; Munthali, K.; Floyd, S.; Fine, P. E.; Glynn, J. R. Recurrent TB: relapse or reinfection? The effect of HIV in a general population cohort in Malawi. ***AIDS*** **2010**, *24*, 417-26.

100. Orme, I. M. A new unifying theory of the pathogenesis of tuberculosis. *Tuberculosis* **2014**, *94*, 8-14.

101. Basaraba, R. J. Experimental tuberculosis: the role of comparative pathology in the discovery of improved tuberculosis treatment strategies. *Tuberculosis* **2008**, *88*. S35-S47.

102. Selvakumar, N.; Kumar, V.; Balaji, S.; Prabuseenivasan, S.; Radhakrishnan, R.; Sekar, G.; Chandrasekaran, V.; Kannan, T.; Thomas, A.; Arunagiri, S.; Dewan, P.; Swaminathan, S. High rates of ofloxacin resistance in *Mycobacterium tuberculosis* among both new and previously treated patients in Tamil Nadu, South India. *PLoS One*. **2010**, *10*, e0117421.

103. Zhang, Y.; Yew, W. W. Mechanisms of drug resistance in *Mycobacterium tuberculosis*. *Int. J. Tuberc. Lung Dis.* **2009**, *11,* 1320-30.

104. Zainuddin, Z. F., and J. W. Dale. Does *Mycobacterium tuberculosis* have plasmids? *Tubercle* **1990**, *71*, 43-49.

105. Adapted from reference 103

106. Smith, T.; Wolff, K. A.; Nguyen, L. Molecular biology of drug resistance in *Mycobacterium tuberculosis*. *Curr. Top Microbiol. Immunol.* **2013**, *374*, 53-80.

107. Kohanski, M. A.; DePristo, M. A.; Collins, J. J. Sublethal antibiotic treatment leads to multidrug resistance *via* radical-induced mutagenesis. *Mol. Cell* **2010**, *37*, 311-20.

108. Chambers, H. F.; Moreau, D.; Yajko, D.; Miick, C.; Wagner, C.; Hackbarth, C.; Kocagöz, S.; Rosenberg, E.; Hadley, W. K.; Nikaido, H. Can penicillins and other beta-lactam antibiotics be used to treat tuberculosis? *Antimicrob. Agents Chemother.* **1995**, *39*, 2620-2624.

109. Zaunbrecher, M. A.; Sikes, R. D. Jr.; Metchock, B.; Shinnick, T. M.; Posey, J. E. Overexpression of the chromosomally encoded aminoglycoside acetyltransferase eis confers kanamycin resistance in *Mycobacterium tuberculosis*. *Proc. Nat. Acad. Sci.* **2009**, *106*, 20004-20009.

110. Quinting, B.; Reyrat, J. M.; Monnaie, D.; Amicosante, G.; Pelicic, V.; Gicquel, B.; Frère, J. M.; Galleni, M. Contribution of beta-lactamase production to the resistance of mycobacteria to beta-lactam antibiotics. *FEBS Lett.* **1997**, *406*, 275-278.

111. Madsen, C. T.; Jakobsen, L.; Buriankova, K.; Doucet-Populaire, F.; Pernodet, J. L.; Douthwaite, S.; Methyltransferase Erm(37) slips on rRNA to confer atypical resistance in *Mycobacterium tuberculosis*. *J. Biol. Chem.* **2005**, *280*, 38942-38947.

112. Buriankova, K.; Doucet-Populaire, F.; Dorson, O.; Gondran, A.; Ghnassia, J. C.; Weiser, J.; Pernodet, J. L. Molecular basis of intrinsic macrolide resistance in the *Mycobacterium tuberculosis* complex. *Antimicrob. Agents Chemother.* **2004**, *48*, 143-150.

113. Ferber, D. Biochemistry. Protein that mimics DNA helps tuberculosis bacteria resist antibiotics. *Science*. **2005**, *308,* 1393.

114. Adams, K. N.; Takaki, K. Connolly, L. E.; Wiedenhoft, H.; Winglee, K.; Humbert, O.; Edelstein, P. H.; Cosma, C. L.; Ramakrishnan, L.; Drug tolerance in replicating mycobacteria mediated by a macrophage-induced efflux mechanism. *Cell* 2011, *145*, 39-53.

115. Panel on Antiretroviral Guidelines for Adults and Adolescents. Guidelines for the use of antiretroviral agents in HIV-1-infected adults and adolescents. Department of Health and Human Services. http://aidsinfo.nih.gov/contentfiles/lvguidelines/adultandadolescentgl.pdf (accessed March 8, 2015).

116. Kwara, A.; Flanigan, T. P.; Carter E. J. Highly active antiretroviral therapy (HAART) in adults with tuberculosis: current status. *Int. J. Tuberc. Lung Dis.* 2005, *9*, 248-257

117. Rathbun, R. C.; Liedtke, M. D. Antiretroviral drug interactions: overview of interactions involving new and investigational agents and the role of

therapeutic drug monitoring for management. *Pharmaceutics* **2011**,*3*, 745-781.

118. Lopéz-Cortés, L. F.; Ruiz-Valderas, R.; Viciana, P.; Alarcón-González, A.; Gómez-Mateos, J.; León-Jimenez, E.; Sarasanacenta, M.; López-Pua, Y.; Pachón, J. Pharmacokinetic interactions between efavirenz and rifampin in HIV-infected patients with tuberculosis. *Clin. Pharmacokinet.* **2002**, *41*, 681-690.

119. Ribera, E.; Pou, L.; Lopez, R. M.; Crespo, M.; Falco, V.; Ocaña, I.; Ruiz, I.; Pahissa, A. Pharmacokinetic interaction between nevirapine and rifampicin in HIV-infected patients with tuberculosis. *AIDS* **2001**, *28*, 450-453.

120. Burman, W. J.; Jones, B. E. Treatment of HIV-related tuberculosis in the era of effective antiretroviral therapy. *Am. J. Respir. Crit. Care Med.* **2001**, *164*, 7-12.

121. American Thoracic Society Documents. American Thoracic Society/Centers of Disease Control and Prevention/Infectious Diseases Society of America. Treatment of tuberculosis. *Am. J. Respir. Crit. Care Med.* **2003**, *167*, 603-662.

122. Zumla, A.; Nahid, P.; Cole, S. T. Advances in the development of new tuberculosis drugs and treatment regimens. *Nat. Rev. Drug Disc.* **2013**, *12*, 388-404.

123. TB alliance: global alliance for TB drug development http://www.tballiance.org/downloads/Pipeline/TBA%20Pipeline%20Q1%202015(2).pdf (accessed March 4, 2015).

124. Working group on new TB drugs— discovery portfolio drug pipeline. http://www.newtbdrugs.org/pipeline.php (accessed March 4, 2015).

125. Ma, Z.; Lienhardt, C.; McIlleron, H.; Nunn, A. J.; Wang, X. Global tuberculosis drug development pipeline: the need and the reality. *Lancet* **2010** *375*, 2100-2109 .

126. Sterling, T. R.; Villarino, M. E.; Borisov, A. S.; Shang, N.; Gordin, F.; Bliven-Sizemore, E.; Hackman, J.; Hamilton, C. D.; Menzies, D.; Kerrigan, A.; Weis, S. E.; Weiner, M.; Wing, D.; Conde, M. B.; Bozeman, L.; Horsburgh, C. R. Jr.; Chaisson, R. E.; TB trials consortium PREVENT TB study team. Three months of rifapentine and isoniazid for latent tuberculosis infection. *N. Engl. J. Med.* 2011, *365*, 2155-2166.

127. Lee, M.; Lee, J.; Carroll, M. W.; Choi, H.; Min, S.; Song, T.; Via, L. E.; Goldfeder, L. C.; Kang, E.; Jin, B.; Park, H.; Kwak, H.; Kim, H.; Jeon, H. S.; Jeong, I.; Joh, J. S.; Chen, R. Y.; Olivier, K. N.; Shaw, P. A.; Follmann, D.; Song, S. D.; Lee, J. K.; Lee, D.; Kim, C. T.; Dartois, V.; Park, S. K.; Cho, S. N.; Barry, C. E. 3rd. Linezolid for treatment of chronic extensively drug-resistant tuberculosis. *N. Engl. J. Med.* 2012, *367*, 1508-1518.

128. Hugonnet, J. E.; Tremblay, L. W.; Boshoff, H. I.; Barry, C. E. 3rd;

Blanchard, J. S. Meropenem-clavulanate is effective against extensively drug-resistant *Mycobacterium tuberculosis*. *Science* 2009, *323*, 1215-1218.

129. 2014 Pipeline report: tuberculosis drug development hobbles forward. http://www.pipelinereport.org/sites/g/files/g575521/f/201407/TB%20Treatment.pdf (accessed March 4, 2015).

130. Andries, K.; Verhasselt. P; Guillemont, J.; Göhlmann, H. W.; Neefs, J. M,; Winkler, H.; Van, Gestel, J.; Timmerman, P.; Zhu, M.; Lee, E.; Williams, P.; de Chaffoy, D.; Huitric, E.; Hoffner, S.; Cambau, E.; Truffot-Pernot, C.; Lounis, N.; Jarlier, V. A diarylquinoline drug active on the ATP synthase of *Mycobacterium tuberculosis*. *Science* **2005**, *307*, 223-227.

131. Food and Drug Administration (U.S.) (Press Release). FDA approves first drug to treat multidrug-resistant tuberculosis. 31 December 2012. www.fda.gov/NewsEvents/Newsroom/ PressAnnouncements/ucm333695.htm (accessed March 4, 2015).

132. Mahajan, R. Bedaquiline: First FDA-approved tuberculosis drug in 40 years. *Int. J. Appl. Basic Med. Res.* 2013, *3*, 1-2.

133. Matsumoto, M.; Hashizume, H.; Tomishige, T.; Kawasaki, M.; Tsubouchi, H.; Sasaki, H.; Shimokawa, Y.; Komatsu, M. OPC-67683, a nitro-dihydro-imidazooxazole derivative with promising action against tuberculosis in vitro and in mice. *PLoS Med.* 2006, *3*, e466.

134. European Medicines Agency. Questions and answers: Positive opinion on the marketing authorisation for Deltyba (delamanid)– Outcome of re-examination. 22 November 2013. http://www.ema.europa.eu/docs/en_GB/document_library/Medicine_QA/human/002552/ WC500155462.pdf (accessed March 4, 2015).

135. Tahlan, K.; Wilson, R.; Kastrinsky, D. B.; Arora, K.; Nair, V.; Fischer, E.; Barnes, S. W.; Walker, J. R.; Alland, D.; Barry, C. E. 3rd; Boshoff, H. I. SQ109 targets MmpL3, a membrane transporter of trehalose monomycolate involved in mycolic acid donation to the cell wall core of *Mycobacterium tuberculosis*. *Antimicrob. Agents Chemother.* 2012, *56*, 1797-1809.

136. Makarov, V.; Lechartier, B.; Zhang, M.; Neres, J.; Sar, A. M.; Raadsen, S. A.; Hartkoorn, R. C.; Ryabova, O. B.; Vocat, A.; Decosterd, L. A.; Widmer, N.; Buclin, T.; Bitter, W.; Andries, K.; Pojer, F.; Dyson, P. J.; Cole, S. T. Towards a new combination therapy for tuberculosis with next generation benzothiazinones. *EMBO Mol. Med.* **2014**, *6*, 372-383

137. Zumla, A. I.; Gillespie, S. H.; Hoelscher, M.; Phillips, P. P. J.; Cole, S. T.; Abubakar, I.; McHugh, T. D.; Shito, M.; Maeurer, M.; Nunn, A. J. New anti-tuberculosis drugs, regimens, and adjunct therapies: needs, advances, and future prospects. *Lancet Infect. Dis.* **2014**, *14*, 327-340.

138. Davies, J. Where have all the antibiotics gone? *Can. J. Infect. Dis. Med. Microbiol.* **2006**, *17*, 287-290.

139. Fischbach, M. A.; Walsh, C. T. Antibiotics for emerging pathogens. *Science*, **2009**, *325*, 1089-1093.

140. Walsh, C. Where will new antibiotics come from? *Nat. Rev. Microbiol.* **2003**, *1*, 65-70.

141. DeBoer, C.; Caron, E. L.; Hinman, J. W. Amicetin, a new *Streptomyces* antibiotic. *J. Am. Chem. Soc.* **1953,** *75*, 499-500.

142. Hinman, J. W.; Caron, E. L.; DeBoer, C. The isolation and purification of amicetin. *J. Am. Chem. Soc.* **1953**, *75*, 5864-5866.

143. McCormick, M. H.; Hoehn, M. M. Isolation of a new antibiotic from *Streptomyces fasciculatis* nov. sp. *Antibiot. Chemother.* **1953**, *3*, 718-720.

144. Hinuma, Y.; Kuroya, M.; Yajima, T.; Ishihara, K.; Hamada, S.; Watanabe, K.; Kuchi, K. Antibiotic substances from actinomycetes. XXXVI. An amicetin (sacromycin) from *Streptomyces* sp. No. 5223. *J. Antibiot.* **1955**, *8A*, 148-152.

145. Haskell, T. H.; Ryder, A.; Frohardt, E. P.; Fusari, S. A.; Jakubowski, Z. L.; Bartz, Q. R. Isolation and characterization of three crystalline antibiotics from *Streptomyces plicatus*. *J. Am. Chem. Soc.* **1958**, *80*, 743-747.

146. Tatsuoka, S.; Nakazawa, K.; Inoue, M.; Fujii, S. Antibiotics. V. Extraction and physicochemical properties of allomycin, an antituberculous antibiotic, and its identity with amicetin. *Yakugaku Zasshi* **1955**, *75*, 1206-1208.

147. Stevens, C. L.; Gasser, R. J.; Mukherjee, T. K.; Haskell, T. H. The structure of amicetin. A new dimethylamino sugar. *J. Am. Chem. Soc.* **1956**, *78*, 6212.

148. Stevens, C. L.; Nagarajan, K.; Haskell, T. H. The structure of amicetin. *J. Org. Chem.* **1962**, *27*, 2991, 3007.

149. Flynn, E. H.; Hinman, J. W.; Caron, E. L.; Woolf, D. O. The chemistry of amicetin, a new antibiotic. *J. Am. Chem. Soc.* **1953**, *78*, 5867-5871.

150. Stevens, C. L.; Blumbergs, P.; Daniher, F. A. Stereochemistry and synthesis of amosamine:4,6-dideoxy-4-dimethylamino-D-glucose. *J. Am. Chem. Soc.* **1963**, *85*, 1552-1553.

151. Stevens, C. L.; Blumbergs, P.; Wood, D. L. Stereochemical identification and synthesis of amicetose and the stereochemical identification of rhodinose and the sugar from streptolydigin. *J. Am. Chem. Soc.* **1964**, *86*, 3592-3594.

152. Hanessian, S.; Haskell, T. Configuration of the anomeric linkages in amicetin. *Tetrahedron* **1964**, *35-36*, 2451-2460.

153. Smith, J. L.; Sundaralaingam, M. The Structure of the antibiotic amicetin consisting of nucleobase, disaccharide and amino acid moieties. *Acta Crystallogr., Sect. B: Struct. Crystallogr. Cryst. Chem.* **1981**, *B37*, 1095-1101.

154. Bu, Y. -Y.; Yamazaki, H.; Ukai, K.; Namikoshi, M. Anti-mycobacterial nucleoside antibiotics from a marine-derived *Streptomyces* sp. TPU1236A *Mar. Drugs* **2014**, *12*, 6102-6112.

155. Ennis, H. L. Mutants of *Escherichia coli* sensitive to antibiotics. *J. Bacteriol.* **1971**, *107*, 486-490.

156. Adapted from reference 141

157. Hoch, A.; Coutsogeorgopoulos, C. Inhibition of protein synthesis by amicetin, a nucleoside antibiotic. *Biochemistry* **1966**, *5*, 3345-3351.

158. Data not shown in reference 145.

159. Renis, H. E. *In vitro* antiviral acitivity of amicetin and its derivatives. *Antimicrob. Agents Chemother.* **1961-1970**, *1965*, 576-57.

160. Smith, C. G.; Lummin, W. L.; Grady, J. E. An improved tissue culture assay. II. Cytotoxicity studies with antibiotics, chemicals, and solvents. *Cancer Res.* **1959**, *19*, 847-852.

161. Burchenal, J. H.; Yuceoglu, M.; Dagg, M. K.; Stock, C. C. Leukemia. VI. Effect of amicetin on transplanted mouse leukemia. *Proc. Soc. Exp. Biol. Med.* **1954**, *86*, 891-893.

162. Tan, C. T.; Burchenal, J. H. Clinical studies with amicetin. *Antibiotic Med. Clin. Ther.* **1956**, *3*, 126-131.

163. Hinshaw, H. C.; Feldman, W. H. Streptomycin in treatment of clinical tuberculosis: a preliminary report. *Proc. Staff Meet. Mayo Clin.* **1945**, *20*, 313-318.

164. Fowler, E. P., Jr.; Feind, C. R. Toxicity of streptomycin for the auditory and vestibular mechanisms. *Am. Rev. Tuberc.* **1949**, *60*, 39-44.

165. Brock, T. D. Effect of antibiotics and inhibitors on M protein synthesis. *J. Bacteriol.* **1963**, *85*, 527-531.

166. Haskell, T. H.; Ryder, A. Frohardt, R.; Fusari, S. A.; Jakubowski, Z. L.; Bartz, Q. R. The isolation and characterization of three crystalline antibiotics from *Streptomyces plicatus. J. Am. Chem. Soc.* **1958**, *80*, 743-747.

167. Haskell, T. H. Amicetin, bamicetin, and plicacetin. chemical studies. *J. Am. Chem. Soc.* **1958**, *80*, 747-751.

168. Gu, Z.; Lovett, P. S. A gratuitous inducer of *cat*-86, amicetin, inhibits bacterial

peptidyl transferase. *J. Bacteriol.* **1995**, *177*, 3616-3618.

169. Cerna, J.; Rychlik, I.; Lichtenhaler, F. W. The effect of the aminoacyl-4-aminohexosyl-cytosine group of antibiotics on ribosomal peptidyl transferase. *FEBS Lett.* **1973**, *30*, 147-150

170. Konishi, M.; Minoru, K.; Tsukiura, H.; Yamamoto, H.; Hoshiya, T.; Miyaki, H.; Fujisawa, K.; Koshiyama, H.; Kawaguchi, H. Oxamicetin, a new antibiotic of bacterial origin. I. Production, isolation and properties. *J. Antibiot.* **1973**, *26*, 752-756.

171. Konishi, M.; Naruishi, M.; Tsuno, T.; Tsukiura, H.; Kawaguchi, H. Oxamicetin, a new antibiotic of bacterial origin. II. Structure of oxamicetin. *J. Antibiot.* **1973**, *26*, 757-764.

172. Adapted from reference 170

173. Itoh, J.; Miyadoh, S. SF2457, a new antibiotic related to amicetin. *J. Antibiot.* **1992**, *45*, 846-853.

174. Haneda, K.; Shinose, M.; Seino, A.; Tabata, N.; Tomoda, Hiroshi.; Iwai, Y.; Omura, S. Cytosaminomycins, new anticoccidial agents produced by *Streptomyces* sp. KO-8119. I. Taxonomy, production, isolation and physio-chemical and biological properties. *J. Antibiot.* **1994**, *47*, 774-781.

175. Adapted from reference 173

176. Shiomi, K.; Haneda, K.; Tomoda, H.; Uzuru, I.: Omura, S. Cytosaminomycins, new anticoccidial agents produced by *Streptomyces* Sp. KO-8119. II. Structure elucidation of cytosaminomycins A, B, C and D. *J. Antibiot.* **1994**, *47*, 782-786.

177. Shumard, R. F.; Callender, M. E. Monensin, a new biologically active compound. VI. Anticoccidial activity. *Antimicrob. Agents Chemother.* **1961-1970**, *1967*, 369-377.

178. Bedrnik, P.; Broz, J.; Sevcik, B.; Jurkovic, P. Efficiency and tolerance evaluation of anticoccidial salinomycin in broilers. *Arch. Gefluegelkd.* **1980**, *44*, 26-29.

179. Frigg, M.; Schramm, H. Comparative anticoccidial activity of lasalocid sodium (Avatec) in chicks: efficacy against european strains of coccidia. *Arch. Gefluegelkd.* **1977**, *41*, 31-34

180. Peek, H. W.; Landman, W. J. M. Resistance to anticoccidial drugs of dutch avian *Eimeria* sp. field isolates originating from 1996, 1999 and 2001. *Avian Pathol.* **2003**, *32*, 391-401.

181. Adapted from reference 174

182. Adapted from reference 174

183. Sensi, P.; Greco, A. M.; Gallo, G. G.; Rolland, G. Isolation and structure determination of a new amicetin-like antibiotic: amicetin B. *Antibiot. Chemother.* **1957**, *7*, 645-652.

184. Lichtenhaler, F. W.; Cerna, J.; Rychlik, I. The effect of oxamicetin and some amicetin analogs on ribosomal peptidyl transferase. *FEBS Lett.* **1975**, *53*, 184-187.

185. Evans, J. R.; Weare, G. Norplicacetin, a new antibiotic from *Streptomyces plicatus*. *J. Antibiot.* **1977**, *30*, 604-606.

186. Adapted from reference 185.

187. Yongle, C.; Zeeck, A.; Chen, Z.; Zahner, H. Studies on metabolites produced by *Streptomyces ramulosus* Tu-34. II. The structural elucidation of oxyplicacetin, a new amicetin. *Kangshengsu* **1985**, *10*, 285-295.

188. Adapted from reference 174.

189. Takeuchi, S.; Hirayama, K.; Ueda, K.; Sakai, H.; Yonehara, H. Blasticidin S, a new antibiotic. *J. Antibiot.* **1958**, *11A*, 1-5.

190. Fukunaga, K.; Misato, T.; Ishii, I.; Asakawa, M. Blasticidin, a new-antiphytopathogenic fungal substance. Part. I. *Bull. Agri. Chem. Soc.* **1955**, *19*, 181-188.

191. Sakuda, S.; Ono, M.; Ikeda, H.; Inagaki, Y.; Nakyama, J.; Suzuki, A.; Isogai, A. Structure of blasticidin A. *Tetrahedron Lett.* **1997**, *38*, 7399-7402.

192. Tanaka, N.; Sakagami, Y.; Nishimura, T.; Yamaki, H. Activity of cytomicin and blasticidin S against transplantable animal tumors. *J. Antibiot.* **1961**, *14A*, 123-126.

193. Cerna, J.; Rychlik, I.; Lichtenthaler, F. W. The effect of the aminoacyl-4-amino-hexosyl-cytosine group of antibiotics on ribosomal peptidyl transferase. *FEBS Lett.* **1973**, *30*, 147-150.

194. Petska, S. The use of inhibitors in studies on protein synthesis. *Methods Enzymol.* **1974**, *30*, 261-282.

195. Adapted from reference 189.

196. Adapted from reference 189.

197. Kalpaxis, D. L.; Theocharis, D. A.; Coutsogeoropolous, C. Kinetic studies on ribosomal peptidyltransferase. The behavior of the inhibitor blasticidin S. *Eur. J. Biochem.* **1986**, *154*, 267-271.

198. Lazaro, E.; Van den Broek, L. A.; San Felix, A.; Ottenheijm, H. C.; Ballesta, J. P. Biochemical and kinetic characteristics of the interaction of the antitumor antibiotic sparsomycin with prokaryotic and eukaryotic ribosomes. *Biochemistry* **1991**, *1991*, 9642-9648.

199. Kuwano, M.; Takena, K.; Ono, M. The cross-resistance of mouse blasticidin S-resistant cell lines to puromycin and sparsomycin, inhibitors of ribosome function. *Biochim. Biophys. Acta* **1979**, *563*, 479-489.

200. Hansen, J. L.; Moore, P. B.; Steitz, T. A. Structures of five antibiotics bound at the peptidyl transferase center of the large ribosomal subunit. *J. Mol. Bol.* **2003**, *330*, 1061-1075.

201 Svidritskiy, E.; Ling, C.; Ermolenko, D. N.; Korostelev, A. A. Blasticidin S inhibits translation by trapping deformed tRNA on the ribosome. *Proc. Nat. Acad. Sci.* **2013**, *110*, 12283-12288.

202. Theocharis, D. A.; Synetos, D.; Kalpaxis, D. L.; Drainas, D.; Coutsogeorgopoulos, C. Kinetics of inhibition of peptide bond formation on bacterial ribosomes. *Arch. Biochem. Biophys.* **1992**, *292*, 266-272.

203. Petropoulos, A. D.; Xaplanteri, M. A.; Dinos, G. P.; Wilson, D. N.; Kalpaxis, D. L. Polyamines affect diversely the antibiotic potency : insight gained from kinetic studies of the blasticidin S and spiramycin interactions with functional ribosomes. *J. Biol. Chem.* **2004**, *279*, 26518-26528.

204. Ermolenko, D. N.; Majumdar, Z. K.; Hickerson, R. P.; Spiegel, P. C.; Clegg, R. M.; Noler, H. F. Observation of intersubunit movement of the ribosome in solution using FRET. *J. Mol. Biol.* **2007**, *370*, 530-540.

205. Wilson, D. N. On the specificity of antibiotics targeting the large ribosomal subunit. *Ann. N. Y. Acad. Sci.* **2011**, *1241*, 1-16.

206. Kanzaki, T.; Higashide, E.; Yamamoto, H.; Shibata, M.; Nakazawa, K.; Iwasaki, H.; Takewaka, T.; Miyake, A. Gougerotin, a new antibacterial antibiotic. *J. Antibiot.* **1962**, *15A*, 93-97.

207. Murao, S.; Hayashi, H. Gougerotin, as a plant growth inhibitor, from *Streptomyces* sp. No. 179. *Agric. Biol. Chem.* **1983**, *47*, 1135-1136.

208. Xue, Y.; Wu, S.; Li, Y.; Zhang, S.; Zhen, Y. Antitumor acitivity of yungumycin. *Yaoxue Xuebao* **1996**, *31*, 171-175.

209. (a) Iwasaki, H. Studies on the structure of gougerotin. Properties of gougerotin. Yakugaku Zasshi 1962, 82, 1358-1561; (b) Components of gougerotin. *Yakugaku Zasshi* **1962**, *82*, 1361-1365; (c) Properties of substance C. *Yakugaku Zasshi* **1962**, *82*, 1365-1367; (d) Catalytic reduction of C substance. A new finding on the reduction of cytosine derivatives. *Yakugaku Zasshi* **1962**, *82*, 1368-1371; (e) Position of the side chain of C substance. *Yakugaku Zasshi* **1962**, *82*, 1372-1376; (f) Structure of the sugar moiety of C substance. (g).

Isolation of uronic acid. *Yakugaku Zasshi* **1962**, *82*, 1376-1380; (h) Structure of the sugar moiety of C substance. (i). Isolation of hyxoamine. *Yakugaku Zasshi* **1962**, *82*, 1380-1383; (j) Structure of the sugar moiety of C substance. (k). Position of amino group. *Yakugaku Zasshi* **1962**, *82*, 1384-1386; (l) The steric configuration of C substance. *Yakugaku Zasshi* **1962**, *82*, 1387-1390; (m) Structure of seryl-C substance. *Yakugaku Zasshi* **1962**, *82*, 1390-1392; (n) Structure of gougerotin. *Yakugaku Zasshi* **1962**, *82*, 1393-1395.

210. Fox, J.; Kuwada, Y.; Watanabe, K. A.; Ueda, To.; Whipple, E. B. Nucleosides. XXV. Chemistry of gougerotin. *Antimicrob. Agents Chemother.* **1961-1970**, *1965*, 518-519.

211. Fox, J. J.; Kuwada, Y.; Watanabe, K. A. Nucleosides LVI. On the structure of the nucleoside antibiotic, gougerotin. *Tetrahedron Lett.* **1968**, *57*, 6029-6032.

212. Clark, J. M. Jr.; Gunther, J. K. Gougerotin, a specific inhibitor of protein synthesis. *Biochim. Biophys. Acta, Spec. Sect. Nucleic Acids Relat. Subj.* **1963**, *76*, 636-638.

213. Sinohara, H.; Sky-Peck, H. H. Effect of gougeroutin on the protein synthesis in the mouse liver. *Biochem. Biophys. Res. Commun.* **1965**, *18*, 98-102.

214. Clark, J. M. Jr.; Chang, A. Y. Inhibitors of the transfer of amino acids from aminoacyl soluble ribonucleic acid to proteins. *J. Biol. Chem.* **1965**, *240*, 4734-4739.

215. Casjens, S. R.; Morris, A. J. The selective inhibition of protein assembly by gougerotin. *Biochim. Et. Biophys. Acta* **1965**, *108*, 677-686.

216. Adapted from reference 206.

217. Hamill, R.L.; Hoehn, M. M. Anthelmycin, a new antibiotic with anthelmintic properties. *J. Antibiot.* **1964**, *17*, 100-103.

218. Uchida, K.; Ichikawa, T.; Shimauchi, Y.; Ishikura, T.; Ozaki, A. Hikizimycin, a new antibiotic. *J. Antibiot.* **1971**, *24*, 259-262.

219. Nagarajan, R.; Nash, S. M. 9th International Symposium on the Chemistry of Natural Products (I.U.P.A.C.), Ottawa, **1974**

220. Das, B. C.; DeFaye, J.; Uchida, K. The structure of hikizimycin. Part I. Identification of 3-amino3-deoxy-D-glucose and cytosine as structural components. *Carbohydrate Res.* **1972**, *22*, 293-299.

221. Uchida, K.; Das, B. C. Hikosamine, a novel C11 aminosugar component of the antibiotic hikizimycin *Biochimie,* **1973,** *55,* 635-636.

222. Adapted from reference 217 and 218.

223. Adapted from reference 217.

224. Alarcon, B.; Lacal, J. C.; Fernandez-Sousa, J. M.; Carrasco, L. Screening for new compounds with anti-herpes activity. *Antiviral Res.* **1984**, *4*, 231-234.

225. Lacal, J. C.; Vazquez, D.; Fernandez-Souza, J. M. Antibiotics that specifically block translation in virus-infected cells. *J. Antibiot.* **1980**, *33*, 441-446.

226. Harries, H. F.; Wiles, W. G. Tests of some antibiotics and other chemosterilants on the green peach aphid. *J. Econ. Entomol.* **1966**, *59*, 694-696.

227. Gonzalez, A.; Vasquez, D.; Jimenez, A. Inhibition of translation in bacterial and eukaryotic systems by the antibiotic anthelmycin (hikizimycin). *Biochim. Biophys. Acta, Nucleic Acid Protein Synth.* **1979**, *561*, 403-409.

228. Rodriguez-Fonseca, C.; Amils, R.; Garrett, R. A. Fine structure of the peptidyl transferace centre on 23 S-Like rRNAs deduced from chemical probing of antibiotic-ribosome complexes. *J. Mol. Biol.* **1995**, *247*, 224-235.

229. Harada, S.; Kishi, T.; Isolation and characterization of mildiomycin, a new nucleoside antibiotic. *J. Antibiot.* **1978**, *31*, 519-524.

230. Harada, S.; Mizuta, E.; Kishi, T. Structure of mildiomycin, a new antifungal nucleoside antibiotic. *Tetrahedron* **1981**, *37*, 1317-1327.

231. Kamiya, K.; Wada, Y.; Takamoto, M. Crystal and molecular structure of mildiomycin monobenzoate heptahydrate. *Tetrahedron Lett.* **1978**, *44*, 4277-4280.

232. Kusaka, T.; Suetomi, K.; Iwasa, T.; Harada, S. TF-138: A new fungicide. *Br. Crop Prot. Conf.— Pests Dis., Proc.* **1979**, 589-595.

233. Adapted from reference 229.

234. Feduchi, E.; Cosin, M.; Carrasco, L. Mildiomycin: a nucleoside antibiotic that inhibits protein synthesis. *J. Antibiot.* **1985**, *38*, 415-419

235. Carrasco, L.; Vasquez, D. Molecular bases for the action and selectivity of nucleoside antibiotics. *Med. Res. Rev.* **1984**, *4*, 471-512.

236. Jiménez, A.; Carrasco L.; Vasquez, D. Enzymic and nonenzymic translocation by yeast polysomes. Site of action of a number of inhibitors. *Biochemistry* **1977**, *16*, 4727-4730.

237. Adapted from reference 234.

238. Sakata, K.; Sakurai, A.; Tamura, S. Ezomycins, antifungal antibiotics. Part III. Isolation of novel antifungal antibiotics, ezomycins A1, A2, B1 and B2. *Agric. Biol. Chem.* **1974**, *38*, 1883-1890.

239. Sakata, K.; Sakurai, A.; Tamura, S. Ezomycins, antifungal antibiotics.

I. L-cystathione as a component of ezomycins A1 and B1 from a *Streptomyces*. *Agric. Biol. Chem.* **1973**, *37*, 687-699.

240. Sakata, K.; Sakurai, A.; Tamura, S. Ezomycins, antifungal antibiotics. II. Ezoaminuroic acid, 3-amino-3,4-dideoxy-D-xylo-hexapyranuroic acid, as a constituent of ezomycins A1 and A2. *Tetrahedron Lett.* **1974**, *16*, 1533-1536.

241. Sakata, K.; Sakurai, A.; Tamura, S. Ezomycins, antifungal antibiotics. V. Degradative studies on ezomycins A1 and A2. *Agric. Biol. Chem.* **1975**, *39*, 885-892.

242. Sakata, K.; Sakurai, A.; Tamura, S. Studies on ezomycins, antifungal antibiotics. Part VII. Structures of ezomycins A1 and A2. *Agric. Biol. Chem.* **1976**, *40*, 1993-1999.

243. Sakata, K.; Sakurai, A.; Tamura, S. Ezomycins, antifungal antibiotics. IV. Structures of ezomycins A1 and A2. *Tetrahedron Lett.* **1974**, *49-50*, 4327-4330.

244. Adapted from reference 238.

CHAPTER 2

A CONVERGENT APPROACH TOWARDS THE SYNTHESIS OF AMICETIN DERIVATIVES

2.1 Background

Pyrimidine nucleosides (Figure 2.1) are a class of ribosomal antibiotics primarily derived from fermentation broths of *Streptomyces* species.[1, 2] Amicetin, a member of this class, is of particular interest to us for its potent antibacterial activity against *Mycobacterium tuberculosis* H37Rv (MIC 0.5 μg/mL) and good selectivity index against mycobacteria over mammalian cells.[3, 4] With the resurgence of drug resistant strains of *M. tuberculosis* (MDR-TB, XDR-TB, and TDR-TB),[5] the need for more efficient therapeutics prompted us to develop a convergent approach

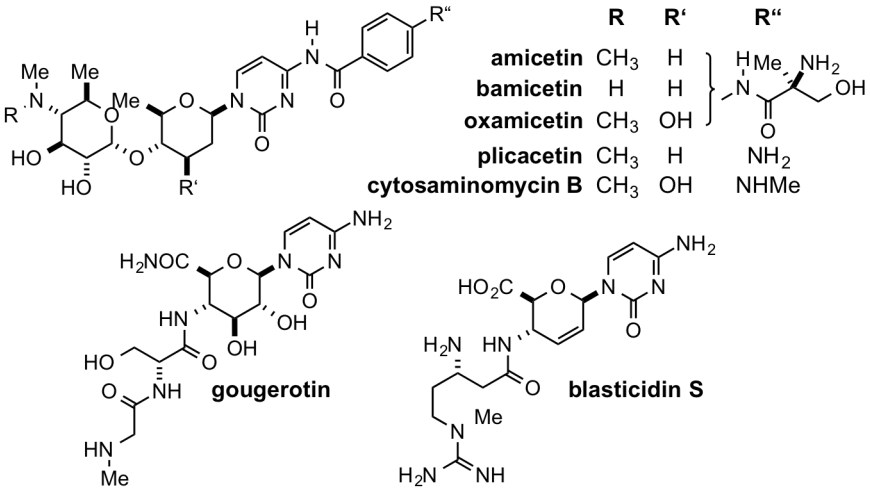

Figure 2.1 Amicetin and other pyrimidine nucleoside class of antibiotics

towards the synthesis of amicetin and its derivatives.

2.2 Retrosynthesis

A convergent retrosynthesis of amicetin is proposed (Figure 2.2). Examining the structure of amicetin **1**, the molecule can be synthesized from the *N*-glycoside coupling[6] of the amicetamine **2** and cytimidine **3**. The disaccharide can be synthesized from the Tsuji-Trost coupling of pyranones derived from the Noyori reduction-Achmatowicz rearrangement sequence on acylfuran **4**.[7] We envision the synthesis of the whole eastern unit of amicetin from the copper catalyzed amidation of halopyrimidine **5**, 4-iodobenzamide **6** and carboxamide **7**.[8]

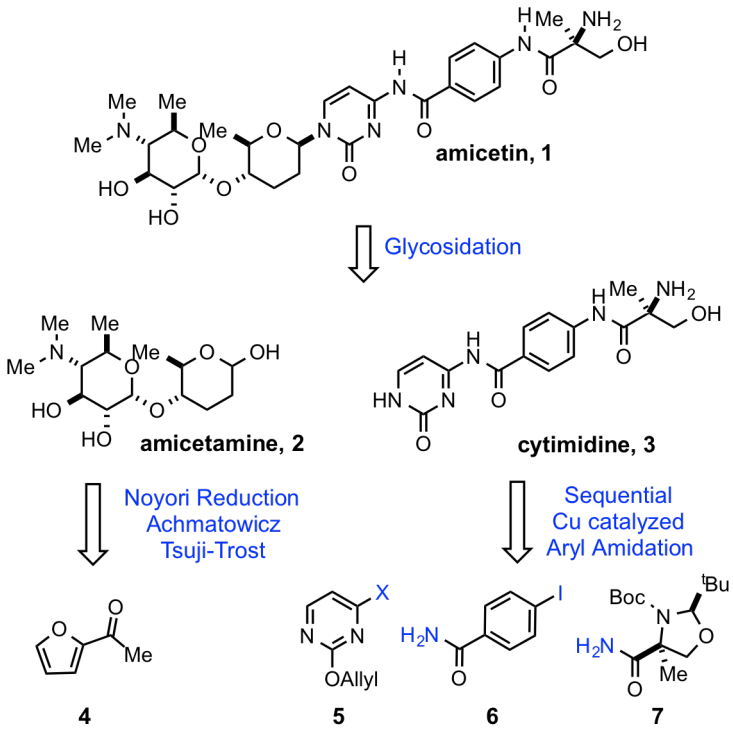

Figure 2.2 Retrosynthetic analysis

2.3 Results and Discussion

2.3.1 Synthesis of Cytimidine Through a One-Pot Copper Amidation Cascade

We began our efforts toward the total synthesis of amicetin by developing a highly efficient route to cytimidine. We sought to prepare cytimidine from a one-pot regioselective coupling of halopyrimidine **5** to 4-iodobenzamide **6**, and carboxamide **7**, *via* copper catalyzed *N*-aryl amidation reactions (Figure 2.3). Our strategy highlights the use of and inexpensive coupling chemistry and avoids a series of protection-deprotection chemistries normally employed in peptide synthesis. We hypothesized that the differences in bond strength and steric constraints among the coupling partners would produce different rates of amidation, enabling us to unite these fragments *via* a one-pot, three component tandem *N*-aryl amidation. We expected **5** and **6** to undergo a faster amidation because the carbon-halogen bond of a halopyrimidine is weaker than an arylhalide bond. In addition, the coupling with **7** would be slower due to the steric hindrance afforded by the quaternary α-stereocenter. To explore our hypothesis and learn more about the subtleties that govern these amidations we studied the coupling reactions individually.

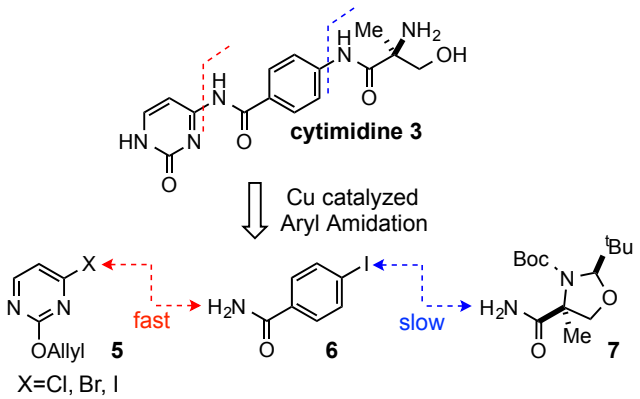

Figure 2.3 One-pot copper-catalyzed tandem amidation

Our synthesis began with the the synthesis of the carboxamide **7** (Figure 2.4), which corresponds to the α-methylserine moiety, we began with the pivaldehyde condensation and subsequent Boc-protection of serine methyl ester **8** to form oxazolidine ester **9** as a single diasteromer.[9] Oxazolidine ester **9** was alkylated employing Seebach's memory of chirality,[10] giving the α-methylated oxazolidine ester **10** in excellent yield and >95:5 *dr*. The alkylated product was saponified to the acid **11**, then converted to carboxamide **7** by treating the corresponding acid chloride (formed *in situ*) with concentrated ammonia.

We proceed with formation of 4-halopyrimidines **5a-c** (Figure 2.5). These halides were prepared by the reaction of commercially available 4-chloro-2-methylthiopyrimidine **12a** with TMSBr or TMSI to give the corresponding bromo and iodopyrimidines **12b** and **12c**.[11] Oxidation of **8a-c** to the sulfone **13a-c**,[12] followed by nucleophilic aromatic substitution[13] with potassium allyloxide gave **5a-c**, in good to excellent yields. The allyl protecting group was introduced to offer the option of selective deprotection to the cytosine moiety for *N*-glycosylation, or con currently deprotection *en route* to cytimidine and its analogues.

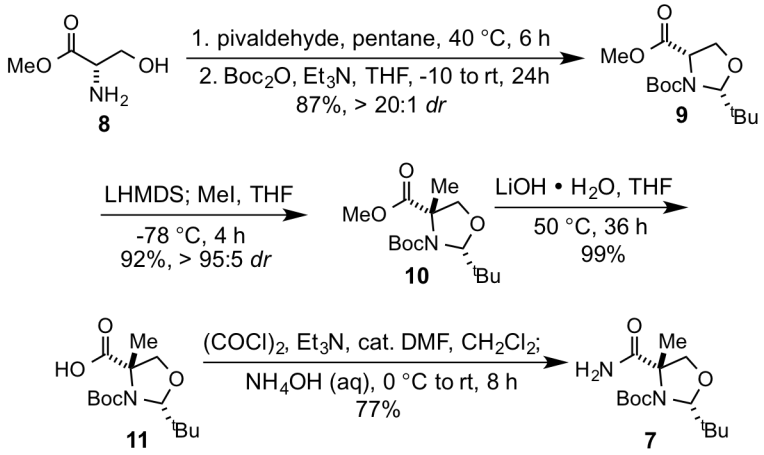

Figure 2.4 Synthesis of carboxamide 7

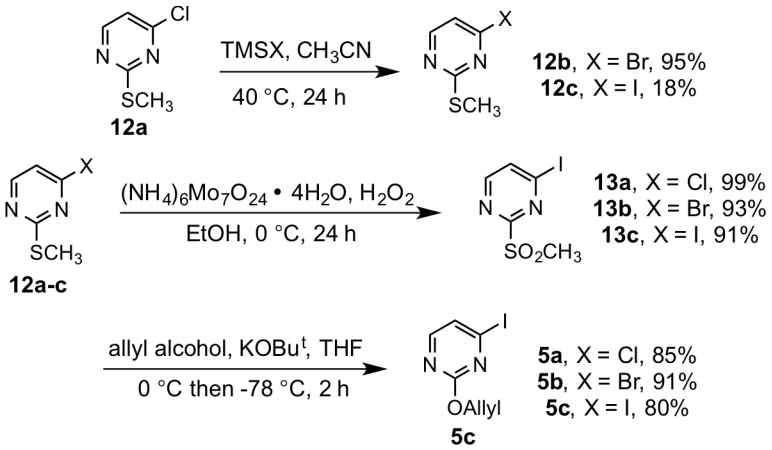

Figure 2.5 Synthesis of 4-halopyrimidines

We proceeded to screen reaction conditions for the copper catalyzed *N*-aryl amidation of **5a-c** with 4-iodobenzamide **6** (Table 2.1). The first example was from Buchwald who reported a the *N*-amidation of cyclohexanecarboxamide with 5-bromopyrimidine using the *trans*-*N,N*'-dimethylcyclohexane-1,2-diamine ligand.[8] The second report was from Legraverend who showed the one-pot synthesis of purines *via* the amidation-condensation of 5-amino-4-iodopyrimidines with benzamides.[14] As a starting point, we applied Buchwald's and Legraverend's conditions to our coupling reaction (entries 1-4). To our surprise, instead of giving the desired pyrimidylbenzamide **14**, these halopyrimidines couple with the diamine ligand, which had been previously described by Fukuyama in the copper-mediated *N*-aryl amination 2-iodopyridine.[15] The ligandless Goldberg protocol was also employed,[16] (entries 5-7) but only gave a trace of the product detected by LCMS. We extended our screening to other ligands typically used in copper-mediated chemistry (entries 8-14).[17] The most promising ligand for the reaction was found to be 1,10-phenanthroline giving pyrimidylbenzamide **14** in good yield. 4-Chloropyrimidine **5a**, however, was unreactive in all reaction conditions

Table 2.1 Optimization of the 1st *N*-aryl amidation*

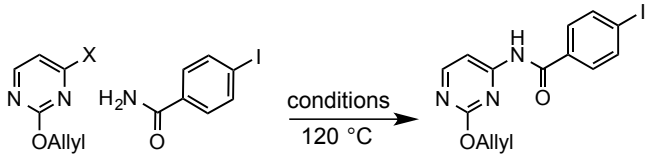

Entry	X	Ligand	Solvent	Base	time	Yield
1	Cl	dmeda	Toluene	K_3PO_4	24h	-
2	Br	dmeda	Toluene	K_3PO_4	24h	-
3	I	dmeda	Toluene	K_3PO_4	24h	-
4	I	diamine 2	Dioxane	Cs_2CO_3	24h	-
5	Cl	-	Dioxane	K_3PO_4	24h	-
6	Br	-	Dioxane	K_3PO_4	24h	<1%
7	I	-	Dioxane	K_3PO_4	24h	<1%
8	Cl	1,10-phen	Toluene	K_3PO_4	18h	-
9	Br	1,10-phen	Toluene	K_3PO_4	18h	69%
10	I	1,10-phen	Toluene	K_3PO_4	24h	71%
11	I	2,2'-bipy	Toluene	K_3PO_4	24h	37%
12	I	8-hq	Toluene	K_3PO_4	24h	14%
13	I	2,4,6-collidine	Toluene	K_3PO_4	24h	14%
14	I	1,10-phen	Dioxane	K_3PO_4	18h	72%

*10 mol% CuI, 20 mol% ligand, 1.0 equiv **5a-c**, 1.0 equiv **6**, and 2.0 equiv base

(entry 8),while 4-bromo and 4-iodopyrimidines **5b** and **5c** exhibited similar yields (entries 9 and 10). This suggests that the coupling process does not occur *via* nucleophilic aromatic substitution mechanism, where chlorides are known to react faster than bromides and iodides.[18] Our data supports the copper-mediated amidation going through through the ion-pair oxidative addition mechanism proposed by Hartwig and co-workers (Figure 2.6).[19]

After optimizing the initial coupling we applied our conditions to the 2nd *N*-arylamidation (Table 2.2). Unfortunately, 1,10-phenanthroline (phen) was found to be a less competent ligand for this reaction (entry 1). Using the ligand *N,N'*-dimethylethylenediamine (dmeda) affords the coupled product in excellent yields. It appears that a very rigid $Cu(phen)_2$ complex[19] is not well suited for the *N*-aryl coup-

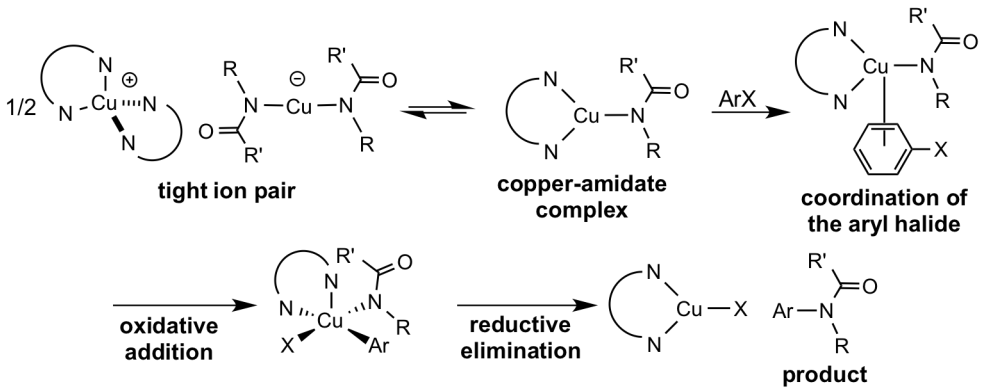

Figure 2.6 Hartwig's proposed mechanism for copper catalyzed amidation

Table 2.2 Optimization of the 2nd *N*-aryl amidation*

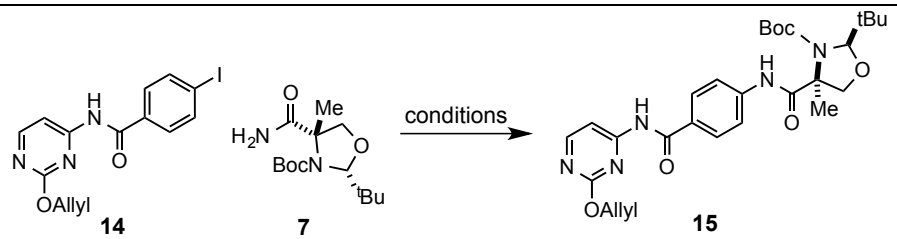

Entry	Ligand	solvent	Base	temp	Time	Yield
1	1,10-phen	dioxane	K_3PO_4	120 °C	48h	20%
2	dmeda	dioxane	K_3PO_4	100 °C	60h	93%

* 10 mol% CuI, 20 mol% ligand, 1.0 equiv **14**, 1.0 equiv 7, and 2.0 equiv base.

ling of a sterically demanding substrate such as carboxamide **7**; however, the more flexible $Cu(dmeda)_2$ complex is well tolerated.

Unfortunately, our initial goal of presenting a three-component tandem route towards cytimidine was not feasible due to the differences in reactivities of the $Cu(phen)_2$ and $Cu(dmeda)_2$ ligand systems with respect to the 1st and 2nd *N*-aryl amidations (Figure 2.3, *vide infra*). The competing reactions (amination vs. amidation) of 4-halopyrimidines **5a-c** in the 1st coupling reaction and the incompatibility of the $Cu(phen)_2$ in the sterically hindered 2nd amidation led us to consider an alternative strategy. So we then decided to examine the one-pot

sequential amidation of cytimidine (Figure 2.7). The *N*-aryl amidation of bromopyrimidine **5b** with 4-iodobenzamide **14** followed by coupling of carboxamide **7** gave masked cytimidine **15** in overall 53% yield. Final deprotection sequences[20] afforded cytimidine in 34% overall yield in 5 steps from the commercially available 4 chloro-2-methylthiopyrimidine.

We also applied our method towards the synthesis of a number of masked cytimidine analogues from simple precursors (Figure 2.8).[21] However, the yields obtained in these Cu-amidation cascades were unsatisfactory. Possible decomposition of the corresponding coupled intermediate or incomplete conversion maybe the reason for the obtained yields. Conducting the two amidation sequences separately gave cleaner reactions and better overall yields for the analogues. Overall, we have developed an efficient route to cytimidine *via* a one-pot sequential Cu-mediated *N*-amidation cascade. Interestingly we found no trace of the

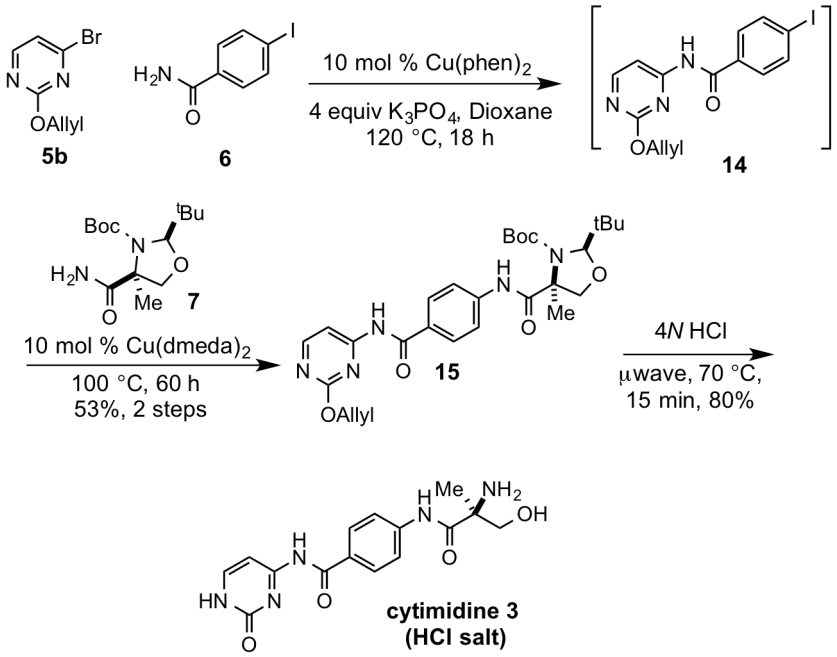

Figure 2.7 One-pot Cu-mediated *N-aryl* amidation and completion of cytimidine synthesis

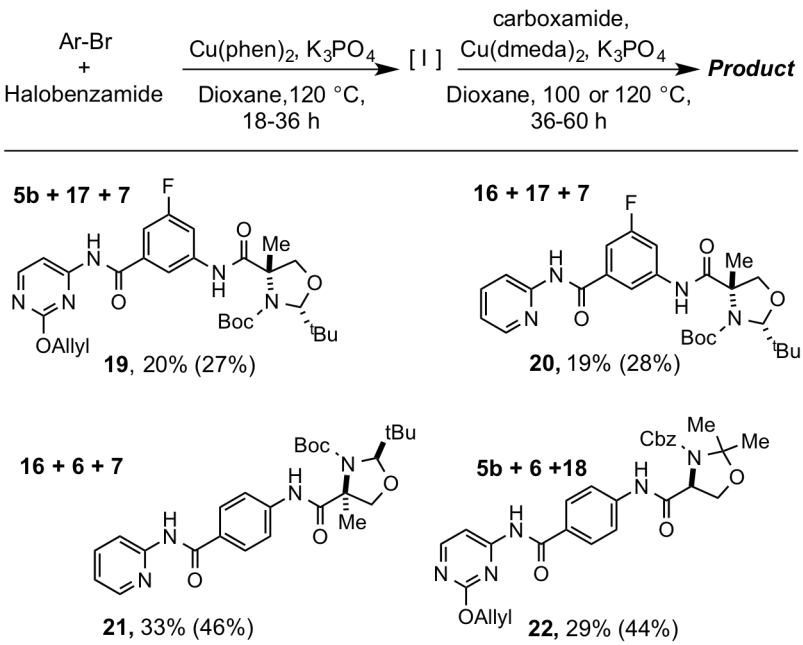

*10-30 mol% CuI, 20-40 mol% ligand, 1.0 equiv **5b** or **16**, 1.0 equiv **6** or 1.5 equiv **17**, 1.0-1.5 equiv **7** or **18**[21]

Figure 2.8 Synthesis of masked cytimidine analogues*

homocoupled halobenzamide and Ullmann[22] product in our reactions by LCMS. The methodology we have developed exploits the regioselective coupling of a halopyrimidine and an iodobenzamide towards the synthesis of cytimidine and analogues.[23]

2.3.2 Efforts Towards the Synthesis of Amicetamine

Continuing on our divergent synthetic strategy, we proceeded with the synthesis of the disaccharide of moiety of amicetin, amicetamine **2** by utilizing the strategy developed by O' Doherty and co-workers in the synthesis of deoxysugars from acylfuran (Figure 2.9). We started our synthesis of amicetose (Figure 2.10) with the asymmetric reduction of acylfuran **4** using the Noyori catalyst and formic acid/triethylamine complex as a hydride source, yielded the corresponding enantio-

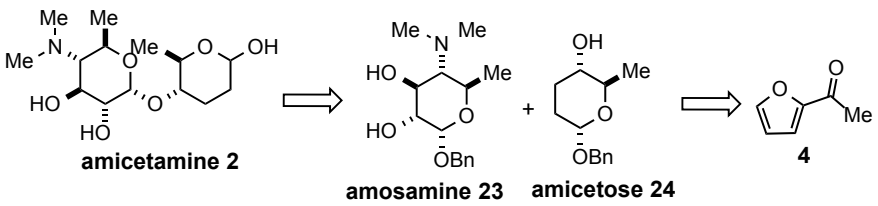

Figure 2.9 Retrosynthesis of amicetamine

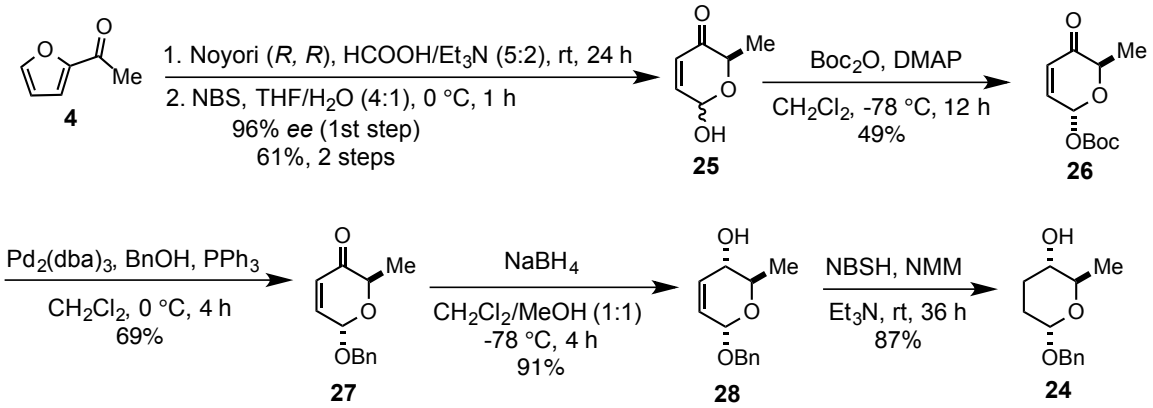

Figure 2.10 Synthesis of amicetose

enriched furfuryl alcohol.[24] The alcohol was obtained in high enantiomeric excess (> 96% ee), however, its exact yield was difficult to determine due its low boiling point. So after aqueous workup, we subjected the semi-crude furfuryl alcohol to the Achmatowicz rearrangement[25, 26] to give pyranose **25** in 61% over two steps. Protection of the hemiacetal with benzoic anyhydride at low temperatures gave the α-Boc-pyranone **26** in 49% isolated yield. Tsuji-Trost reaction was employed on **26** to install the benzyloxy group in excellent yield and complete anomeric selectivity. Controlled low temperature reduction of the Tsuji-Trost product **27** with $NaBH_4$ selectively formed allyl alcohol **27** in excellent isolated yield. Alkene reduction of **27** was achieved by 2-Nitrobenzenesulfonylhydrazide (NBSH) giving benzyloxyamicetose **24** in 87%.

We envisioned that the aminopyranoside amosamine **23** could come from the same strategy. We began our synthesis (Figure 2.11) with the Boc protection of the equatorial alcohol **28,** which gave carbonate **29** in good yields. Unfortunately, the attempted Tsuji-Trost reaction with dimethylamine on **29** was unsuccessful. We then proceed with the Tsuji-Trost reaction using di-Cbz imide[27] as our nitrogen nucleophile, which then gave the protected aminodihydropyran **30** in modest yields. We attempted the Prevost reaction[28] on **30**, but instead of the dihydroxylation product, iodopyran **31** was formed. From here, we decided to access the diol from the epoxide. Solvolysis of the cyclic carbamate[29] in **31**, gave an isolatable mixture of benzyl and ethyl carbamate epoxides **32** and **33** in modest yields. At this point, we have reached a major roadblock in our synthesis to open epoxide, however, we only found tosic acid to work to give a mixture of diols as all attempts in transforming our tosylated products **34** and **35** only lead to undesired transformations. While we ventured to synthesize amosamine from the same precursor alcohol **28**, however, our

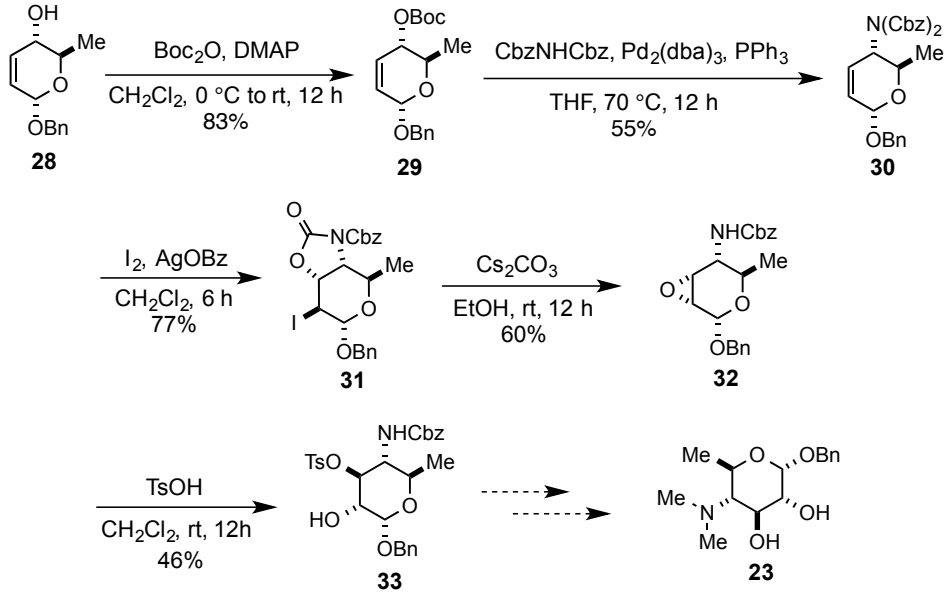

Figure 2.11 Synthetic efforts towards the synthesis of amosamine

efforts did not afford us the aminosugar.

2.4 Conclusion

We were able to synthesize cytimidine, the eastern half of amicetin through a one-pot copper-catalyzed amidation cascade. Our efforts towards the synthesis of amicetamine, the disaccharide portion of amicetin, resulted in the completion of the dideoxy sugar amicetose, but not the aminosugar amosamine. During our attempts to complete the synthesis of amicetin, we also sought other more viable ways of producing the compound for further studies. It was then we opted to produce the natural product through actinomycete fermentation and isolation procedures.

2.5 References

1. Fox, J. J. Watanabe, K.A.; Bloch, A. Nucleoside antibiotics. *Prog. Nucleic Acid Res. Mol. Biol.* **1966**, *5*, 251-313.

2. Isono, K. Nucleoside antibiotics: structure, biological activity, and biosynthesis. *J. Antibiot.* **1988**, *41*, 1712-1739.

3. DeBoer, C.; Caron, E. L.; Hinman, J. W. Amicetin, a new *Streptomyces* antibiotic. *J. Am. Chem. Soc.* **1953**, *75*, 499-500.

4. Smith, C. G.; Lummin, W. L.; Grady, J. E. An improved tissue culture assay. II. Cytotoxicity studies with antibiotics, chemicals, and solvents. *Cancer Res.* **1959**, *19*, 847-852.

5. World Health Organization Global Tuberculosis Report 2014. http://www.who.int/tb/publications/global_report/en/ (accessed March 7, 2015).

6. Crich, D.; Sun, S. Direct synthesis of ß-mannopyranosides by the sulfoxide method. *Journal of Organic Chemistry* **1997**, *62*, 1198-1999.

7. Guo, H.; O' Doherty, G. A. *De novo* asymmetric synthesis of D- and L- swainsonine. *Org. Lett.* **2006**, *8*, 1609-1612.

8. Klapars, A.; Huand, X.; Buchwald, S. L. A general and efficient catalyst for the amidation of aryl halides. *J. Am. Chem. Soc.* **2002**, *124*, 7421-7428.

9. Brunner, M.; Saakrento, P.; Straub, T.; Rissanen, K.; Koshinen, A. M. P. Stereocontrolled α-alkylation of fully protected L-serine. *Eur. J. Org. Chem.* **2004**, 3879-3883.

10. Seebach, D.; Aebi, J. D. α-Alkylation of serine with self-reproduction of the center of chirality. *Tetrahedron Lett.* **1984**, *25*, 2545-2548.

11. Hocková, D.; Antonín, H.; Masojídková, K. D. T.; de Jersey, J.; Guaddat, L. W. W. Synthesis of branched 9-[2-(2-phosphonoethoxy)ethyl]purines as a new class of acyclic nucleoside phosphonates which inhibit *Plasmodium falciparum* hypoxanthine-guanine-xanthine phosphoribosyltransferase. *Bioorg. Med. Chem.* **2009**, *17*, 6218-6232.

12. Baudin, J. B.; Julia, S. A.; Lorne, R.; Ruel, O. Stereochemistry of direct olefin formation from carbonyl compounds and lithiated heterocyclic sulfones. *Bull. Chim. Soc. Fr.* **1993**, *130*, 856-878.

13. Falck-Pedersen, M. L.; Benneche, T.; Undheim, K. Palladium-catalyzed rearrangements of 2-cyclopentenyloxypyrimidines in the preparation of pyrimidine carbonucleosides. *Acta Chim. Scan.* **1993**, *47*, 72-79.

14. Ibrahim, N.; Legraverend, M. Synthesis of 6,7,8-trisubstituted purines *via* a copper-catalyzed amidation reaction. *J. Org. Chem.* **2009**, *74*, 463-465.

15. Okano, K.; Tokuyama, H.; Fukuyama, T. Synthesis of secondary arylamines through copper-mediated intermolecular aryl amination. *Org. Lett.* **2003**, *5*, 4987-4990.

16. Goldberg, I. Phenylation in the presence of copper as catalyst. *Ber. Dtsch. Chem. Ges.* **1906**, *39*, 1691-1692.

17. (a) Lin, J.; Elangovan, A.; Ho, T. Structure-property relationships in conjugated donor-acceptor molecules based on cyanoanthracence: computational and experimental studies. *J. Org. Chem.* **2005**, *70*, 7397-7407. (b) Lai, C.; Gum, R. J.; Daly, M.; Fry, E. H.; Hutchins, C.; Abad-Zapatero, C.; von Geldern, T. W. Benzoxazole benzenesulfonamides as allosteric inhibitors of fructose-1,6-bisphosphatase. *Biorg. Med. Chem. Lett.* **2006**, *16*, 1807-1810. (c) Guzzo, P. Preparation of 5-pyridinone substituted indazoles as melanin-concentrating hormone (MCH1) receptor selective antagonists. (AMR Technology, Inc. USA). US Patent 20090082359, January 29, 2009. (d) Maruyama, T.; Fujiwara, K.; Fukuhara, M. A new method for the synthesis of N-phenyl-uracil and -pyrimidine nucleosides. *J. Chem. Soc. Perkin Trans. 1* **1995**, 733.

18. Ritchie, C. D.; Sawada, M. Cation-anion combination reactions. 15. Rates of nucleophilic aromatic substitution reactions in water and methanol solutions. *J. Am. Chem. Soc.* **1977**, *99*, 3754.

19. Tye. J. W.; Johns, A. M.; Incarvito, C. D.; Hartwig, J. F. Copper complexes of anionic nitrogen ligands in the amidation and imidation of aryl halides *J. Am. Chem. Soc.* **2008**, *130*, 9971-9983.

20. Doi, T. Kinbara, A.; Inoue, H. Takahasi, T. Donor-bound glycosylation for various glycosyl acceptors: bidirectional solid-phase semisynthesis of vancomycin and its derivatives. *Chem.- Asian J.* **2007**, *2,* 188-198.

21. Shin, C.; Ito, A.; Okumura, K.; Nakamura, Y. A convenient synthesis of methyl 2-[2-(1-amino)ethenyl-bithiazolyl]thiazoline-4-carboxylate, an important skeleton of cyclothiazomycin. *Chem. Lett.* **1995**, *1,* 45-46.

22. Ullmann, F. Ueber synthesen in der biphenylreihe. *Ber. Dtsch. Chem. Ges.* **1901**, *34*, 2174-2185.

23. Serrano, C. M.; Looper, R. E. Synthesis of cytimidine through a one-pot copper-mediated amidation cascade. *Org. Lett.* **2011**, *13*, 5000-5003.

24. Shan, M.; Xing, Y.; O' Doherty, G. A. *De novo* asymmetric synthesis of an α-6-deoxyaltropyranoside as well as its 2-3-deoxy and 2,3-dideoxy congeners. *J. Org. Chem.* **2009**, *74*, 5961-5066.

25. Fujii, A.; Hashiguchi, S.; Uematsu, N.; Ikariya, T. Noyori, R. Ruthenium(II)-catalyzed asymmetric transfer hydrogenation of ketones using a formic acid−triethylamine mixture. *J. Am. Chem. Soc.* **1996**, *118*, 2521-2522.

26. Achmatowicz, O.; Bielski, R. Stereoselective total synthesis of methyl α-D- and α-L-glucopyranosides. *Carbohydr. Res.* **1977**, *55*, 165-176.

27. Guo, H.; O' Doherty, G. A. *De novo* asymmetric synthesis of daumone via a palladium-catalyzed glycosylation. *Org. Lett.* **2005**, *7*, 3921-3924.

28. Fairhurst, R. A.; Taylor, R. J.; Cox, B. Preparation of carbocyclic nucleosides as anti-inflammatory agents. PCT Int. Appl. (2007), WO 2007121920 A2, November 1, 2007.

29. Hodgson, R.; Majid, T.; Nelson, A. Towards complete stereochemical control: complementary Mmethods for the synthesis of six diastereomeric monosaccharide mimetics. *J. Chem. Soc., Perkin Trans. 1* **2002**, 1444-14454.

30. Ishizuka, T.; Kunieda, T. Mild and selective ring-cleavage of cyclic carbamates to amino alcohols. *Tetrahedron Lett.* **1987**, *28*, 4185-4188.

2.6 Supplemental Information

2.6.1 General Experimental Considerations

All reactions requiring anhydrous conditions were conducted in flame-dried glassware under a positive pressure of either nitrogen or argon. Commercially available reagents were used as received; otherwise, materials were purified according to *Purification of Laboratory Chemicals*.[1] Dichloromethane (CH_2Cl_2), *N,N'*-dimethylformamide (DMF), and tetrahydrofuran (THF) were degassed with nitrogen and passed through a solvent purification system (Innovative Technologies Pure Solv). Dry 1,4-dioxane was purchased from Acros Organics in a Acros Seal™ bottle. Triethylamine (Et_3N) was distilled from CaH_2 immediately prior to use. Microwave reactions were done in CEM Discover System Model 908005. Reactions were monitored by TLC and visualized by a dual short wave/long wave UV lamp and stained with ethanolic solution of 12-phosphomolybdic acid and *p*-anisaldehyde. Flash chromatography was performed on Merck silica gel Kieselgel 60 (230-400 mesh) from EM Science with the indicated HPLC grade solvent.

Melting points were determined using Mel-Temp® Capillary Melting Point Apparatus. Infrared spectra were obtained using Nicolet 380-FT IR spectrometer fitted with a Smart Orbit sample system. Optical rotations were obtained at ambient temperature on a Perkin Elmer Model 343 polarimeter (Na D line) using a microcell with a 1 decimeter path length. Mass spectra were determined on a Micromass Quattro II (ESI/APCI-TOF) for HRMS at the University of Utah Mass Spectrometry Facility. ^{1}H NMR spectra were recorded at 300 MHz and 500 MHz. and ^{13}C NMR

---

[1] *Purification* of *Laboratory Chemicals.* 2003, 5th Ed. Armarego, W. L. F.; Chai, C. L. L.

spectra were recorded at 125 MHz. Proton resonances were reported relative to the deuterated solvent peak: 7.27 ppm for $CDCl_3$ and 3.31 ppm (center line signal) for CD_3OD using the following format: chemical shift (δ) [multiplicity (s= singlet, bs= broad singlet, d= doublet, dd= doublet of doublet, dd= doublet of triplet, dq= doublet of quartet, ddd=doublet of doublet of exitdoublet, t= triplet, tdd= triplet of doublet of doublet, q= quartet, m= multiplet), coupling constant(s) *J* in Hz, integration].[2] Carbon resonances were reported as chemical shifts (δ) in parts per million, relative to the center line signal of the respective solvent peak: 77.23 ppm for $CDCl_3$ and 49.15 ppm for CD_3OD.

2.6.2 Experimental Procedures

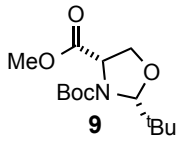

9

3-(*tert*-butyl) 4-methyl (2*R*,4*S*)-2- ((*tert*-butyl)oxazolidine-3,4-dicarboxylate (9). In a round bottom flask, Et_3N (5.75 mL, 41.3 mmol, 100 mol) was added to a suspension of commercially available serine methyl ester hydrochloride **8** (5.83 g, 37.5 mmol, 1 equiv) in pentane (50 mL), after which pivaldehyde (4.54 mL, 41.25 mmol, 1.1 equiv) was added to the mixture. A reflux condenser and Dean-Stark trap was then attached to the flask and the reaction was heated to 45 ˚C for about 6h, until no further water was collected in the Dean-Stark trap. The reaction was allowed to cool down to room temperature. The precipitated

---

[2] Hoye, T.R.; Hansen, P.R.; Vyvyan, J.R. *J. Org. Chem.* **1994**, *59*, 4096-4103.

$Et_3N \cdot HCl$ salt was filtered, washed with Et_2O (3 × 30 mL) and the organic layer dried over Na_2SO_4. The yellow filtrate was concentrated under reduced pressure and to give a yellow oil (6.6 g) containing a 1:1 mixture of epimers. The condensation product was subjected to Boc-protection without further purification.

Afterwards, the condensation product (6.6 g, 35.2 mmol, 1 equiv) was dissolved in THF (20 mL) and was cooled to 0 °C. $(Boc)_2O$ (14.6 mL, 71.8 mmol, 2 equiv) was added dropwise. The reaction mixture was allowed to warm to room temperature overnight and was then poured into a mixture of ice (ca. 10 g) and saturated $NaHCO_3$ solution (50 mL). The product was extracted with Et_2O (50 mL) and was washed with saturated NaHCO3 solution (4 × 20 mL) and dried over Na_2SO_4. Excess solvent was removed under reduced pressure giving the crude product. Further purification by flash chromatography using 15% ether/hexanes gave a single isomer of the title compound **9** as a colorless oil (9.37 g, 87% yield over two steps). R_f = 0.31 (15% Et_2O /hexanes). $[\alpha]^{20}_D$ -28.45 (*c* = 4.67, $CHCl_3$). ^1H NMR (500 MHz, $CDCl_3$): δ 5.01 (s, 1H), 4.68 (bs, 1H), 4.26 (dd, *J* = 8.3, 5.9 Hz, 1H), 4.12 (dd, *J* = 8.8, 8.8 Hz, 1H), 3.73 (s, 1H), 1.46 (s, 9H), 0.92 (s, 9H) ppm. ^{13}C NMR (125 MHz, $CDCl_3$) δ 171.2, 155.3, 97.8, 81.5, 68.5, 59.9, 52.5, 37.9, 28.4, 25.9 ppm.^{13}C DEPT (125 MHz, $CDCl_3$) δ CH_3: 52.5, 28.4, 25.9; CH_2: 68.5; CH: 97.8, 59.9; CH_0: 171.2, 155.3, 81.5, 37.9 ppm. IR (neat) 2974, 2906, 1761, 1704 cm^{-1}. HRMS (ESI) Calculated for $C_{14}H_{25}NO_5Na$ *m/z* 310.1630 (M+Na), Obsd. 310.1628.

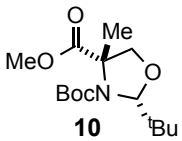

10

(2*R*,4*S*)-3-*tert*-Butyl 4-methyl 2-(*tert*-butyl)-4-methyloxazolidine-3,4-

dicarboxylate (10). A 100 mL flask under N_2 was charged with THF (1 mL) and was cooled to -78 °C. 1M LHMDS in THF (1.60 mL, 1.60 mmol, 1.2 equiv) was added. A solution of oxazolidine **9** (0.377 g, 1.31 mmol, 1.0 equiv) in THF (4 mL) was slowly added to the solution, maintaining the internal temperature of the reaction mixture at -78 °C. The reaction was allowed to stir for another 30 min at -78 °C. Iodomethane (0.250 mL, 4.00 mmol, 3.1 equiv) was added dropwise. After stirring for another 6h at -78 °C, the solution was allowed to warm to room temperature. The reaction mixture was then poured into a mixture of saturated solution of NH_4Cl (15 mL) and EtOAc (50 mL). The organic layer was separated, washed with distilled H_2O (15 mL) and brine (15 mL), dried over anhydrous Na_2SO_4, filtered and concentrated under reduced pressure. The crude product was purified by flash chromatography using 10% EtOAc/hexanes, giving the alkylated product **10** (0.365 g, 92% yield) as a colorless oil. R_f = 0.32 (10% EtOAc/hexanes). $[\alpha]^{20}_D$ = -3.9, (*c* = 0.4, $CHCl_3$). ^{1}H NMR (500 MHz, $CDCl_3$): δ 5.11 (s, 1H), 4.25 (d, *J* = 8.3 Hz, 1H), 3.82 (d, *J* = 8.3 Hz, 1H), 3.77 (s, 3H), 1.64 (s, 3H), 1.44 (s, 9H), 1.01 (s, 9H) ppm. ^{13}C NMR (125 MHz, $CDCl_3$) δ 172.7, 153.9, 97.2, 81.0, 77.3, 66.6, 52.6, 39.4, 28.3, 26.8 21.4 ppm. ^{13}C DEPT (125 MHz, $CDCl_3$) δ CH_3: 52.6, 28.3, 26.8, 21.4; CH_2: 77.3; CH 97.2; CH_0: 172.7, 153.9, 81.0, 66.6, 39.4 ppm. IR (neat) 2976, 2907, 1744, 1713, 1478 cm^{-1}. HRMS (ESI) Calculated for $C_{15}H_7NO_5Na$ *m/z* 324.1787 (M+Na), Obsd. 324.1789.

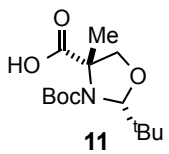

11

(2*R*,4*S*)-3-(*tert*-Butoxycarbonyl)-2-(*tert*-butyl)-4-methyloxazoli-dine-4-

carboxylic acid (11). To a stirring solution of alkylated oxazolidine **10** (0.847 g, 2.81 mmol, 1.0 equiv) in THF (16 mL), LiOH・H_2O (1.18 g, 28.1 mmol, 10.0 equiv) was added. Distilled H_2O (4 mL) was added to the mixture. The reaction was allowed to stir at 50 °C over 36h. The reaction mixture was poured into a mixture of diethyl ether (30 mL) and distilled H_2O (20 mL). The aqueous layer was separated, carefully acidified to pH 3 with 1N HCl solution, extracted with EtOAc (3 × 20 mL), dried over anhydrous Na_2SO_4, filtered and concentrated under reduced pressure. The crude product was purified by flash chromatography using 50% EtOAc/hexanes, giving the acid oxazolidine **11** (0.797 g, 99% yield) as a white solid. R_f = 0.41 (50% MeOH/hexanes). Mp 117-118 °C. $[\alpha]^{20}_D$ = -104.5 (*c* = 0.4, $CHCl_3$). ^{1}H NMR (500 MHz, $CDCl_3$): δ 5.13 (s, 1H), 4.60 (bs, 1H), 3.88 (d, *J* = 9.3 Hz, 1H), 1.68 (s, 3H), 1.49 (s, 9H), 0.93 (s, 9H) ppm. ^{13}C NMR (125 MHz, $CDCl_3$) δ 174.3, 156.4, 97.4, 83.5, 76.5, 66.5, 39.0, 28.1, 26.4, 21.5 ppm. ^{13}C DEPT (125 MHz, $CDCl_3$) δ CH_3: 28.1, 26.4, 21.5; CH_2: 76.5; CH 97.4; CH_0: 174.3, 156.4, 83.5, 66.5, 39.0 ppm. IR (neat) 2978, 2957, 1729, 1648, 1365 cm^{-1}. HRMS (ESI) Calculated for $C_{14}H_{25}NO_5Na$ *m/z* 320.1630 (M+Na), Obsd. 320.1628.

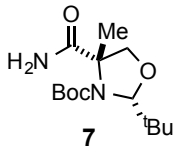

7

(2*R*,4*S*)-*tert*-Butyl 2-(*tert*-butyl)-4-carbamoyl-4-methyloxazoli-dine-3-carboxylate (7). To a stirring solution of acid oxazolidine **11** (0.344 g, 1.20 mmol, 1.0 equiv) in CH_2Cl_2 (10 mL) at 0 °C under N_2, dry Et_3N (0.84 mL, 6.0 mmol, 5.0 equiv) was added dropwise. A few drops of dry DMF were added into the mixture. Afterwards, Oxalyl chloride (0.16 mL, 1.84 mmol, 1.5 equiv) was added

dropwise into the reaction. The reaction was allowed to warm slowly to room temperature and was stirred for another 2 h. Excess concentrated NH_4OH solution (2 mL) was slowly added to the reaction mixture and was stirred for another 6h at room temperature. The reaction mixture was quenched with saturated solution of NH_4Cl (30 mL) and extracted with EtOAc (3 × 20 mL). The combined organic layers was washed with brine (20 mL), dried with anhydrous Na_2SO_4, filtered and concentrated under reduced pressure. The crude product was purified by flash chromatography using 40% EtOAc/hexanes giving the carboxamide **7** (0.263 g, 77% yield) as a white solid. R_f = 0.32 (40% EtOAc/hexanes). Mp 101-102 °C. $[\alpha]^{20}_D$ = -68.8 (*c* = 0.4, $CHCl_3$). ^{1}H NMR (500 MHz, $CDCl_3$): δ 6.16 (bs, 1H), 5.16 (s, 1H), 4.57 (d, d, *J* = 5.9 Hz, 1H), 3.76 (d, *J* = 8.8 Hz, 1H), 1.64 (s, 3H), 1.47 (s, 9H), 0.91 (s, 9H) ppm. ^{13}C NMR (125 MHz, $CDCl_3$) δ 176.5, 155.3, 98.1, 82.2, 76.8, 67.5, 38.5, 28.3, 26.4, 22.3 ppm. ^{13}C DEPT (125 MHz, $CDCl_3$) δ CH_3: 28.3, 26.4, 22.3; CH_2: 76.8; CH: 98.1; CH_0: 176.5, 153.3, 82.2, 67.5, 38.8 ppm. IR (neat) 3485, 3350, 2975, 1688, 1680, 1365 cm^{-1}. HRMS (ESI) Calculated for $C_{14}H_{26}NO_4Na$ *m/z* 309.1790 (M+Na), Obsd. 309.1793.

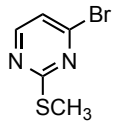

12b

4-Bromo-2-(methylthio)pyrimidine (12b). Trimethylsilyl bromide (3.10 mL, 23.4 mmol, 13.6 equiv) was added to a stirring solution of 4-Chloro-2-(methylthio)pyrimidine **12a** (0.200 mL, 1.72 mmol, 1.0 equiv) in CH_3CN (20 mL) under N_2 atmosphere. The mixture was heated to 40 ºC and was stirred for 24h. The reaction mixture was quenched with a saturated solution of $NaHCO_3$ (20 mL)

and was extracted with EtOAc (50 mL). The organic layer was washed with distilled H_2O (30 mL) and brine solution (30 mL), dried with anhydrous Na_2SO_4, and concentrated under reduced pressure. The crude orange oil was purified by flash chromatography using 10% EtOAc/hexanes giving the title compound **12b** (0.335 g, 95% yield) as a colorless oil. R_f= 0.26 (10% EtOAc/hexanes). ^{1}H NMR (500 MHz, $CDCl_3$): δ 8.18 (d, *J* = 5.4 Hz, 1H), 7.09 (d, *J* = 4.9 Hz, 1H), 2.56 (s, 3H) ppm. ^{13}C NMR (125 MHz, $CDCl_3$) δ 173.7, 157.2, 152.3, 120.3, 14.3 ppm. ^{13}C DEPT (125 MHz, $CDCl_3$) δ CH_3: 14.3; CH: 157.2, 120.3; CH_0: 173.7, 152.5 ppm. IR (neat) 3096, 2926, 1537, 1393, 1331, 1304cm^{-1}. HRMS (ESI) Calculated for $C_5H_6N_1O_xSBr$ *m/z* 204.9435 (M+H), Obsd. 204.9438.

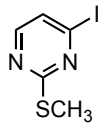

12c

4-Iodo-2-(methylthio)pyrimidine (12c). Trimethylsilyl iodide (10.0 mL, 10.3 mmol, 20.0 equiv) was added to a stirring solution of 4-Chloro-2-(methylthio)pyrimidine **12a** (0.400 mL, 3.43 mmol, 1.0 equiv) in CH_3CN (12 mL) under N_2 atmosphere. The mixture was heated to 40 ºC and was stirred for 24h. The mixture was then cooled down to 0 ºC. The reaction mixture was carefully quenched with a saturated solution of $NaHCO_3$ (20 mL) and was extracted with EtOAc (50 mL). The organic layer was washed with distilled H_2O (30 mL) and brine solution (30 mL), dried with anhydrous Na_2SO_4, filtered through silica and concentrated under reduced pressure giving a brown crude product. The crude product was then dry packed into silica gel and purified using flash chromatography using 10% EtOAc/hexanes giving the title compound **12c** (0.163 g, 18% yield) as

colorless solid. R_f= 0.26 (10% EtOAc/hexanes). Mp 38-39 °C. ^{1}H NMR (500 MHz, $CDCl_3$): δ 8.00 (d, *J* = 5.4 Hz, 1H), 7.41 (d, *J* = 4.9 Hz, 1H), 2.54 (s, 3H) ppm. ^{13}C NMR (125 MHz, $CDCl_3$) δ 173.5, 156.0, 129.5, 127.5, 14.5 ppm. ^{13}C DEPT (125 MHz, $CDCl_3$) δ CH_3: 14.5; CH: 156.0, 127.5; CH_0: 173.5, 129.5 ppm. IR (neat) 3089, 3009, 2923, 1526, 1387 cm^{-1}. HRMS (ESI) Calculated for $C_5H_6N_2OSI$ *m/z* 252.9296 (M+H), Obsd. 252.9297.

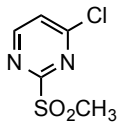

13a

4-Chloro-2-(methylsulfonyl)pyrimidine (13a). Ammonium molybdate tetrahydrate (0.218 g, 0.187 mmol, 0.03 equiv) was added to a 30% solution of Hydrogen peroxide (1.44 mL, 18.7 mmol, 3.0 equiv). The mixture was then cooled to 0 °C and slowly added to a stirring solution of 4-Chloro-2-(methylthio)pyrimidine **12a** (0.725 mL, 6.23 mmol, 1.0 equiv) in 95% ethanol (10 mL) at 0 °C. The reaction was allowed to stir for another 24h at 0 °C, at which time, the bulk of the solvent was removed from the reaction mixture under reduced pressure. The remaining crude reaction mixture was diluted with H_2O (20 mL) and CH_2Cl_2 (20 mL). The layers were separated and the aqueous layer was extracted with CH_2Cl_2 (3 × 20 mL). The combined organic layers were washed with 5% H_2SO_4, dried with anhydrous Na_2SO_4, filtered, and concentrated under reduced pressure. The crude product was purified by flash chromatography using 30% EtOAc/hexanes giving the chlorosulfone **13a** (1.19 g, 99% yield) as a white solid. R_f= 0.21 (50% EtOAc/hexanes). Mp 88-89 °C (lit. 87-89 °C). ^{1}H NMR (500 MHz, $CDCl_3$): δ 8.82 (d, *J* = 5.4 Hz, 1H), 7.63 (d, *J* = 4.9 Hz, 1H), 3.33 (s, 3H) ppm. ^{13}C NMR

(125 MHz, $CDCl_3$) δ 166.0, 163.3, 159.7, 124.9, 39.3 ppm. ^{13}C DEPT (125 MHz, $CDCl_3$) δ CH_3: 39.3; CH: 159.7, 124.9; CH_0: 166.0, 163.3 ppm. IR (neat) 3077, 3013, 2931, 1307, 1162 cm^{-1}. HRMS (ESI) Calculated for $C_5H_6N_2O_2SCl$ *m/z* 192.9839 (M+H), Obsd. 192.9844.

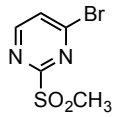

13b

4-Bromo-2-(methylsulfonyl)pyrimidine (13b). Ammonium molybdate tetrahydrate (0.258 g, 0.0221 mmol, 0.03 equiv) was added to a 30% solution of Hydrogen peroxide (0.154 mL, 2.21 mmol, 3.0 equiv). The mixture was then cooled to 0 °C and slowly added to a stirring solution of 4-Bromo-2-(methylthio)pyrimidine **12b** (0.151 g, 0.738 mmol, 1.0 equiv) in 95% ethanol (5 mL) at 0 °C. The reaction was allowed to stir for another 24 h at 0 °C, at which time, the bulk of the solvent was removed from the reaction mixture under reduced pressure. The remaining crude reaction mixture was diluted with H_2O (20 mL) and CH_2Cl_2 (20 mL). The layers were separated and the aqueous layer was extracted with CH_2Cl_2 (3 × 20 mL). The combined organic layers were washed with 5% H_2SO_4, dried with anhydrous Na_2SO_4, filtered, and concentrated under reduced pressure. The crude product was purified by flash chromatography using 30% EtOAc/hexanes giving the bromosulfone **13b** (0.163 g, 93% yield) as a white solid. R_f= 0.21 (50% EtOAc/hexanes). Mp 111-112 °C. ^1H NMR (500 MHz, $CDCl_3$): δ 8.69 (d, *J* = 5.4 Hz, 1H), 7.79 (d, *J* = 4.9 Hz, 1H), 3.35 (s, 3H) ppm. ^{13}C NMR (125 MHz, $CDCl_3$) δ 166.0, 158.8, 154.8, 128.9, 39.3 ppm. ^{13}C DEPT (125 MHz, $CDCl_3$) δ CH_3: 39.3; CH: 158.8, 128.9; CH_0: 166.0, 154.8 ppm. IR (neat) 3058, 2910,

1523, 1333, 1309 cm^{-1}. HRMS (ESI) Calculated for $C_5H_5N_2O_2BNaSBr$ *m/z* 258.9153 (M+Na), Obsd. 258.9160.

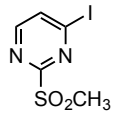

13c

4-Iodo-2-(methylsulfonyl)pyrimidine (13c). Ammonium molybdate tetrahydrate (0.182 g, 0.0156 mmol, 0.03 equiv) was added to a 30% solution of Hydrogen peroxide (1.20 mL, 15.6 mmol, 3.0 equiv). The mixture was then cooled to 0 °C and slowly added to a stirring solution of 4-Iodo-2-(methylthio)pyrimidine **12c** (1.31 g, 5.21 mmol, 1.0 equiv) in 95% ethanol (10 mL) at 0 °C. The reaction was allowed to stir for another 24h at 0 °C, at which time, the bulk of the solvent was removed from the reaction mixture under reduced pressure. The remaining crude reaction mixture was diluted with H_2O (50 mL) and CH_2Cl_2 (50 mL). The layers were separated and the aqueous layer was extracted with CH_2Cl_2 (3 × 25 mL). The combined organic layers were washed with 5% H_2SO_4, dried with anhydrous Na_2SO_4, filtered, and concentrated under reduced pressure. The crude product was purified by flash chromatography using 30% EtOAc/hexanes giving the iodosulfone **13c** (1.38 g, 93% yield) as a white solid. R_f= 0.21 (50% EtOAc/hexanes). Mp 130-131 °C. ^{1}H NMR (500 MHz, $CDCl_3$): d 8.44 (d, *J* = 4.9 Hz, 1H), 8.02 (d, *J* = 5.4 Hz, 1H), 3.37 (s, 3H) ppm. ^{13}C NMR (125 MHz, $CDCl_3$) δ 165.8, 157.3, 135.7, 131.0, 39.3 ppm. ^{13}C DEPT (125 MHz, $CDCl_3$) δ CH_3: 39.3; CH: 157.3, 135.7; CH_0: 165.8, 131.0 ppm. IR (neat) 3100, 3010, 2927, 1534, 1516, 1403, 1304 cm^{-1}. HRMS (ESI) Calculated for $C_5H_6N_2O_2SI$ *m/z* 284.9195 (M+H), Obsd. 284.9198.

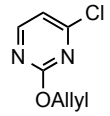

5a

2-(Allyloxy)-4-chloropyrimidine (5a). To a stirring solution of allyl alcohol (0.25 mL, 2.86 mmol, 1.1 equiv) in THF (5 mL) at 0 °C, 1M $KOBu^t$ in THF (4.0 mL, 4.0 mmol, 1.2 equiv) was slowly added. The reaction was allowed to stir for 15 min and was cooled to -78 °C. The resulting potassium salt of allyl alcohol was added dropwise to a stirring suspension of chlorosulfone **13a** (0.650 g, 3.37 mmol, 1 equiv) in THF (5 mL) at -78 °C. The internal temperature during addition was maintained around -78 °C to prevent the formation of 2,4-bis(allyloxypyrimidine). The reaction was allowed to react for another 2 h at -78 °C. The mixture was diluted with diethyl ether (25 mL) and was washed with distilled H_2O (2 × 20 mL) and brine (20 mL). The organic layer was then dried with anhydrous sodium sulfate, filtered, and concentrated under reduced pressure. The crude product was further purified by flash chromatography using 30% EtOAc/hexanes affording allyloxypyrimidine **5a** (0.490 g, 85% yield) as a yellow oil, which was stored at sub-zero temperatures to avoid decomposition. R_f = 0.34 (30% EtOAc/hexanes). ^{1}H NMR (500 MHz, $CDCl_3$): δ 8.38 (d, J = 5.4 Hz, 1H), 6.97 (d, J = 5.4 Hz, 1H), 6.05 (tdd, J = 17.6, 10.3, 5.4 Hz, 1H), 5.42 (tdd, J = 17.6, 1.5, 1.0 Hz, 1H), 5.27 (tdd, J = 10.7, 2.0, 1.5 Hz, 1H), 4.88 (ddd, J = 5.9, 2.0, 2.0 Hz, 2H) ppm. ^{13}C NMR (125 MHz, $CDCl_3$) δ 164.9, 162.6, 160.2, 132.1, 118.6, 115.2, 68.9 ppm. ^{13}C DEPT (125 MHz, $CDCl_3$) δ CH_2: 118.6, 68.9; CH: 160.2, 132.1, 115.2; CH_0: 166.0, 163.3 ppm. IR (neat) 3116, 2946, 1456, 1398 cm^{-1}. HRMS (ESI) Calculated for $C_7H_8N_2OCl$ *m/z* 171.0325 (M+H), Obsd. 171.0334.

5b

2-(Allyloxy)-4-bromopyrimidine (5b). To a stirring solution of allyl alcohol (0.081 mL, 1.19 mmol, 1.1 equiv) in THF (5 mL) at 0 °C, 1M $KOBu^t$ in THF (1.3 mL, 1.3 mmol, 1.2 equiv) was slowly added. The reaction was allowed to stir for 15 min. The resulting potassium salt of allyl alcohol was added dropwise to a stirring solution of bromosulfone **13b** (0.253 g, 1.07 mmol, 1.0 equiv) in THF (10 mL) at -78 °C. The internal temperature during addition was maintained around -78 °C to prevent the formation of 2,4-bis(allyloxypyrimidine). The reaction was allowed to react for another 2h at -78 °C. The mixture was diluted with diethyl ether (20 mL) and was washed with distilled H_2O (2 × 10 mL) and brine (10 mL). The organic layer was then dried with anhydrous sodium sulfate, filtered, and concentrated under reduced pressure. The crude product was further purified by flash chromatography using 30% EtOAc/hexanes affording allyloxypyrimidine **5b** (0.208 g, 91% yield) as a colorless oil, which was stored at sub-zero temperatures to avoid decomposition. R_f = 0.34 (30% EtOAc/hexanes). ^{1}H NMR (500 MHz, $CDCl_3$): δ 8.26 (d, J = 4.9Hz, 1H), 7.13 (d, J = 5.4 Hz, 1H), 6.05 (tdd, J = 17.1, 10.3, 5.9 Hz, 1H), 5.42 (tdd, J = 17.1, 1.5, 1.5 Hz, 1H), 5.27 (tdd, J = 10.8, 1.5, 1.5 Hz, 1H), 4.88 (ddd, J = 5.4, 1.5, 1.5 Hz, 2H) ppm. ^{13}C NMR (125 MHz, $CDCl_3$) δ 164.4, 159.5, 153.9, 132.1, 119.2, 118.6, 69.0 ppm. ^{13}C DEPT (125 MHz, $CDCl_3$) δ CH_2: 118.6, 69.0; CH: 159.5, 132.1, 118.2; CH_0: 164.4, 153.9 ppm. IR (neat) 3110, 2987, 2946, 1558, 1534cm^{-1}. HRMS (ESI) Calculated for $C_7H_8N_2OBr$ *m/z* 214.9820 (M+H), Obsd. 214.9823.

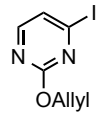

5c

2-(Allyloxy)-4-iodopyrimidine (5c). To a stirring solution of allyl alcohol (0.0240 mL, 0.352 mmol, 1.1 equiv) in THF (5 mL) at 0 °C, 1M $KOBu^t$ in THF (0.378 mL, 0.378 mmol, 1.2 equiv) was slowly added. The reaction was allowed to stir for 15 min. The resulting potassium salt of allyl alcohol was added dropwise to a stirring solution of iodosulfone **13c** (0.0894 g, 0.315 mmol, 1.0 equiv) in THF (5 mL) at -78 °C. The internal temperature during addtion was maintained around -78 °C to prevent the formation of 2,4-bis(allyloxypyrimidine). The reaction was allowed to react for another 2h at -78 °C. The mixture was diluted with diethyl ether (25 mL) and was washed with distilled H_2O (2 × 20 mL) and brine (20 mL). The organic layer was then dried with anhydrous sodium sulfate, filtered, and concentrated under reduced pressure. The crude product was further purified by flash chromatography using 30% EtOAc/hexanes affording allyloxypyrimidine **5c** (0.0825 g, 82% yield) as a colorless oil. R_f = 0.34 (30% EtOAc/hexanes). ^{1}H NMR (500 MHz, $CDCl_3$): δ 8.01 (d, J = 5.4 Hz, 1H), 7.38 (d, J = 5.4 Hz, 1H), 6.05 (tdd, J = 16.6, 10.3, 5.9 Hz, 1H), 5.42 (tdd, J = 17.1, 1.5, 1.5 Hz, 1H), 5.27 (tdd, J = 10.3, 1.5, 1.4 Hz, 1H), 4.88 (ddd, J = 5.9, 1.5, 1.5 Hz, 2H) ppm. ^{13}C NMR (125 MHz, $CDCl_3$) δ 163.7, 158.3, 132.2, 130.7, 126.3, 118.7, 69.0 ppm. ^{13}C DEPT (125 MHz, $CDCl_3$) δ CH_2: 118.7, 69.0; CH: 158.3, 132.2, 126.3; CH_0: 163.7, 158.3 ppm. IR (neat) 3099, 3019, 2942, 1548, 1529 cm^{-1}. HRMS (ESI) Calculated for $C_7H_7N_2ONaI$ *m/z* 284.9501 (M+Na), Obsd. 284.9503.

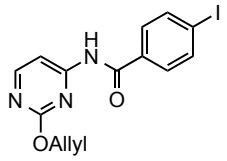

14

***N*-(2-(Allyloxy)pyrimidin-4-yl)-4-iodobenzamide (14).** Representative procedure: Under a positive pressure of argon, a dry pressure flask was charged with recrystallized CuI (0.0032 g, 0.0166 mmol, 0.1 equiv), 1,10-Phenanthroline (0.0066 g, 0.0332 mmol, 0.2 equiv), anhydrous K_3PO_4 (0.0705 g, 0.332 mmol, 2.1 equiv), allyloxypyrimidine **5c** (0.0408 g, 0.156 mmol, 1.0 equiv), and 4-Iodobenzamide **6** (0.0410 g, 0.166 mmol, 1.1 equiv). The flask was then quickly fitted with a rubber septum. 1,4-Dioxane (2.0 mL) was added to the mixture and was used to wash the walls of the pressure tube. The rubber septum was quickly replaced with the pressure tube cap. The reaction was stirred and heated at 120 °C for 18h. The reaction mixture was then diluted with EtOAc (10 mL), filtered through a pad of celite and concentrated. Flash chromatography (10% EtOAc/hexanes) afforded the title compound (0.0428 g, 72%) as white solid. R_f = 0.23 (20% EtOAc/hexanes). Mp 110 °C. ^{1}H NMR (500 MHz, $CDCl_3$) δ 8.62 (s, 1H), 8.47 (d, J = 5.4 Hz, 1H), 7.94 (d, J = 5.4 Hz, 1H), 7.86 (d, J = 8.8 Hz, 2H), 7.61 (d, J = 8.8, Hz 2H), 6.05 (tdd, J = 17.6, 10.8, 5.4 Hz, 1H), 5.40 (tdd, J = 17.1, 3.4, 2.0 Hz, 1H), 5.27 (tdd, J = 10.3, 2.9, 1.5 Hz, 1H), 4.85 (ddd, J= 5.9, 1.5, 1.5 Hz, 1H). ^{13}C NMR (125 MHz, $CDCl_3$) δ 165.5, 164.7, 161.0, 159.2, 138.4, 132.8, 132.7, 128.9, 118.1, 104.4, 100.6, 68.3 ppm. ^{13}C DEPT (125 MHz, $CDCl_3$) δ CH_2: 118.1, 68.3; CH: 161.0, 138.5, 132.7, 128.9, 104.4; CH_0: 165.4, 164.6, 159.2, 100.6 ppm. IR (neat) 3299, 3164, 2987, 1687, 1574, 1346, 1282 cm^{-1}. HRMS (ESI) Calculated for $C_{14}H_{12}N_3O_2NaI$ *m/z* (M+Na) 403.9872, Obsd. 403.9870.

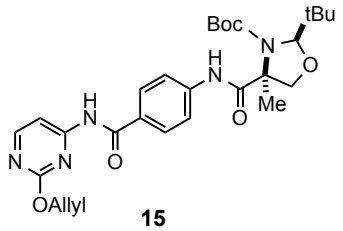

15

(2*R*,4*S*)-*tert*-Butyl 4-((4-((2-(allyloxy)pyrimidin-4-yl)carbamoyl) phenyl) carbamoyl)-2-(*tert*-butyl)-4-methyloxazolidine-3-carboxylate (15).

METHOD A (single *N*-aryl amidation reaction): Under a positive pressure of argon, a dry pressure flask was charged with recrystallized CuI (0.0166 g, 0.0872 mmol, 0.1 equiv), anhydrous K_2CO_3 (0.2419 g, 1.75 mmol, 2.0 equiv), pyrimidylbenzamide **14** (0.330 g, 0.865 mmol, 0.99 equiv), and carboxamide **7** (0.250 g, 0.872 mmol, 1.0 equiv). The flask was then quickly fitted with a rubber septum. N^1,N^2-Dimethylethane-1,2-diamine (0.019 mL, 0.175 mmol, 0.2 equiv) was added into the reaction mixture. 1,4-Dioxane (3.0 mL) was added to the mixture and was used to wash the walls of the pressure tube. The rubber septum was quickly replaced with the pressure tube cap. The reaction was stirred and heated at 100 ^oC for 60h. The reaction mixture was then diluted with EtOAc (10 mL), washed with CH_2Cl_2 (10 mL), and filtered through a pad of celite and concentrated. Flash chromatography (10% EtOAc/hexanes) afforded the title compound (0.4711 g, 92%) as colorless oil.

METHOD B (one-pot sequential *N*-amidation): Under a positive pressure of argon, a dry pressure flask was charged with recrystallized CuI (0.0046 g, 0.0240 mmol, 0.1 equiv), 1,10-Phenanthroline (0.0095 g, 0.0480 mmol, 0.2 equiv), anhydrous K_3PO_4 (0.203 g, 0.960 mmol, 4.0 equiv), allyloxypyrimidine **5b** (0.0517 g, 0.240 mmol, 1.0 equiv), and 4-Iodobenzamide **6** (0.0593 g, 0.240 mmol, 1.0 equiv).

The flask was then quickly fitted with a rubber septum. 1,4-Dioxane (3.0 mL) was added to the mixture and was used to wash the walls of the pressure tube. The rubber septum was quickly replaced with the pressure tube cap. The reaction was stirred and heated at 120 °C for 18h. The reaction was monitored by thin layer chromatography. After the first reaction was done, carboxamide **7** (0.0687 g, 0.240 mmol, 1.0 equiv) was added to the reaction mixture. A solution of recrystallized CuI (0.0046 g, 0.0240 mmol, 0.1 equiv) and N^1,N^2-Dimethylethane-1,2-diamine (0.0052 mL, 0.0480 mmol, 0.2 equiv) in 1,4-Dioxane (1 mL) was added into the reaction mixture. The reaction was stirred and heated at 100 °C for 60h. The reaction cooled down to room temperature and was then diluted with EtOAc (10 mL), filtered through a pad of celite, washed with CH_2Cl_2 (10 mL), and concentrated. Flash chromatography (10% EtOAc/hexanes) afforded the title compound (0.0685 g, 53%) as colorless oil. R_f = 0.23 (20% EtOAc/hexanes). $[\alpha]^{20}_D$ = -67.5 (*c* = 0.45, $CHCl_3$). ^{1}H NMR (500 MHz, CD_3OD): δ 8.38 (d, *J* = 5.9 Hz, 1H), 7.97 (d, *J* = 8.3 Hz, 2H), 7.90 (d, *J* = 5.4 Hz, 1H), 7.67 (d, *J* = 8.3 Hz, 2H), 6.08 (tdd, *J* = 17.6, 10.3, 5.4 Hz, 1H), 5.41 (tdd, *J* = 17.6, 2.0, 1.5 Hz, 1H), 5.24 (tdd, *J* = 17.6, 1.5, 1.0 Hz, 1H), 5.17 (s, 1H), 4.86 (ddd, *J* = 5.4, 1.5, 1.5 Hz, 2H), 4.69 (d, *J* = 8.3 Hz, 1H), 3.78 (d, *J* = 8.8 Hz, 1H), 1.69 (s, 3H), 1.53 (s, 9H), 0.91 (s, 9H) ppm. ^{13}C NMR (125 MHz, CD_3OD) δ 173.2, 168.2, 165.7, 161.8, 161.3, 157.2, 143.5, 134.3, 130.6, 130.4, 120.4, 118.3, 105.5, 99.2, 84.1, 77.0, 69.5, 69.1, 39.2, 28.6, 26.8, 22.2 ppm. ^{13}C DEPT (125 MHz, $CDCl_3$) δ CH_3: 28.6, 26.8, 22.2; CH_2: 118.3, 77.0, 69.2; CH: 161.3, 134.3, 130.6, 120.4, 105.5, 99.2; CH_0: 173.2, 168.2, 165.7, 161.8, 157.2, 143.5, 130.4, 99.2, 84.1, 69.6, 39.2 ppm. IR (neat) 3260, 3052, 2975, 1689, 1587 cm^{-1}. HRMS (ESI) Calculated for $C_{28}H_{37}N_5O_6Na$ *m/z* 562.2642 (M+Na), Obsd. 562.2650.

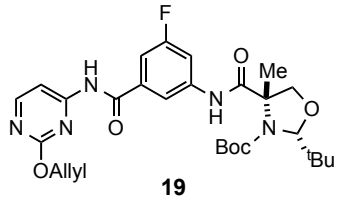

19

(2*R*,4*S*)-*tert*-Butyl 4-((3-((2-(allyloxy)pyrimidin-4-yl)carbamoyl)-5-fluorophenyl)carbamoyl)-2-(*tert*-butyl)-4-methyloxazolidine-3-carboxylate (19). METHOD A (separate *N*-aryl amidation reaction) 1st Amidation reaction: Under a positive pressure of argon, a dry pressure flask was charged with recrystallized CuI (0.0045 g, 0.0236 mmol, 0.1 equiv), 1,10-Phenanthroline (0.0094g, 0.047 mmol, 0.2 equiv), anhydrous K_3PO_4 (0.100 g, 0.471 mmol, 2.1 equiv), allyloxypyrimidine **5c** (0.0510 g, 0.237 mmol, 1.0 equiv), and 3-Bromo-5-Flurobenzamide **17** (0.0518 g, 0.237 mmol, 1.0 equiv). The flask was then quickly fitted with a rubber septum. 1,4-Dioxane (4.0 mL) was added to the mixture and was used to wash the walls of the pressure tube. The rubber septum was quickly replaced with the pressure tube cap. The reaction was stirred and heated at 120 °C for 36h. The reaction mixture was then diluted with EtOAc (10 mL), filtered through a pad of celite and concentrated. Flash chromatography (10% EtOAc/hexanes) afforded the title compound (0.0475 g, 56%) as white solid. R_f = 0.37 (20% EtOAc/hexanes). The product was carried on forward without further characterization.

2nd Amidation reaction: Under a positive pressure of argon, a dry pressure flask was charged with recrystallized CuI (0.0070 g, 0.0368 mmol, 0.2 equiv), anhydrous K_3PO_4 (0.2419 g, 1.75 mmol, 2.0 equiv), product from 1st amidation reaction: *N*-(2-(allyloxy)pyrimidin-4-yl)-3-bromo-5-fluorobenzamide (0.0673 g, 0.191 mmol, 1.0 equiv), and carboxamide **7** (0.547 g, 0.191 mmol, 1.0 equiv). The flask was

then quickly fitted with a rubber septum. N^1,N^2-Dimethylethane-1,2-diamine (0.0080 mL, 0.0743 mmol, 0.4 equiv) was added into the reaction mixture. 1,4-Dioxane (4.0 mL) was added to the mixture and was used to wash the walls of the pressure tube. The rubber septum was quickly replaced with the pressure tube cap. The reaction was stirred and heated at 120 °C for 36h. The reaction mixture was then diluted with EtOAc (10 mL), filtered through a pad of celite, washed with CH_2Cl_2 (10 mL), and concentrated. Flash chromatography (10% EtOAc/hexanes) afforded the title compound (0.0499 g, 48%) as colorless oil.

METHOD B (one-pot sequential *N*-amidation): Under a positive pressure of argon, a dry pressure flask was charged with recrystallized CuI (0.0134 g, 0.0704 mmol, 0.1 equiv), 1,10-Phenanthroline (0.0279 g, 0.141 mmol, 0.2 equiv), anhydrous K_3PO_4 (0.597 g, 2.82 mmol, 4.0 equiv), allyloxypyrimidine **5b** (0.151 g, 0.702 mmol, 1.0 equiv), and 3-Bromo-5-fluorobenzamide **17** (0.230 g, 1.51 mmol, 1.5 equiv). The flask was then quickly fitted with a rubber septum. 1,4-Dioxane (5 mL) was added to the mixture and was used to wash the walls of the pressure tube. The rubber septum was quickly replaced with the pressure tube cap. The reaction was stirred and heated at 120 °C for 36h. The reaction was monitored by thin layer chromatography. The reaction did not appear to go to completion; it was then decided to add carboxamide **7** (0.3024 g, 1.06 mmol, 1.5 equiv) was added to the reaction mixture. A solution of recrystallized CuI (0.0270 g, 0.142 mmol, 0.2 equiv) and N^1,N^2-Dimethylethane-1,2-diamine (0.030 mL, 0.279 mmol, 0.4 equiv) in 1,4-Dioxane (1 mL) was added into the reaction mixture. The reaction was stirred and heated at 120 °C for 60h. The reaction cooled down to room temperature and was then diluted with EtOAc (15 mL), filtered through a pad of celite, washed with CH_2Cl_2 (10 mL), and concentrated. Flash chromatography (10%-20%

EtOAc/hexanes) afforded title compound (0.080 g, 20%) as a colorless oil. Rf= 0.43 (30% EtOAc/hexanes). $[\alpha]^{20}_{D}$ = -17.2 (*c*= 0.62, $CHCl_3$). ^{1}H NMR (500 MHz, CD_3OD): δ 8.45 (d, *J* = 5.4 Hz, 1H), 7.92 (d, *J* = 5.9 Hz, 1H), 7.84 (ddd, *J* = 9.8, 2.4, 2.0 Hz, 1H), 7.78 (ddd, *J* = 10.7, 2.0, 2.0 Hz, 1H), 7.77 (dd, *J* =3.42, 2.0 Hz, 1H), 7.47 (ddd, *J* = 8.8, 2.0, 1.5 Hz, 1H), 6.10 (tdd, *J* = 17.1, 10.7, 5.1 Hz, 1H), 5.43 (tdd, *J* = 17.6, 2.9, 1.5 Hz, 1H), 5.26 (tdd, *J* = 10.3, 2.9, 1.5 Hz, 1H), 5.18 (s, 1H), 4.90 (tdd, *J* = 5.4, 1.5, 1.5 Hz, 1H), 4.68 (d, *J* = 8.3 Hz, 1H), 3.81 (d, *J* = 8.8 Hz, 1H), 1.72 (s, 3H), 1.55 (s, 9H), 0.95 (s, 9H) ppm. ^{13}C NMR (125 MHz, CD_3OD) δ 173.5, 167.6, 164.3 (δ, $J_{C\text{-}F}$ = 244.9 Hz), 163.3, 161.7, 161.6, 157.3, 141.5 (δ, $J_{C\text{-}F}$ = 10.7 Hz), 137.9 (δ, $J_{C\text{-}F}$ = 8.4 Hz), 134.3, 118.3, 116.6, 112.1 (δ, $J_{C\text{-}F}$ = 26.7 Hz), 111.7 (δ, $J_{C\text{-}F}$ = 23.7 Hz), 105.7, 99.3, 84.3, 77.1, 69.6, 69.3, 39.3, 28.6, 26.8, 22.1ppm. ^{13}C DEPT (125 MHz, CD_3OD) δ CH_3: 28.6, 26.8, 22.1; CH_2: 118.3, 77.1, 69.3; CH: 161.6, 134.3, 116.6, 112.1 (δ, $J_{C\text{-}F}$ = 26.7 Hz), 111.7 (δ, $J_{C\text{-}F}$ = 23.7 Hz), 105.7, 99.3; CH_0: 173.5, 167.6, 164.3 (δ, $J_{C\text{-}F}$ = 244.9 Hz), 161.7, 161.6, 84.3, 69.6, 39.3 ppm. IR (neat) 3277, 3085, 2975, 1695, 1582 cm^{-1}. HRMS (ESI) Calculated for $C_{28}H_{36}N_5O_6FNa$ 580.2547 *m/z* (M+Na), Obsd. 580.2551.

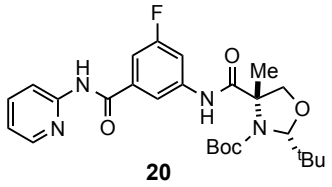

20

(2*R*,4*S*)-*tert*-Butyl 2-(*tert*-butyl)-4-((3-fluoro-5-(pyridin-2-ylcarbamoyl) phenyl)carbamoyl)-4-methyloxazolidine-3-carboxylate (20). METHOD A (separate *N*-aryl amidation reaction) 1st Amidation reaction: Under a positive pressure of argon, a dry pressure flask was charged with recrystallized CuI

(0.0291 g, 0.0153 mmol, 0.1 equiv), 1,10-Phenanthroline (0.0607g, 0.306 mmol, 0.2 equiv), anhydrous K_3PO_4 (0.650 g, 3.06 mmol, 2.1 equiv), 2-Bromopyridine **16** (0.146 mL, 0.153 mmol, 1.0 equiv), and 3-Bromo-5-Flurobenzamide **17** (0.500 g, 2.29 mmol, 1.5 equiv). The flask was then quickly fitted with a rubber septum. 1,4-Dioxane (8.0 mL) was added to the mixture and was used to wash the walls of the pressure tube. The rubber septum was quickly replaced with the pressure tube cap. The reaction was stirred and heated at 120 °C for 36h. The reaction mixture was then diluted with EtOAc (10 mL), filtered through a pad of celite and concentrated. Flash chromatography (10% EtOAc/hexanes) afforded the title compound (0.2577 g, 57%) as white solid. R_f = 0.36 (20% EtOAc/hexanes). The product was carried on forward without further characterization.

2nd Amidation reaction: Under a positive pressure of argon, a dry pressure flask was charged with recrystallized CuI (0.0070 g, 0.0172 mmol, 0.2 equiv), anhydrous K_3PO_4 (0.0730 g, 0.344 mmol, 2.0 equiv), product from 1st amidation reaction: 3-Bromo-5-fluoro-*N*-(pyridin-2-yl)benzamide (0.0508 g, 0.172 mmol, 1.0 equiv), and carboxamide **7** (0.0492 g, 0.171 mmol, 1.0 equiv). The flask was then quickly fitted with a rubber septum. N^1,N^2-Dimethylethane-1,2-diamine (0.0080 mL, 0.0743 mmol, 0.4 equiv) was added into the reaction mixture. 1,4-Dioxane (4.0 mL) was added to the mixture and was used to wash the walls of the pressure tube. The rubber septum was quickly replaced with the pressure tube cap. The reaction was stirred and heated at 120 °C for 36h. The reaction mixture was then diluted with EtOAc (10 mL), filtered through a pad of celite, washed with CH_2Cl_2 (10 mL), and concentrated. Flash chromatography (10% EtOAc/hexanes) afforded the title compound (0.0509 g, 48%) as colorless oil.

METHOD B (one-pot sequential *N*-amidation): Under a positive pressure of

argon, a dry pressure flask was charged with recrystallized CuI (0.0133 g, 0.0698 mmol, 0.1 equiv), 1,10-Phenanthroline (0.0277 g, 0.140 mmol, 0.2 equiv), anhydrous K_3PO_4 (0.593 g, 2.79 mmol, 4.4 equiv), 2-Bromopyridine **16** (0.060 mL, 0.629 mmol, 1.0 equiv), and 3-Bromo-5-fluorobenzamide **17** (0.206 g, 0.0944 mmol, 1.5 equiv). The flask was then quickly fitted with a rubber septum. 1,4-Dioxane (5 mL) was added to the mixture and was used to wash the walls of the pressure tube. The rubber septum was quickly replaced with the pressure tube cap. The reaction was stirred and heated at 120 °C for 36h. The reaction was monitored by thin layer chromatography. The reaction did not appear to go to completion; it was then decided to add carboxamide **7** (0.2702 g, 0.943 mmol, 1.5 equiv) was added to the reaction mixture. A solution of recrystallized CuI (0.0266 g, 0.140 mmol, 0.2 equiv) and N^1,N^2-Dimethylethane-1,2-diamine (0.030 mL, 0.279 mmol, 0.4 equiv) in 1,4-Dioxane (1 mL) was added into the reaction mixture. The reaction was stirred and heated at 120 °C for 60 h. The reaction cooled down to room temperature and was then diluted with EtOAc (15 mL), filtered through a pad of celite, washed with CH_2Cl_2 (15 mL), and concentrated. Flash chromatography (10-20% EtOAc/hexanes) afforded the title compound (0.0595 g, 19%) as a colorless oil. Rf= 0.38 (30% EtOAc/hexanes). $[\alpha]^{20}_D$ = -27.0, (*c* = 0.32 , $CHCl_3$). ^{1}H NMR (500 MHz, CD_3OD): δ 8.36 (dd, *J* = 4.9, 1.0 Hz, 1H), 8.20 (d, *J* = 8.3 Hz, 1H), 7.84 (ddd, *J* = 10.3, 7.3, 2.0 Hz, 1H), 7.79 (ddd, *J* = 10.7, 2.0, 2.0 Hz, 1H), 7.77 (dd, *J* =3.42, 2.0 Hz, 1H), 7.49 (ddd, *J* = 8.8, 2.4, 1.5 Hz, 1H), 7.18 (ddd, *J* = 7.3, 4.9, 1.0 Hz, 1H), 5.19 (s, 1H), 4.69 (d, *J* = 8.8 Hz, 1H), 3.81 (d, *J* = 8.8 Hz, 1H), 1.71 (s, 3H), 1.55 (s, 9H), 0.95 (s, 9H) ppm. ^{13}C NMR (125 MHz, CD_3OD) δ 173.5. 166.9, 164.3 (δ, $J_{C\text{-}F}$ = 244.9 Hz), 157.3, 153.2, 149.3, 141.5 (δ, $J_{C\text{-}F}$ = 11.5 Hz), 139.8, 138.6 (δ, $J_{C\text{-}F}$ = 7.6 Hz), 121.6, 116.6, 116.3, 111.7 (δ, $J_{C\text{-}F}$ = 26.7 Hz), 111.4 (δ, $J_{C\text{-}F}$ = 24.4 Hz), 99.3, 84.2, 77.1, 69.6,

39.3, 28.6, 26.8, 22.1 ppm. ^{13}C DEPT (125 MHz, CD_3OD) δ CH_3: 28.6, 26.8, 22.1; CH_2: 77.1; CH: 149.3, 139.8, 121.6, 116.6, 116.3, 111.7 (δ, $J_{C\text{-}F}$ = 26.7 Hz), 111.4 (δ, $J_{C\text{-}F}$ = 24.4 Hz), 99.3; CH_0: 173.5, 167.6, 164.3 (δ, $J_{C\text{-}F}$ = 244.9 Hz), 173.5, 166.9, 164.3 (δ, $J_{C\text{-}F}$ = 244.9 Hz), 157.3, 84.2, 69.6, 39.3 ppm. IR (neat) 3257, 2975, 1685, 1433 cm^{-1}. HRMS (ESI) Calculated for $C_{26}H_{33}N_4O_5FNa$ 523.2333 *m/z* (M+Na), Obsd. 523.2334.

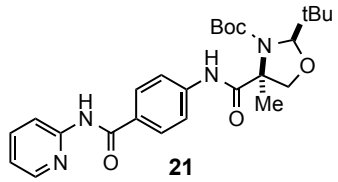

21

(2*R*,4*S*)-*tert*-Butyl 2-(*tert*-butyl)-4-methyl-4-((4-(pyridin-2-ylcarbamoyl) phenyl)carbamoyl)oxazolidine-3-carboxylate (21). METHOD A: (separate *N*-aryl amidation reaction) 1st Amidation reaction: Under a positive pressure of argon, a dry pressure flask was charged with recrystallized CuI (0.0120 g, 0.0633 mmol, 0.1 equiv), 1,10-Phenanthroline (0.0250 g, 0.131 mmol, 0.2 equiv), anhydrous K_3PO_4 (0.2687 g, 0.127 mmol, 2.0 equiv), 2-Bromopyridine **16** (0.060 mL, 0.237 mmol, 1.0 equiv), and 4-Iodobenzamide **6** (0.1564 g, 0.633 mmol, 1.0 equiv). The flask was then quickly fitted with a rubber septum. 1,4-Dioxane (6.0 mL) was added to the mixture and was used to wash the walls of the pressure tube. The rubber septum was quickly replaced with the pressure tube cap. The reaction was stirred and heated at 120 °C for 36h. The reaction mixture was then diluted with EtOAc (10 mL), filtered through a pad of celite and concentrated. Flash chromatography (10% EtOAc/hexanes) afforded the title compound (0.119 g, 58%) as white solid. R_f = 0.35 (20% EtOAc/hexanes). The product was carried on forward without further

characterization.

2nd Amidation reaction: Under a positive pressure of argon, a dry pressure flask was charged with recrystallized CuI (0.0062 g, 0.0326 mmol, 0.1 equiv), anhydrous K_3PO_4 (0.1327 g, 0.652 mmol, 2.0 equiv), product from 1st amidation reaction: 4-Iodo-*N*-(pyridin-2-yl)benzamide (0.1057 g, 0.326 mmol, 1.0 equiv), and carboxamide **7** (0.0933 g, 0.326 mmol, 1.0 equiv). The flask was then quickly fitted with a rubber septum. N^1,N^2-Dimethylethane-1,2-diamine (0.0080 mL, 0.0743 mmol, 0.2 equiv) was added into the reaction mixture. 1,4-Dioxane (4.0 mL) was added to the mixture and was used to wash the walls of the pressure tube. The rubber septum was quickly replaced with the pressure tube cap. The reaction was stirred and heated at 100 °C for 36h. The reaction mixture was then diluted with EtOAc (10 mL), filtered through a pad of celite, washed with CH_2Cl_2 (10 mL), and concentrated. Flash chromatography (10% EtOAc/hexanes) afforded the title compound (0.128 g, 81%) as colorless oil.

METHOD B (one-pot sequential *N*-amidation): Under a positive pressure of argon, a dry pressure flask was charged with recrystallized CuI (0.0070 g, 0.0368 mmol, 0.1 equiv), 1,10-Phenanthroline (0.0138 g, 0.0696 mmol, 0.2 equiv), anhydrous K_3PO_4 (0.296 g, 1.39 mmol, 4.4 equiv), 2-Bromopyridine **16** (0.030 mL, 0.314 mmol, 1.0 equiv), and 4-Iodobenzamide **6** (0.0593 g, 0.240 mmol, 1.0 equiv). The flask was then quickly fitted with a rubber septum. 1,4-Dioxane (3.0 mL) was added to the mixture and was used to wash the walls of the pressure tube. The rubber septum was quickly replaced with the pressure tube cap. The reaction was stirred and heated at 120 °C for 36h. The reaction was monitored by thin layer chromatography. The reaction did not appear to go to completion; it was then decided to add carboxamide **7** (0.150 g, 0.523 mmol, 1.5 equiv) was added to the

reaction mixture. A solution of recrystallized CuI (0.014 g, 0.0735 mmol, 0.2 equiv) and N^1,N^2-Dimethylethane-1,2-diamine (0.015 mL, 0.140 mol, 0.4 equiv) in 1,4-dioxane (1 mL) was added into the reaction mixture. The reaction was stirred and heated at 120 °C for 60h. The reaction was cooled down to room temperature and then diluted with EtOAc (15 mL), filtered through a pad of celite, washed with CH_2Cl_2 (15 mL), and concentrated. Flash chromatography (10%-20% EtOAc/hexanes) afforded title compound (0.0548 g, 36%) as a colorless oil. Rf= 0.26 (30% EtOAc/hexanes). $[\alpha]^{20}_D$ = -25.8, (*c* = 0.71 , $CHCl_3$). ^{1}H NMR (500 MHz, CD_3OD): δ 8.36 (d, *J* = 8.3, 1.0 Hz, 1H), 8.22 (d, *J* = 8.3 Hz, 1H), 7.99 (d, *J* = 8.3, Hz, 2H), 7.81 (ddd, *J* = 8.8, 8.8, 1.5 Hz, 1H), 7.68 (d, *J* =8.8 Hz, 2H), 7.14 (dd, *J* = 7.3, 5.3 Hz, 1H), 5.18 (s, 1H), 4.69 (d, *J* = 8.3 Hz, 1H), 3.79 (d, *J* = 8.8 Hz, 1H), 1.70 (s, 3H), 1.54 (s, 9H), 0.94 (s, 9H) ppm. ^{13}C NMR (125 MHz, CD_3OD) δ 173.3, 167.7, 157.2, 153.4, 149.2, 143.1, 139.7, 131.3, 130.2, 121.3, 120.5, 116.4, 99.2, 84.1, 77.1, 69.6, 39.3, 28.6, 26.8, 22.2 ppm. ^{13}C DEPT (125 MHz, CD_3OD) δ CH_3: 28.6, 26.8, 22.2; CH_2: 77.1; CH: 149.2, 139.7, 130.2, 121.3, 120.5, 116.4, 99.2; CH_0: 173.3, 167.7, 157.2, 153.4, 143.1, 131.3, 84.1, 69.6, 39.2 ppm. IR (neat) 3291, 2974, 1675, 1507, 1432 cm^{-1}. HRMS (ESI) Calculated for $C_{26}H_{34}N_4O_5Na$ 505.2427 *m/z* (M+Na), Obsd. 505.2425.

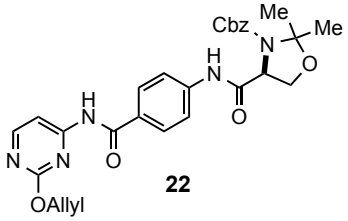

22

(*S*)-Benzyl 4-(4-(2-(allyloxy)pyrimidin-4-ylcarbamoyl)phenylcarbamoyl) -2,2-dimethyloxazolidine-3-carboxylate, (22). METHOD A (single *N*-aryl

amidation reaction): Under a positive pressure of argon, a dry pressure flask was charged with recrystallized CuI (0.0030 g, 0.016 mmol, 0.1 equiv), anhydrous K_2CO_3 (0.0365 g, 0.264 mmol, 2.0 equiv), pyrimidylbenzamide **14** (0.055 g, 0.131 mmol, 1.0 equiv), and *des*-methyl carboxamide **18**:[3] *(S)*-Benzyl 4-carbamoyl-2,2-dimethyloxazolidine-3-carboxylate (0.0506 g, 0.182 mmol, 1.4 equiv). The flask was then quickly fitted with a rubber septum. N^1,N^2-Dimethylethane-1,2-diamine (0.005 mL, 0. 046 mmol, 0.35 equiv) was added into the reaction mixture. 1,4-Dioxane (4.0 mL) was added to the mixture and was used to wash the walls of the pressure tube. The rubber septum was quickly replaced with the pressure tube cap. The reaction was stirred and heated at 100 °C for 36h. The reaction mixture was then diluted with EtOAc (10 mL), filtered through a pad of celite, washed with CH_2Cl_2 (10 mL), concentrated. Flash chromatography (10% EtOAc/hexanes) afforded the title compound (0.045 g, 64%) as colorless oil.

METHOD B (one-pot sequential *N*-amidation): Under a positive pressure of argon, a dry pressure flask was charged with recrystallized CuI (0.0064 g, 0.0335 mmol, 0.1 equiv), 1,10-Phenathroline (0.0133 g, 0.0676 mmol, 0.2 equiv), anhydrous K_3PO_4 (0.287 g, 1.35 mmol, 4.0 equiv), allyloxypyrimidine **5b** (0.0720 g, 0.335 mmol, 1.0 equiv), and 4-Iodobenzamide **6** (0.0827 g, 0.335 mmol, 1.0 equiv). The flask was then quickly fitted with a rubber septum. 1,4-Dioxane (4.0 mL) was added to the mixture and was used to wash the walls of the pressure tube. The rubber septum was quickly replaced with the pressure tube cap. The reaction was stirred and heated at 120 °C for 24h. The reaction was monitored by thin layer

---

[3] Cossu, S.; Conti, S.; Giacomelli, G.; Falorni, M. *Synthesis*, **1994**, *12*, 1429-1432.

chromatography. After the first reaction was done, *des*-methyl carboxamide **18**:[5] (*S*)-Benzyl 4-carbamoyl-2,2-dimethyloxazolidine-3-carboxylate (0.0930 g, 0.334 mmol, 1.0 equiv) was added to the reaction mixture. A solution of recrystallized CuI (0.0128 g, 0.0676 mmol, 0.2 equiv) and N^1,N^2-Dimethylethane-1,2-diamine (0.0146 mL, 0.135 mmol, 0.4 equiv) in 1,4-dioxane (1 mL) was added into the reaction mixture. The reaction was stirred and heated at 100 °C for 36 h. The reaction was cooled down to room temperature and was then diluted with EtOAc (10 mL), filtered through a pad of celite, washed with CH_2Cl_2 (10 mL), and concentrated. Flash chromatography (50% EtOac/hexanes) afforded title compound (0.0520 g, 29%) as a colorless oil. Rf= 0.25 (50% EtOAc/hexanes). $[\alpha]^{20}_D$ = -63.6, (*c* = 0.805, $CHCl_3$). ^{1}H NMR (500 MHz, CD_3OD) mixture of rotomers (3:1), minor rotamer indicated by an asterisk: δ 8.40 (d, *J*= 5.4 Hz, 1H), 7.95 (d, *J*= 8.3 Hz, 2H), 7.92 (d, *J*= 5.7 Hz, 1H), 7.72 (d, *J*= 8.3 Hz, 1H), 7.67 (d, *J*= 8.3 Hz, 1H), 7.41-7.35 (m, 2H), 7.21 (d, *J*= 6.8 Hz, 1H), 7.15 (t, *J*= 6.9 Hz, 1H), 7.10 (t, *J*= 7.3 Hz, 1H), 6.09 (tdd, *J*= 17.1, 10.7, 5.4 Hz, 1H), 5.41 (dd, *J*= 17.1, 1.0, 1H), 5.25 (dd, *J*= 10.7, 1.0 Hz, 1H), 5.17 (dd, *J*= 19.0, 11.7 Hz, 1H), 5.11 (d, *J*= 12.2 Hz, 1H), 4.96 (d, *J*= 12.2 Hz, 1H), 4.89 (s, 1H), 4.61* (bs, 1H), 4.31 (dd, *J*= 6.8, 3.9 Hz, 1H), 4.34* (dd, *J*= 8.8, 7.3 Hz, 1H), 4.30 (dd, *J*= 8.8, 7.3 Hz, 1H), 4.11* (dd, *J*= 7.3 Hz, 3.4 Hz, 1H), 4.07 (dd, *J*= 8.8 Hz, 3.4 Hz, 1H), 1.73 (s, 3H), 1.66* (s, 3H), 1.59 (s, 3H), 1.52* (s, 3H) ppm. ^{13}C NMR (125 MHz, CD_3OD) δ 171.3, 170.9*, 168.5, 165.8, 161.9, 161.4, 154.8*, 153.8, 144.0, 137.5, 134.3, 130.4, 130.2*, 129.8, 129.5*, 129.4*, 129.2, 128.9, 120.5, 118.3, 105.5, 96.8, 96.4*, 69.2, 68.9, 68.9*, 68.4, 68.3, 67.9, 62.6*, 62.0*, 26.4*, 25.7*, 25.2, 24.9 ppm. IR (neat) 2986, 2940, 1682, 1585, 1502 cm^{-1}. HRMS (ESI) Calculated for $C_{28}H_{30}N_5O_6$ *m/z* (M+) 532.2196, Obsd. 532.2198.

3

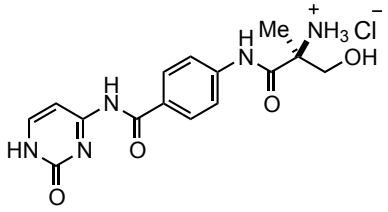

(S)-3-Hydroxy-2-methyl-1-oxo-1-((4-((2-oxo-1,2-dihydropyrimidin-4-yl) carbamoyl)phenyl)amino)propan-2-aminium chloride (3). A dry microwave reaction tube was charged with masked cytimidine **15** (0.0306 g, 0.0567 mmol, 1.0 equiv). 4*N* HCl (1 mL) was then added. The reaction was heated to 70 ºC for 15 min in the microwave (200 W). The reaction was monitored every 2 minutes. The reaction was allowed to cool down to room temperature and transferred to a round bottom flask. Excess HCl was removed by addition of MeOH (7 × 10 mL) and concentrating the mixture. The excess H_2O was then removed azeotropically by rotovaping the crude product with toluene (3 × 10 mL). The crude product was then washed with ether (3 × 10 mL). The product was then dried under reduced pressure to give the pure title compound **3** (0.0167 g, 80%) as a white solid. R_f = 0.22 (50% MeOH/EtOAc). Mp 260-262 °C. $[\alpha]^{20}_D$ = -2.0 (*c* = 0.20, CH_3OH). ^{1}H NMR (500 MHz, CD_3OD): δ 7.99 (d, *J* = 8.3 Hz, 2H), 7.77 (d, *J* = 8.8 Hz, 2H), 7.74 (d, *J* = 6.8 Hz, 1H), 6.02 (d, *J* = 6.8 Hz, 2H), 4.11 (d, *J* = 12.1 Hz, 1H), 3.83 (d, *J* = 11.7 Hz, 1H), 1.65 (s, 3H) ppm. ^{13}C NMR (125 MHz, CD_3OD) δ 170.2, 169.4, 162.5, 149.23 148.2, 143.7, 131.8, 127.9, 121.4, 94.0, 65.5, 63.7, 19.1 ppm. ^{13}C DEPT (125 MHz, CD_3OD) δ CH_3: 19.1; CH_2: 65.5; CH: 148.2, 131.8, 121.4, 94.0; CH_0: 170.2, 169.4, 162.5, 149.3, 143.7, 127.9, 63.7 ppm. IR (neat) 3551, 3048, 2983, 1715, 1659, 1604 cm^{-1}. HRMS (ESI) Calculated for $C_{15}H_{18}N_5O_4$ 332.1359 *m/z* (M+H), Obsd. 332.1370.

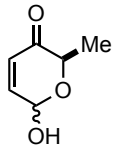

25

(2*R*)-6-hydroxy-2-methyl-2*H*-pyran-3(6*H*)-one (25). To a flask was added acetylfuran **4** (15.0 g, 136 mmol, 1 equiv), CH_2Cl_2 (240 mL), formic acid/triethylamine (5:2 (molar ratio), 50 mL) and Noyori asymmetric transfer hydrogenation catalyst (*R*)-Ru(η6-*p*-cymene)-(*R,R*)-TsDPEN (290 mg, 0.36 mol%). The resulting solution was stirred at room temperature for 24 h. The reaction mixture was diluted with water (500 mL) and extracted with Et_2O (100 mL × 3). The combined organic layers were washed with saturated aqueous NaHCO3, dried over Na2SO4. The excess solvent was removed by carefully evaporating the solvent under atmospheric pressure. The resulting semi-crude furfuryl alcohol was dissolved in of THF/H_2O (1000 mL, 3:1 (v/v)) and cooled to 0 ˚C. To this solution, solid $NaHCO_3$ (22.9 g, 272.4 mmol, 2 equiv), $NaOAc \cdot 3H_2O$ (18.5 g, 136.2 mmol, 1 equiv), and recrystallized NBS (64.3 g, 136.2 mmol, 1 equiv) were added and the mixture was stirred for 1h at 0 ˚C. The reaction mixture was extracted with cold Et_2O (3 × 200 mL) and the combined organic layer was washed by cold saturated brine (100 mL), dried over Na_2SO_4. The solvent was removed under reduced pressure to give a residue, which was rapidly subjected to purification *via* flash chromatography on silica gel. Elution with 50% EtOAc/hexane gave a diastereomeric mixture of pyranone hemiacetal **25** (10.6 g, 61%, α:ß=2.3:1) as a yellow oil. *Rf*= 0.35 (50% EtOAc/hexanes). ^{1}H NMR (500 MHz, $CDCl_3$) α isomer: δ 6.90 (dd, *J* = 10.2, 3.4 Hz, 1H), 6.10 (d, *J* = 10.3, 1H), 5.63 (dd, *J* = 4.4, 3.6 Hz, 1H), 4.71 (q, *J* = 6.8 Hz, 1H), 3.73 (d, *J* = 5.1, 1H) OH, 1.38 (d, *J* = 6.8 Hz, 3H) ppm; ß isomer: δ 6.94 (dd, *J* = 10.3,

1.47 Hz, 1H), 6.14, (dd, *J* = 10.3, 1.7, 1H), 5.67 (dd, *J* = 7.3, 1.2 Hz, 1H), 4.23 (dq, *J* = 6.8, 1.2 Hz, 1H), 4.04 (d, *J* = 7.3, 1H) OH, 1.45 (d, *J* = 6.8 Hz, 3H) ppm. ^{13}C NMR (125 MHz, $CDCl_3$) α isomer: δ 197.2, 144.7, 127.4, 87.7, 70.6, 15.5 ppm; β isomer: 196.8, 148.4, 128.7, 91.2, 75.4, 16.4 ppm. ^{13}C DEPT (125 MHz, $CDCl_3$) α isomer: δ CH_3: 15.5; CH: 144.7, 127.4, 87.7, 70.6 ; CH_0: 197.2 ppm; β isomer: δ CH_3: 16.4; CH: 148.4, 128.7, 91.2, 75.4 ; CH_0: 196.8 ppm. IR (neat) 3388, 2987, 2940, 1691 cm^{-1}. HRMS (ESI) Calculated for $C_6H_8O_3Na$ 151.0371 *m/z* (M+Na), Obsd. 151.0381.

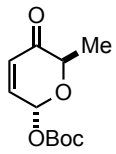

26

***tert*-butyl ((2*R*,6*R*)-6-methyl-5-oxo-5,6-dihydro-2*H*-pyran-2-yl) carbonate (26).** The mixture of pyranone hemiacetal **25** (0.162 g, 1.26 mmol, 1 equiv) was dissolved in CH_2Cl_2 (10 mL) and the solution was cooled to –78 ˚C. $(Boc)_2O$ (0.550 g, 2.82 mmol, 2.2 equiv) and DMAP (10.8 mg, 0.0882 mmol, 7 mol %) was added to the reaction mixture. After stirring for 12h, the reaction was quenched with aqueous saturated $NaHCO_3$, extracted with Et_2O, dried over Na_2SO_4, and concentrated under reduced pressure. The crude product was subjected to purification *via* flash chromatography using silica gel and eluting with 15% EtOAc/hexanes to give α-Boc-pyranone **26** (0.138 g, 49%) as a colorless oil. *Rf*= 0.48 (20% EtOAc/hexane); $[\alpha]^{20}_D$ = -1.84 (*c* = 2.64, $CHCl_3$). ^{1}H NMR (500 MHz, $CDCl_3$) δ 6.87 (dd, *J* = 10.3, 3.9 Hz, 1H), 6.22 (d, *J* = 3.4 Hz, 1H), 6.20 (d, *J* = 10.3 Hz, 1H), 4.65 (q, *J* = 6.8 Hz, 1H), 1.53 (s, 9H), 1.42 (d, *J* = 6.35 Hz, 3H) ppm. ^{13}C NMR (125 MHz, $CDCl_3$) δ 196.0, 152.1, 141.2, 128.7, 89.4, 83.9, 72.4, 27.9, 15.4 ppm. ^{13}C DEPT

(125 MHz, $CDCl_3$) δ CH_3: **27**.9, 15.4; CH: 141.2, 128.7, 89.4, 72.4 ; CH_0: 196.0 ppm. IR (neat) 2983, 2941, 1748, 1701 cm^{-1}. HRMS (ESI): Calculated for $C_{11}H_{16}O_5Na$ *m/z* (M+Na) 251.0895, Obsd. 251.0896.

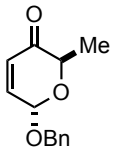

27

(2*R*,6*S*)-6-(benzyloxy)-2-methyl-2*H*-pyran-3(6H)-one (27) Benzyl alcohol (0.144 mL, 1.39 mmol, 2 equiv) was added to a solution of α-Boc pyranone **26** (0.158 g, 0.694 mmol, 1 equiv) in CH_2Cl_2 (5 mL). The mixture was cooled to 0 °C. A solution of $Pd_2(dba)_3$ (15.9 mg, 0.01735 mmol, 2.5 mol%) and PPh_3 (18.2 mg, 0.0694 mmol, 10 mol%) in CH_2Cl_2 (4 mL) was added to the reaction mixture at 0 °C. The reaction was kept at 0 °C. After 24 h, the reaction mixture was quenched with saturated aqueous $NaHCO_3$ (10 mL), extracted with CH_2Cl_2 (3 × 5 mL), dried over Na_2SO_4, and concentrated under reduced pressure. The crude product was purified *via* silica gel flash chromatography eluting with 20% EtOAc/hexanes to give the title compound **27** (0.104, 69%) as colorless oil. *Rf*= 0.43 (20% EtOAc/hexanes). $[\alpha]^{20}_D$ = -22.7 (*c* = 1.35, $CHCl_3$). ^{1}H NMR (500 MHz, $CDCl_3$) δ 7.39-7.32 (m, 5H), 6.85 (dd, *J* = 10.3, 3.9 Hz, 1H), 6.10 (d, *J* = 10.3 Hz, 1H), 5.29 (d, *J* = 3.4 Hz, 1H), 4.83 (d, *J* = 11.7 Hz, 1H), 4.70 (d, *J* = 11.7 Hz, 1H), 4.57 (q, *J* = 6.8 Hz, 1H), 1.37 (d, *J* = 6.4 Hz, 3H) ppm. ^{13}C NMR (125 MHz, $CDCl_3$) δ 197.2, 143.6, 137.4, 128.8, 128.8, 128.4, 128.3, 128.3, 127.7, 92.6, 71.0, 70.7, 15.4 ppm. ^{13}C DEPT (125 MHz, $CDCl_3$) δ CH_3: 15.4; CH_2: 71.0; CH: 143.6, 128.8, 128.8, 128.4, 128.3, 128.3, 127.7, 92.6, 70.7; CH_0: 197.2, 137.4 ppm. IR (neat) 3031, 2985, 2938, 1696 cm^{-1}. HRMS (ESI): Calculated for $C_{13}H_{15}O_3$

219.1021 *m/z* (M+H), Obsd. 219.1021.

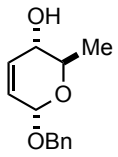

28

(2*R*,3*S*,6*S*)-6-(benzyloxy)-2-methyl-3,6-dihydro-2*H*-pyran-3-ol) (28) A solution of dihydropyranone **27** (0.1005 g, 0.46 mmol, 1 equiv) was dissolved in CH_2Cl_2 /MeOH (6mL, 1:1 (v/v)). The solution was cooled to −78 °C, to which $NaBH_4$ (17.4 mg, 0.46 mmol, 1 equiv) was added. The reaction mixture was stirred at −78 °C for 4h. The reaction was quenched with saturated aqueous $NaHCO_3$ (10 mL), extracted with EtOAc (3 × 5 mL). The organic phase was dried over Na_2SO_4 and concentrated under reduced pressure. The product was purified using silica gel flash chromatography eluting with 20% EtOAc/hexanes to give allyl alcohol **28** (91.7 mg, 91%) as a colorless oil: *Rf*= 0.22 (20% EtOAc/hexanes). $[\alpha]^{20}_D$ = +34.9 (*c* = 0.935, $CHCl_3$). ^{1}H NMR (500 MHz, $CDCl_3$) δ 7.37-7.28 (m, 5H), 5.93 (dd, *J* = 9.8, 1.0 Hz, 1H), 5.76 (ddd, *J* = 10.3, 2.9, 1.6 Hz, 1H), 5.03 (d *J* = 1.5, 0.97 Hz, 1H), 4.78 (d, *J* = 11.7 Hz, 1H), 4.60 (d, *J* = 12.2 Hz, 1H), 3.84 (dt, *J* = 8.9, 1.5 Hz, 1H), 3.76 (dq, *J* = 12.7, 6.3 Hz, 1H), 1.9 (d, *J*= 8.3 Hz, 1H) OH, 1.30 (d, *J* = 5.9 Hz, 3H) ppm. ^{13}C NMR (125 MHz, $CDCl_3$) δ 138.1, 133.8, 128.6, 128.6, 128.2, 128.2, 127.9, 126.7, 93.7, 70.2, 69.9, 68.3, 18.1 ^{13}C DEPT (125 MHz, $CDCl_3$) δ CH_3: 18.1; CH_2: 69.9; CH: 133.8, 128.6, 128.6, 128.2, 128.2, 127.9, 126.7, 93.7, 70.2, 69.9, 68.3; CH_0: 138.1 ppm. IR (neat) 3386, 2973, 2931, 2877 cm^{-1}. HRMS (ESI): Calculated for $C_{13}H_{16}O_3Na$ *m/z* (M+Na) 243.0997, Obsd. 243.0996.

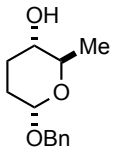

24

(2*R*,3*S*,6*S*)-6-(Benzyloxy)-2-methyltetrahydro-2*H*-pyran-3-ol (24).

O-nitro- benzenesulfonyl hydrazide (NBSH) (0.272 g, 1.25 mmol, 3 equiv) was added to a solution of allylic alcohol **28** (91.7 mg, 0.416 mmol, 1 equiv) in *N*-methylmorpholine (NMM) (0.5 mL) at rt. Et_3N (200 µL) was added to the reaction mixture and was stirred for 24h. Additional NBSH (0.181 g, 0.832 mmol, 2 equiv) was added to the reaction, which was stirred for another 12h. The reaction mixture was diluted with EtOAc (5 mL) and was quenched with NH_4Cl solution (5 mL). The aqueous layer was extracted with ethyl acetate (2 × 5 mL). The organic layers were combined and were washed with saturated aqueous $NaHCO_3$, dried over Na_2SO_4, and concentrated under reduced pressure. The product was purified by silica gel column chromatography eluting with 10% EtOAc/hexane afforded the benzyloxy amicetose **24** (80.3 mg, 83%) as a clear oil. *Rf*= 0.33 (30% EtOAc/hexanes. $[\alpha]^{20}_D$ = +108.3 (*c* = 2.21, $CHCl_3$). ^1H NMR ($CDCl_3$, 500 MHz) δ 7.38-7.33 (m, 5H), 4.85 (dd, *J* = 3.0, 1.2 Hz, 1 H), 4.72 (d, *J* = 12.0 Hz, 1 H), 4.49 (d, *J* = 12.0 Hz, 1H), 3.67 (dq, *J* = 9.3, 6.3 Hz, 1H), 3.29 (dddd, *J* = 9.8, 9.3, 4.9, 4.9 Hz, 1 H), 1.88 (m, 2H), 1.80 (m, 2H), 1.45 (d, *J*=4.8 Hz, OH), 1.27 (d, *J*=6.6 Hz, 3 H) ppm. ^{13}C NMR ($CDCl_3$, 125 MHz) δ 138.3, 128.6, 128.6, 128.0, 128.0, 127.8, 95.7, 72.3, 69.8, 68.8, 29.8, 27.9, 18.1 ppm. ^{13}C DEPT (125 MHz, $CDCl_3$) δ CH_3: 18.1; CH_2: 68.8, 29.8, 27.9; CH: 128.6, 128.6, 128.0, 128.0, 95.7, 72.3, 69.8, 68.8; CH_0: 138.3 ppm. IR (neat) 3405, 2933, 2894, 1027 cm^{-1}. HRMS (ESI) calculated for $C_{13}H_{18}O_3Na$ *m/z* (M+Na) 245.1154, Obsd. 245.1156.

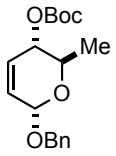

29

tert-Butyl (2*R*,3*S*,6*S*)-6-(Benzyloxy)-2-methyl-3,6-dihydro-2*H*-pyran-3-ylcarbonate (29). Boc_2O (0.954 g, 4.37 mmol, 1.5 equiv) was added to a solution of allylic alcohol **28** (0.642 g, 2.92 mmol, 1 equiv) and DMAP (17.8 mg, 0.146 mmol, 5 mol%) in CH_2Cl_2 (20 mL) at 0 ˚C. The reaction allowed to warm up to rt and was stirred for 1h. It was quenched with saturated aqueous $NaHCO_3$. It was then extracted with CH_2Cl_2 (3 × 10 mL). The combined organic layer was washed with saturated aqueous $NaHCO_3$, and dried over Na_2SO_4. The solvent was removed under reduced pressure. The product was purified by silica gel flash column chromatography eluting with 10-20% EtOAc/hexane to afforded the carbonate **29** (0.773 g, 83%) as a white solid. Mp. 60-62 ˚C. *Rf*= 0.63 (20% EtOAc/hexanes). $[\alpha]^{20}_D$ = +88.6 (*c* = 2.99, $CHCl_3$). ^{1}H NMR (500 MHz, $CDCl_3$) δ 7.37-7.27 (m, 5H), 5.94 (ddd, *J* = 10.1, 1., 1.22 Hz, 1 H), 5.82 (ddd, *J* = 10.4, 2.7, 1.8 Hz, 1 H), 5.06 (bs, 1H), 4.87 (ddd, *J* = 9.2, 3.1, 1.5 Hz, 1H), 4.79 (d, *J* = 11.9 Hz, 1H), 4.61 (d, *J* = 11.9 Hz, 1H), 4.02 (dq, *J* = 9.2, 6.4 Hz, 1H), 1.50 (s, 9H), 1.23 (d, *J* = 6.0 Hz, 3 H) ppm. ^{13}C NMR (125 MHz, $CDCl_3$) δ 153.3, 138.3, 129.9, 128.6, 128.1, 128.0, 127.6, 93.9, 82.8, 73.7, 70.3, 65.1, 28.0, 18.0 ppm. ^{13}C DEPT (125 MHz, $CDCl_3$) δ CH_3: 28.0, 18.0; CH_2: 70.3; CH: 129.9, 128.6, 128.1, 128.0, 127.6, 93.9, 73.7, 65.1; CH_0: 153.3, 138.3 ppm. IR (neat) 2892, 2953, 1732 cm-1. HRMS (ESI) calculated for $C_{18}H_{24}O_5Na$ *m/z* (M+Na) 343.1516, Obsd. 343.1517.

2.6.3 ^{1}H NMR, ^{13}C NMR and DEPT Spectra

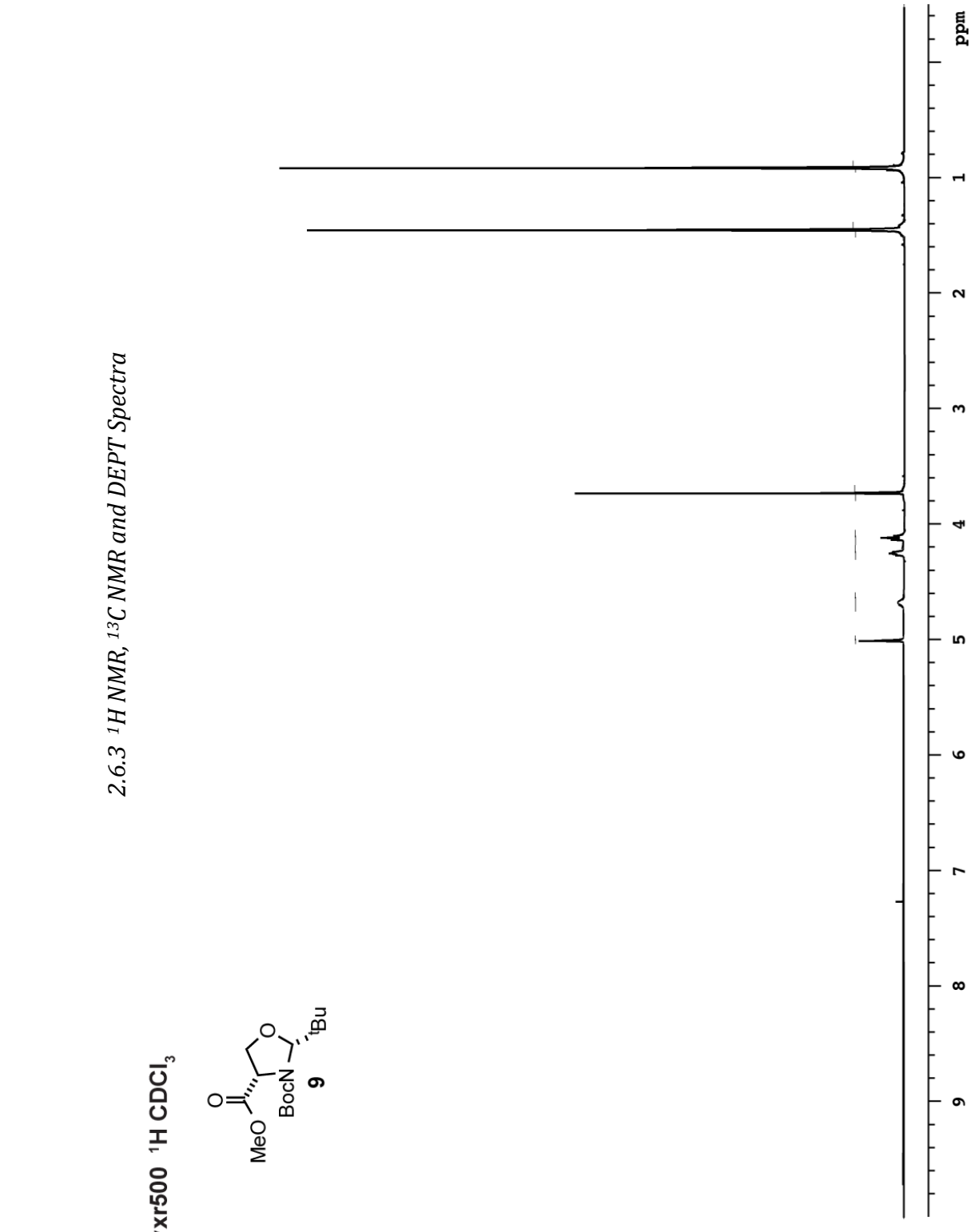

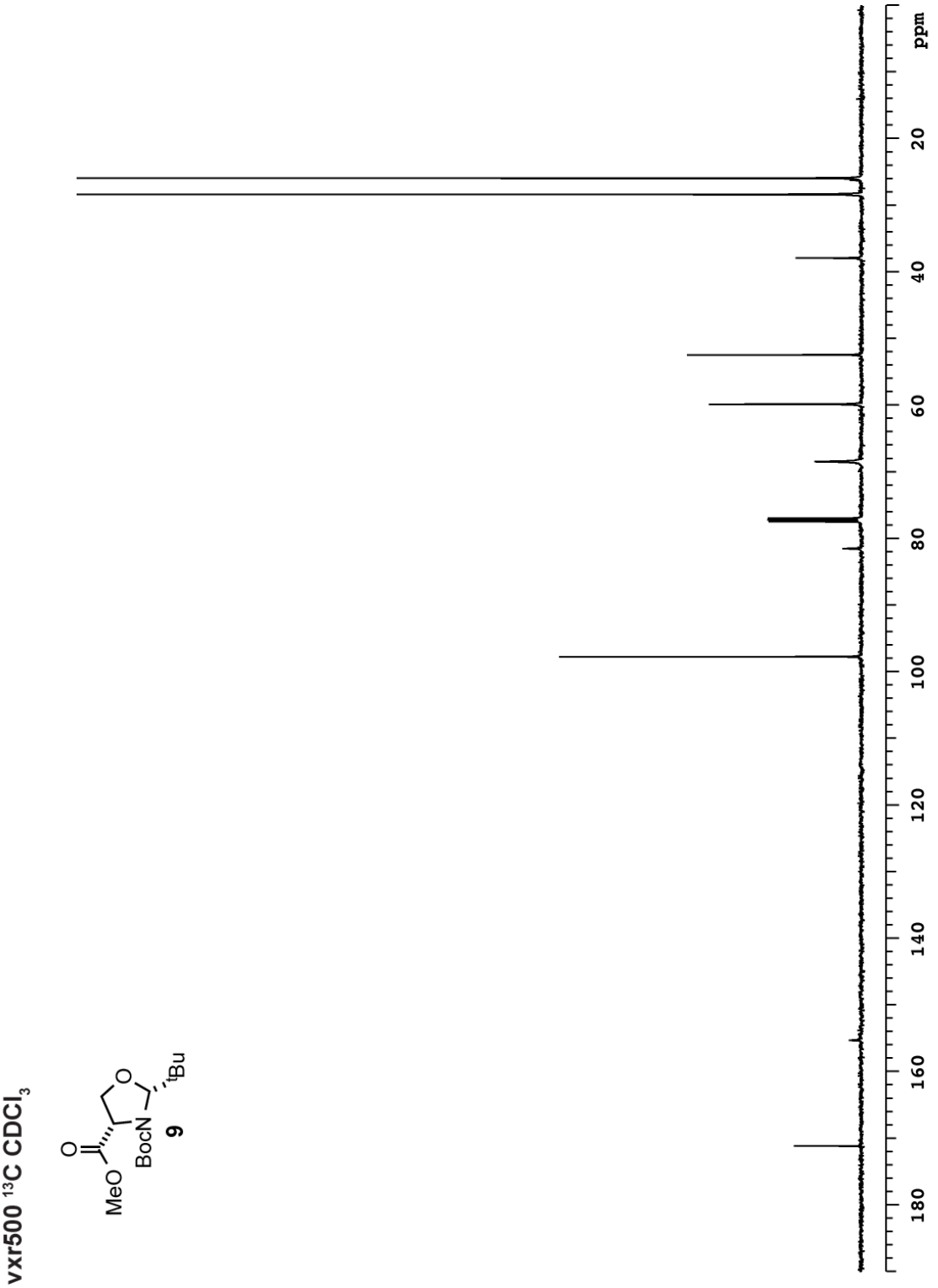
vxr500 13C CDCl3
MeO
O
BocN
O
tBu
9
ppm
180
160
140
120
100
80
60
40
20

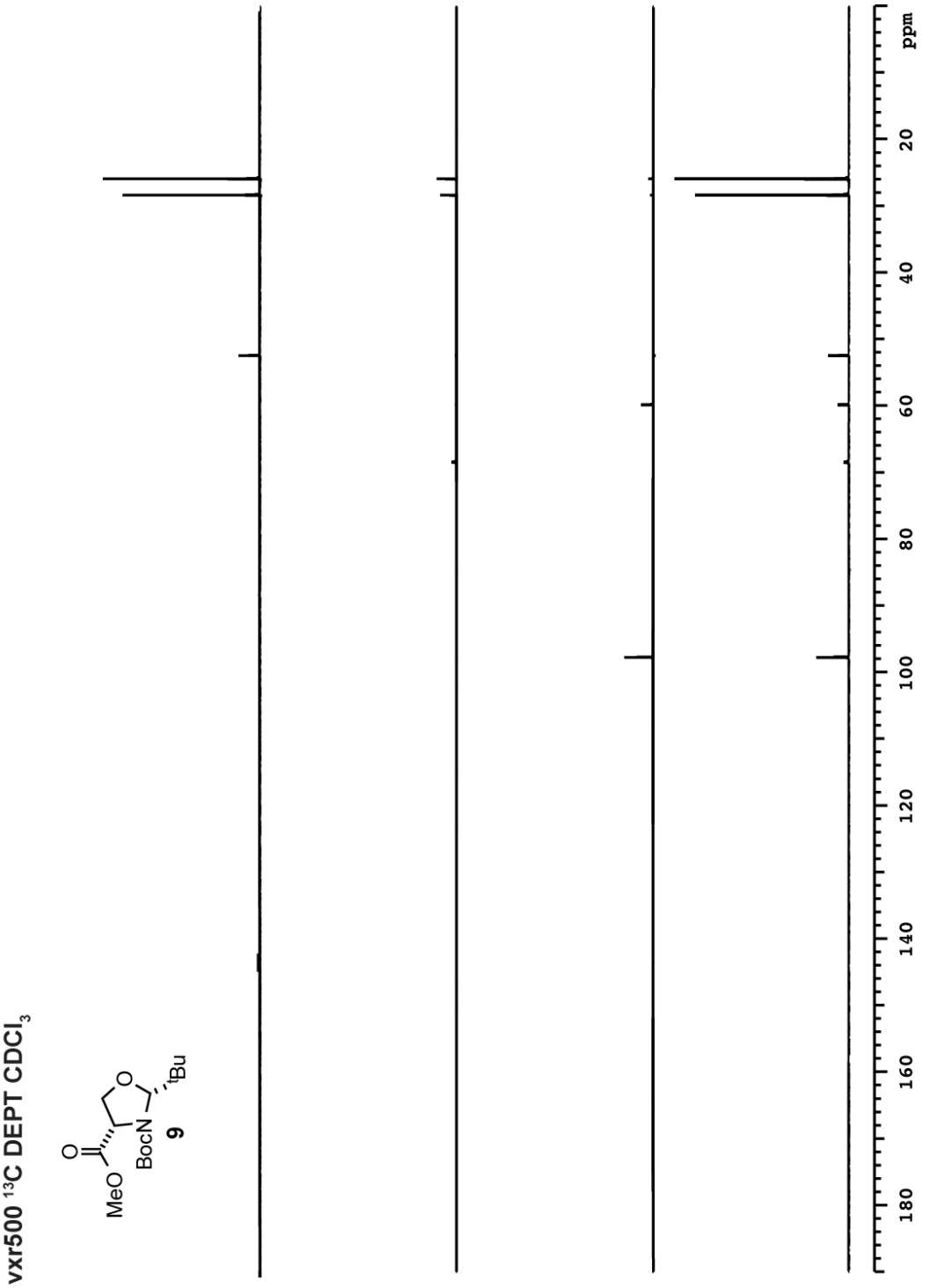
vxr500 13C DEPT CDCl3
MeO
O
BocN
O
tBu
9
ppm
20
40
60
80
100
120
140
160
180

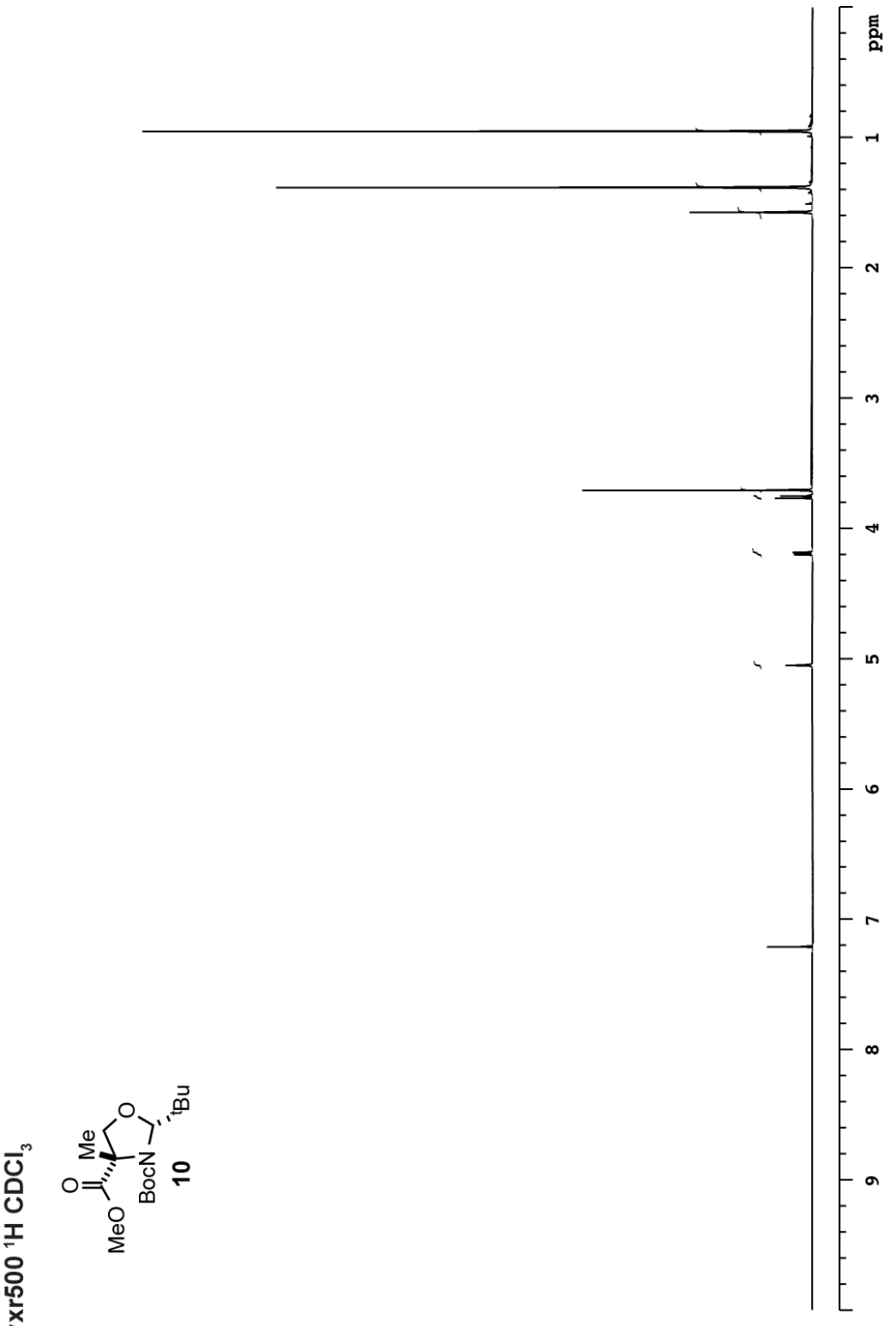
vxr500 1H CDCl3
MeO
O
Me
BocN
O
tBu
10
ppm
1
2
3
4
5
6
7
8
9

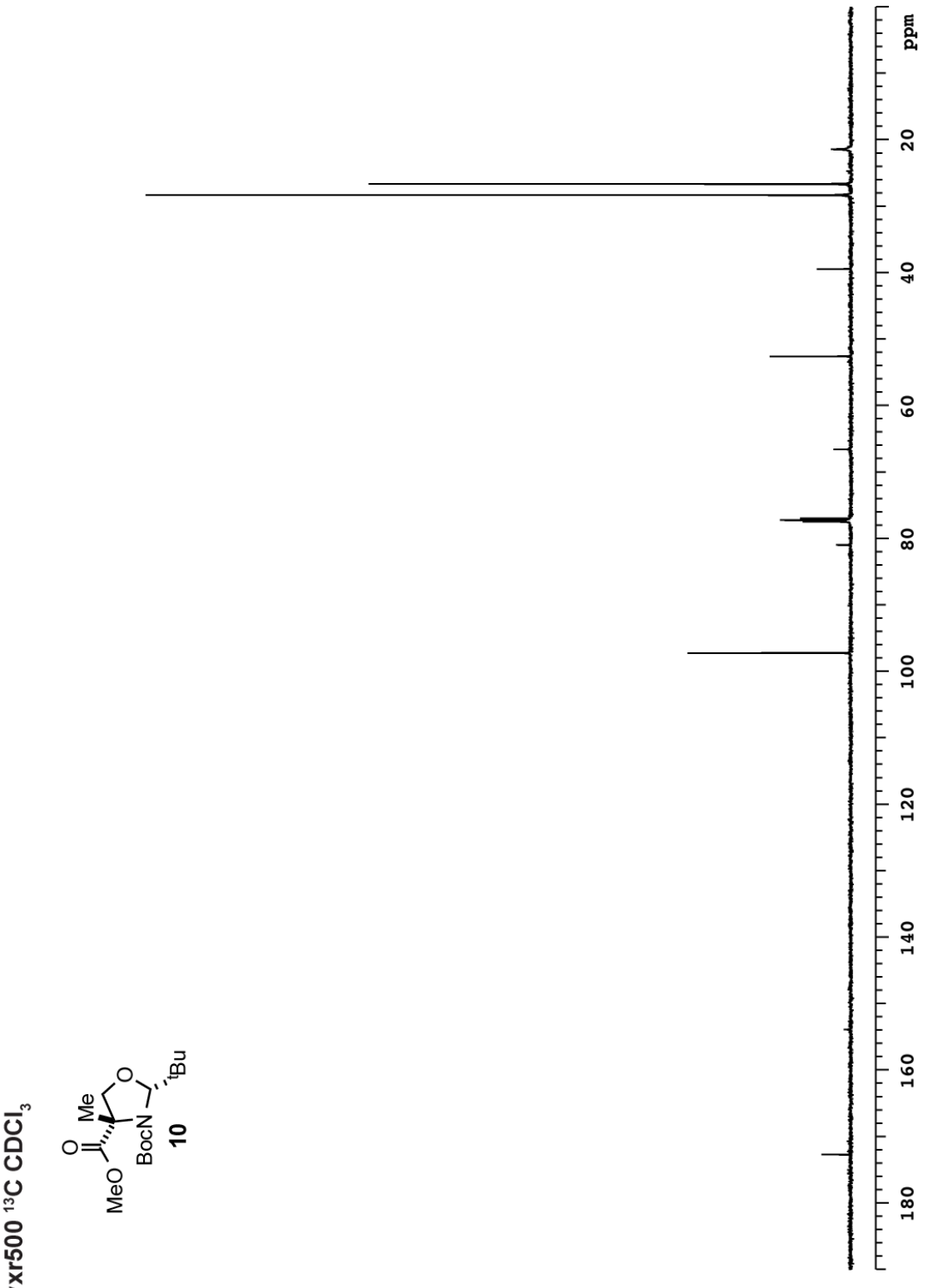
vxr500 13C CDCl3
Me
O
MeO
BocN
O
tBu
10
ppm
20
40
60
80
100
120
140
160
180

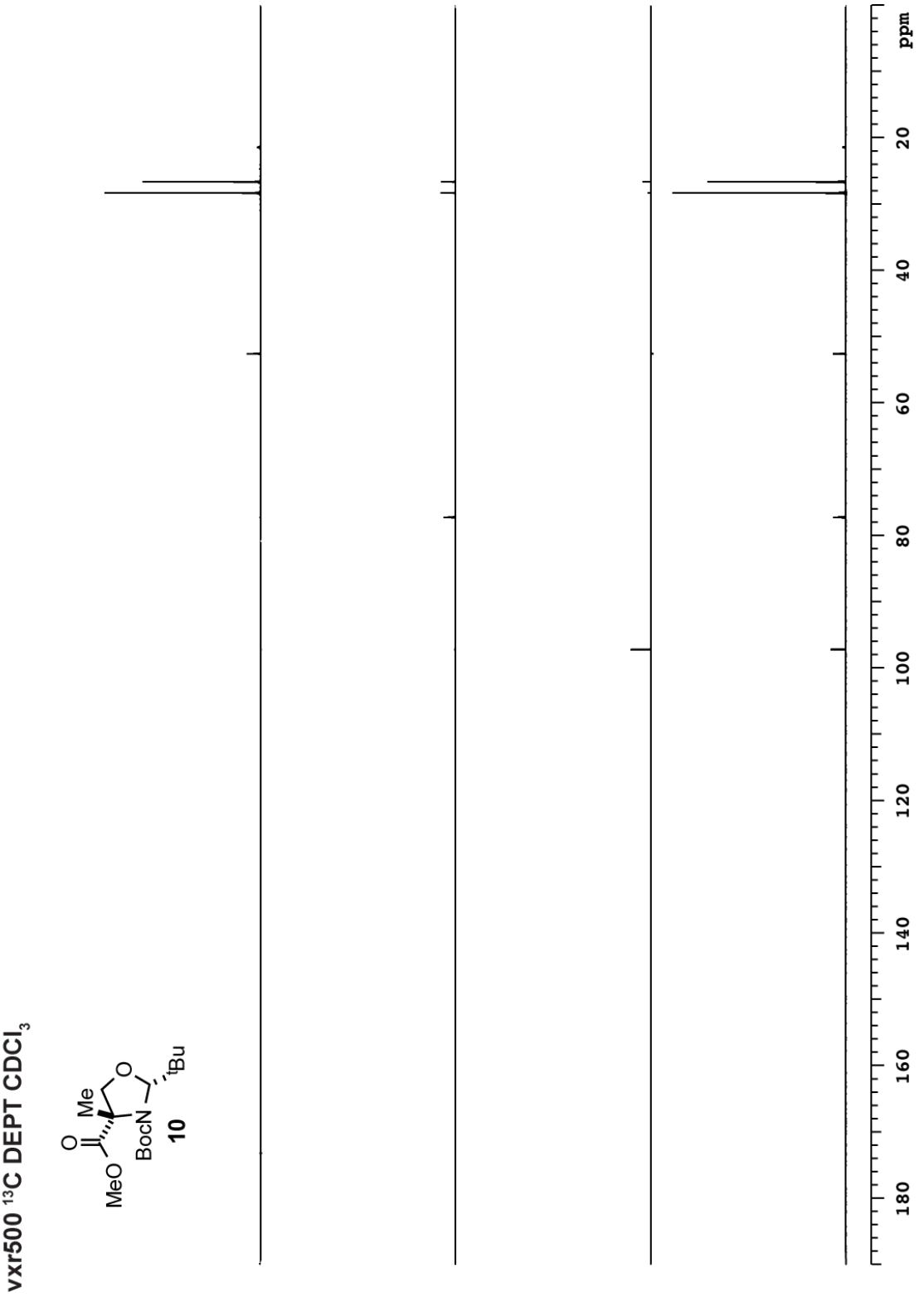
vxr500 13C DEPT CDCl3
Me
O
MeO
BocN
O
tBu
10
ppm
180
160
140
120
100
80
60
40
20

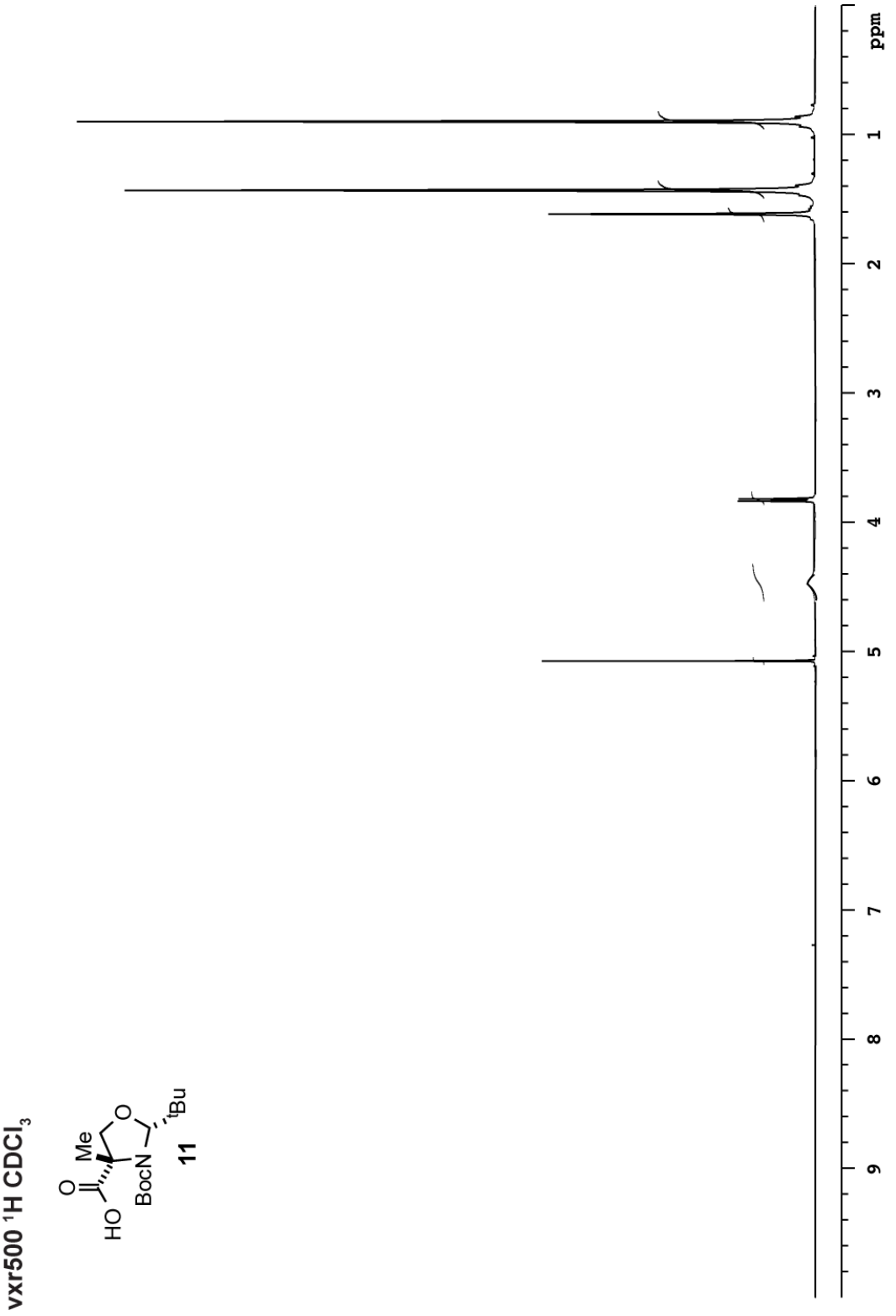
vxr500 1H CDCl3
HO
O
Me
BocN
O
tBu
11
ppm
1
2
3
4
5
6
7
8
9

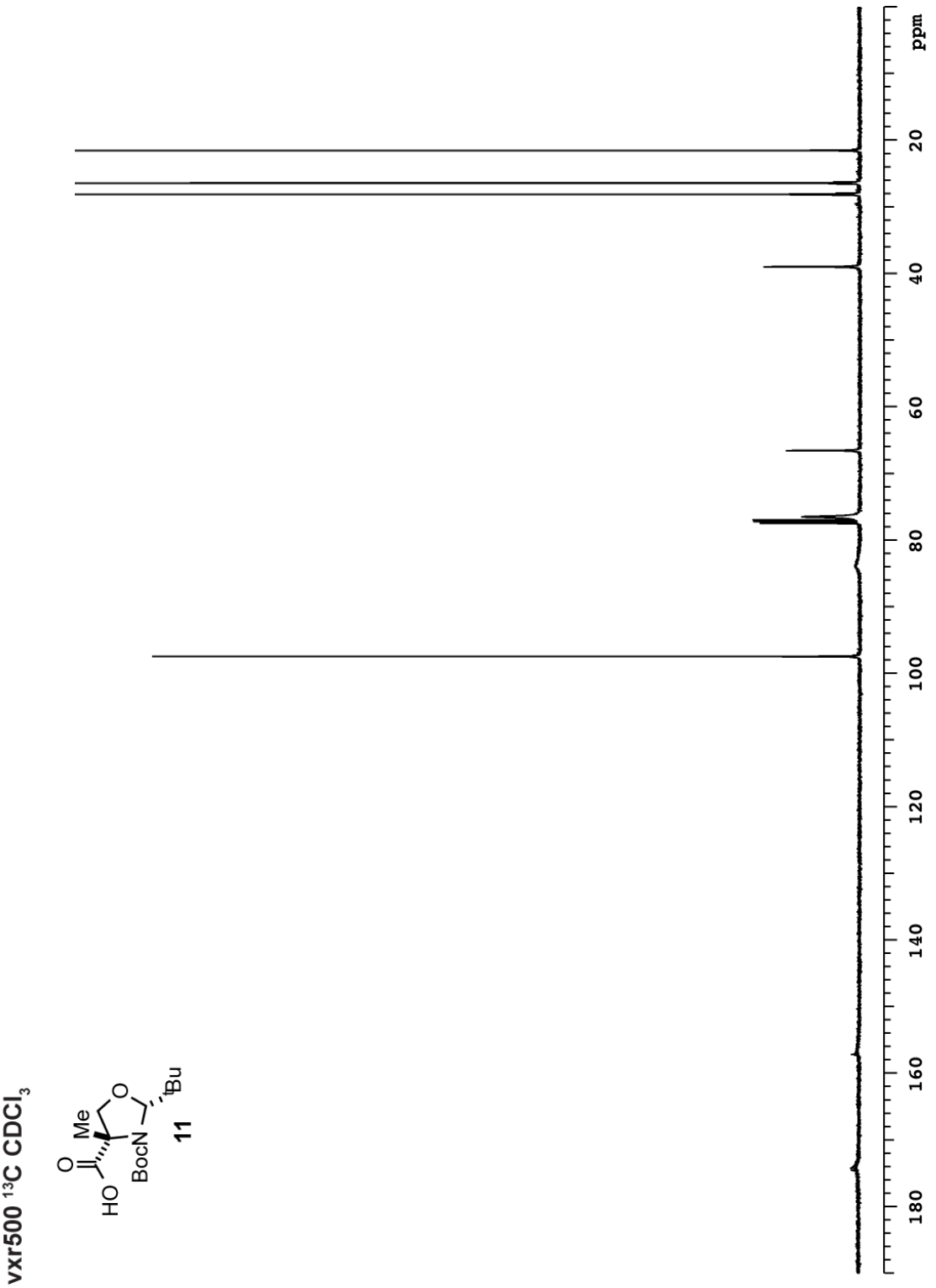
vxr500 13C CDCl3
HO
O
Me
BocN
O
tBu
11
ppm
180
160
140
120
100
80
60
40
20

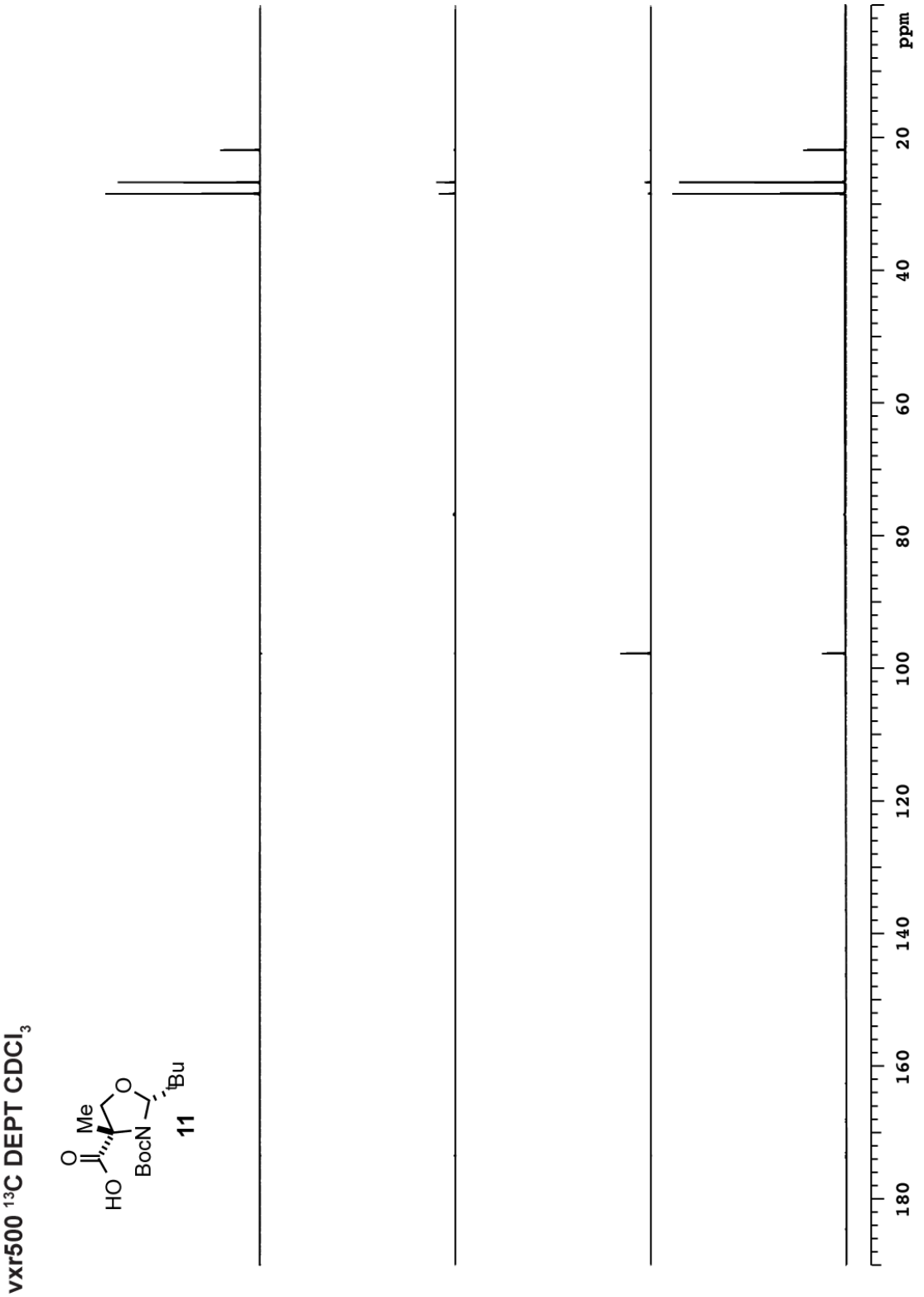
vxr500 13C DEPT CDCl3
Me
O
HO
BocN
O
tBu
11
ppm
20
40
60
80
100
120
140
160
180

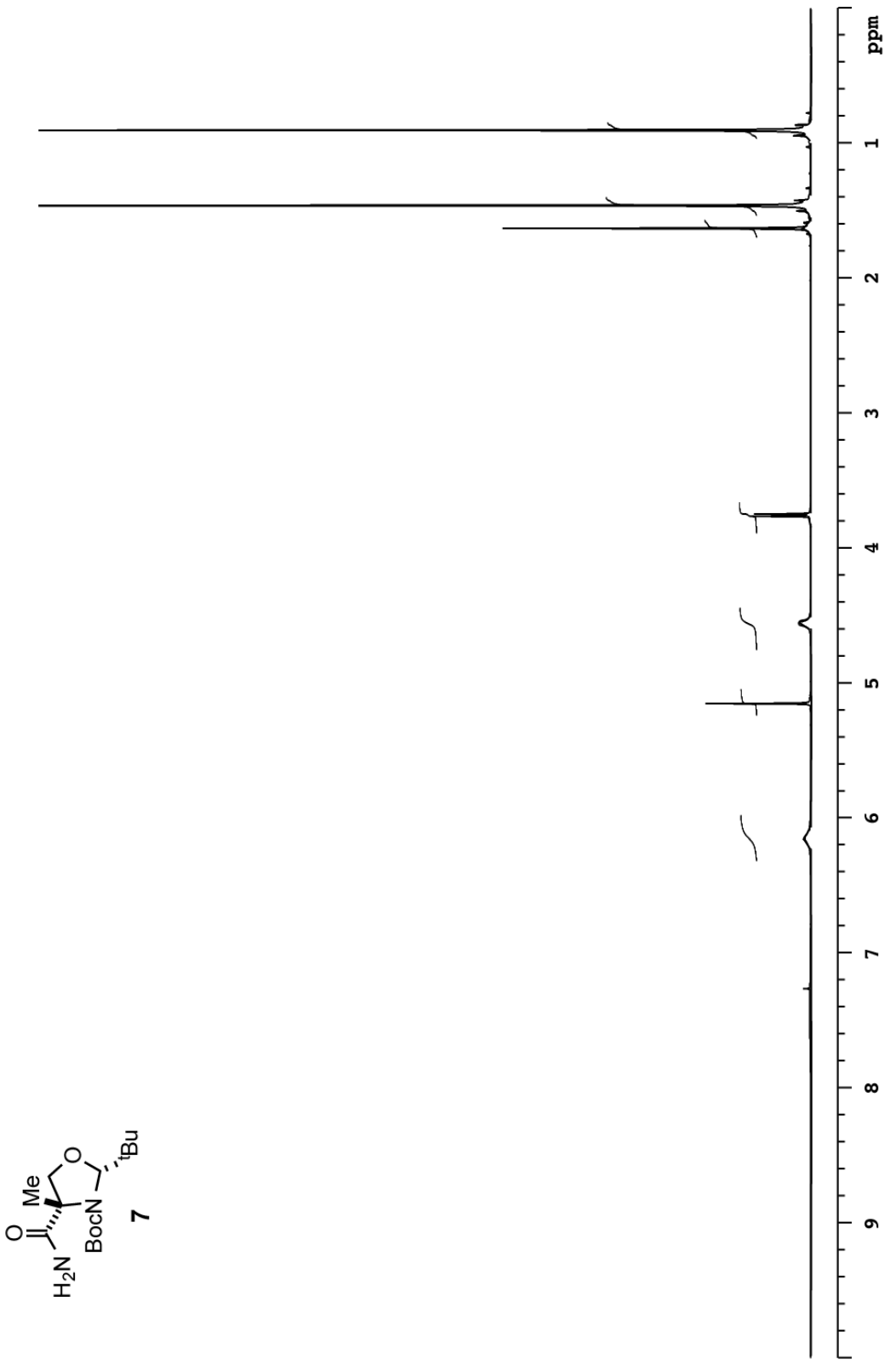
O
Me
H2N
BocN
O
tBu
7
ppm
1
2
3
4
5
6
7
8
9

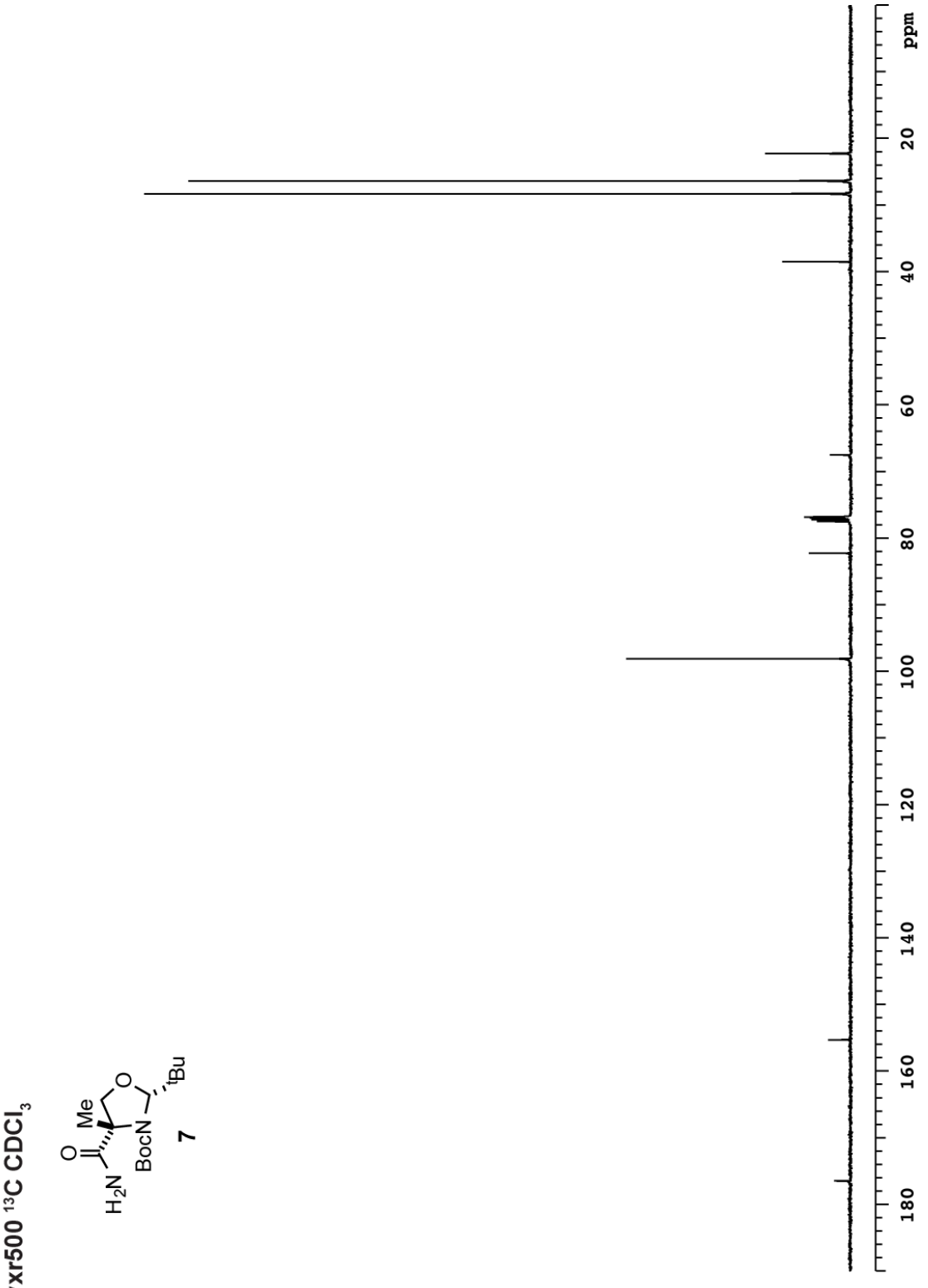
vxr500 13C CDCl3
Me
O
H2N
BocN
O
tBu
7
ppm
180
160
140
120
100
80
60
40
20

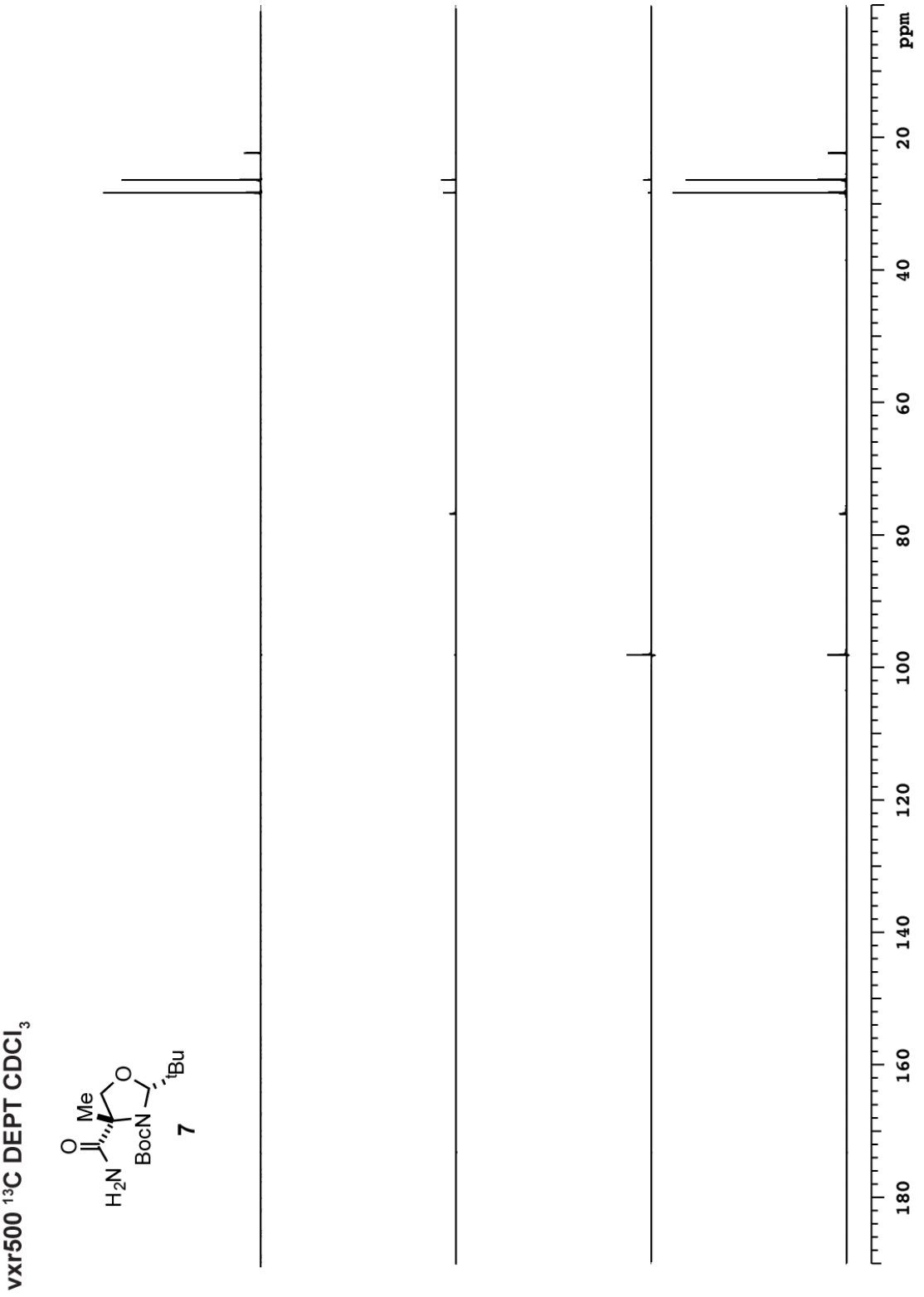
vxr500 13C DEPT CDCl3
O
Me
H2N
BocN
O
tBu
7
180
160
140
120
100
80
60
40
20
ppm

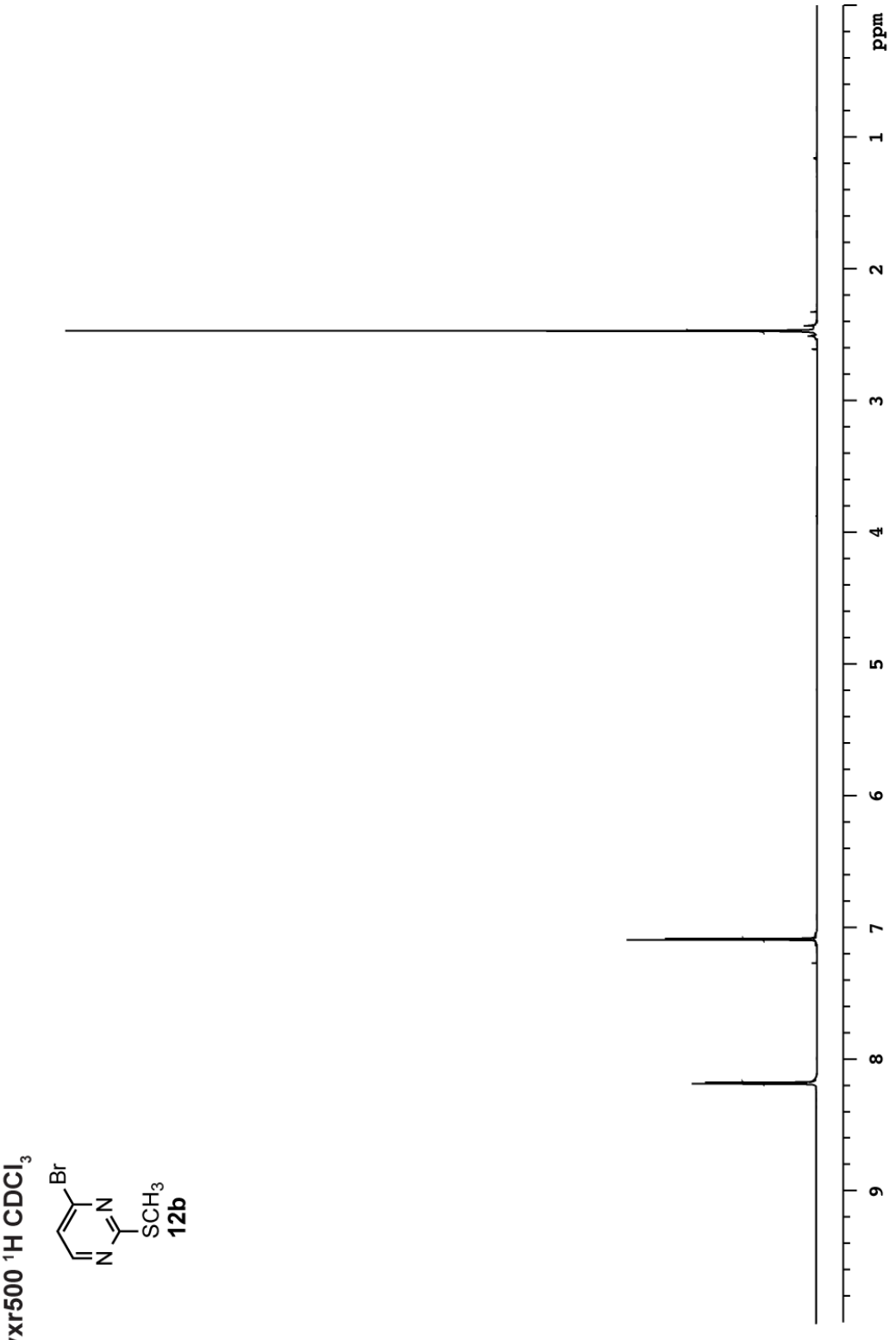
vxr500 1H CDCl3
Br
N
N
SCH3
12b
9
8
7
6
5
4
3
2
1
ppm

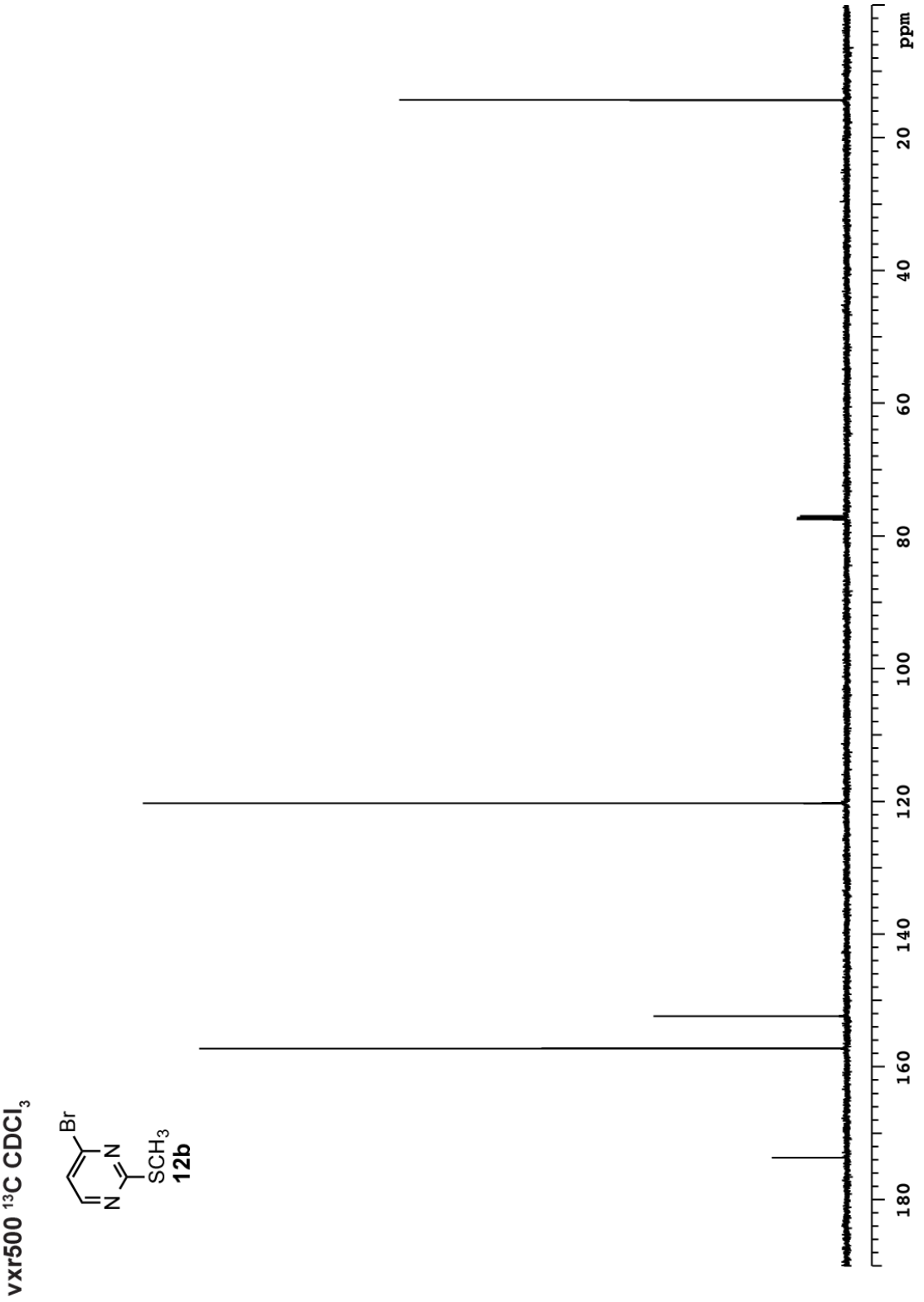
vxr500 13C CDCl3
Br
N
N
SCH3
12b
180
160
140
120
100
80
60
40
20
ppm

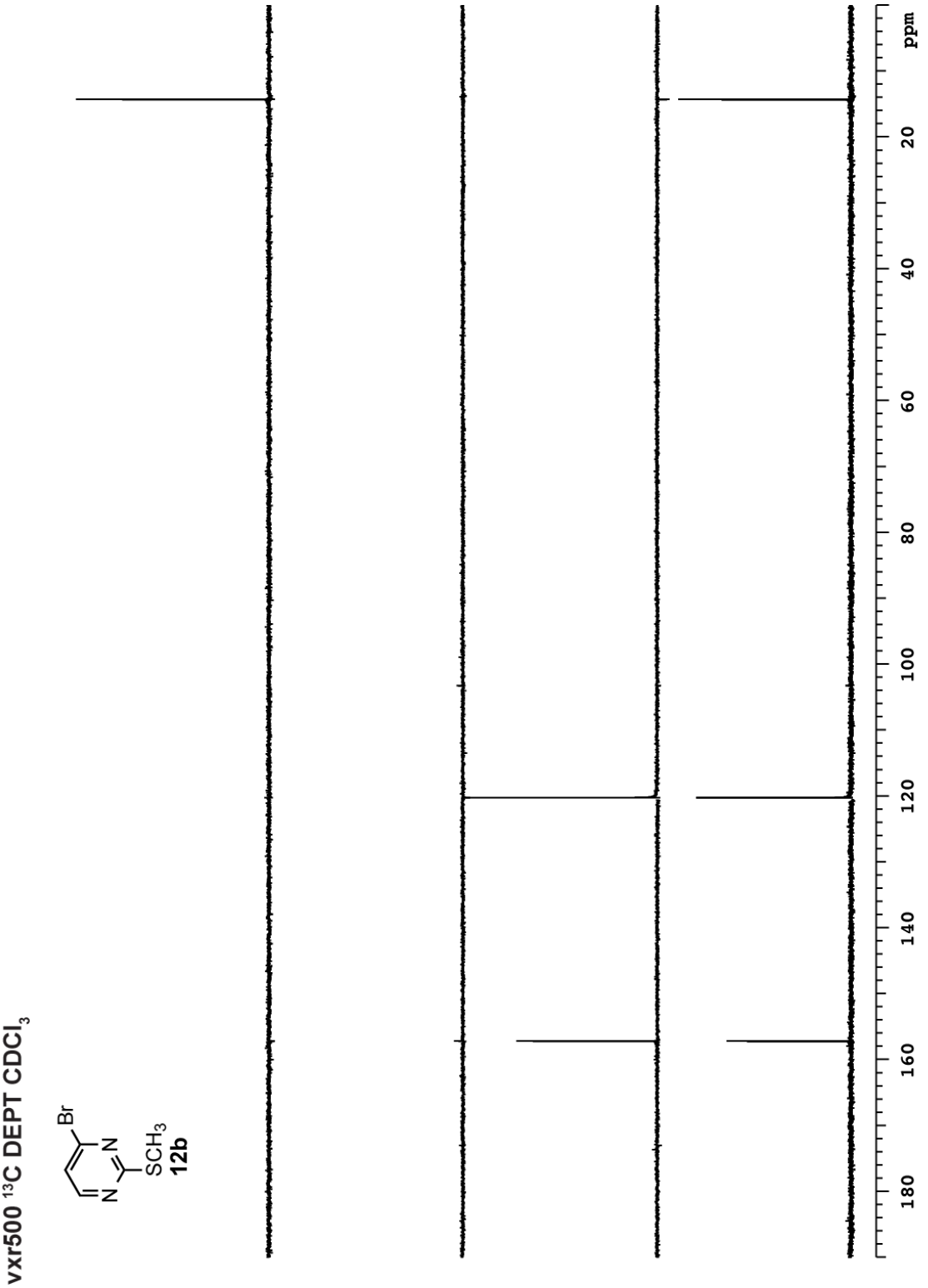
vxr500 13C DEPT CDCl3
Br
N
N
SCH3
12b
180
160
140
120
100
80
60
40
20
ppm

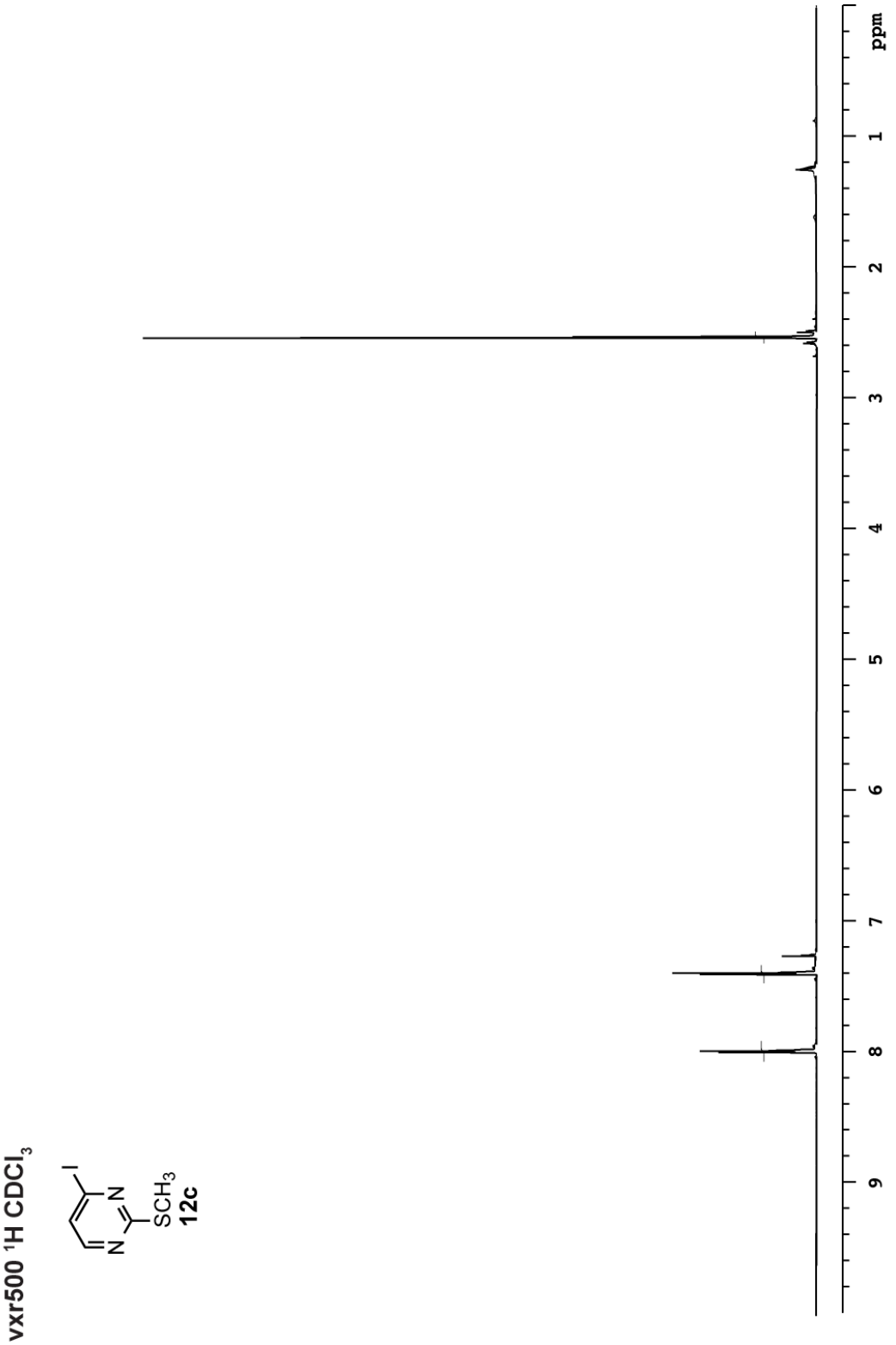
vxr500 1H CDCl3
I
N
N
SCH3
12c
9
8
7
6
5
4
3
2
1
ppm

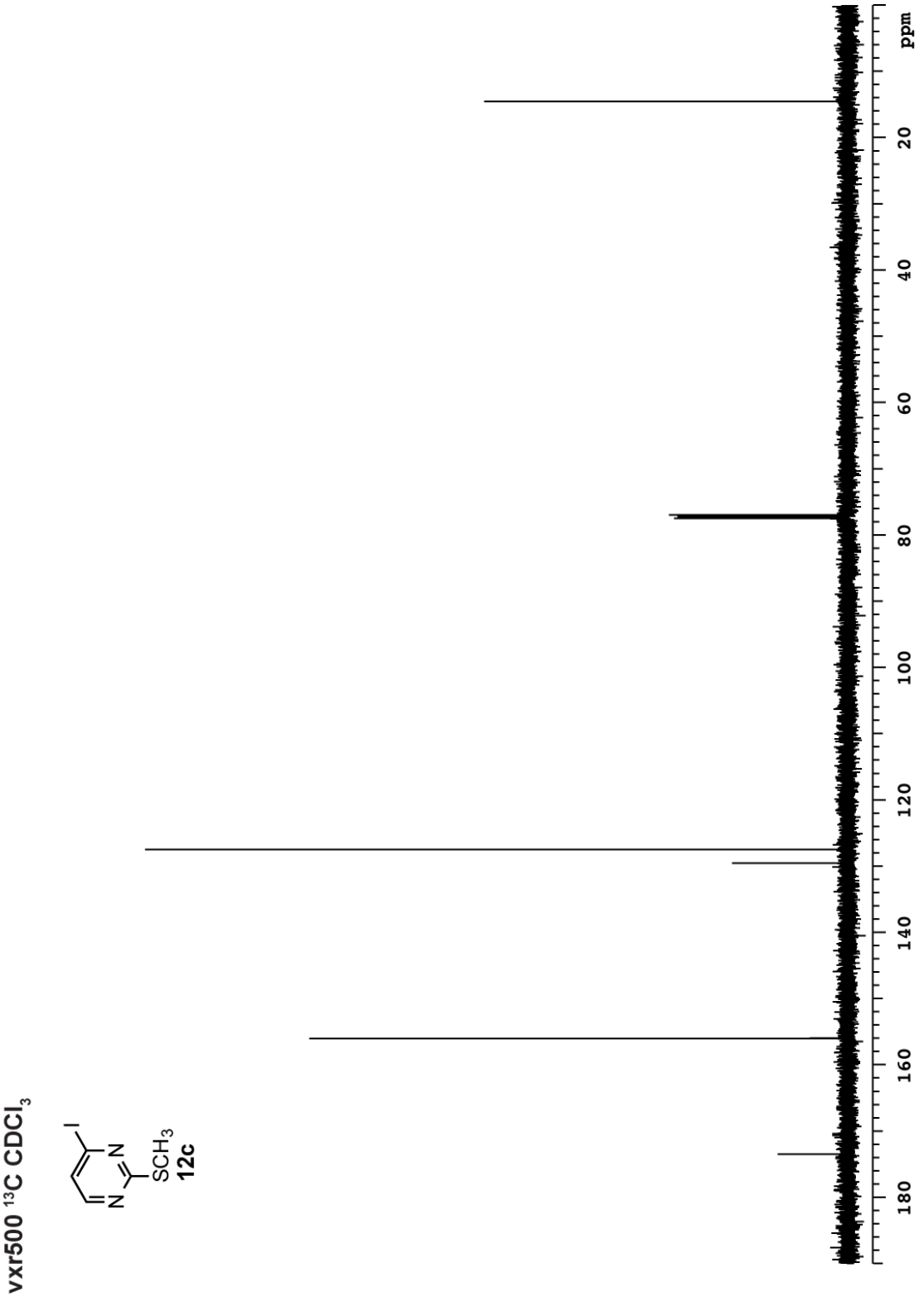
vxr500 13C CDCl3
I
N
N
SCH3
12c
180
160
140
120
100
80
60
40
20
ppm

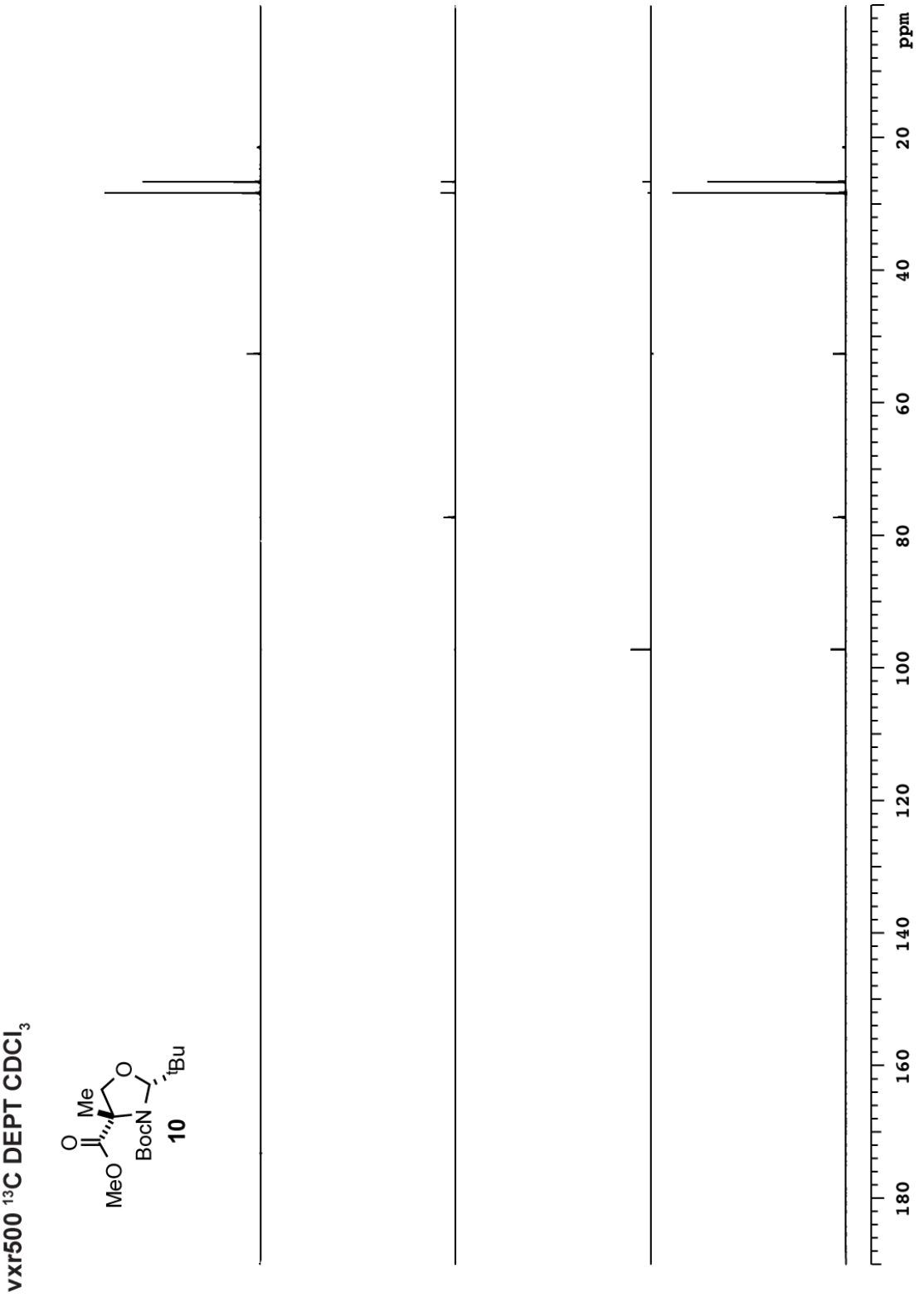
vxr500 13C DEPT CDCl3
Me
O
MeO
BocN
O
tBu
10
180
160
140
120
100
80
60
40
20
ppm

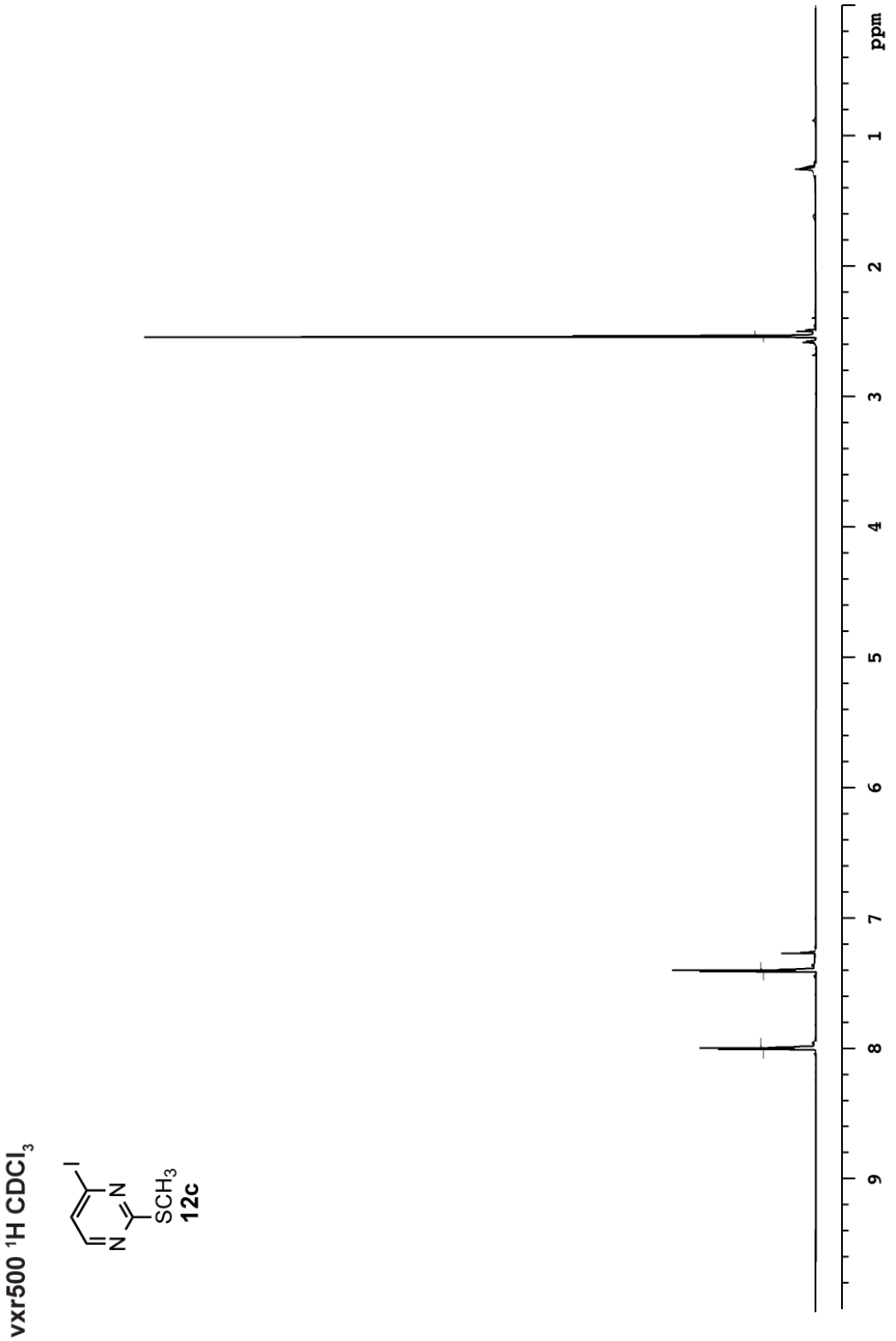
vxr500 1H CDCl3
I
N
N
SCH3
12c
ppm
1
2
3
4
5
6
7
8
9

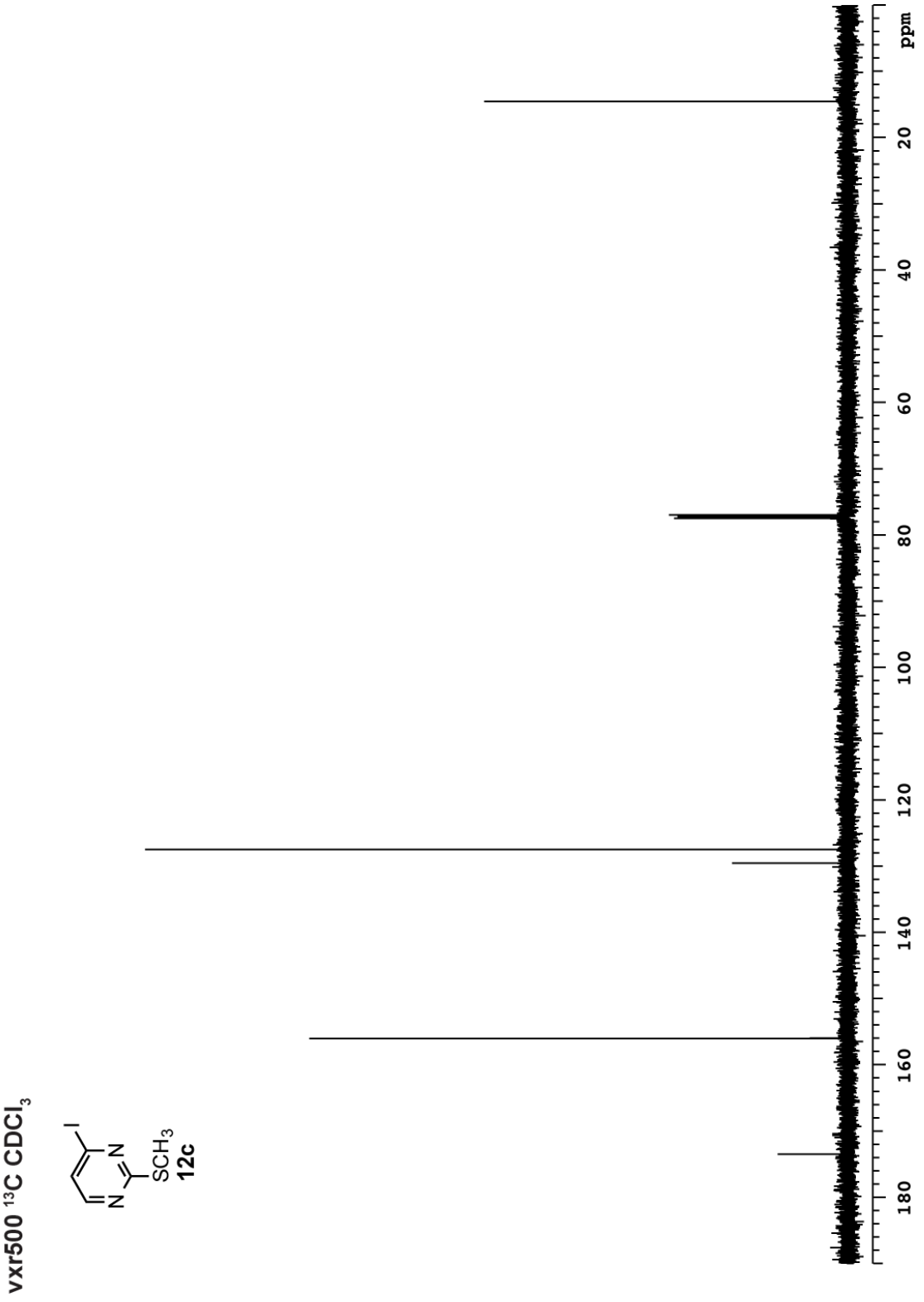
vxr500 13C CDCl3
I
N
N
SCH3
12c
180
160
140
120
100
80
60
40
20
ppm

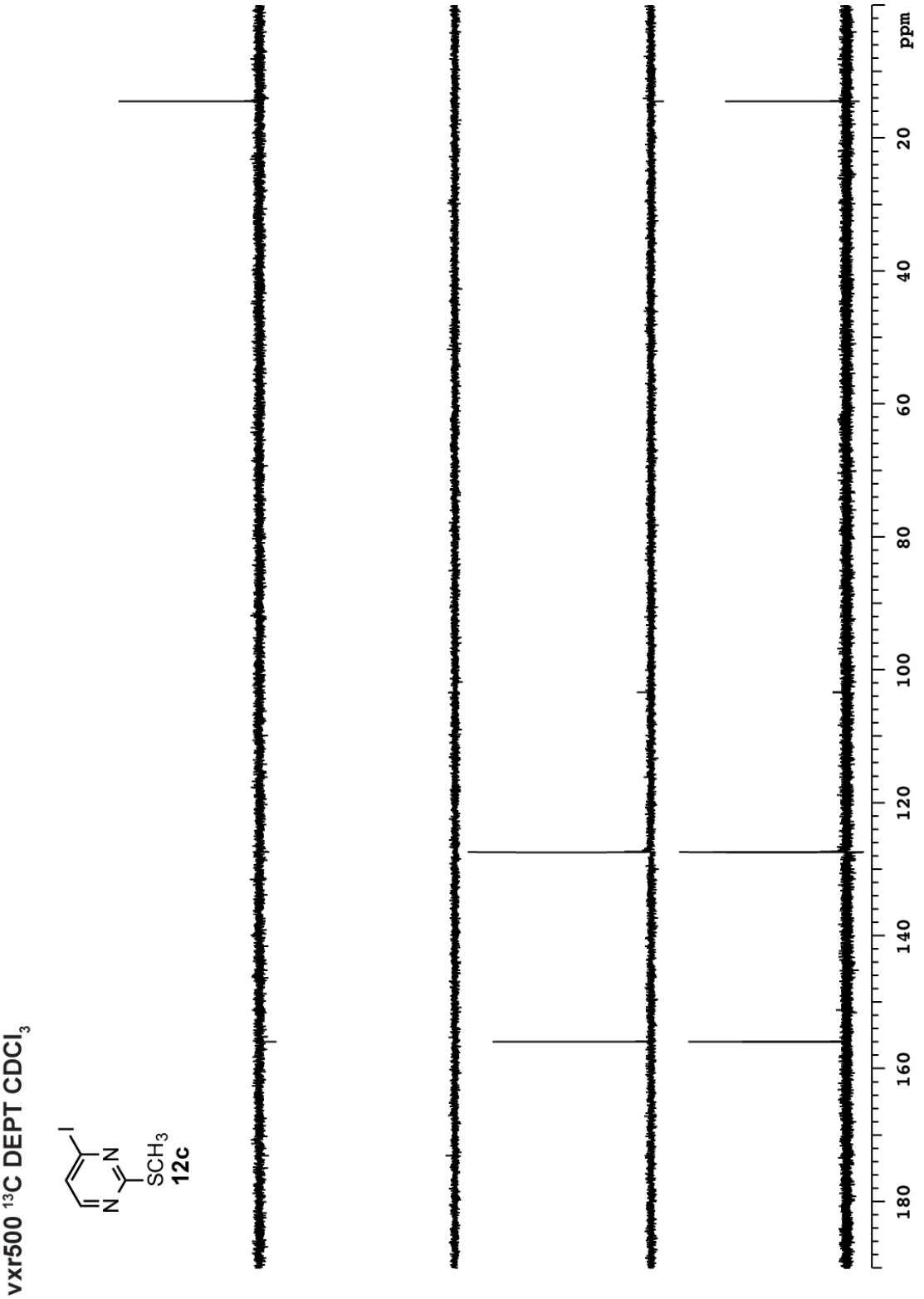
vxr500 13C DEPT CDCl3
I
N
N
SCH3
12c
180
160
140
120
100
80
60
40
20
ppm

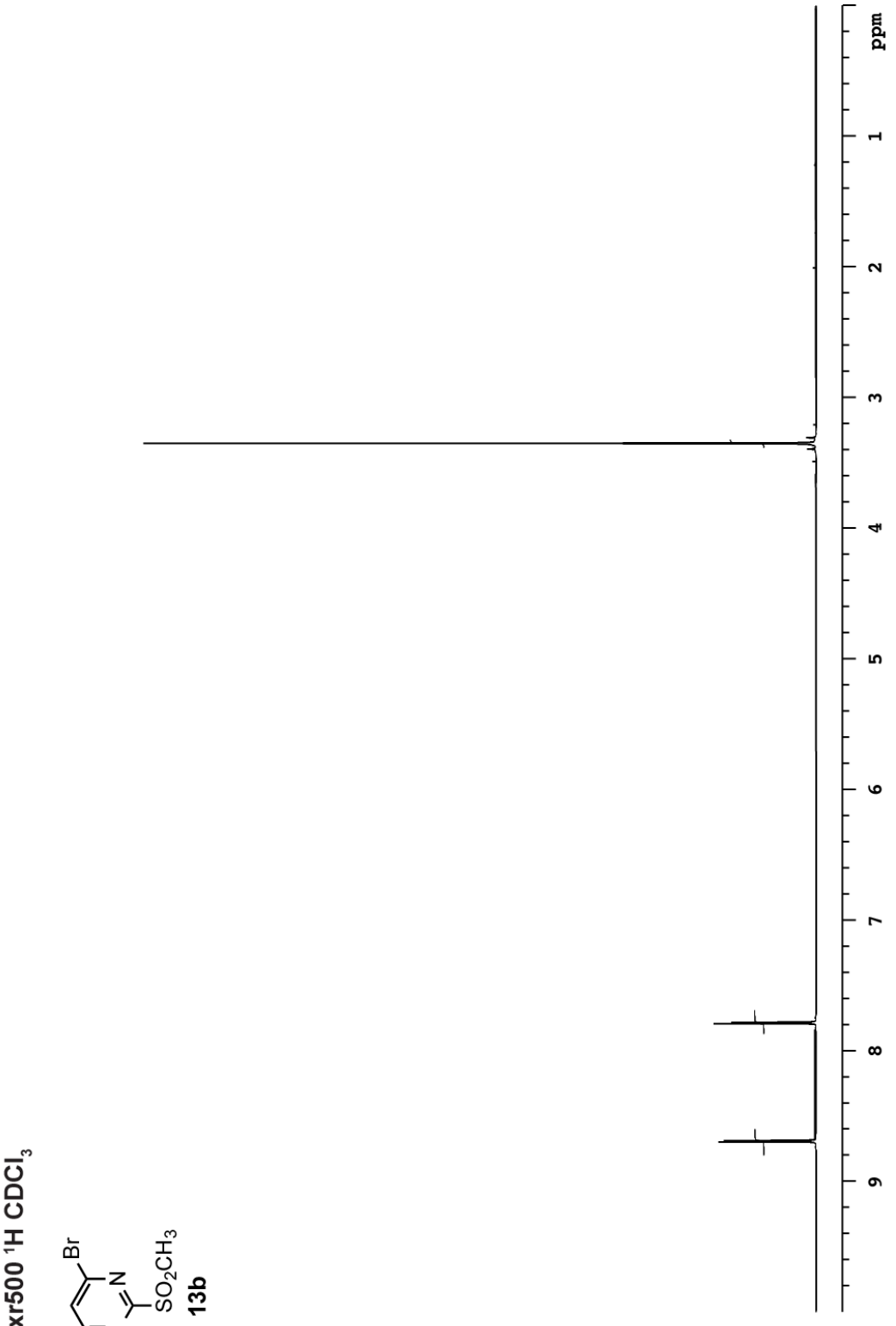
vxr500 1H CDCl3
Br
N
N
SO2CH3
13b
9
8
7
6
5
4
3
2
1
ppm

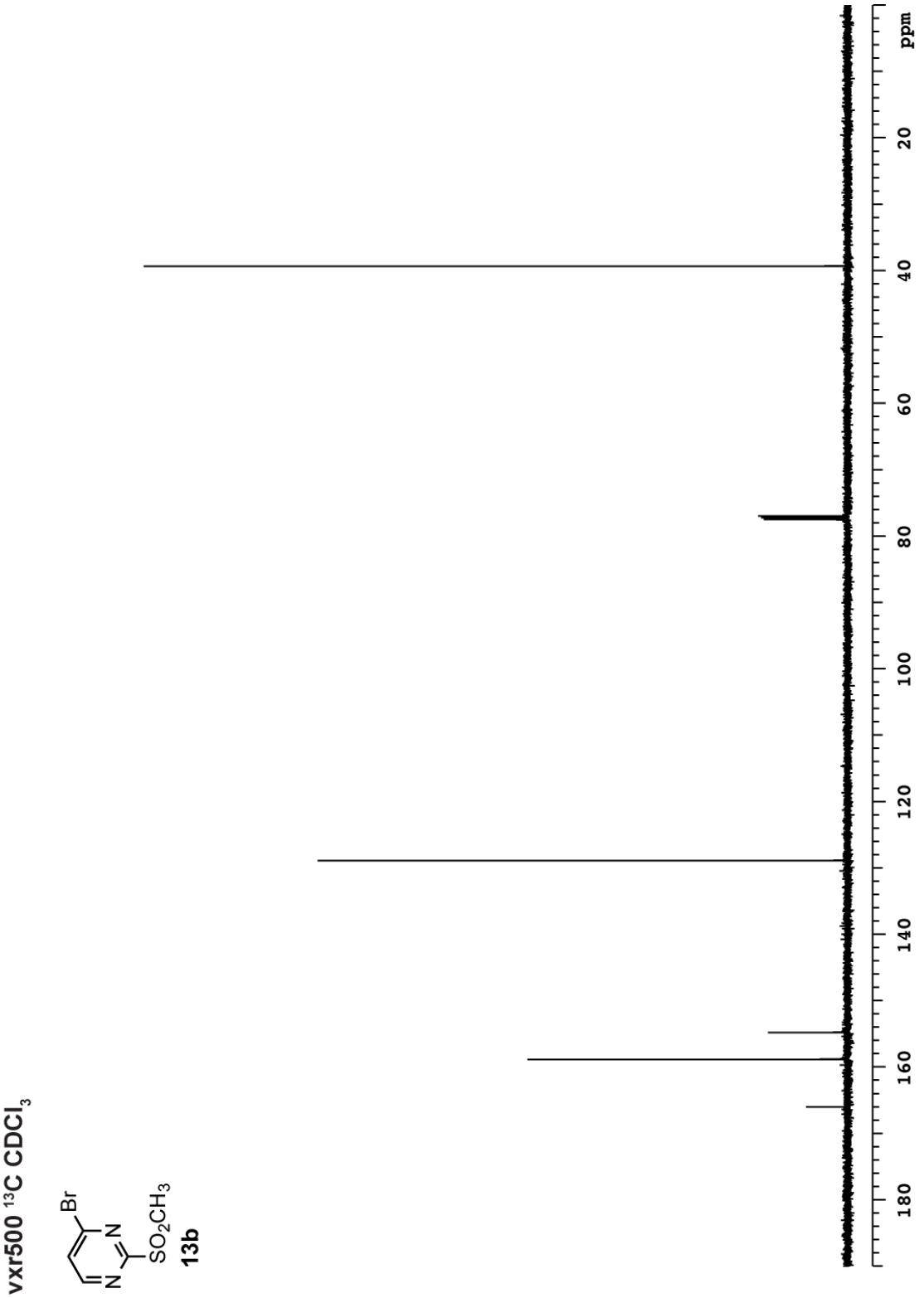
vxr500 13C CDCl3
Br
N
N
SO2CH3
13b
180
160
140
120
100
80
60
40
20
ppm

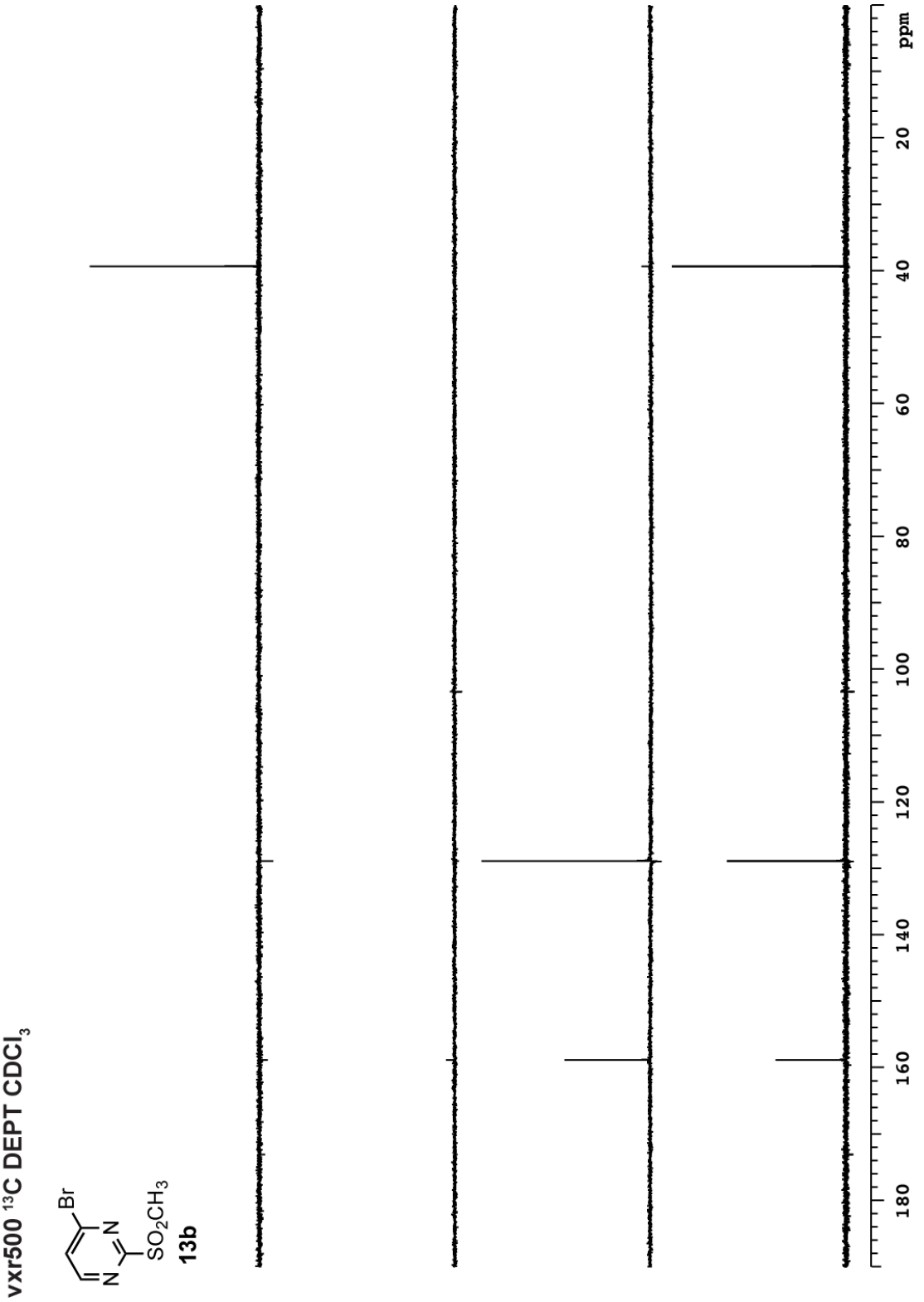
vxr500 13C DEPT CDCl3
Br
N
N
SO2CH3
13b
180
160
140
120
100
80
60
40
20
ppm

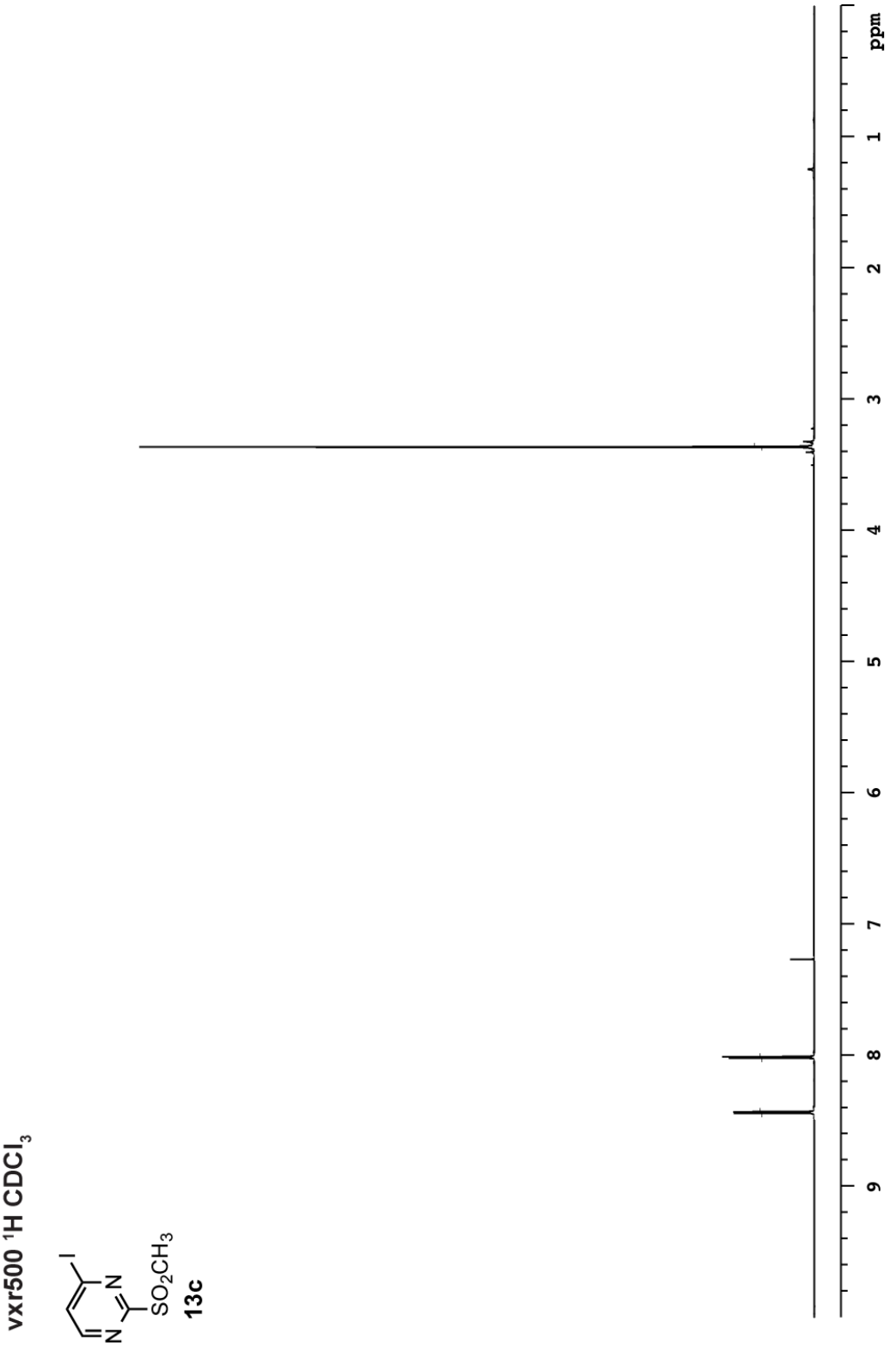
vxr500 1H CDCl3
I
N
N
SO2CH3
13c
9
8
7
6
5
4
3
2
1
ppm

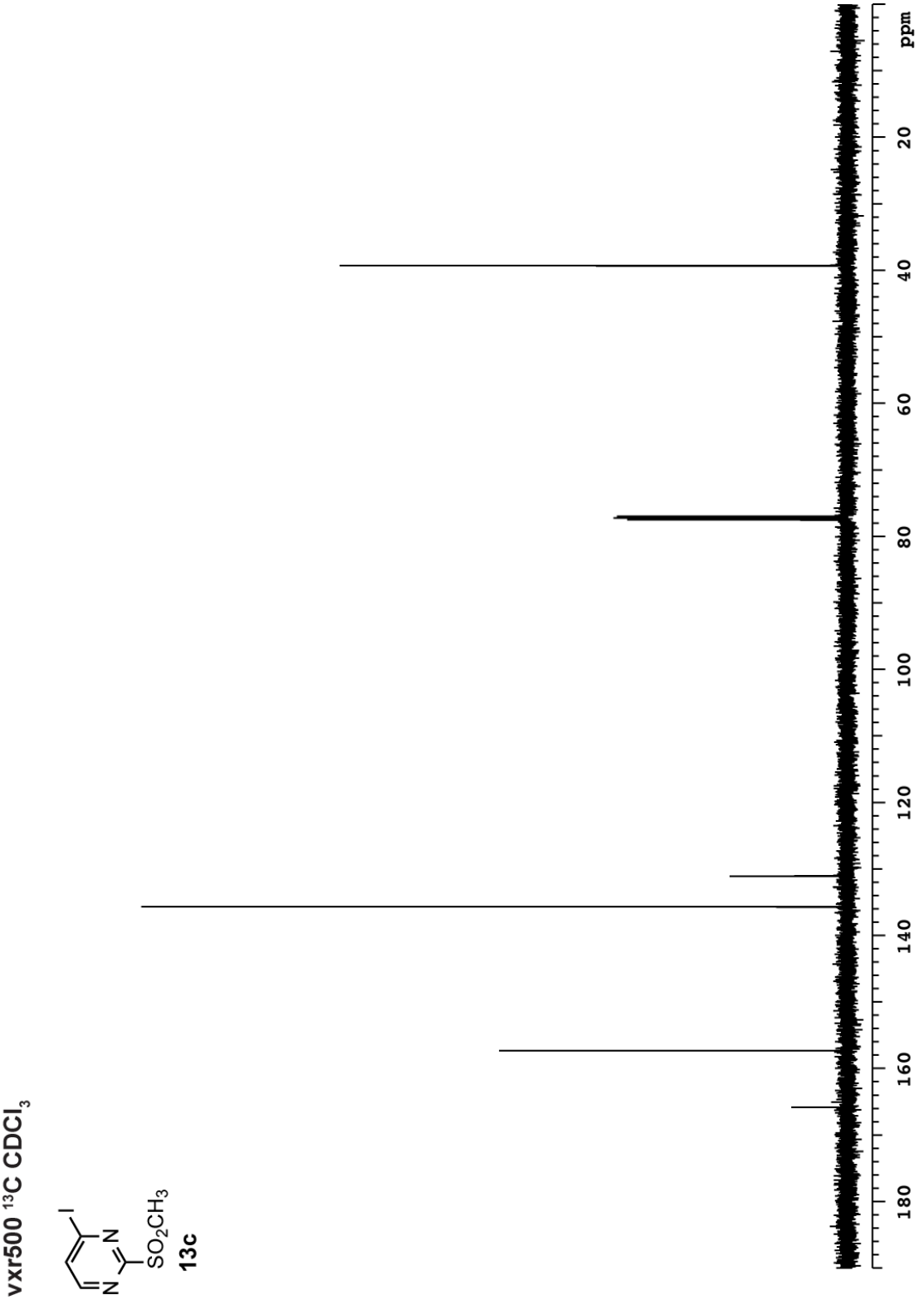
vxr500 13C CDCl3
I
N
N
SO2CH3
13c
180
160
140
120
100
80
60
40
20
ppm

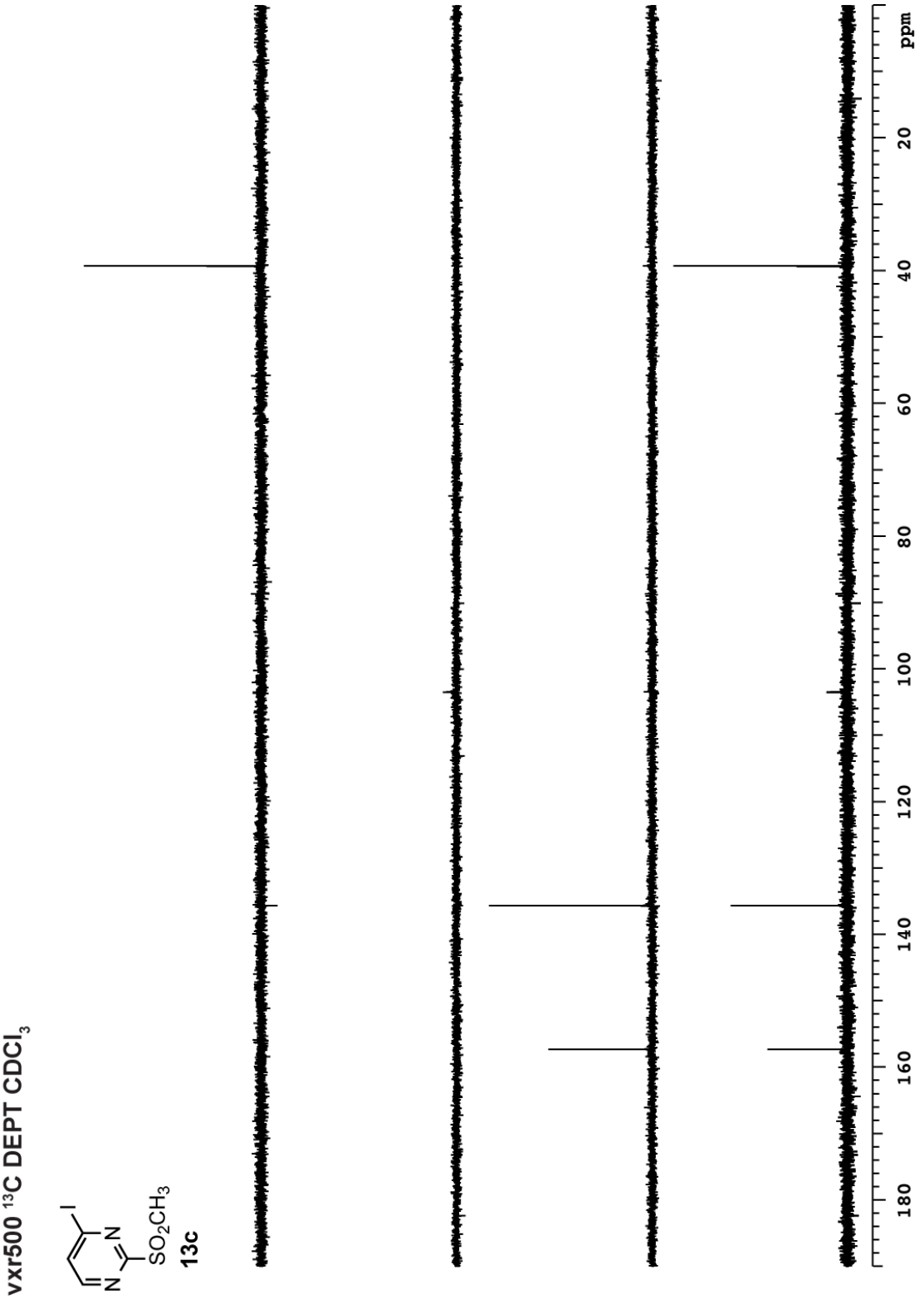
vxr500 13C DEPT CDCl3
I
N
N
SO2CH3
13c
180
160
140
120
100
80
60
40
20
ppm

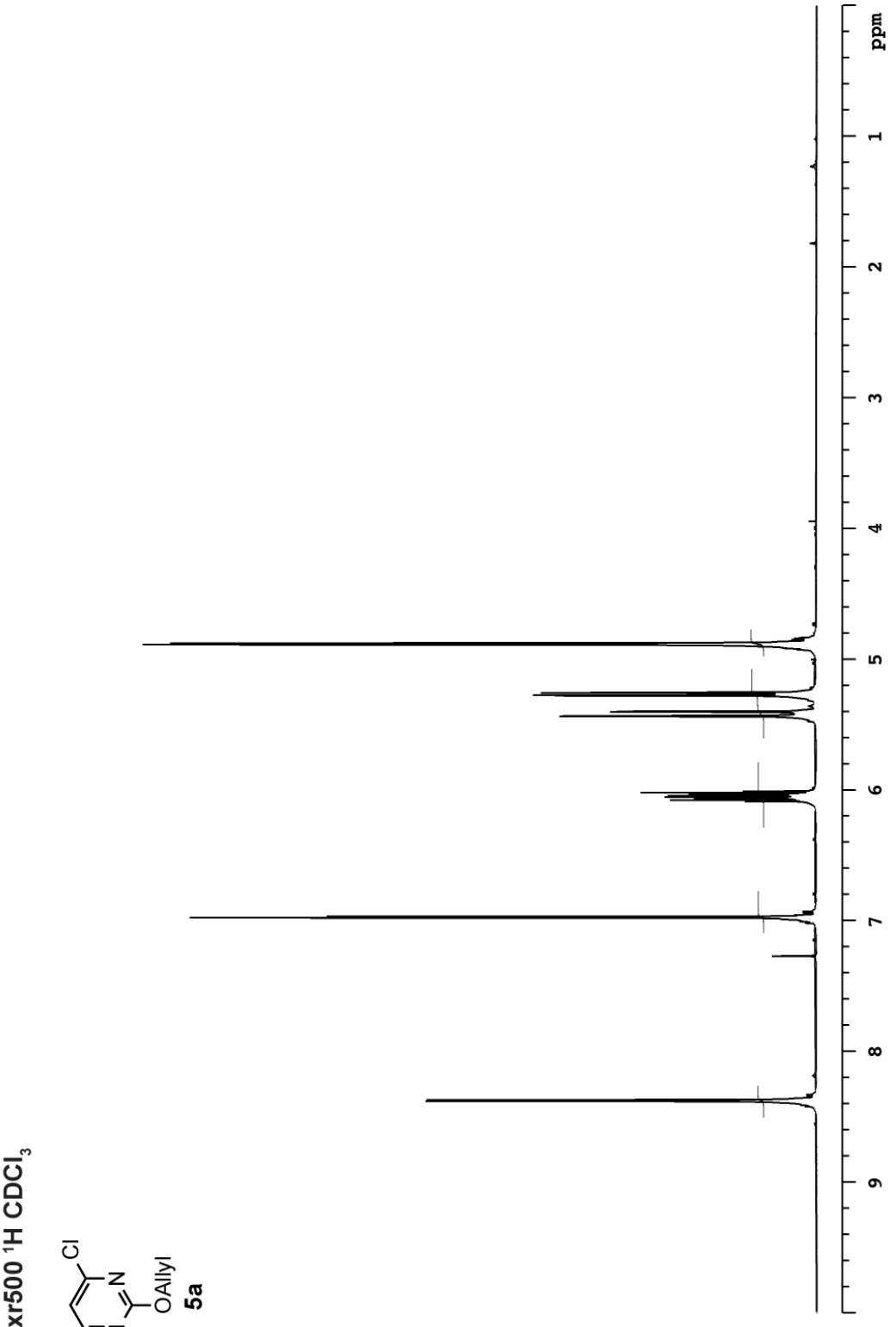
vxr500 1H CDCl3
Cl
N
N
OAllyl
5a
9
8
7
6
5
4
3
2
1
ppm

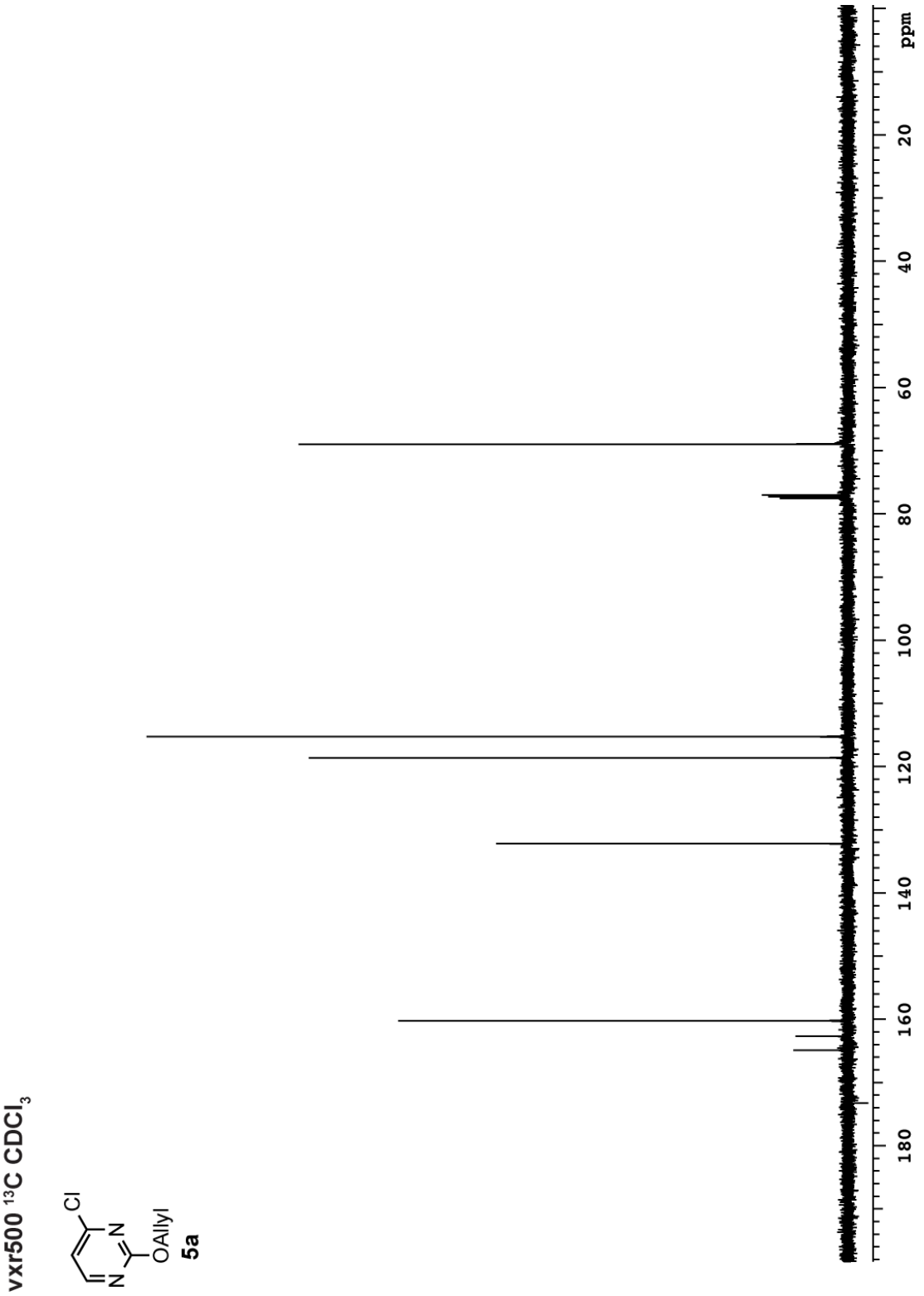
vxr500 13C CDCl3
Cl
N
N
OAllyl
5a
180
160
140
120
100
80
60
40
20
ppm

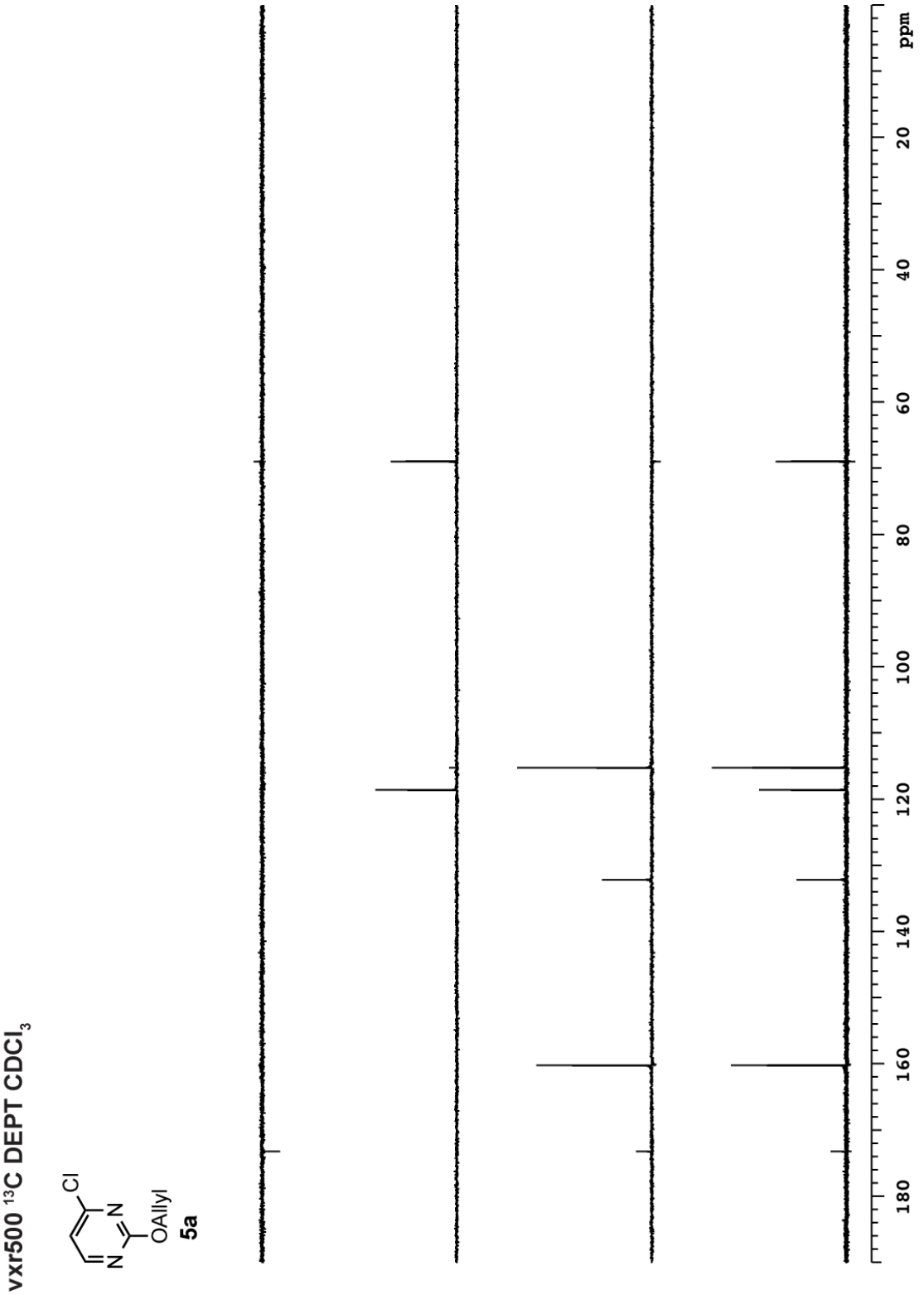
vxr500 13C DEPT CDCl3
Cl
N
N
OAllyl
5a
180
160
140
120
100
80
60
40
20
ppm

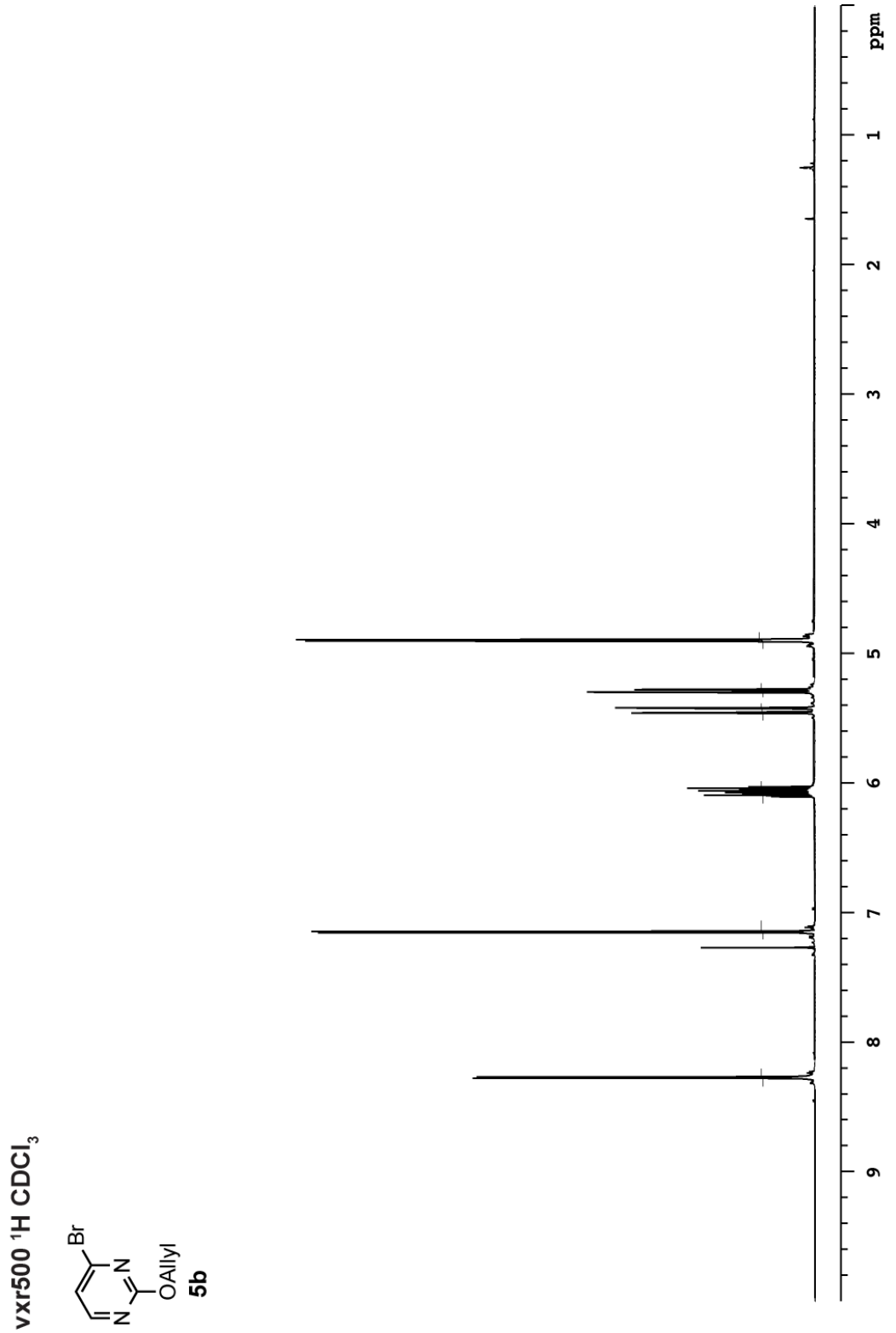
vxr500 1H CDCl3
Br
N
N
OAllyl
5b
ppm
9
8
7
6
5
4
3
2
1

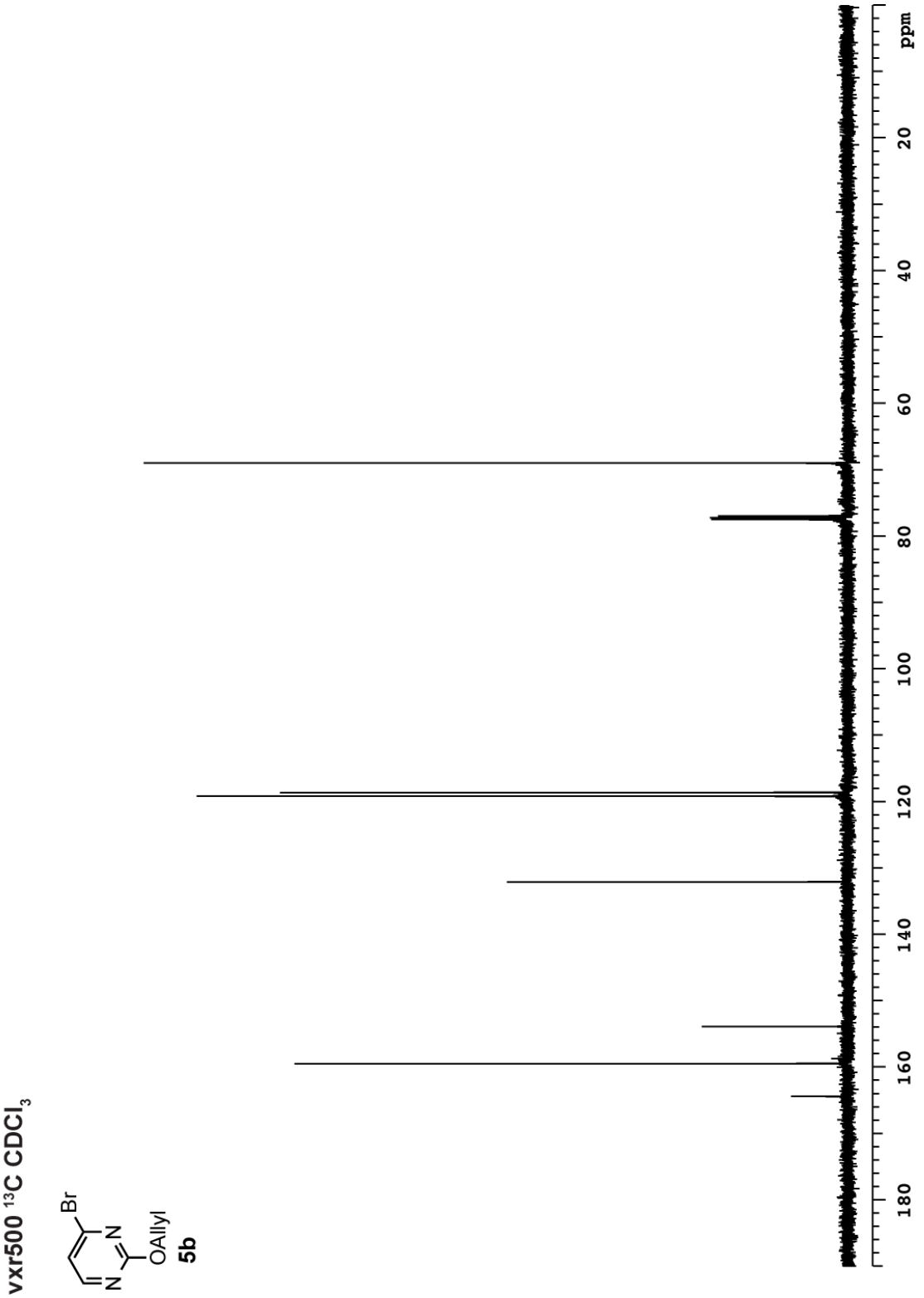
vxr500 13C CDCl3
Br
N
N
OAllyl
5b
180
160
140
120
100
80
60
40
20
ppm

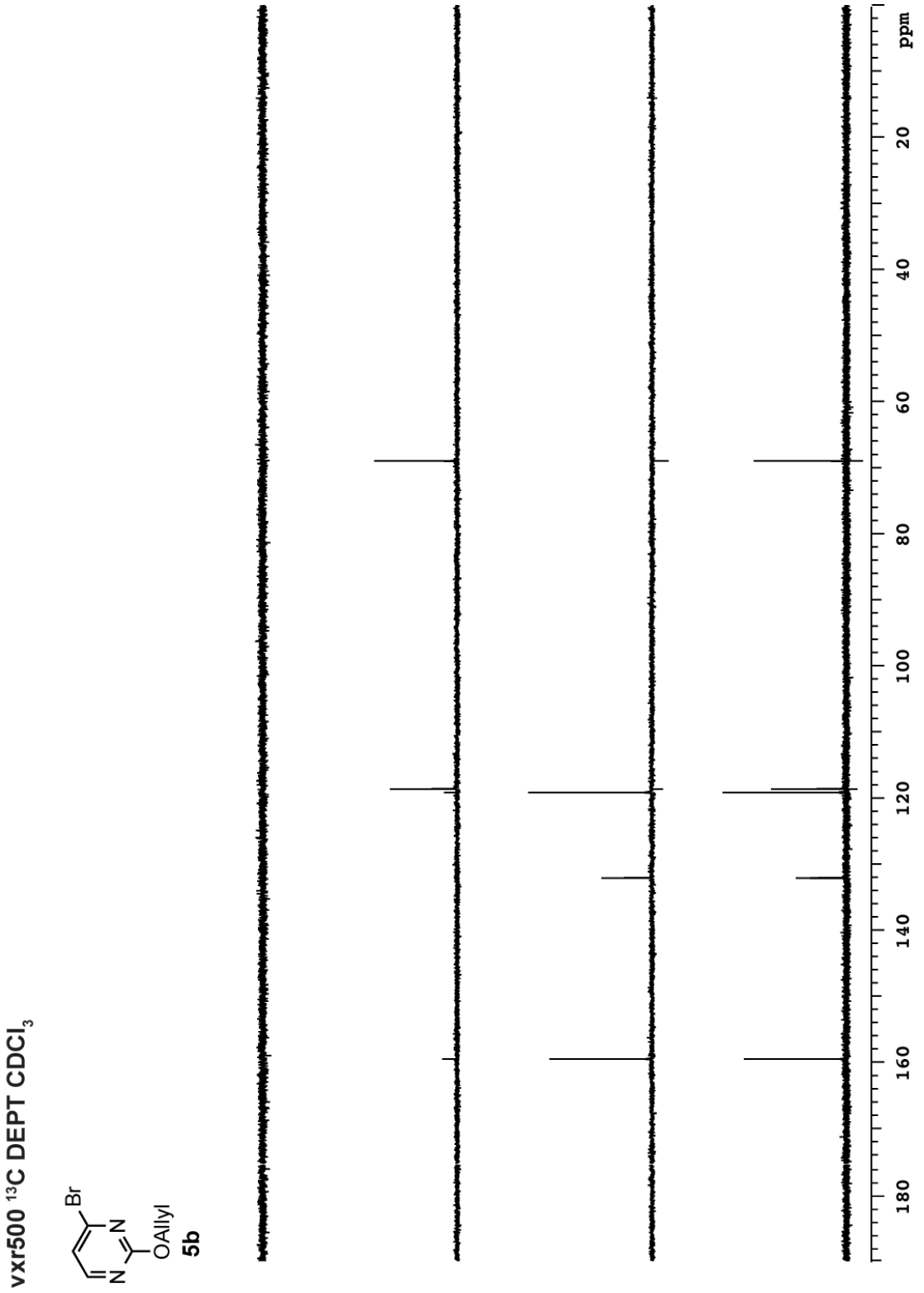
vxr500 13C DEPT CDCl3
Br
N
N
OAllyl
5b
180
160
140
120
100
80
60
40
20
ppm

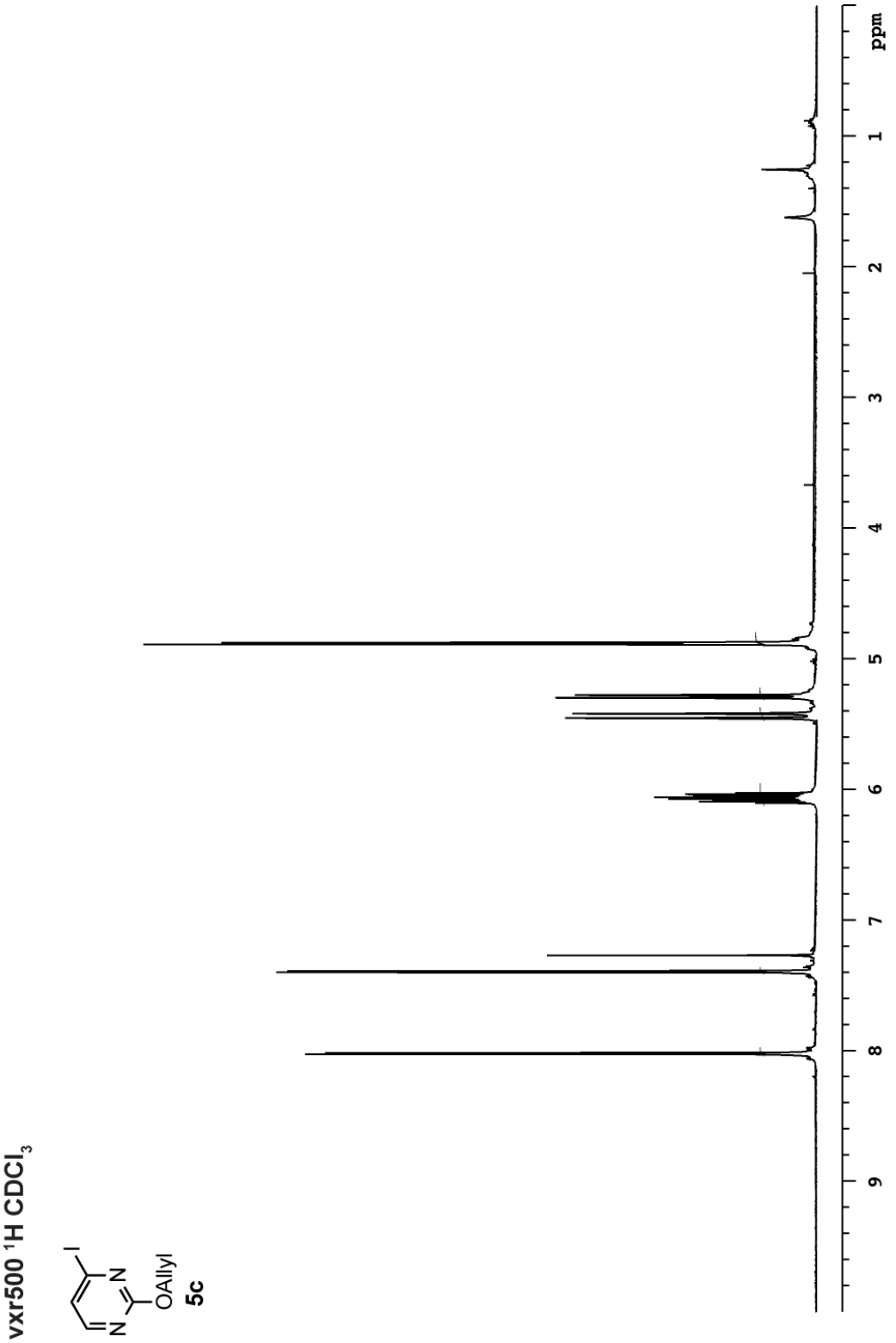
vxr500 1H CDCl3
I
N
N
OAllyl
5c
ppm
9
8
7
6
5
4
3
2
1

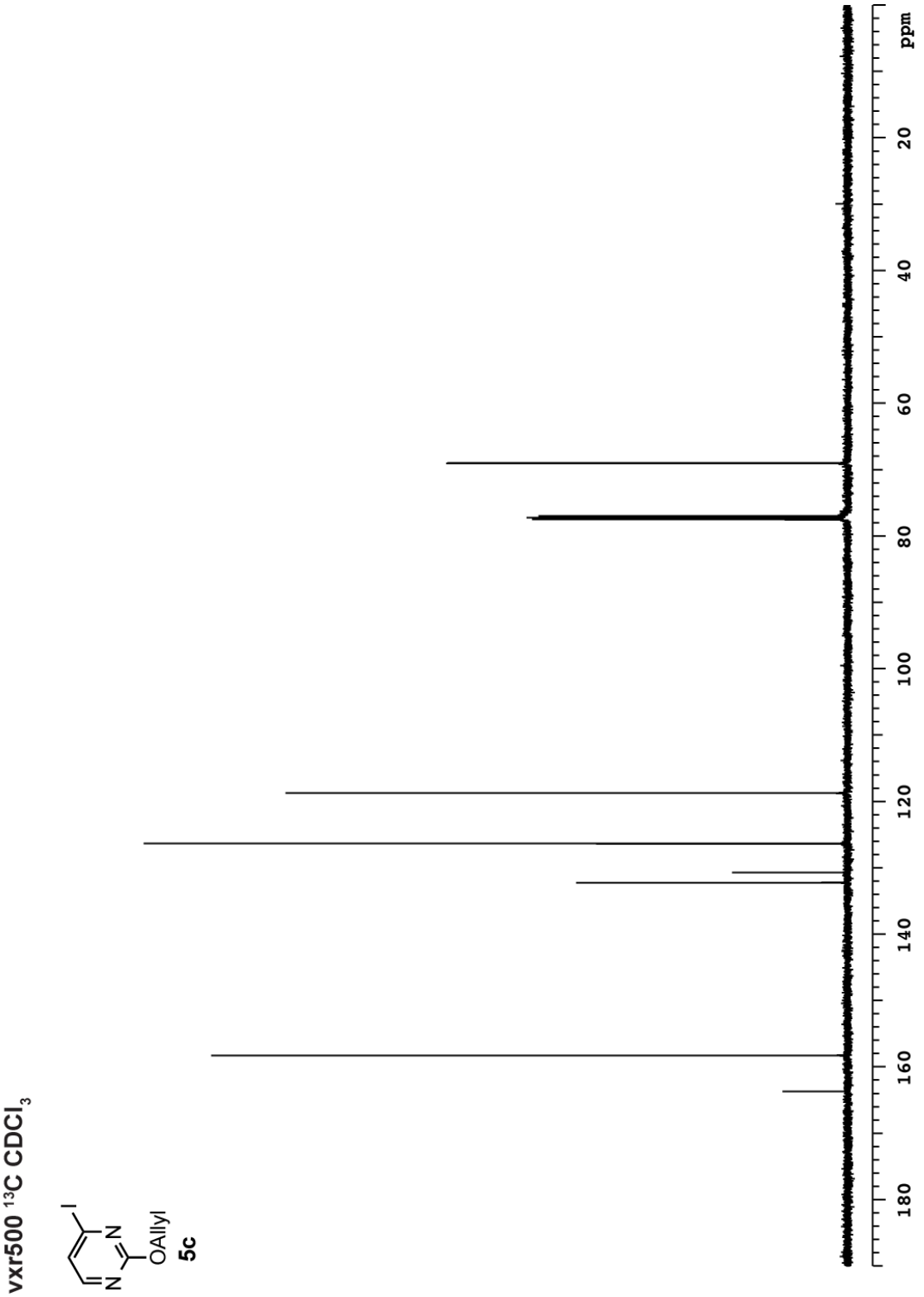
vxr500 13C CDCl3
I
N
N
OAllyl
5c
180
160
140
120
100
80
60
40
20
ppm

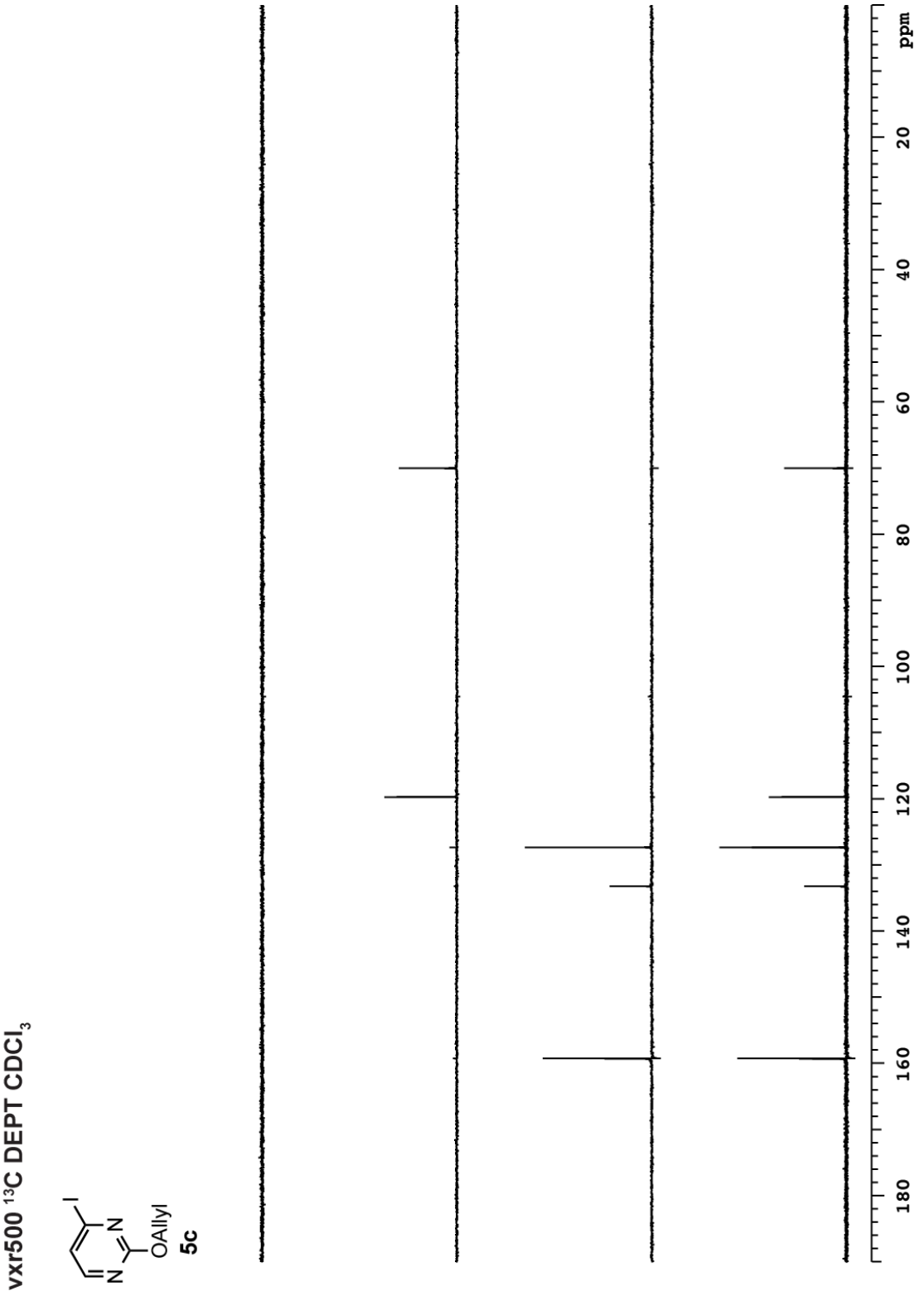
vxr500 13C DEPT CDCl3
I
N
N
OAllyl
5c
180
160
140
120
100
80
60
40
20
ppm

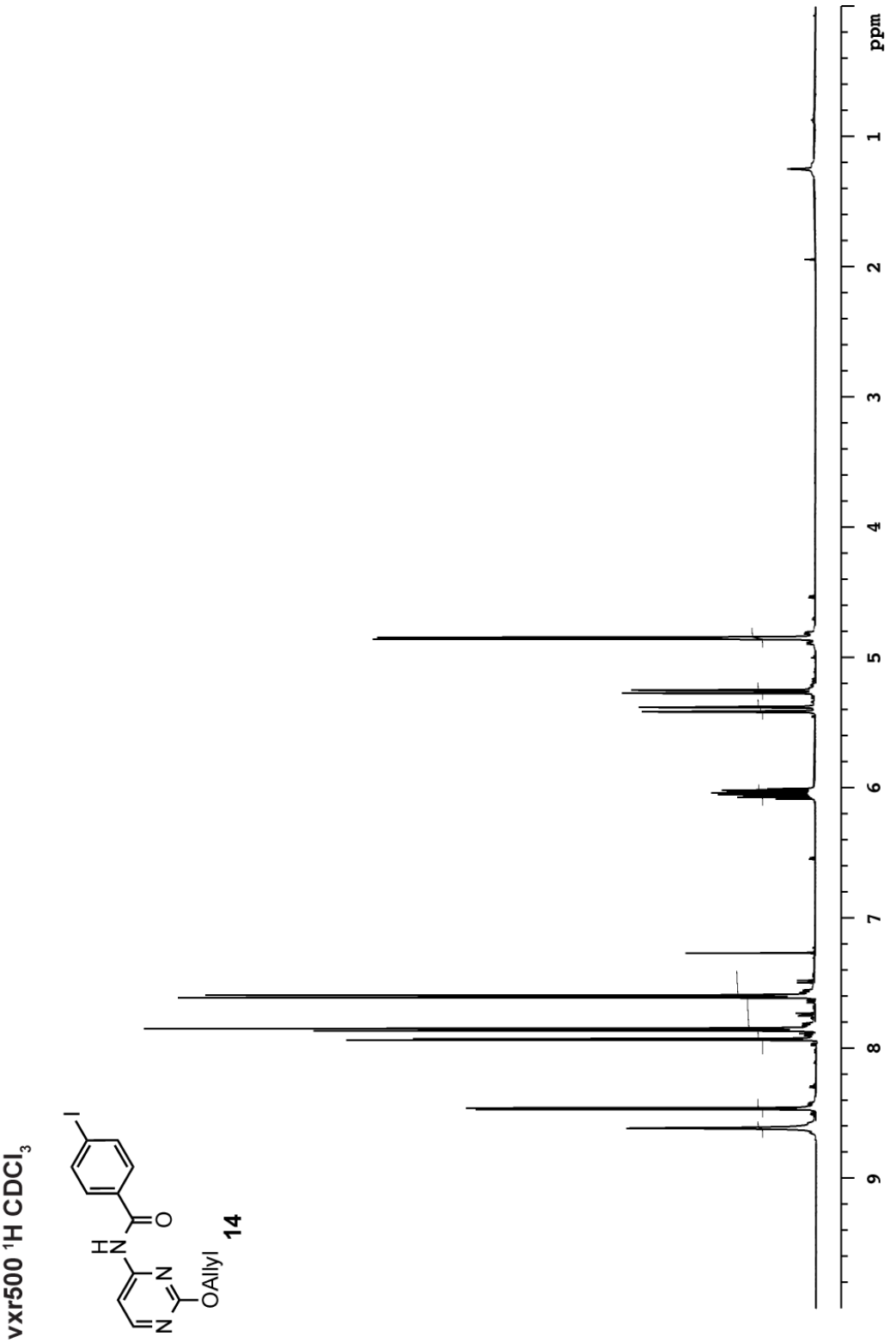
vxr500 1H CDCl3
I
H
N
O
N
N
OAllyl
14
ppm
9
8
7
6
5
4
3
2
1

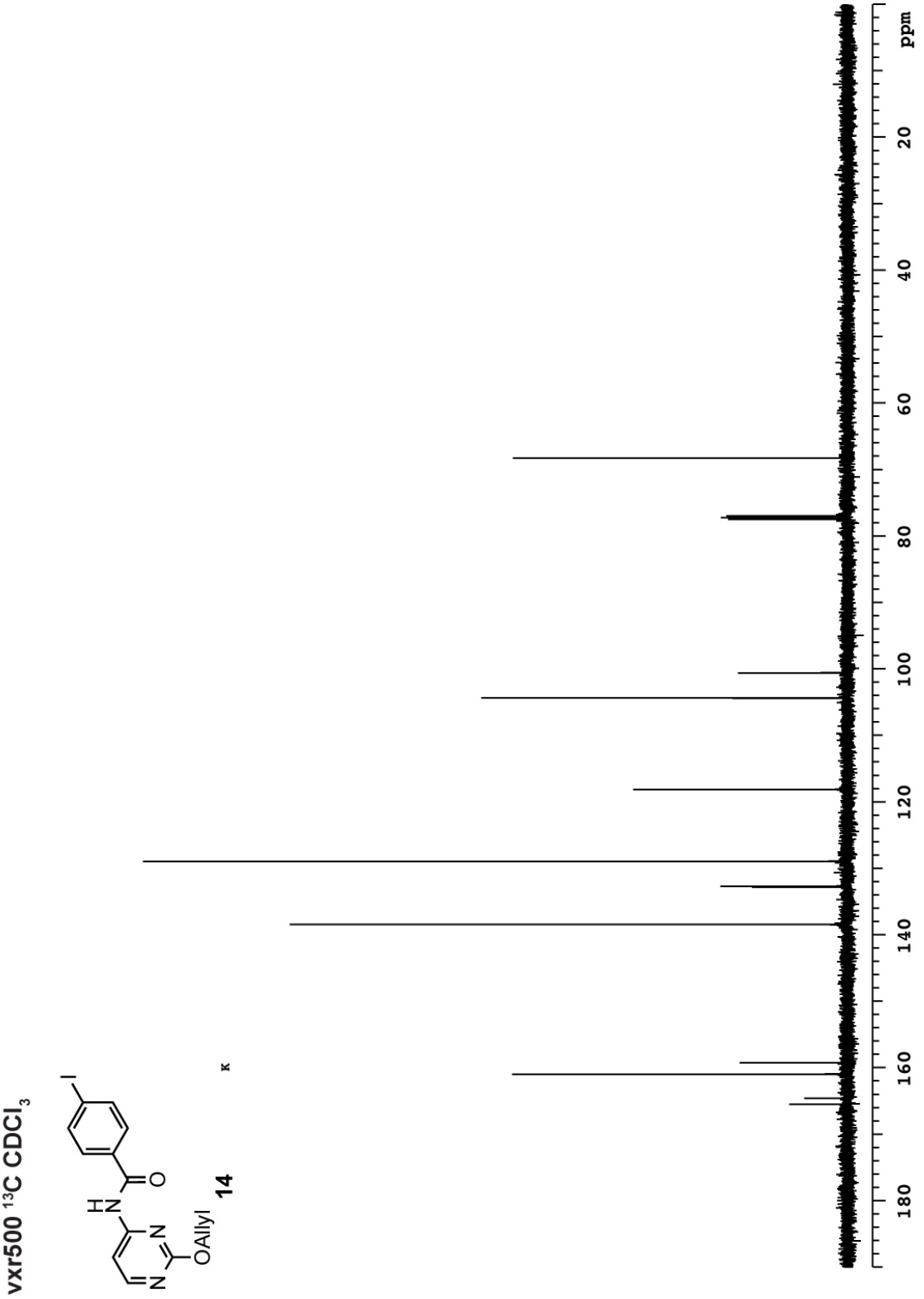
vxr500 13C CDCl3
I
O
HN
N
N
OAllyl
14
ppm
20
40
60
80
100
120
140
160
180

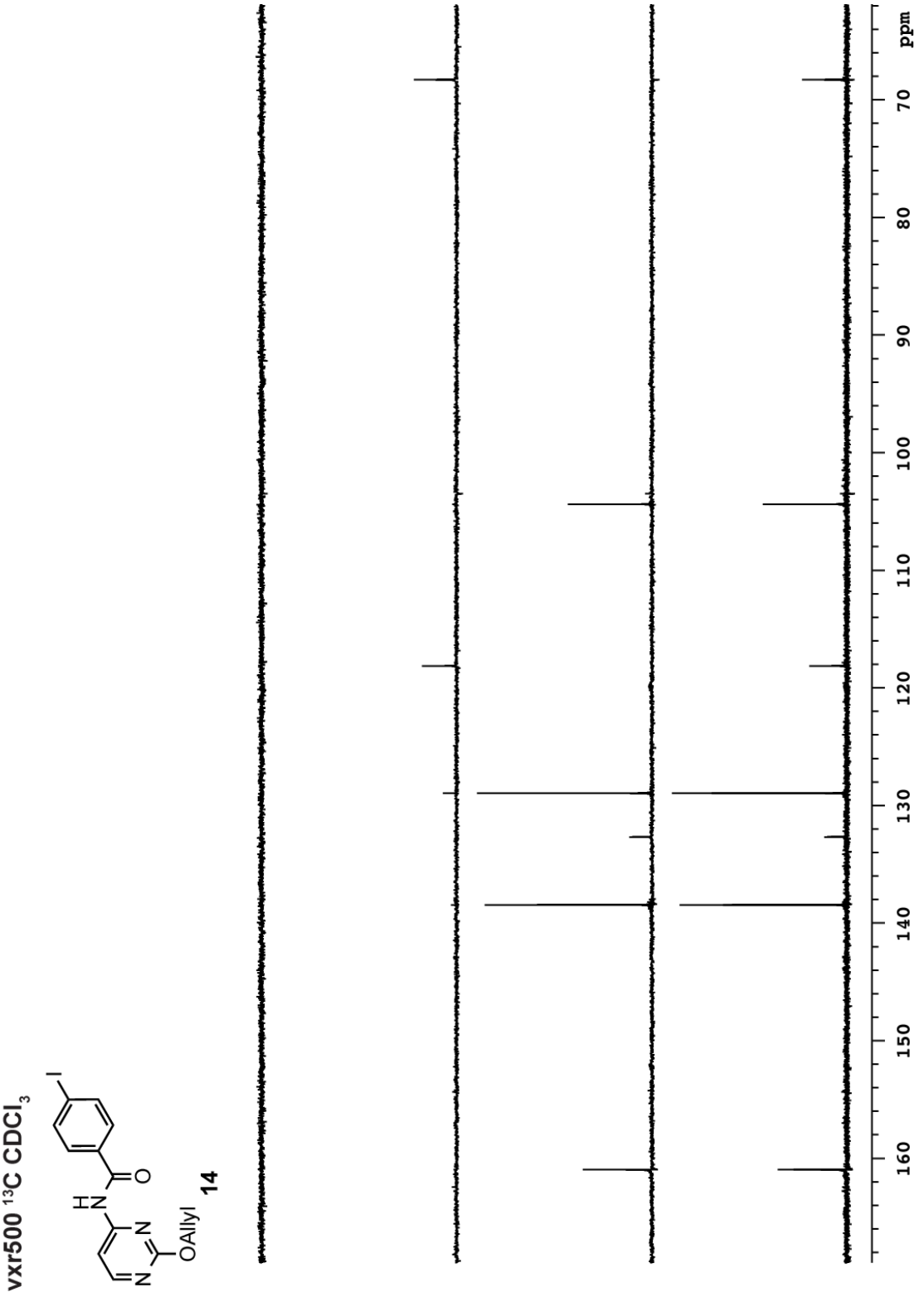
vxr500 13C CDCl3
I
O
N
H
N
N
OAllyl
14
160
150
140
130
120
110
100
90
80
70
ppm

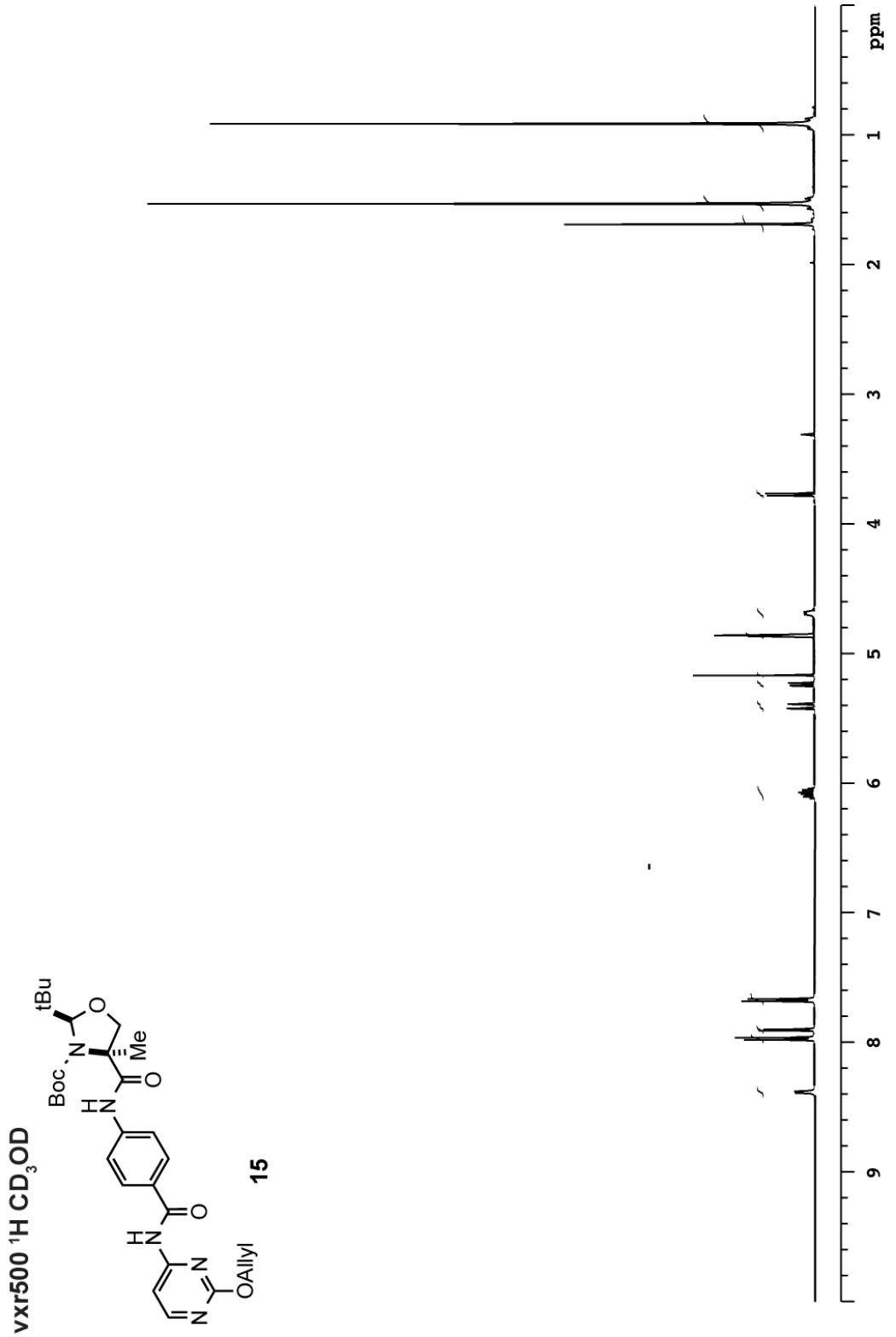
vxr500 1H CD3OD
tBu
Boc
Me
OAllyl
15
ppm

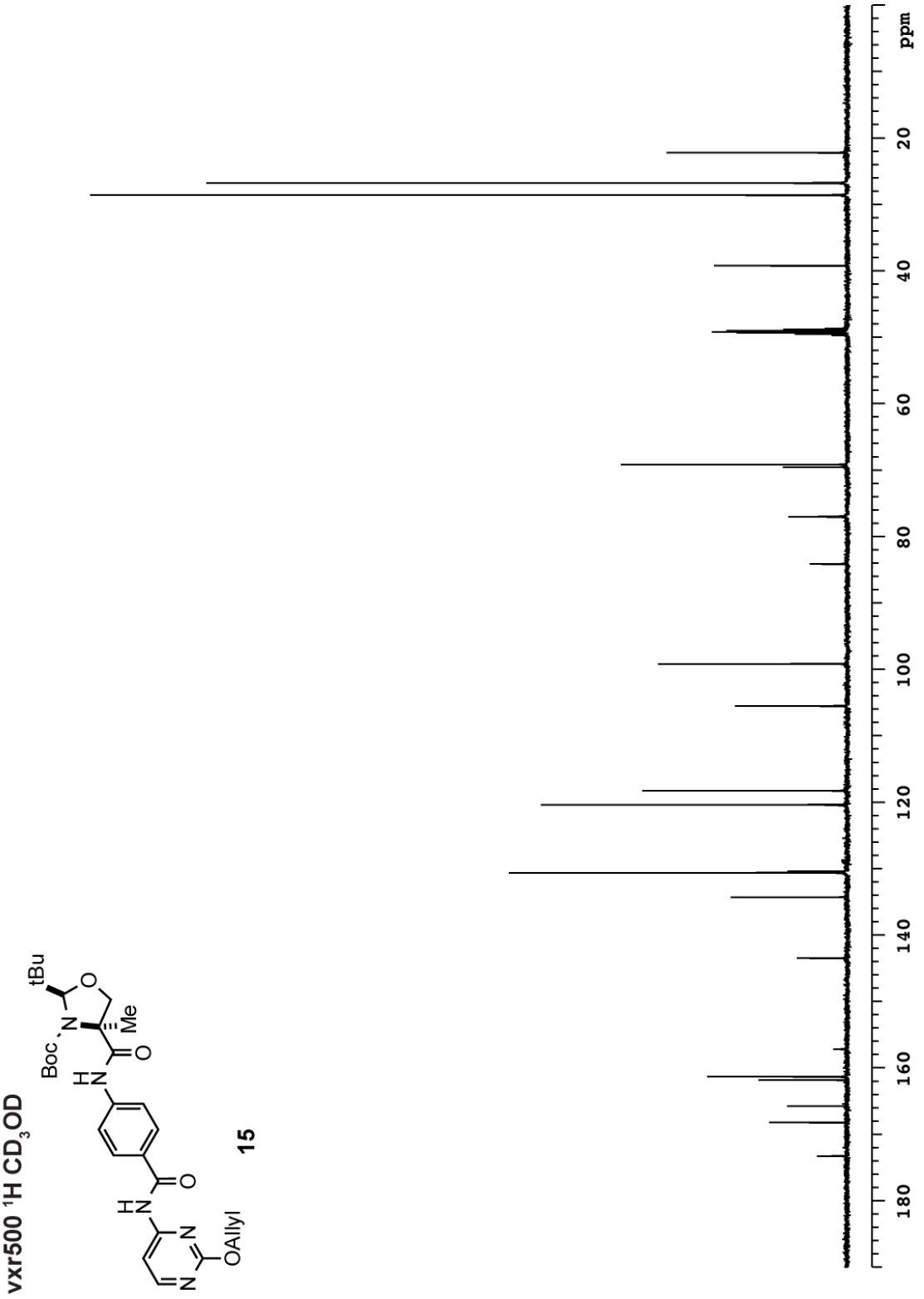
vxr500 1H CD3OD
tBu
Boc
Me
OAllyl
15
ppm
20
40
60
80
100
120
140
160
180

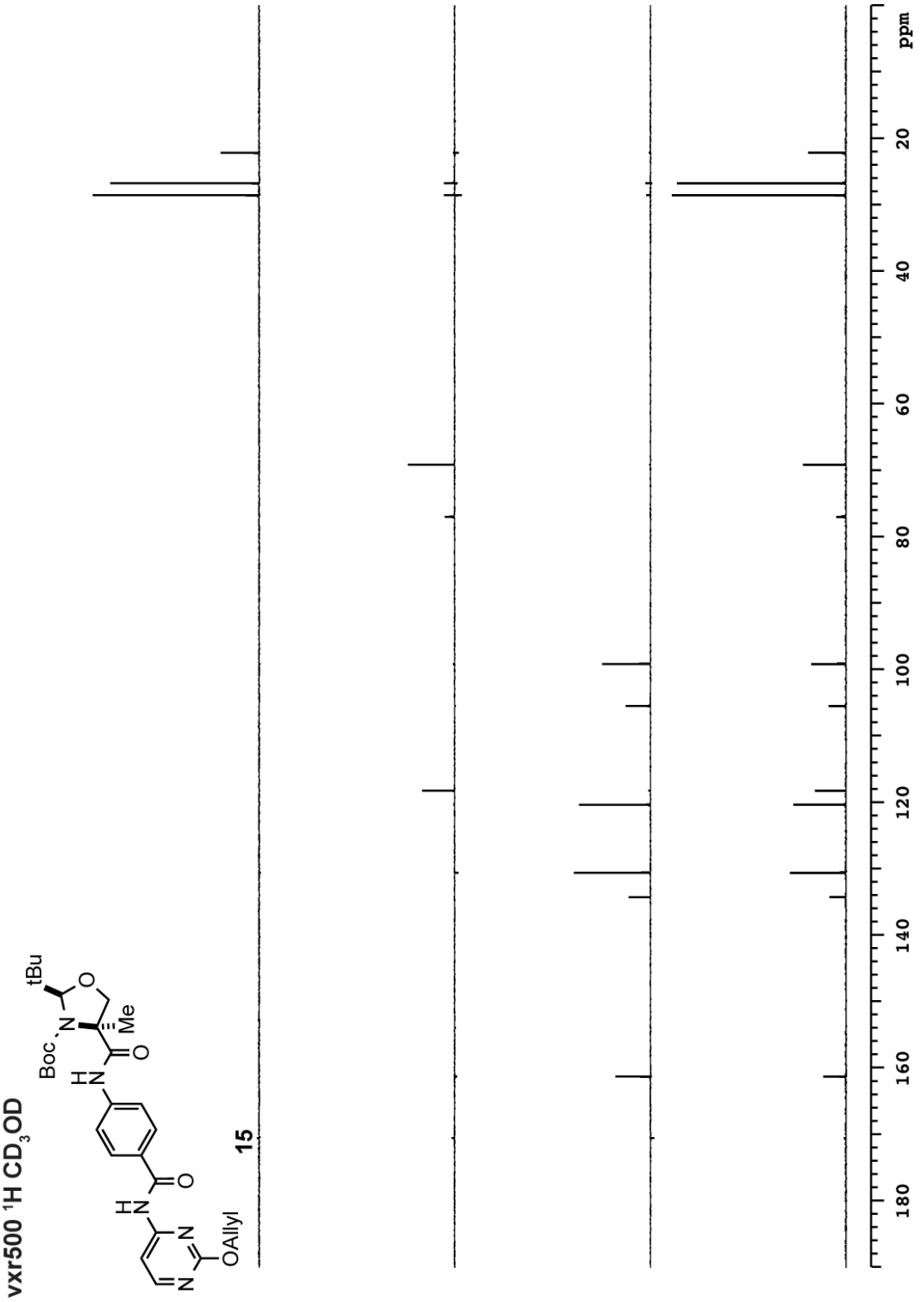
vxr500 1H CD3OD
15
tBu
Boc
Me
OAllyl
ppm
20
40
60
80
100
120
140
160
180

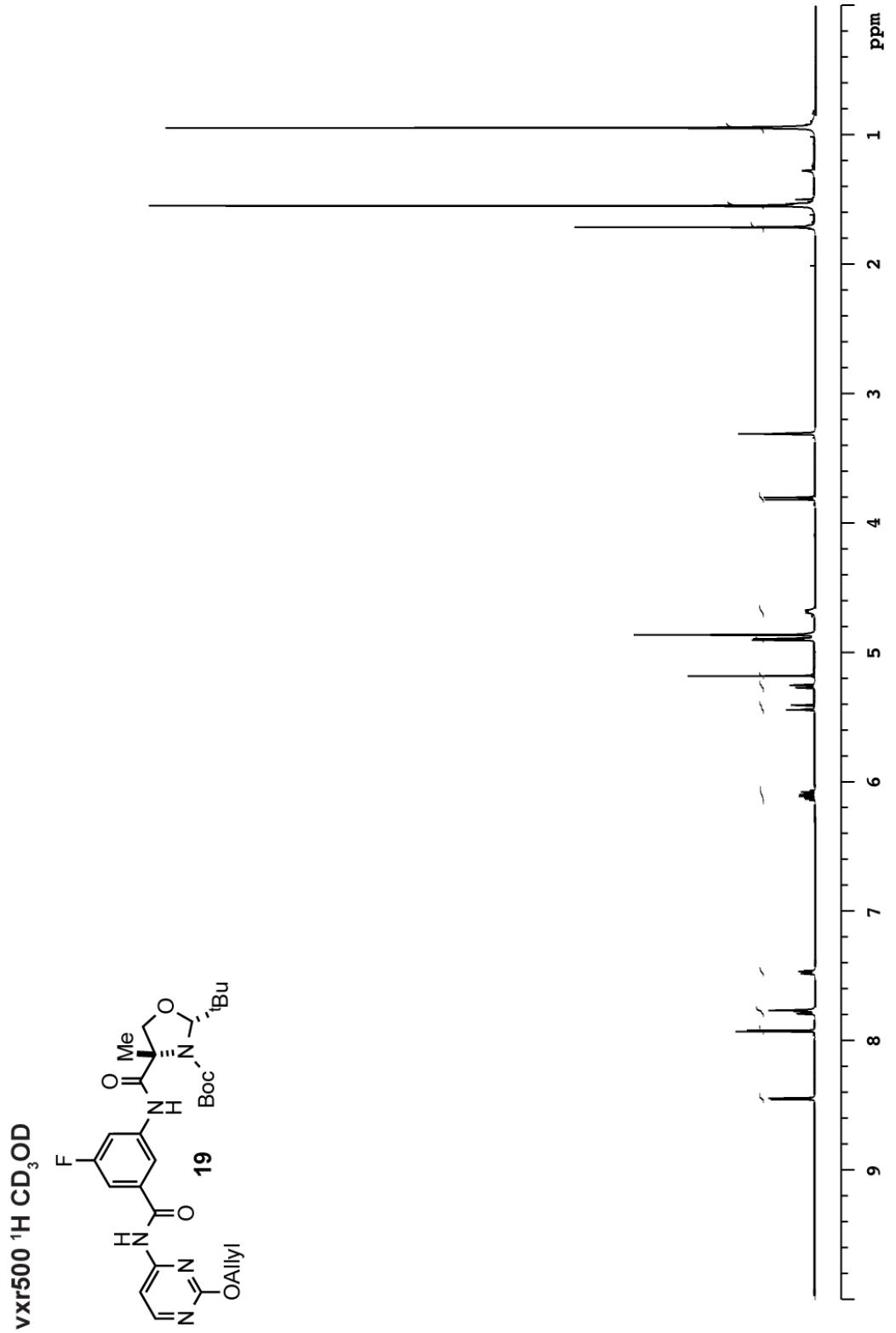
vxr500 1H CD3OD
F
O
Me
O
N
H
N
Boc
tBu
19
N
H
N
N
OAllyl
ppm
1
2
3
4
5
6
7
8
9

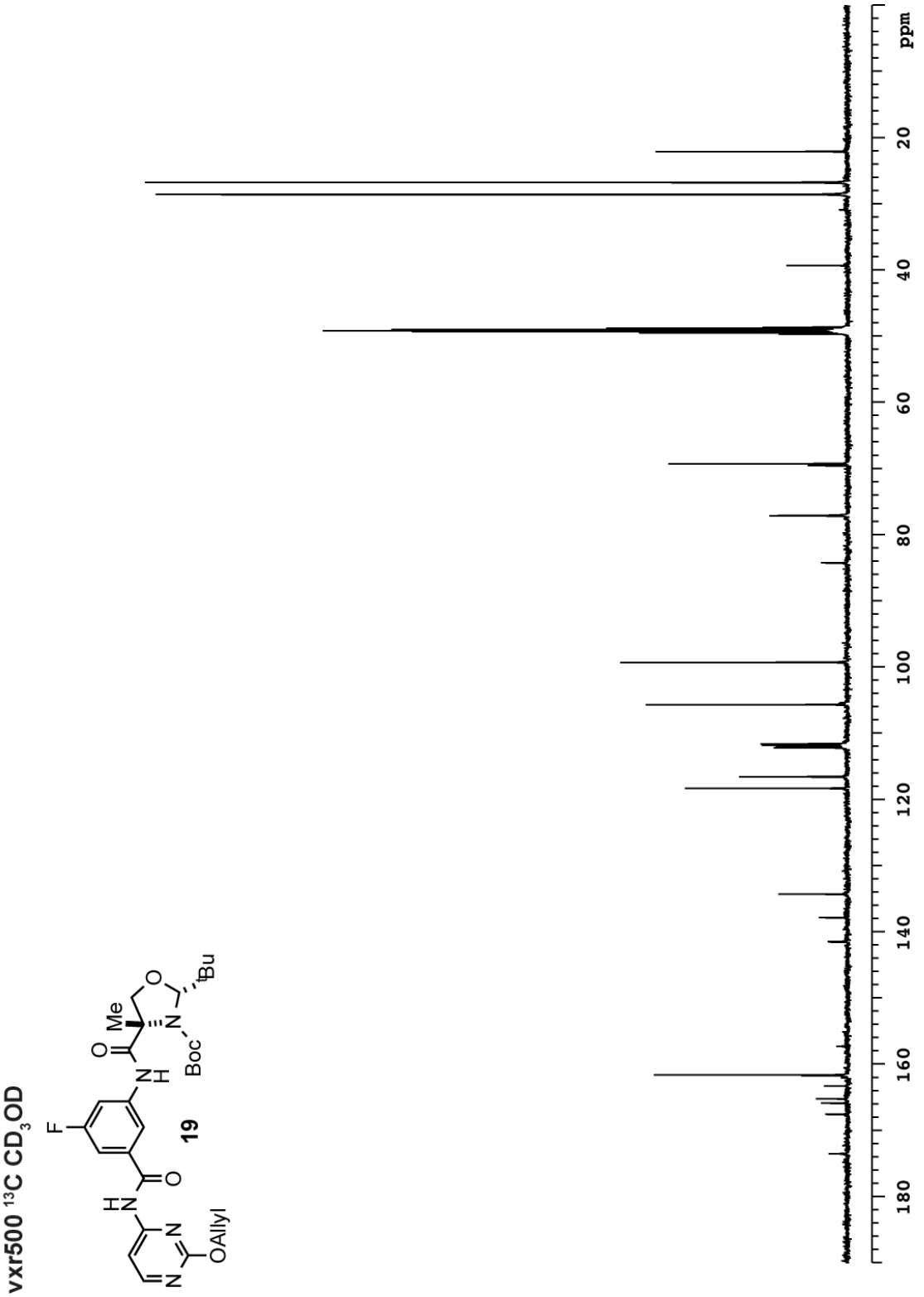
vxr500 13C CD3OD
19
ppm
20
40
60
80
100
120
140
160
180

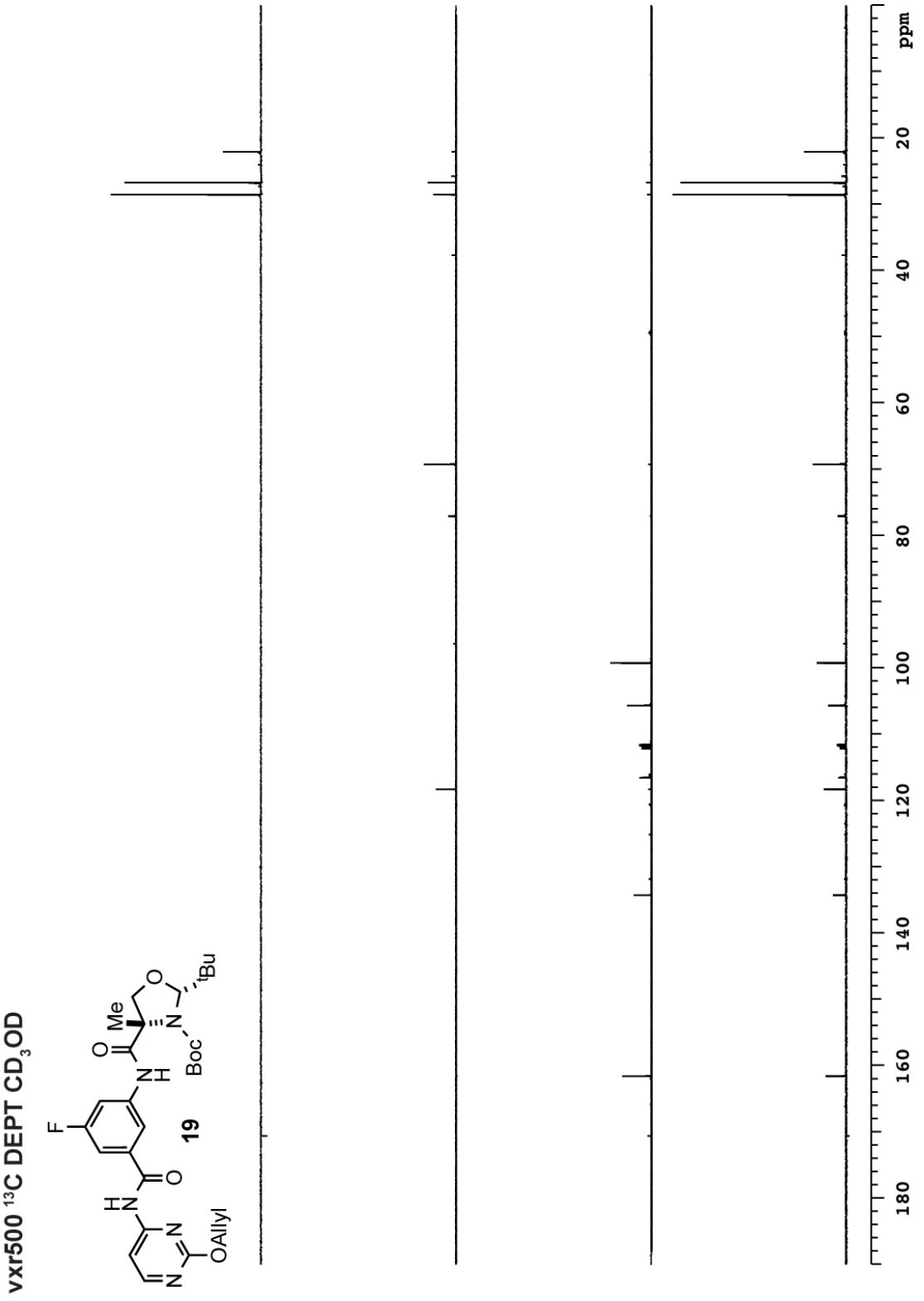
vxr500 13C DEPT CD3OD
19
ppm
20
40
60
80
100
120
140
160
180

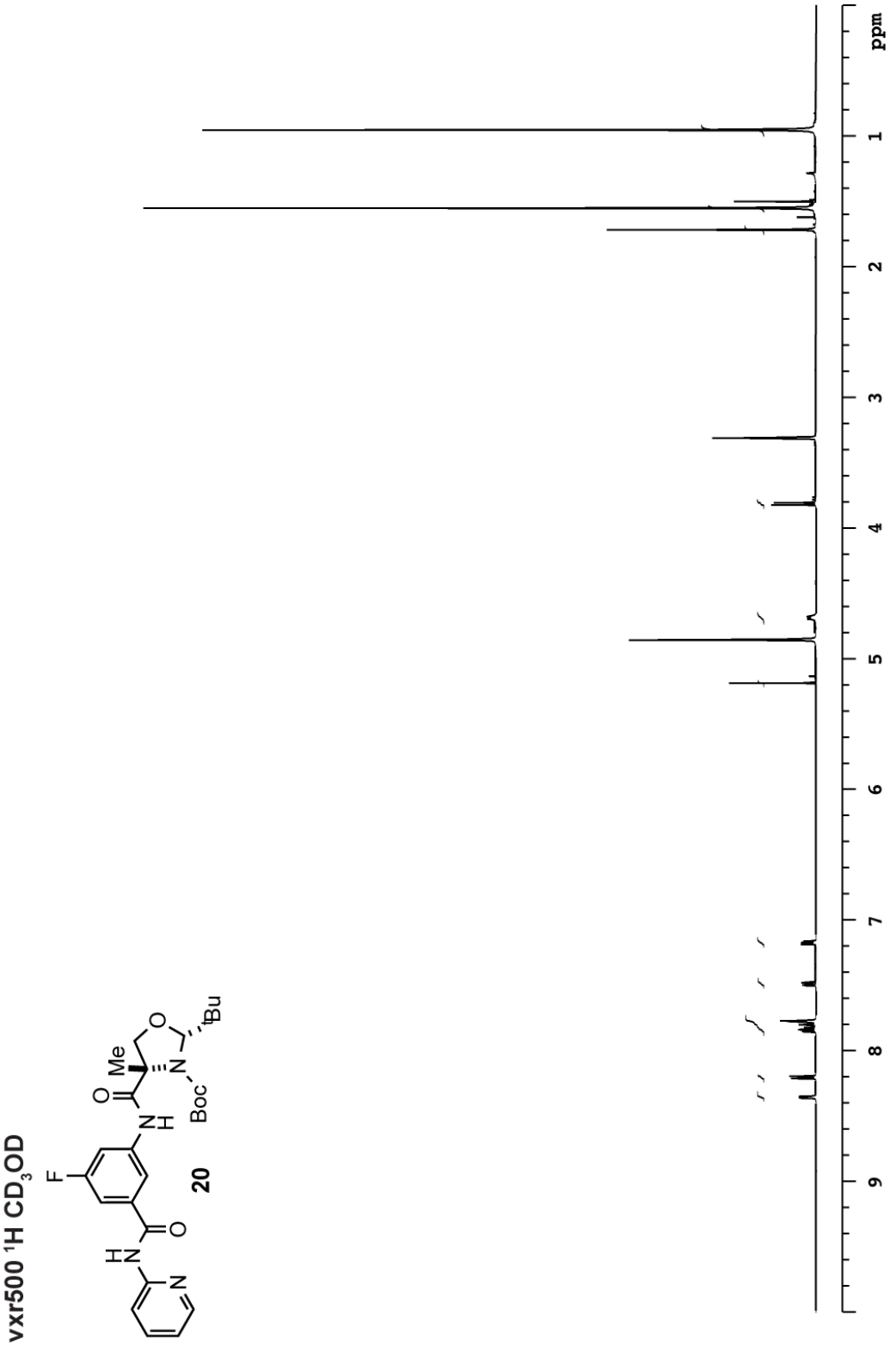
vxr500 1H CD3OD
F
O
N
H
N
O
Me
N
Boc
O
tBu
20
ppm
1
2
3
4
5
6
7
8
9

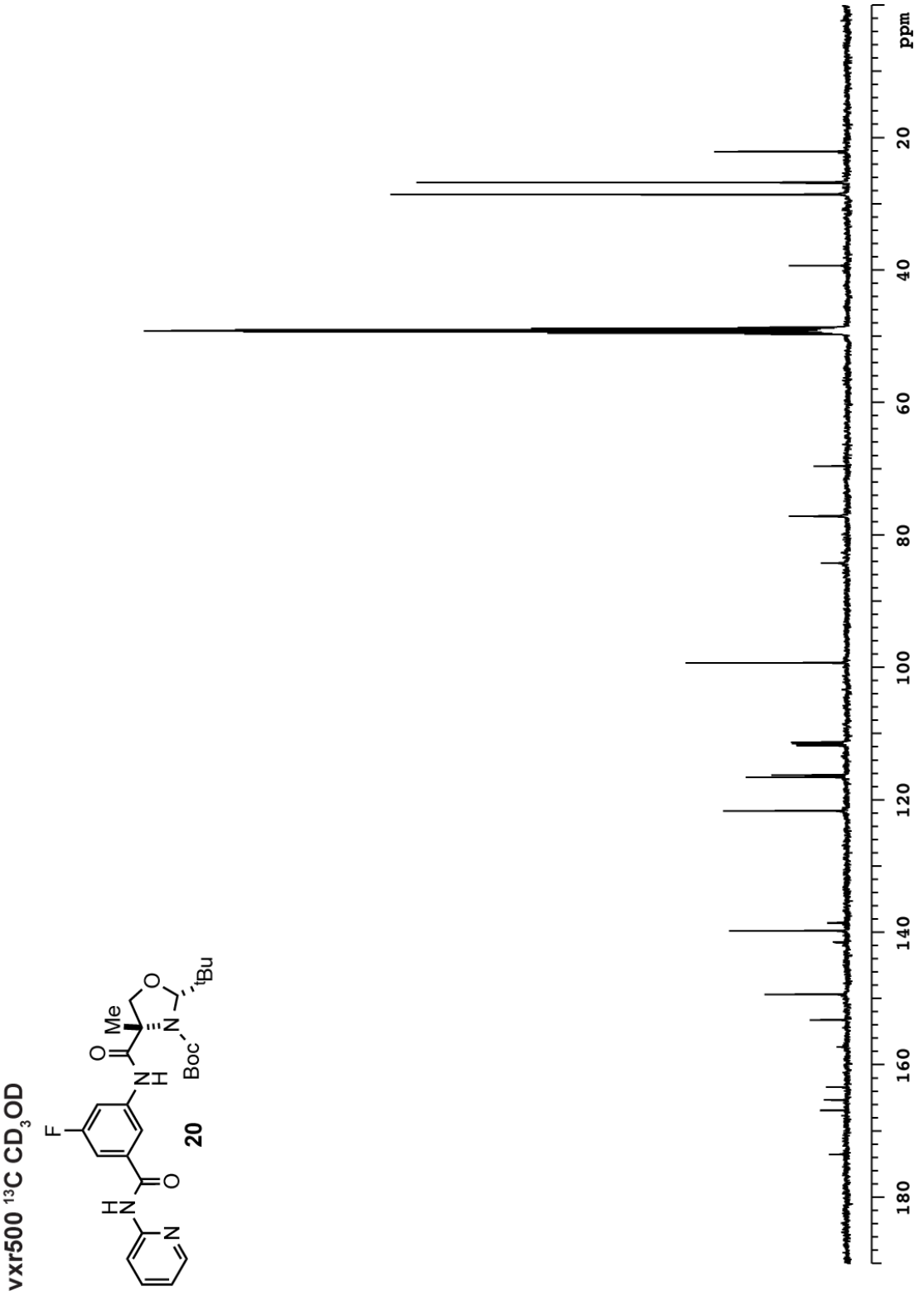
vxr500 13C CD3OD
F
O
Me
N
H
O
N
Boc
O
tBu
20
N
H
O
N
ppm
180
160
140
120
100
80
60
40
20

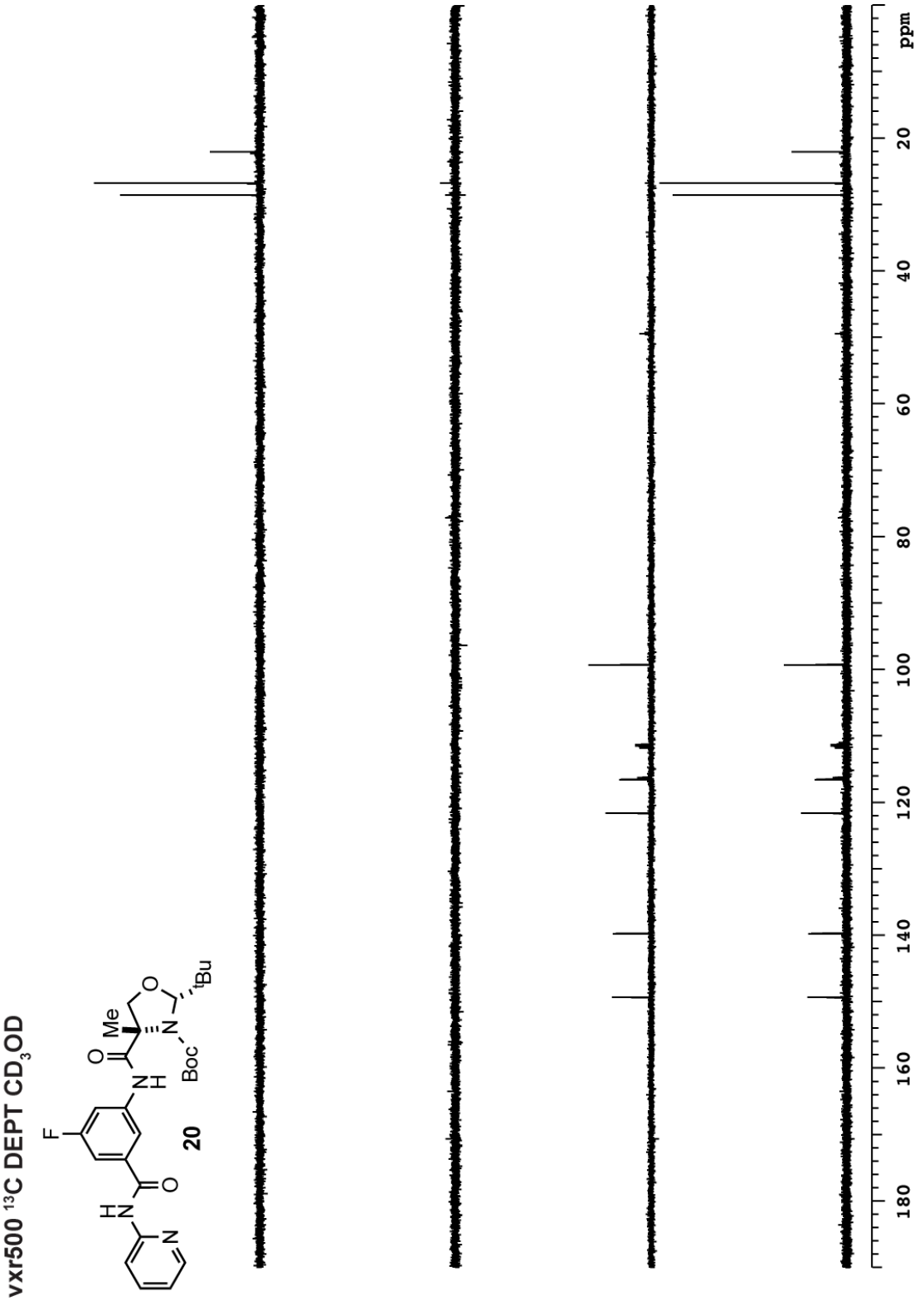
vxr500 13C DEPT CD3OD
20
ppm
180
160
140
120
100
80
60
40
20

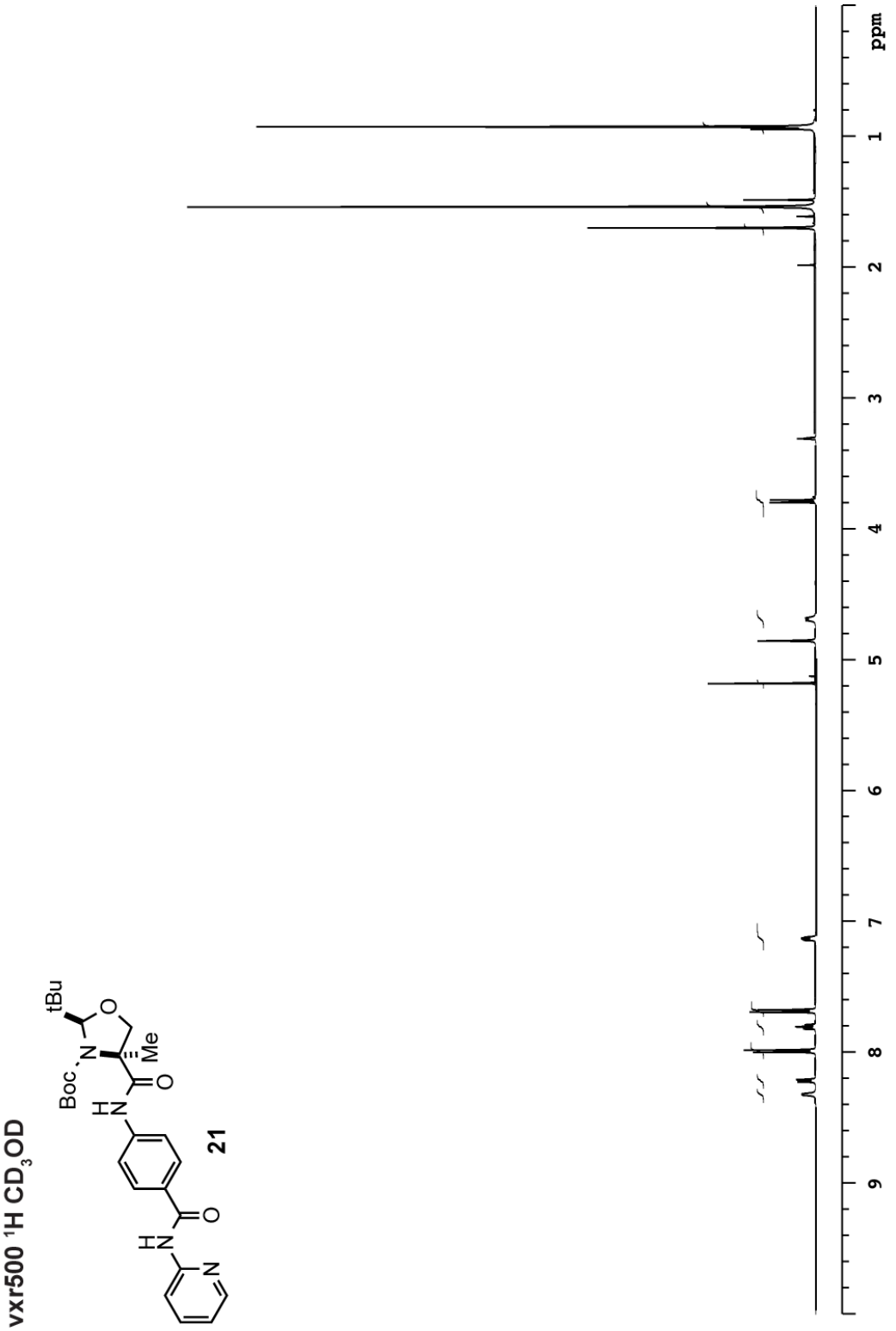
vxr500 ^{1}H CD_3OD
tBu
Boc
N
O
Me
O
H
N
21
O
H
N
N
ppm
1
2
3
4
5
6
7
8
9

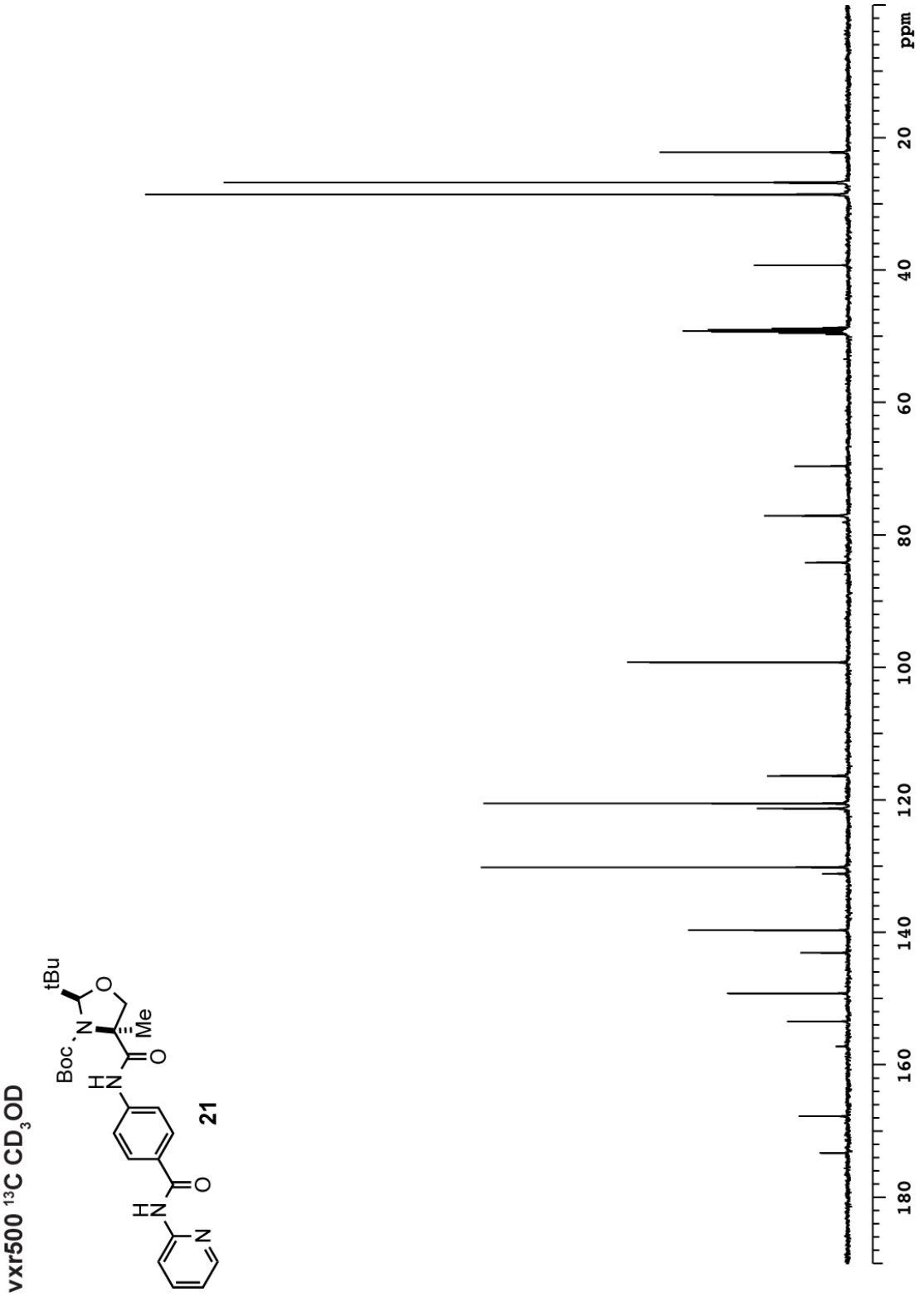
vxr500 13C CD3OD
tBu
Boc
N
O
Me
H
N
O
H
N
N
21
ppm
20
40
60
80
100
120
140
160
180

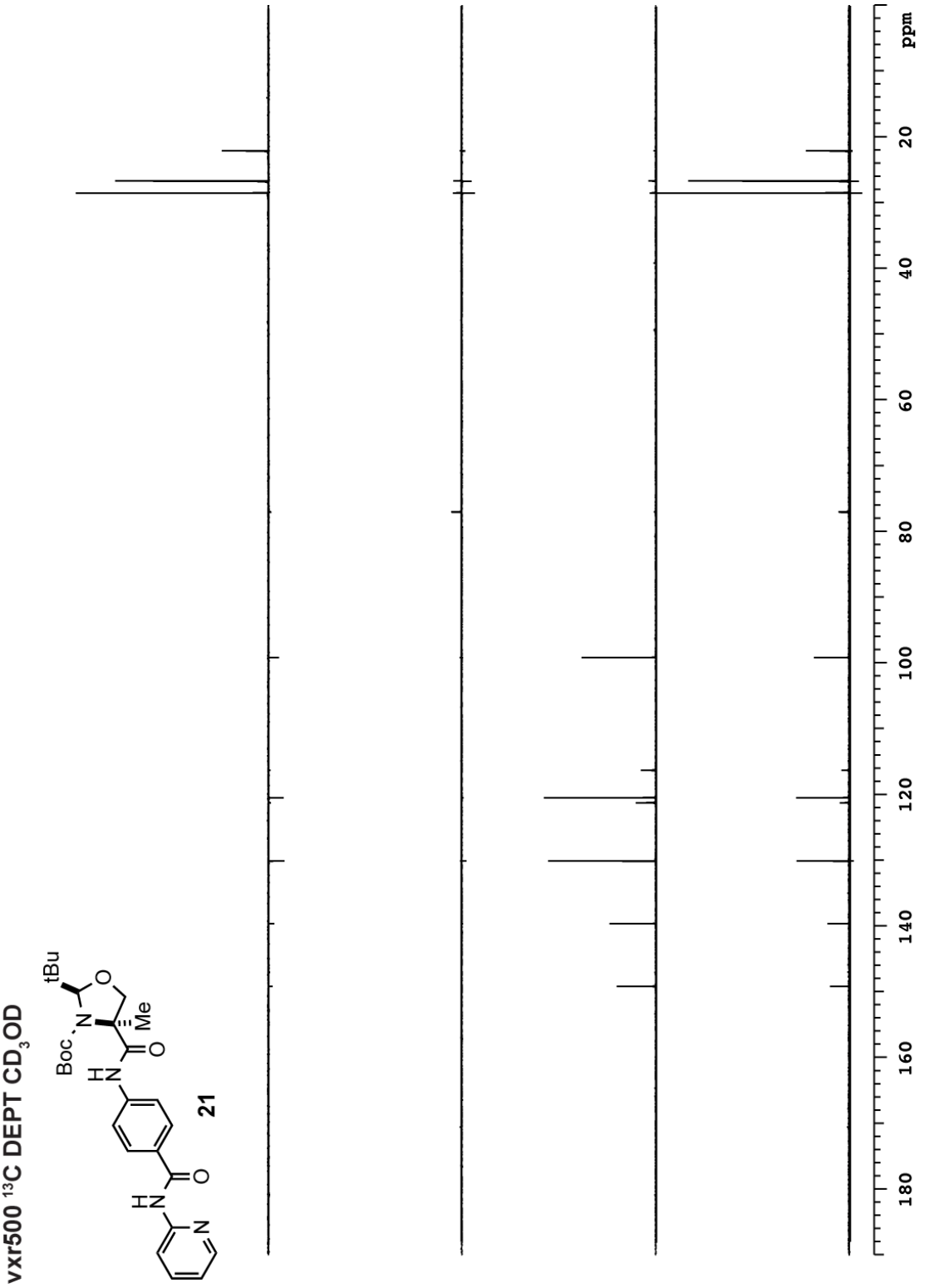
vxr500 13C DEPT CD3OD
21
ppm
20
40
60
80
100
120
140
160
180

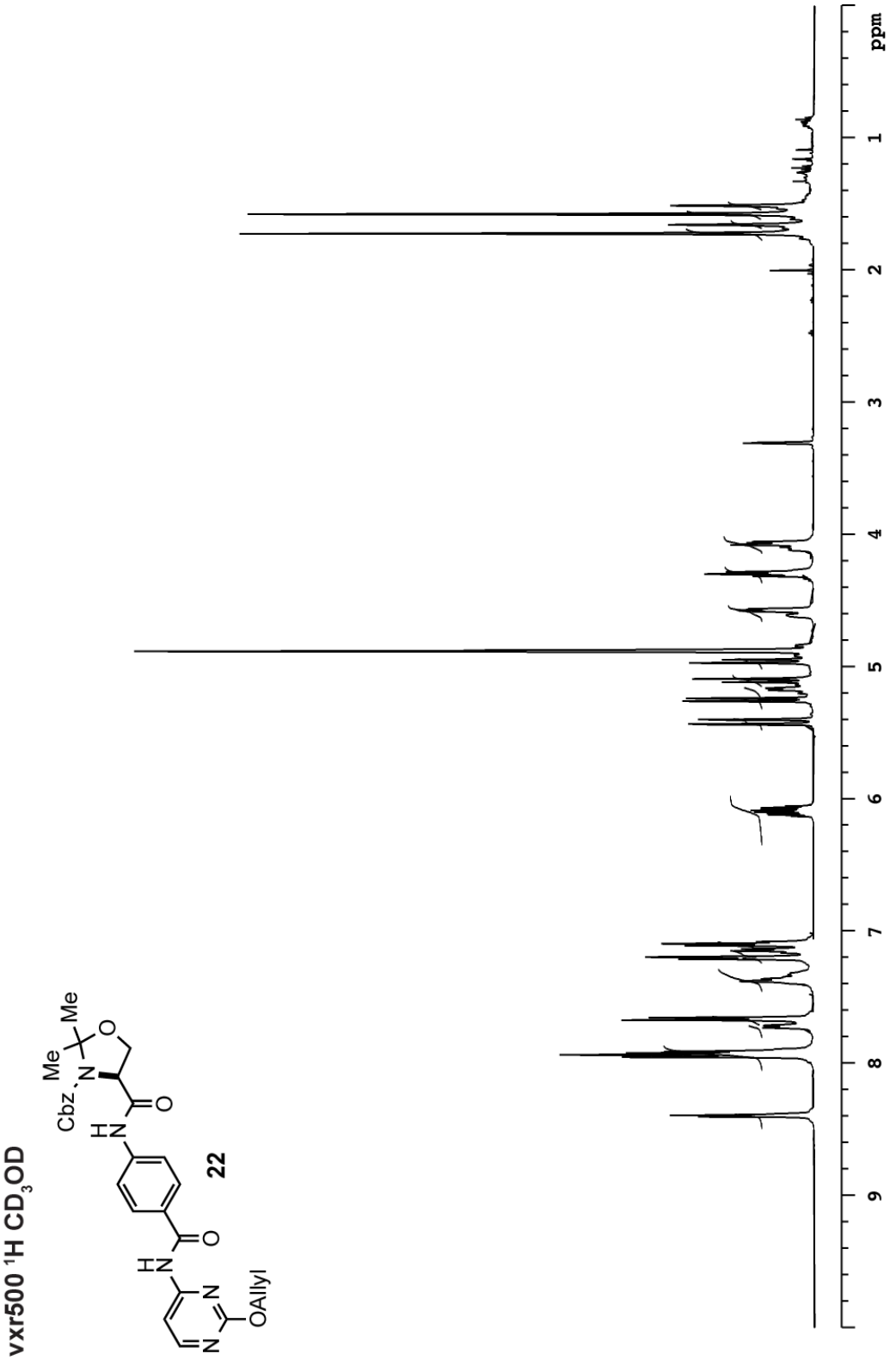
vxr500 1H CD3OD
Cbz
Me
Me
O
N
H
N
O
H
N
N
N
OAllyl
22
ppm
9
8
7
6
5
4
3
2
1

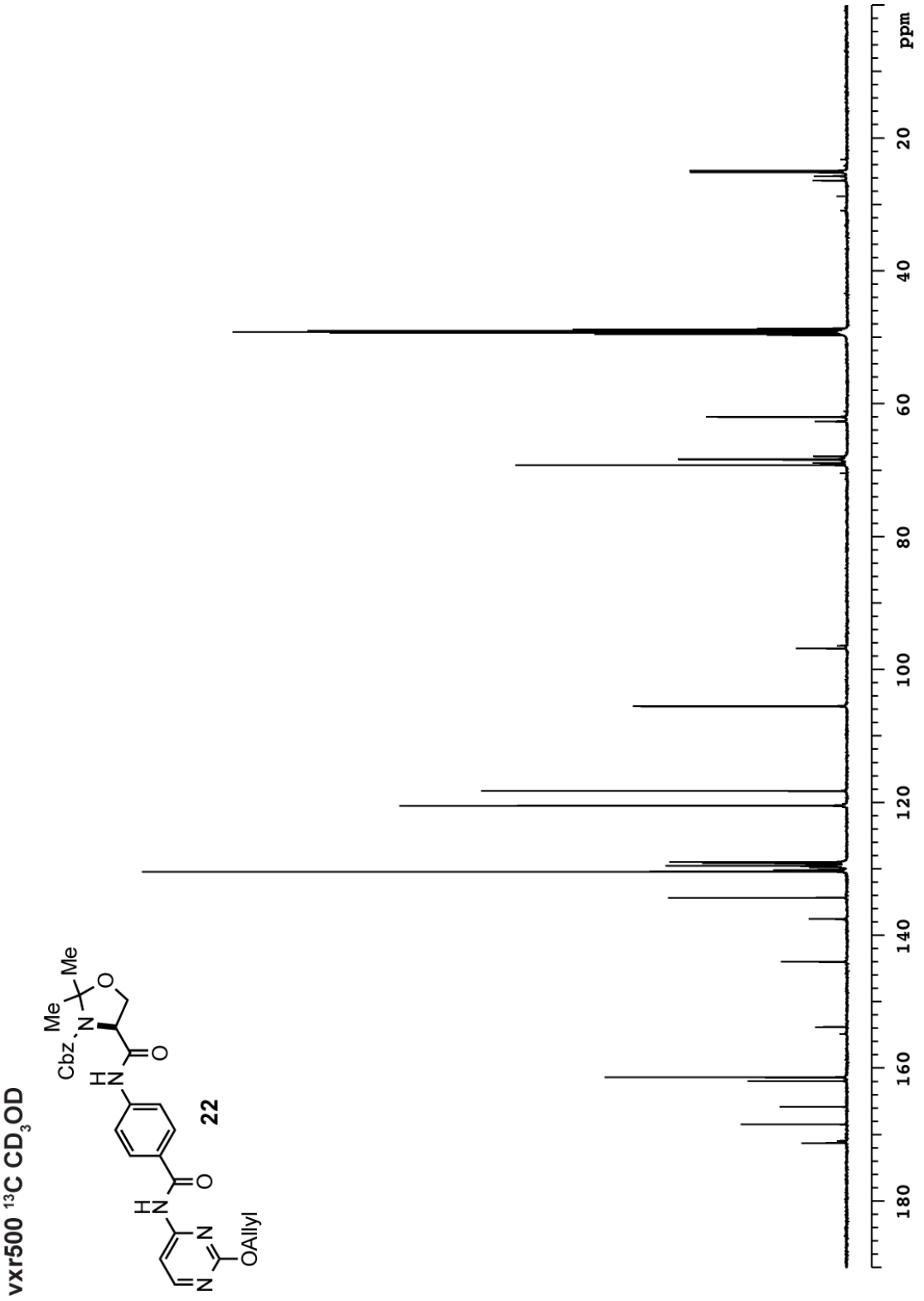
vxr500 13C CD3OD
Cbz
Me
Me
O
N
H
N
O
O
H
N
N
N
OAllyl
22
ppm
20
40
60
80
100
120
140
160
180

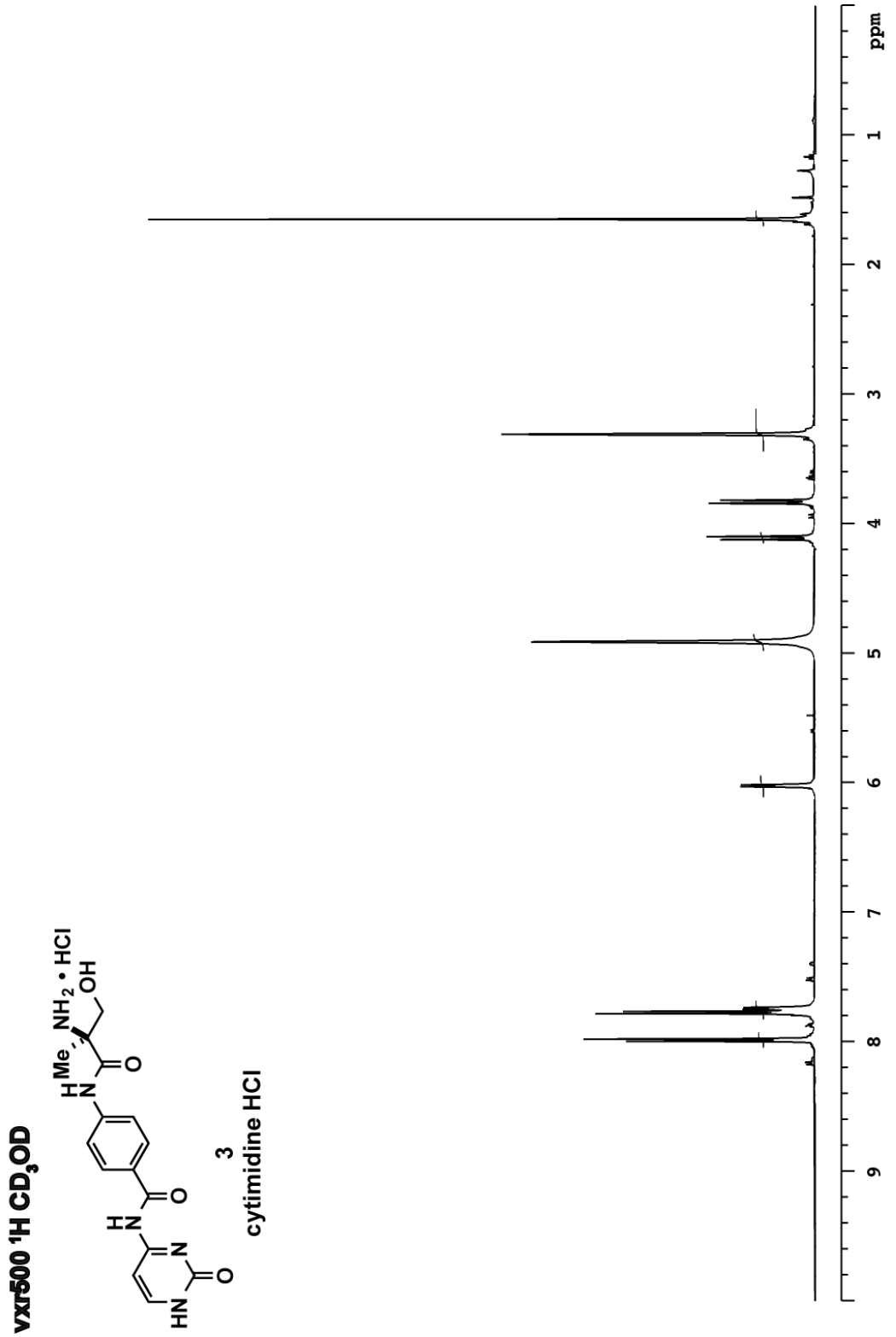
vxr500 1H CD3OD
3
cytimidine HCl
ppm

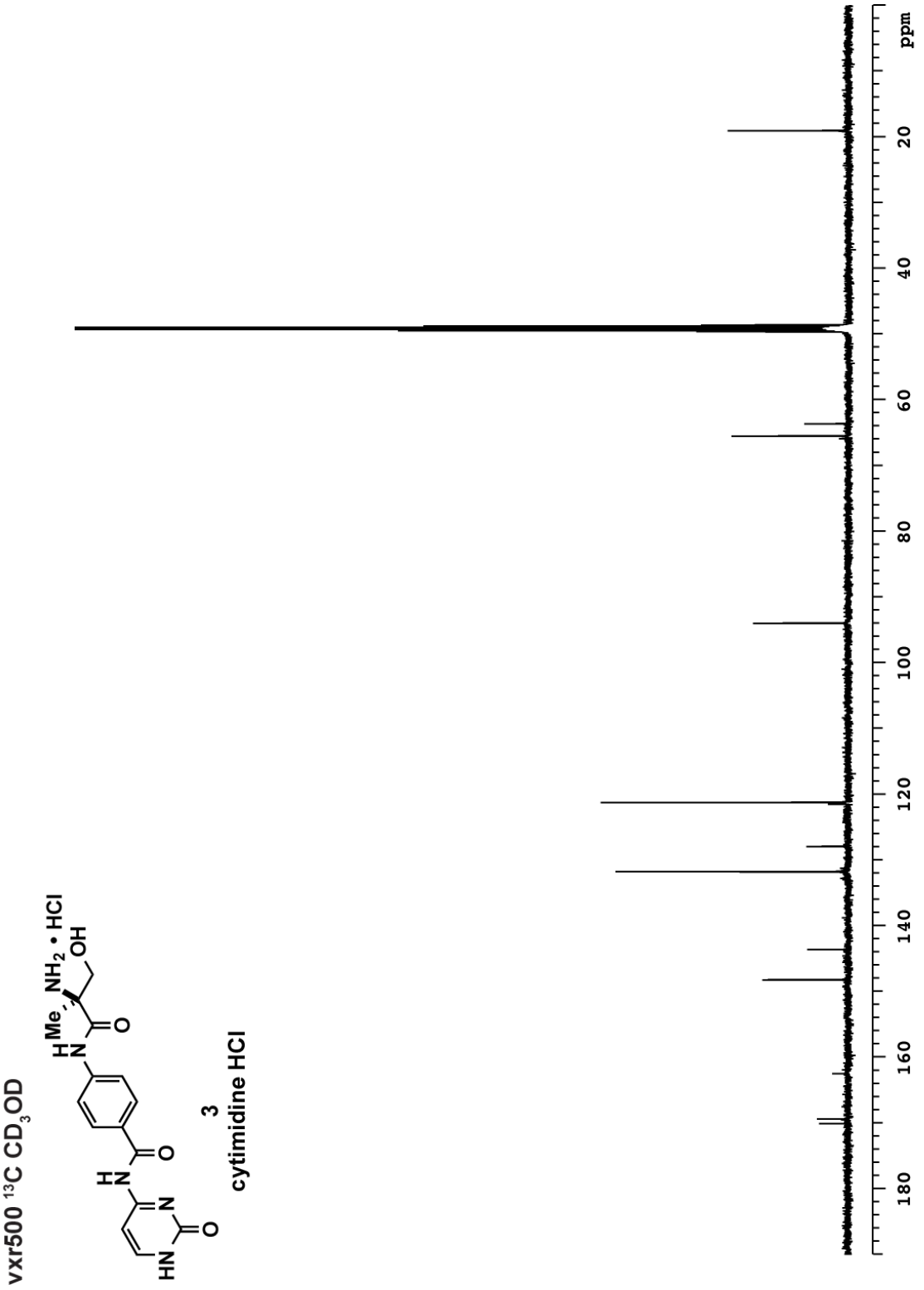
vxr500 13C CD3OD
3
cytimidine HCl
ppm
20
40
60
80
100
120
140
160
180

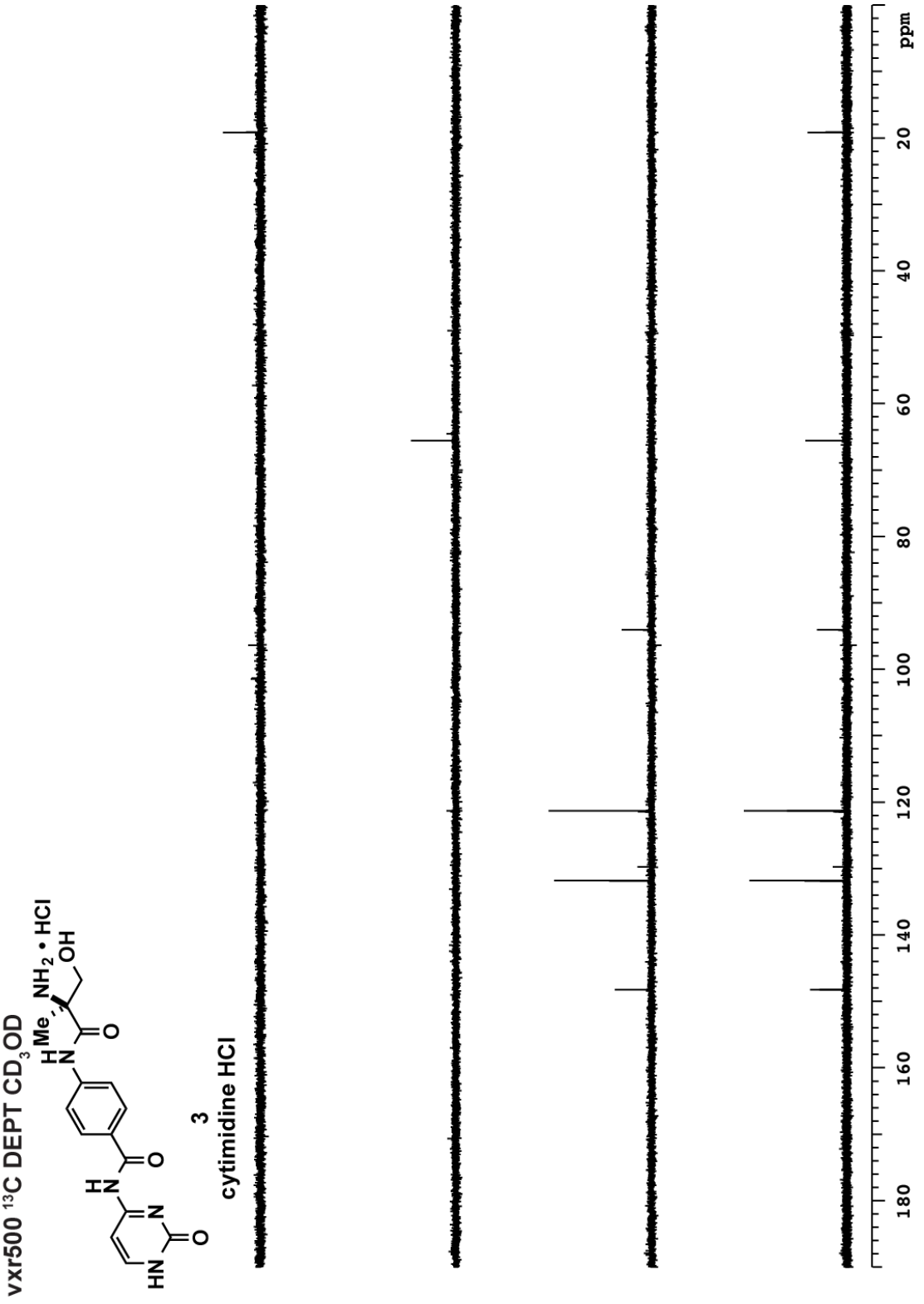
vxr500 13C DEPT CD3OD
3
cytimidine HCl
ppm
20
40
60
80
100
120
140
160
180

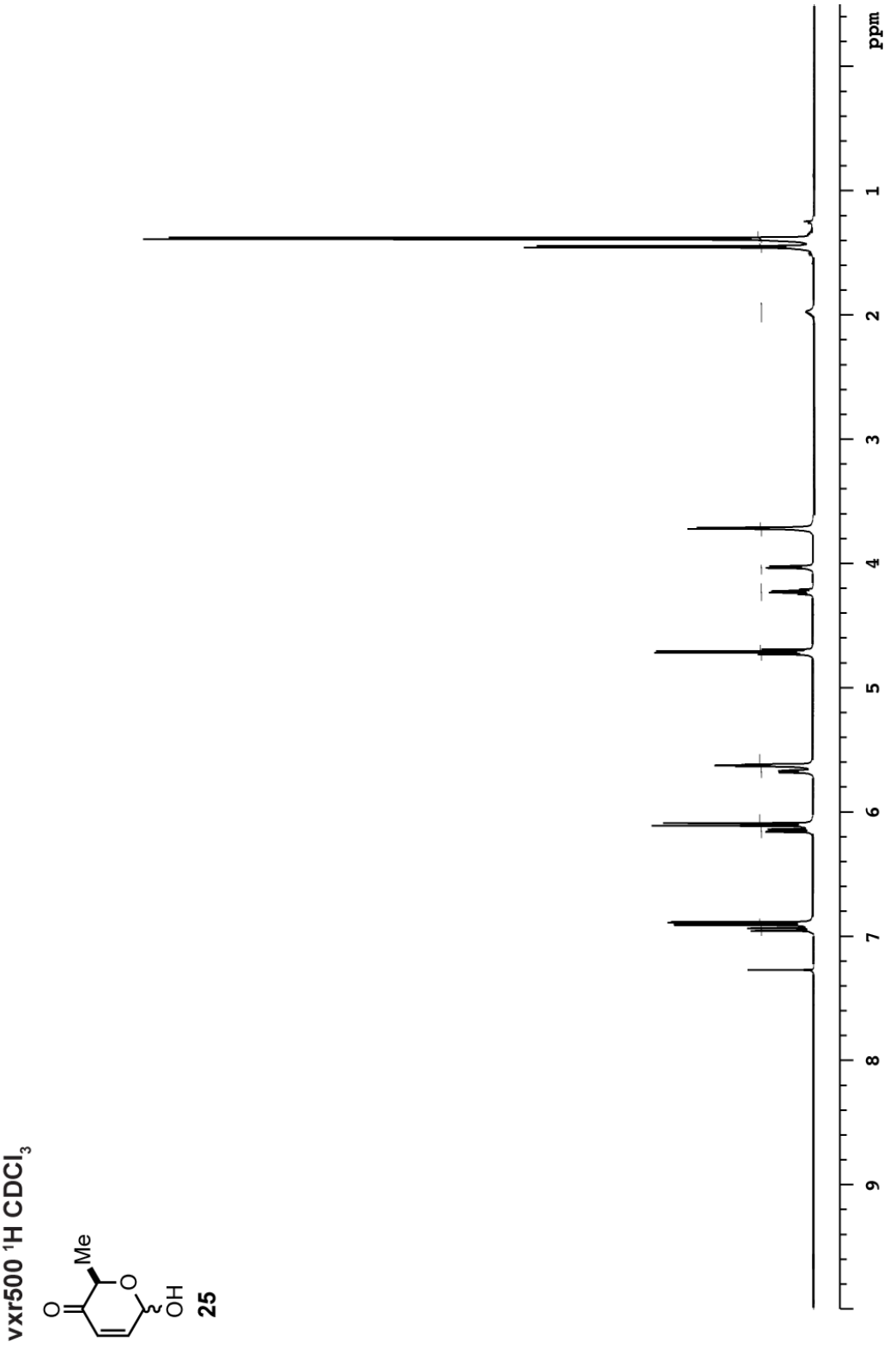
vxr500 1H CDCl3
Me
O
O
OH
25
ppm
1
2
3
4
5
6
7
8
9

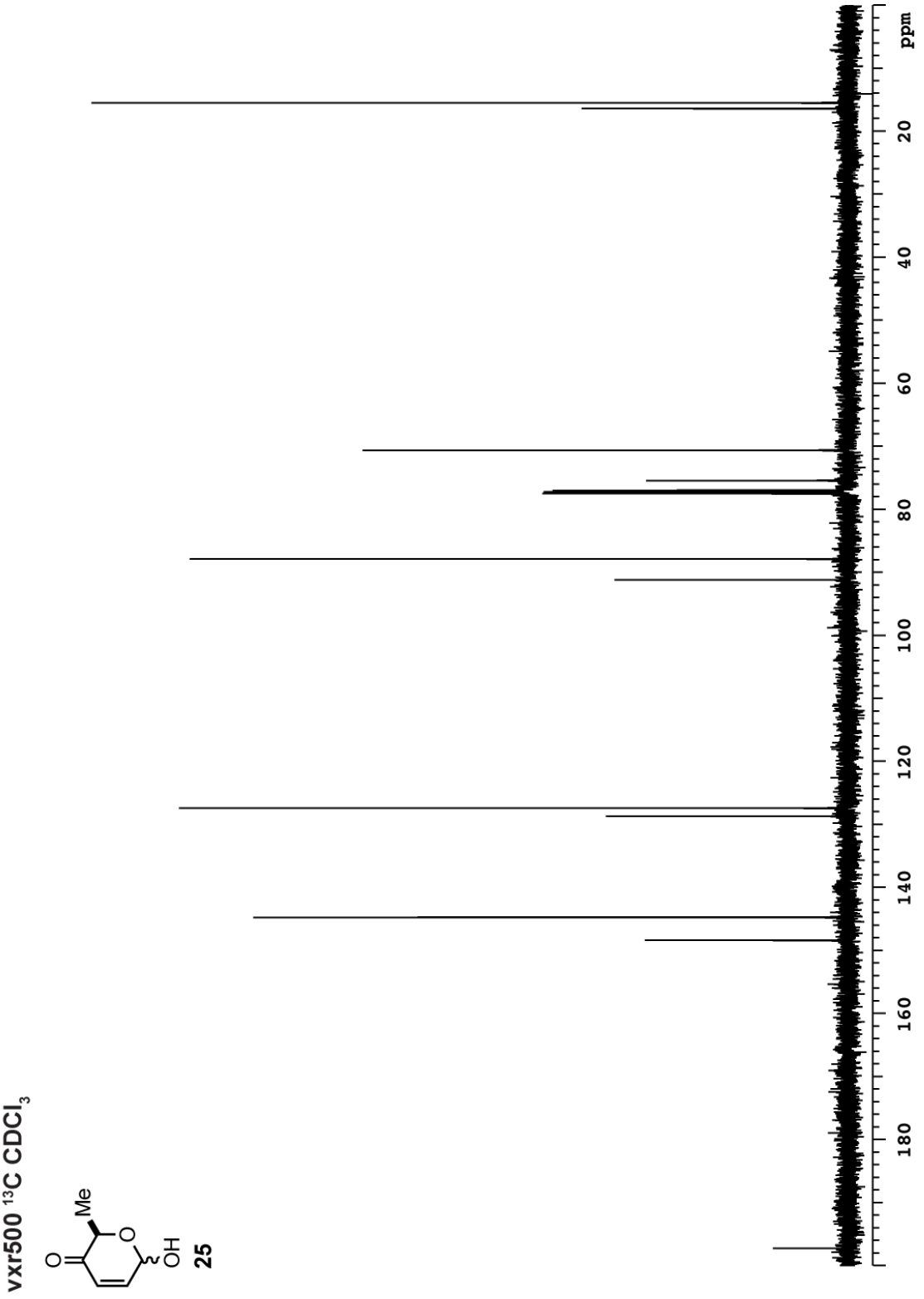
vxr500 13C CDCl3
Me
O
O
OH
25
ppm
20
40
60
80
100
120
140
160
180

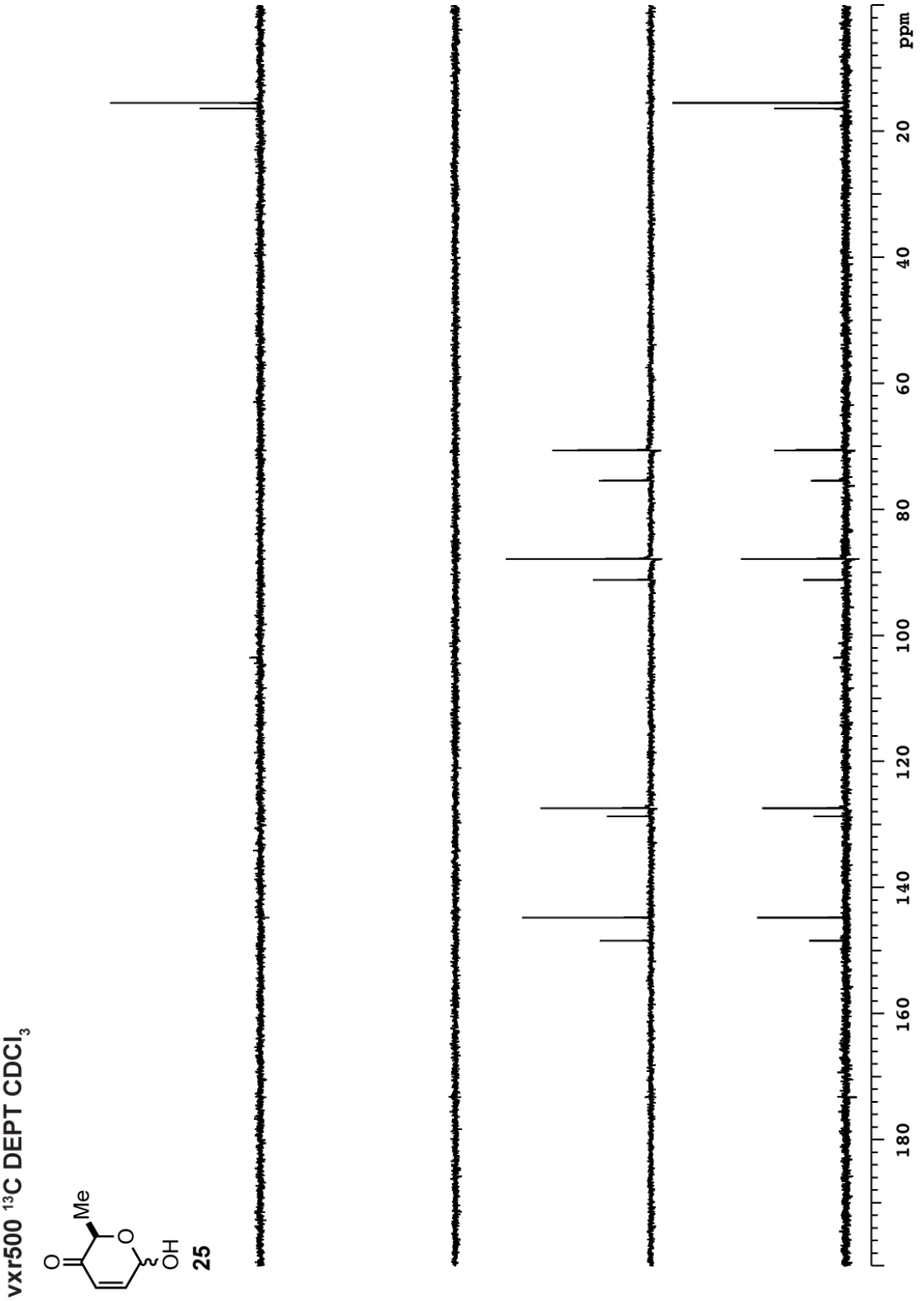
vxr500 13C DEPT CDCl3
Me
O
O
OH
25
ppm
20
40
60
80
100
120
140
160
180

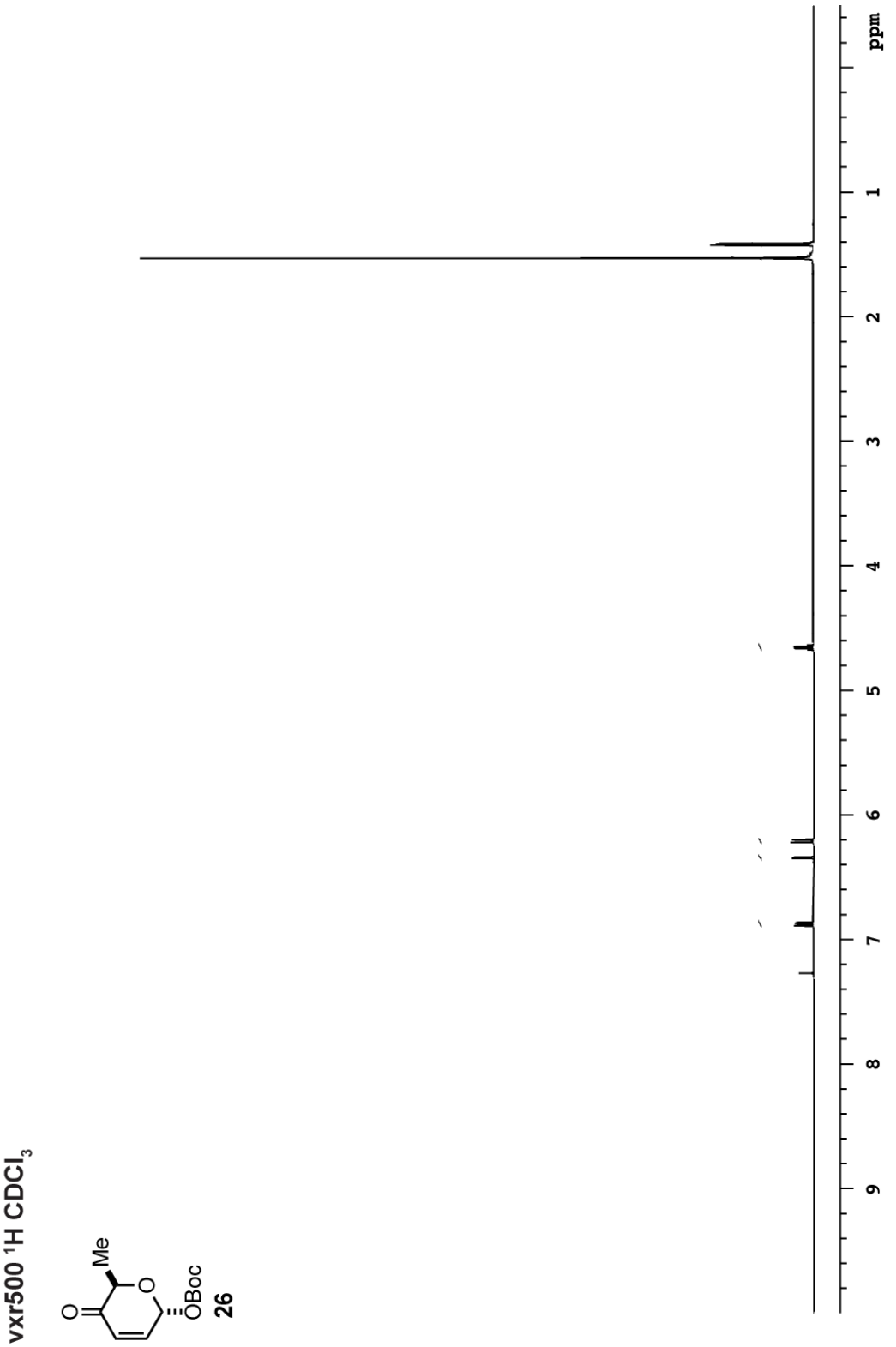
vxr500 1H CDCl3
Me
O
O
OBoc
26
ppm
9
8
7
6
5
4
3
2
1

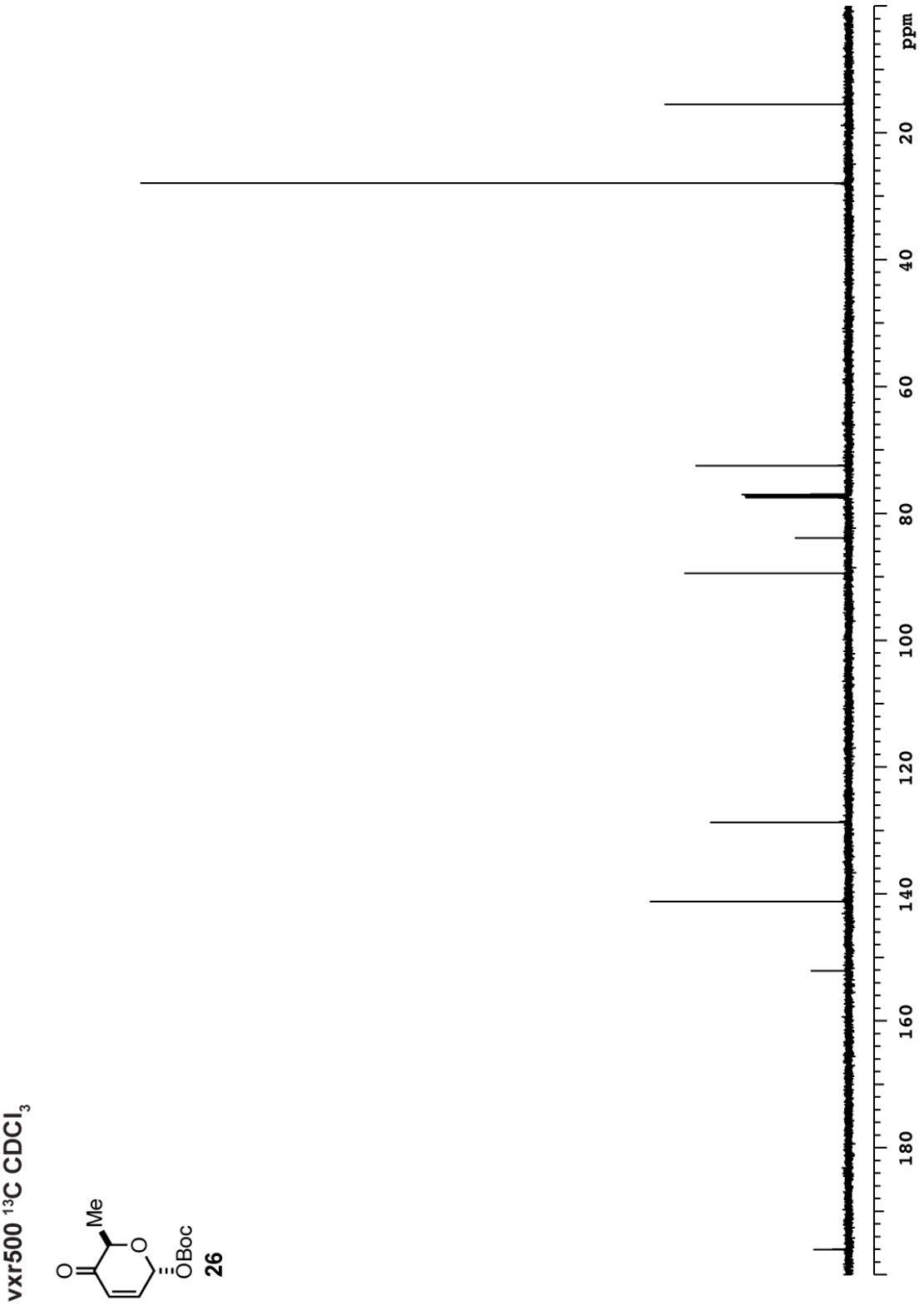
vxr500 13C CDCl3
Me
O
O
OBoc
26
ppm
180
160
140
120
100
80
60
40
20

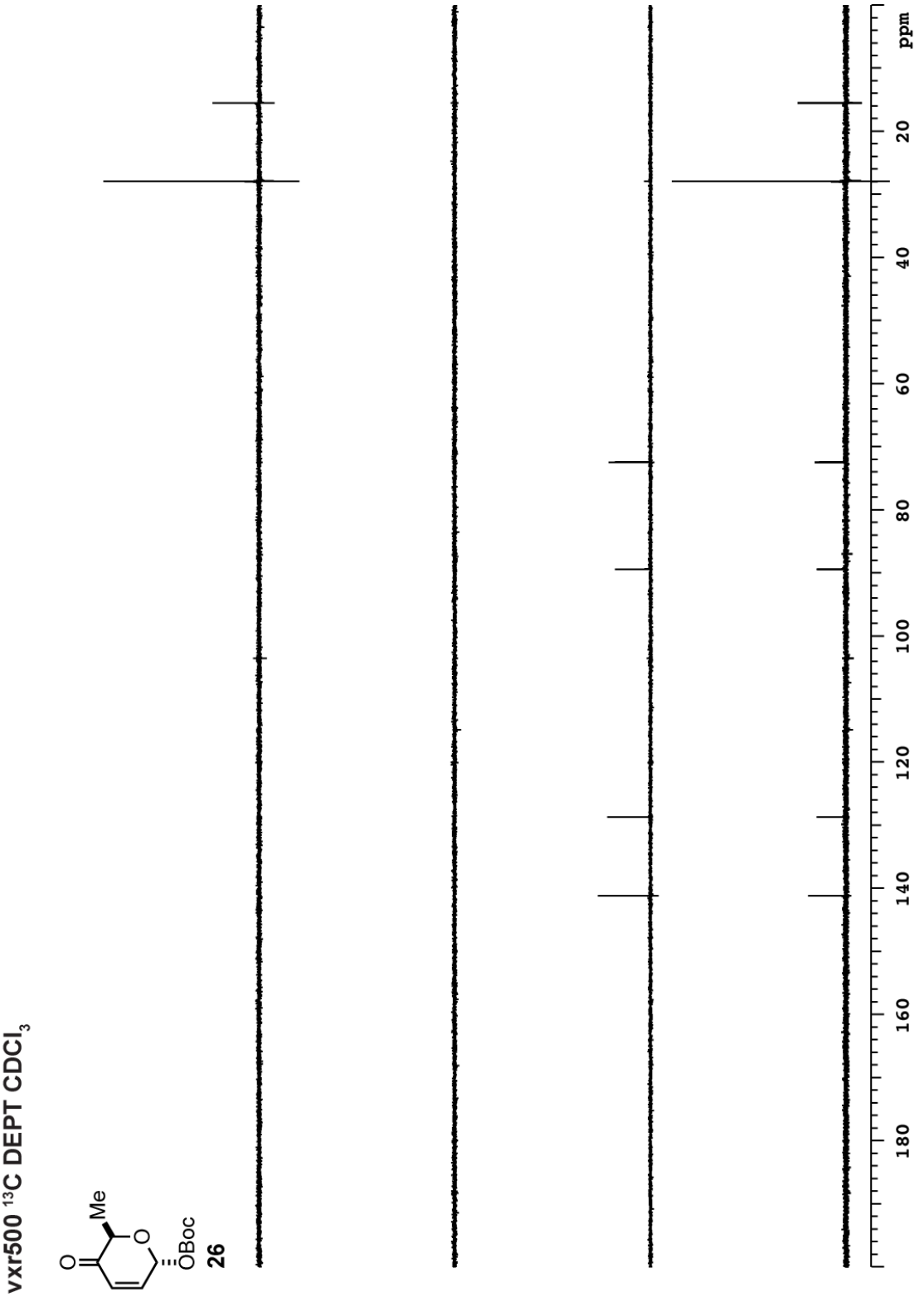
vxr500 13C DEPT CDCl3
Me
OBoc
26
ppm
20
40
60
80
100
120
140
160
180

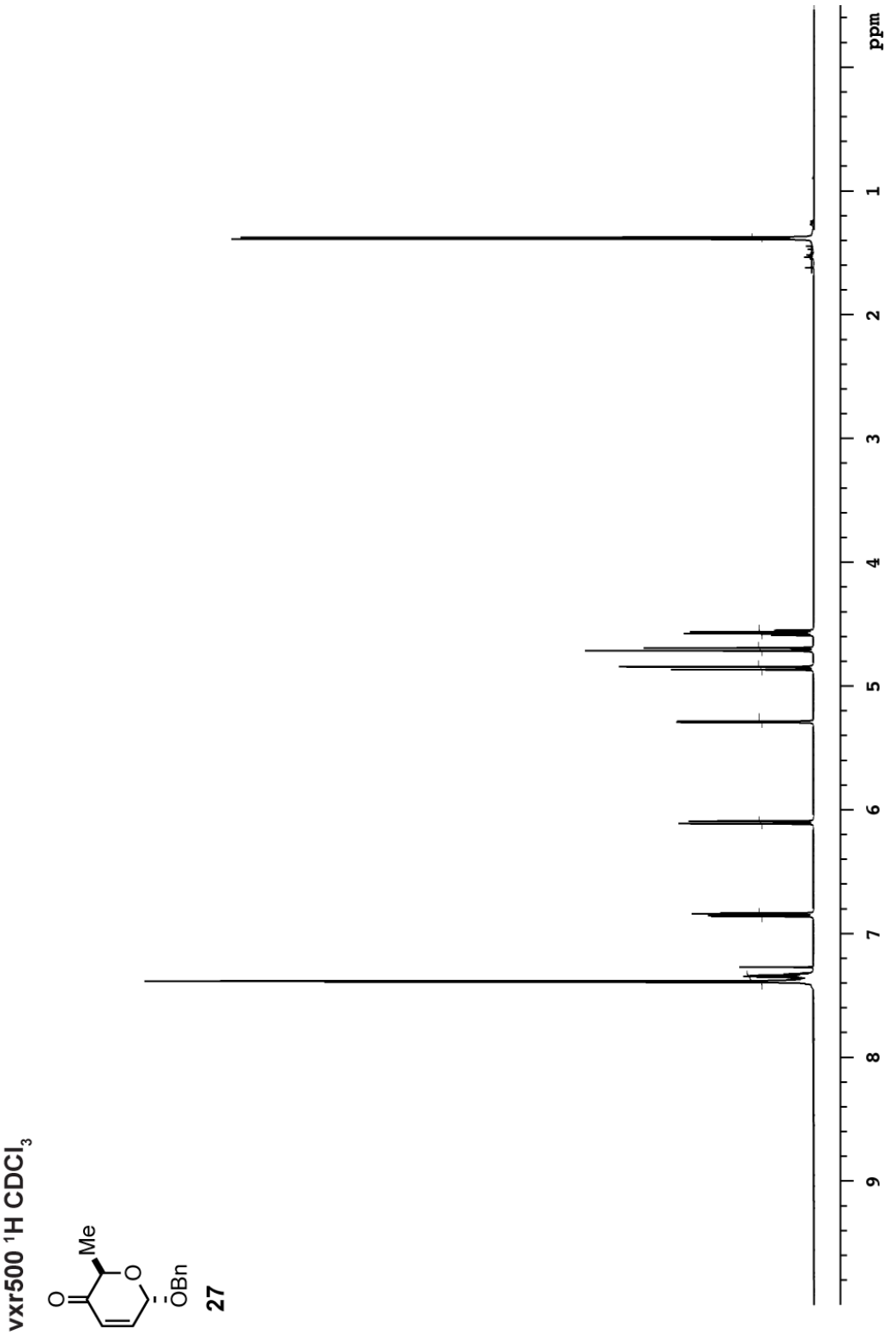
vxr500 1H CDCl3
Me
O
O
OBn
27
ppm
9
8
7
6
5
4
3
2
1

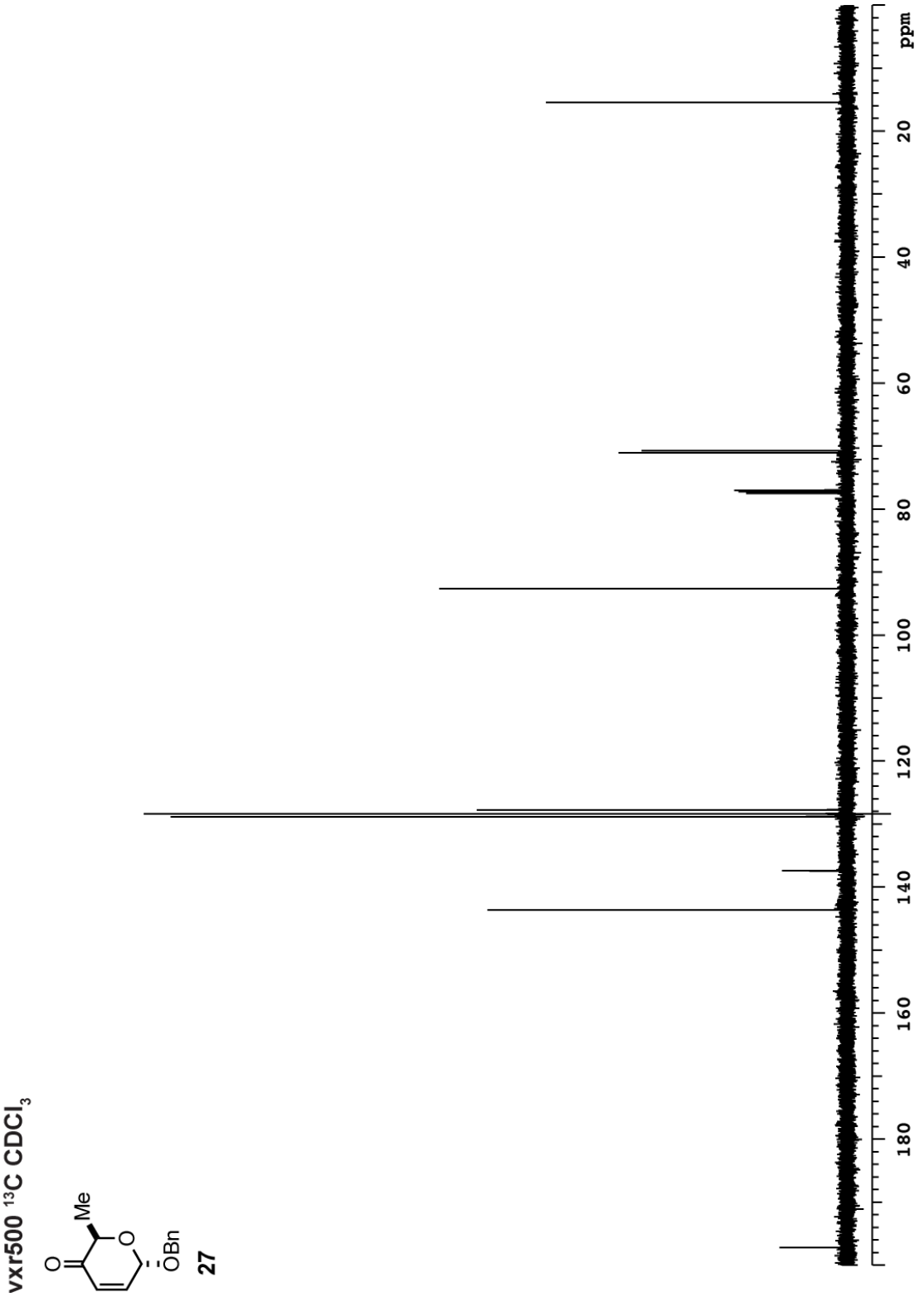
vxr500 13C CDCl3
Me
O
O
OBn
27
ppm
20
40
60
80
100
120
140
160
180

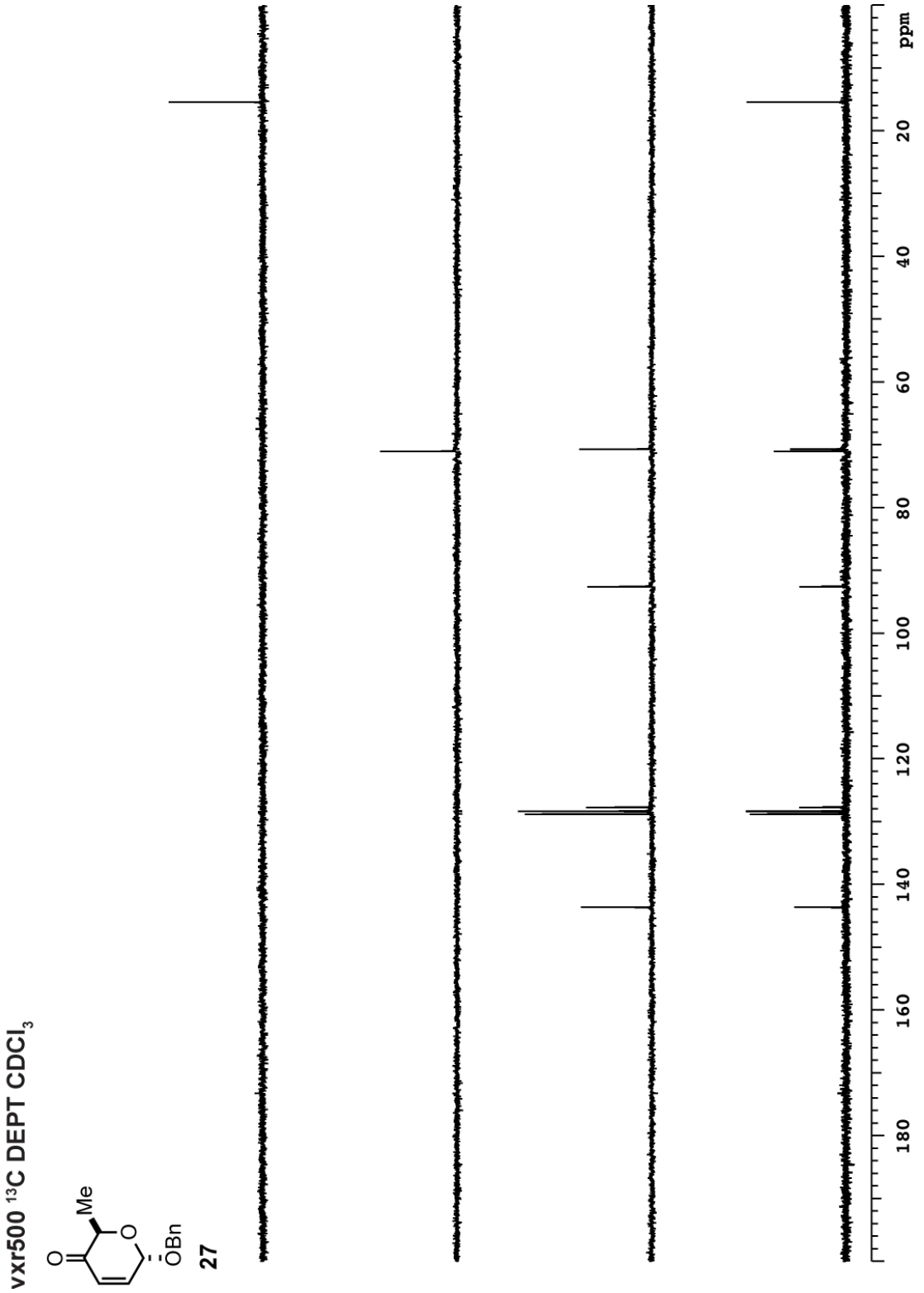
vxr500 13C DEPT CDCl3
Me
O
O
OBn
27
180
160
140
120
100
80
60
40
20
ppm

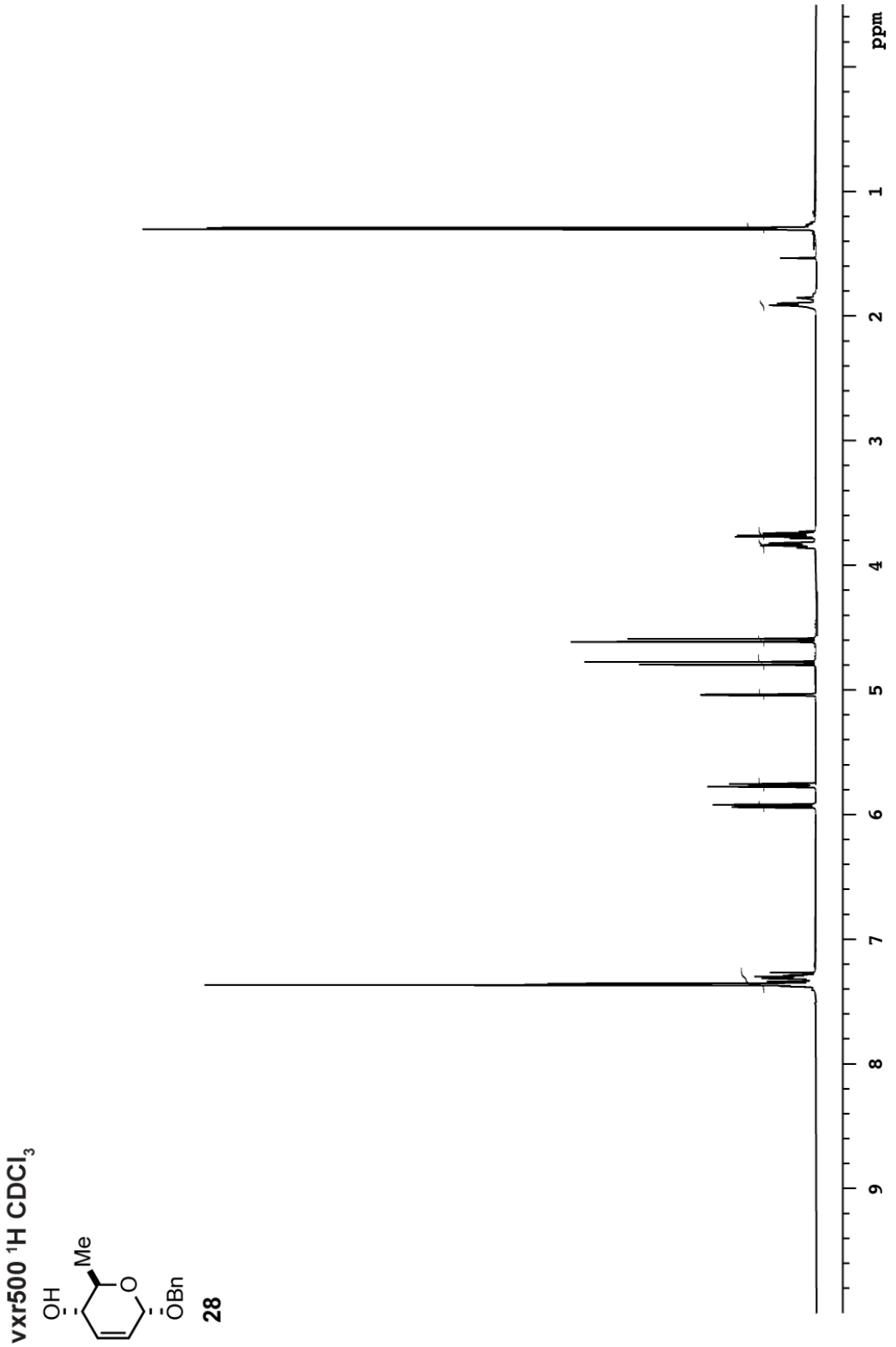
vxr500 1H CDCl3
OH
Me
O
OBn
28
ppm
9
8
7
6
5
4
3
2
1

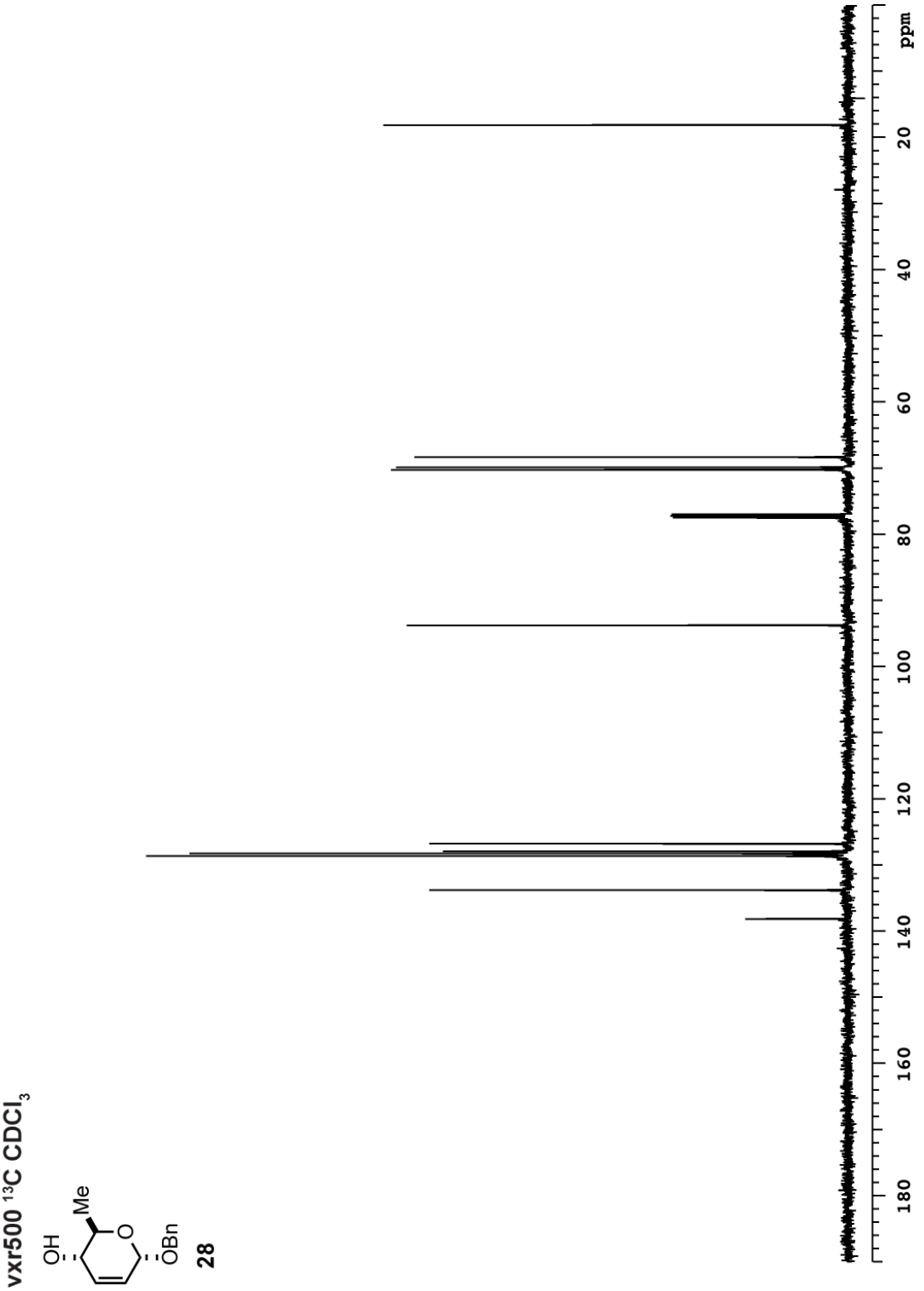
vxr500 13C CDCl3
OH
Me
O
OBn
28
180
160
140
120
100
80
60
40
20
ppm

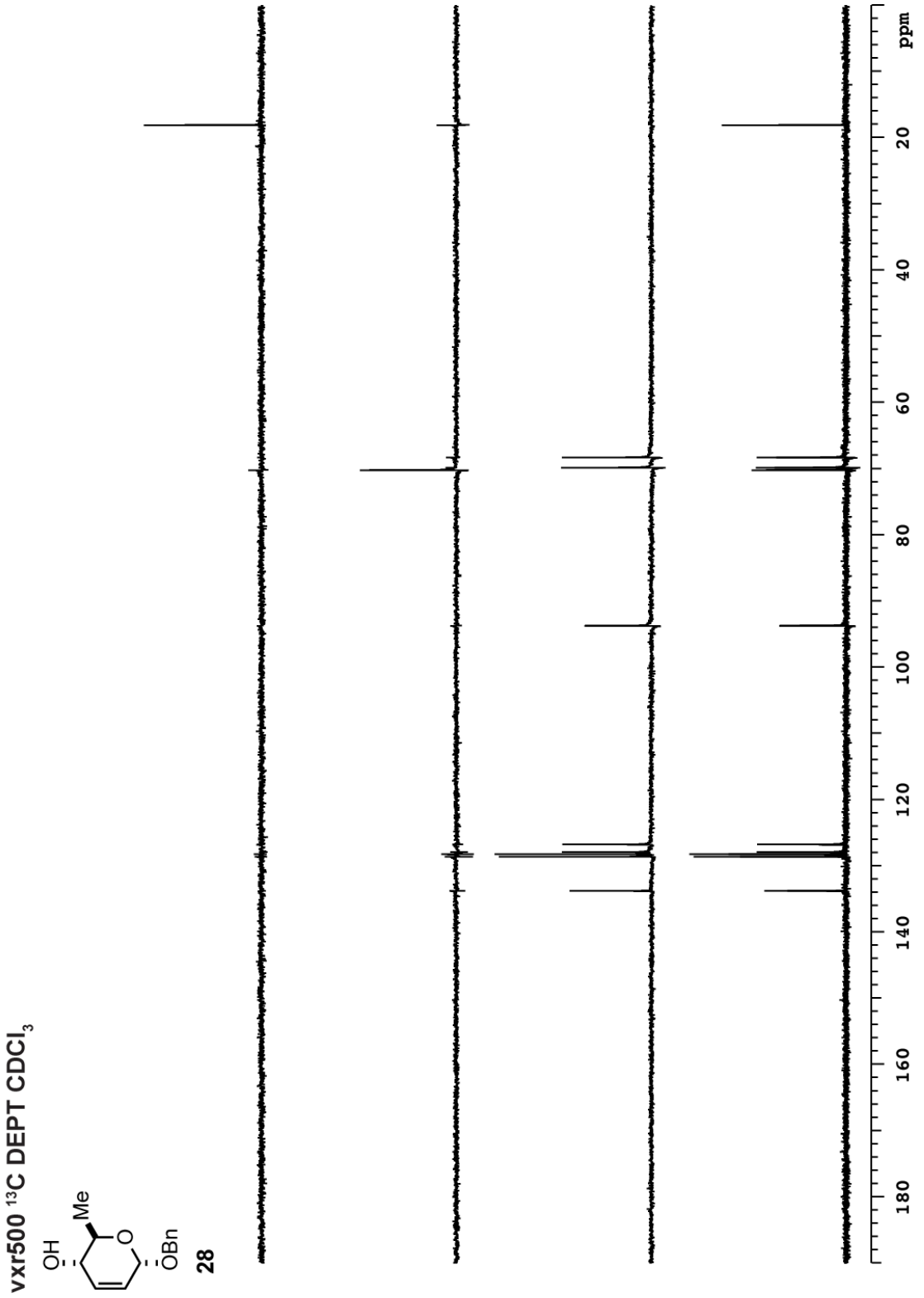
vxr500 13C DEPT CDCl3
OH
Me
O
OBn
28
180
160
140
120
100
80
60
40
20
ppm

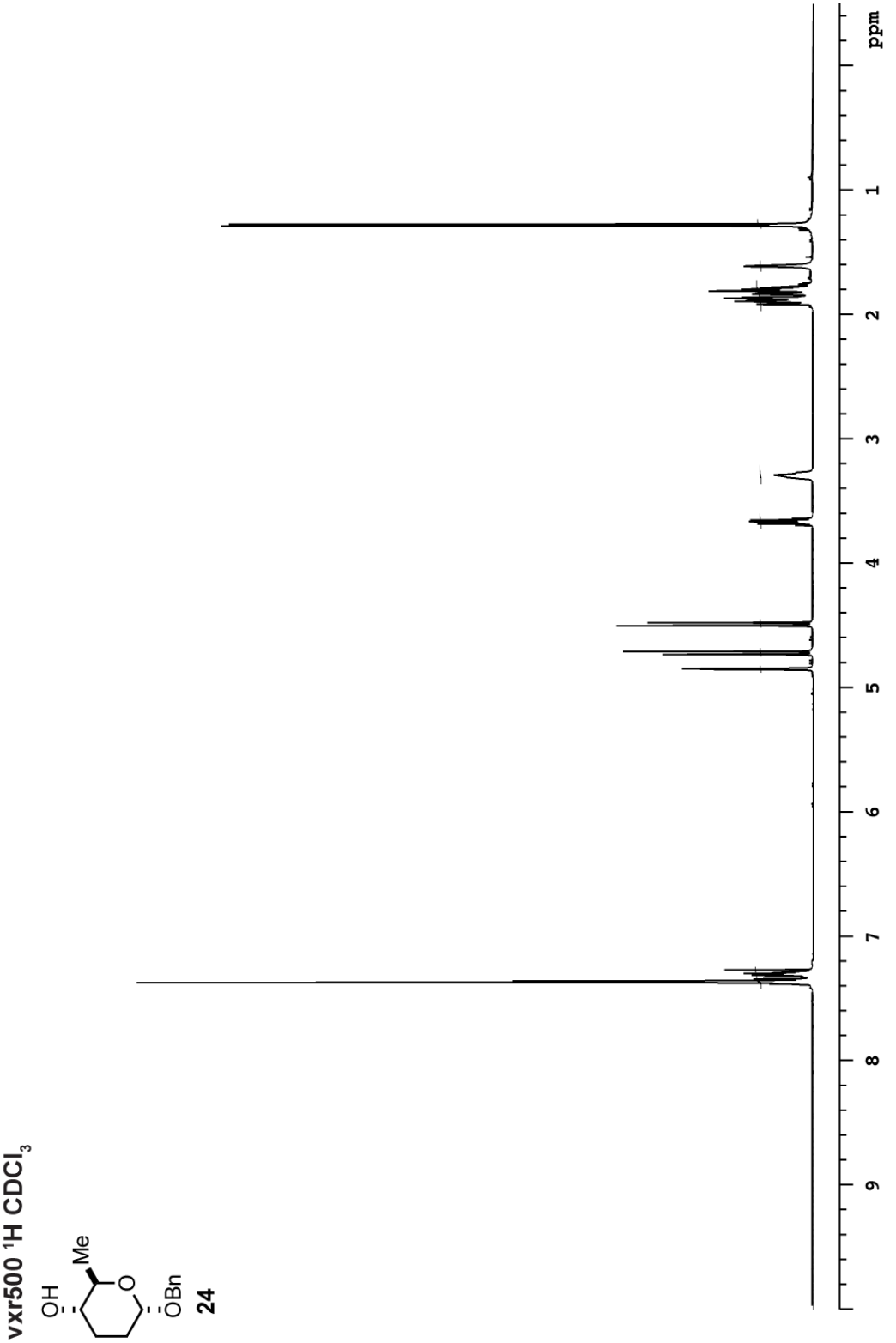
vxr500 ^{1}H CDCl$_3$
OH
Me
O
OBn
24
ppm
9
8
7
6
5
4
3
2
1

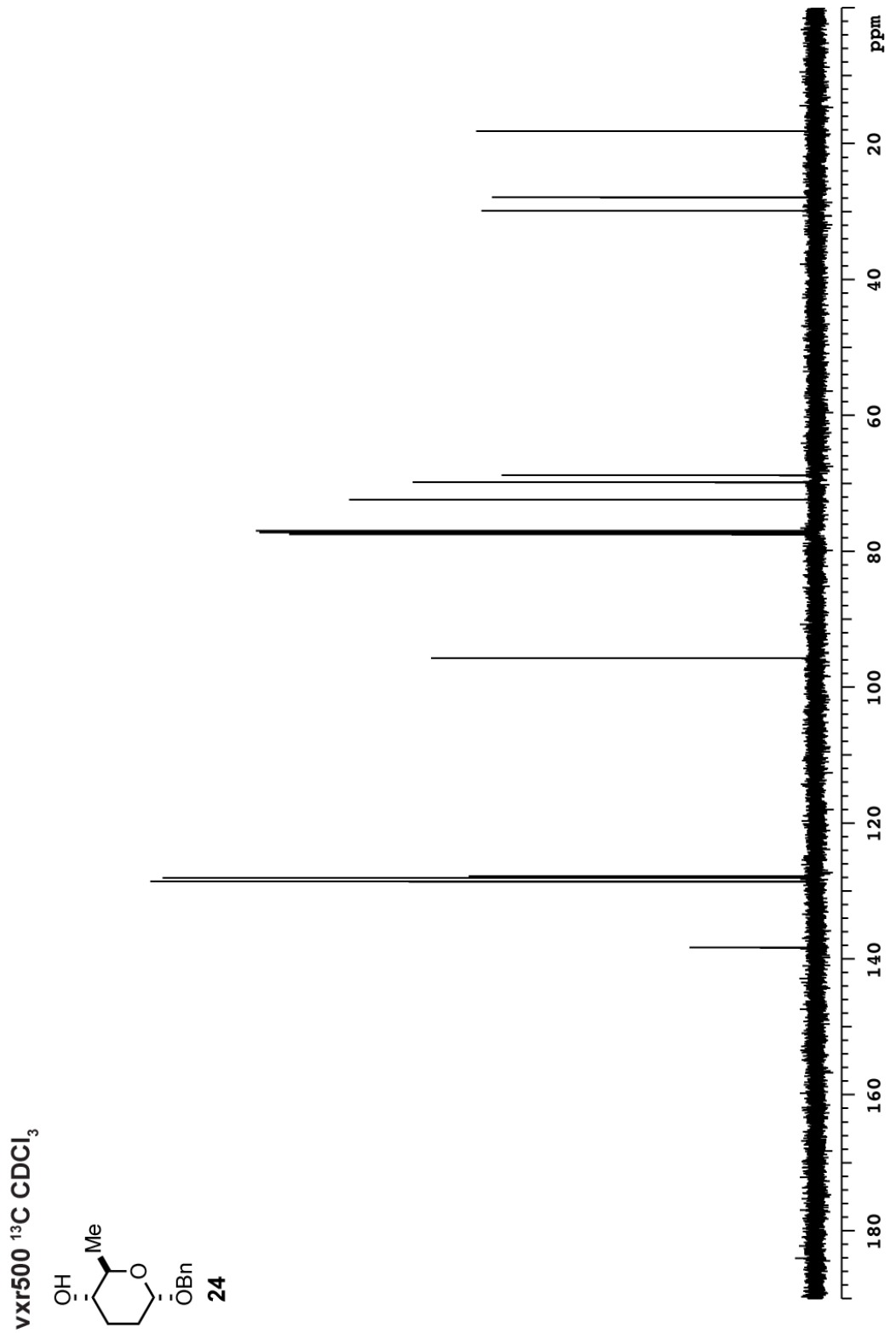
vxr500 13C CDCl3
OH
Me
O
OBn
24
ppm
20
40
60
80
100
120
140
160
180

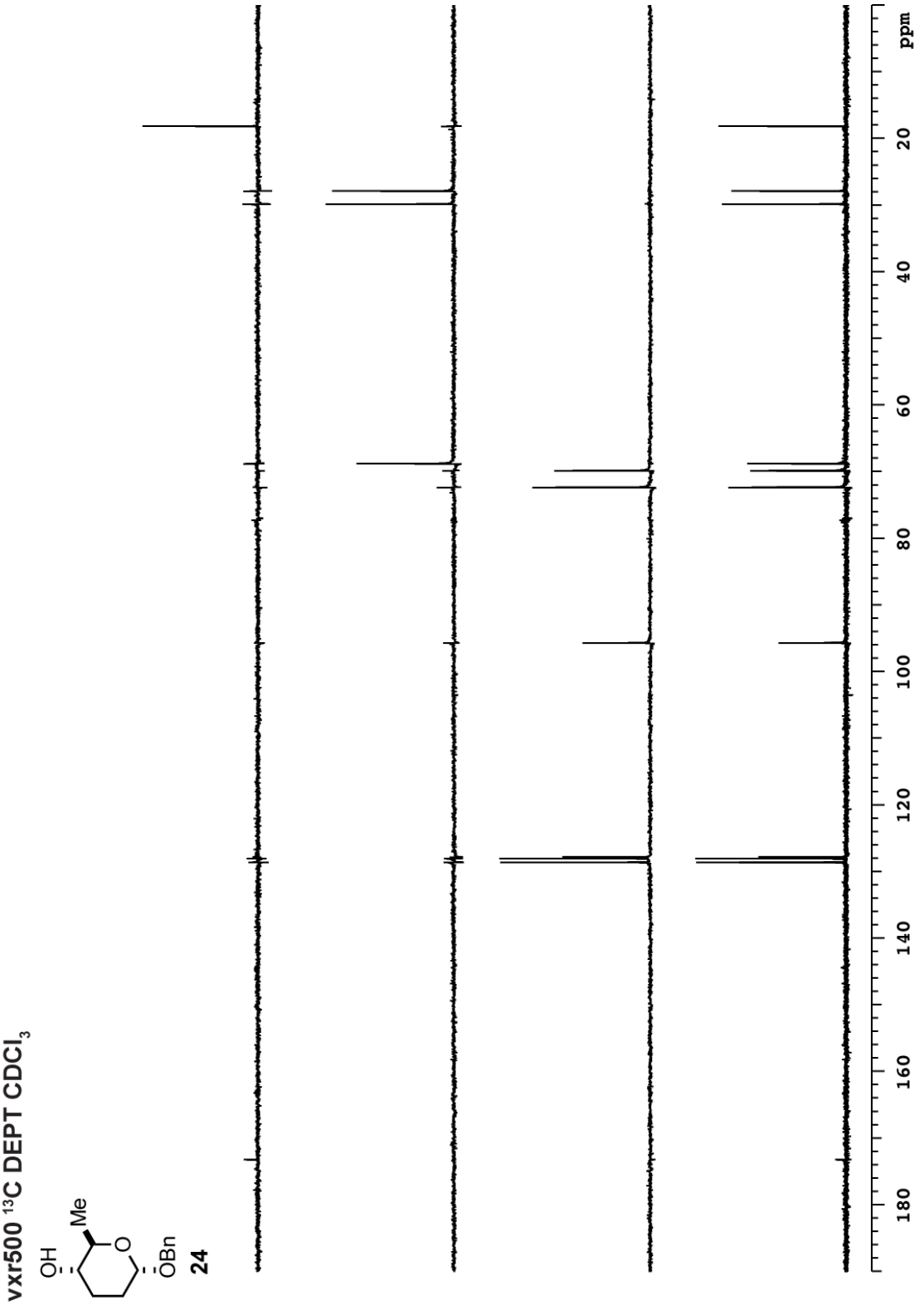
vxr500 13C DEPT CDCl3
OH
Me
O
OBn
24
180
160
140
120
100
80
60
40
20
ppm

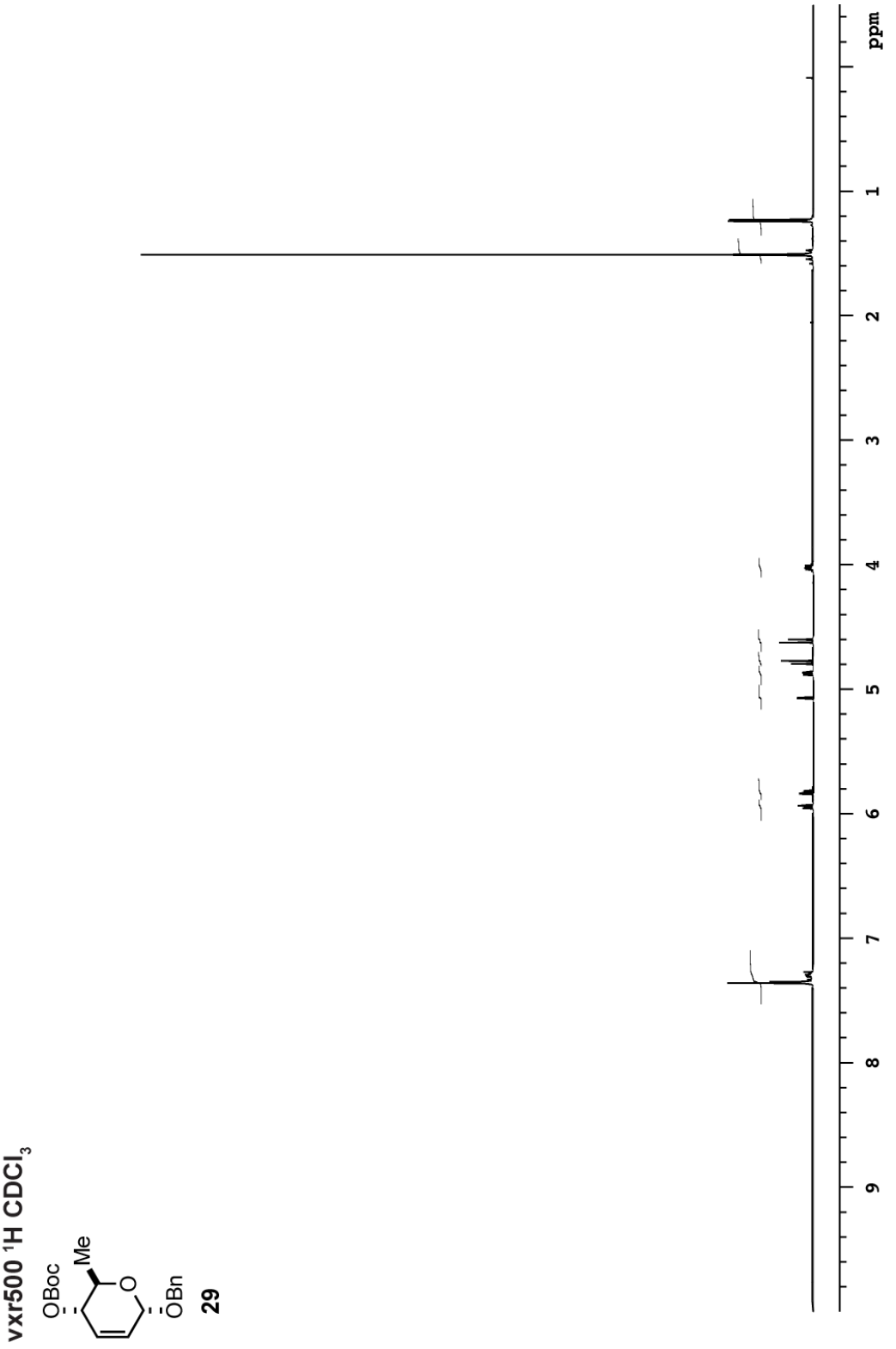
vxr500 1H CDCl3
OBoc
Me
O
OBn
29
ppm
1
2
3
4
5
6
7
8
9

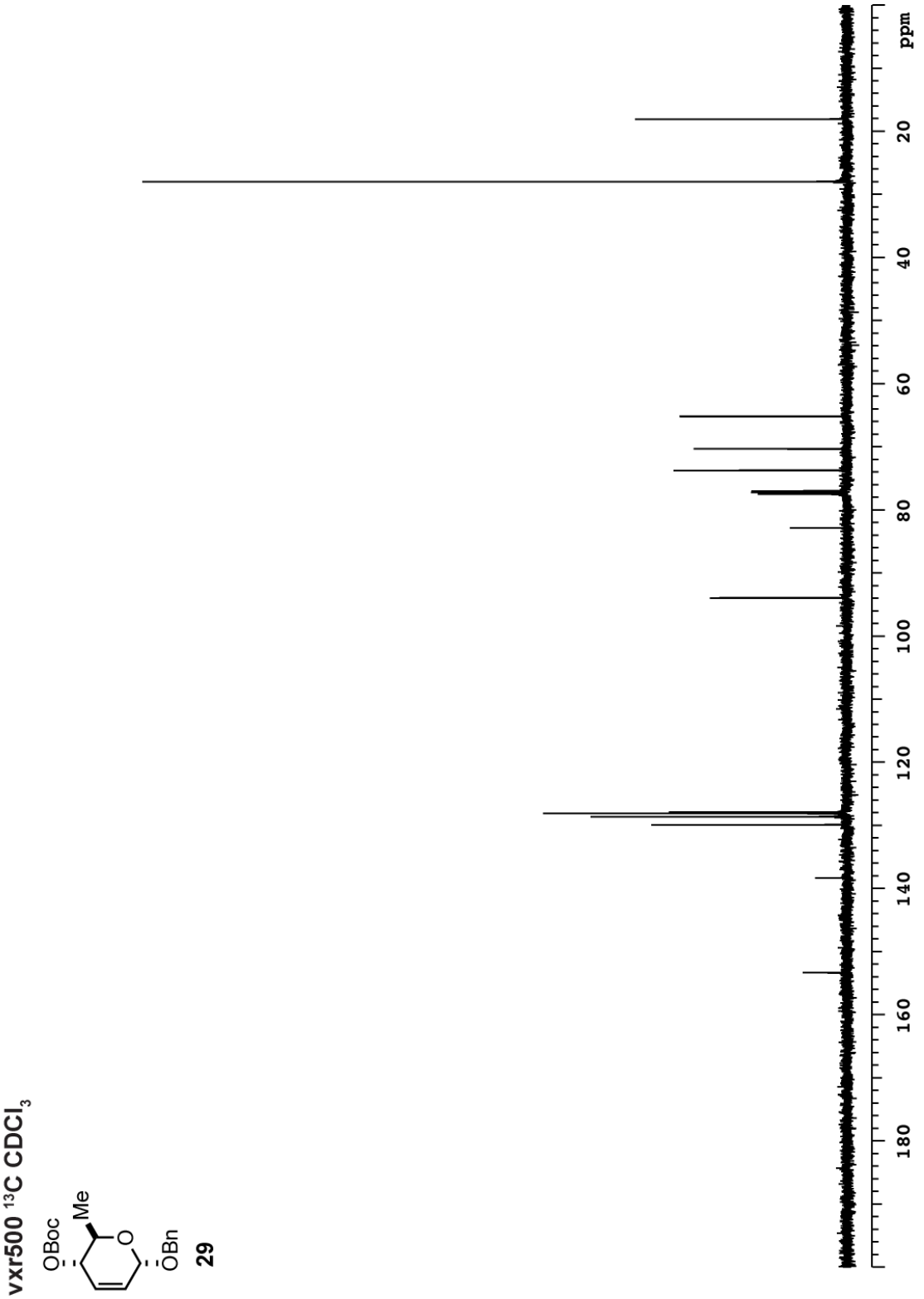
vxr500 13C CDCl3
OBoc
Me
O
OBn
29
ppm
20
40
60
80
100
120
140
160
180

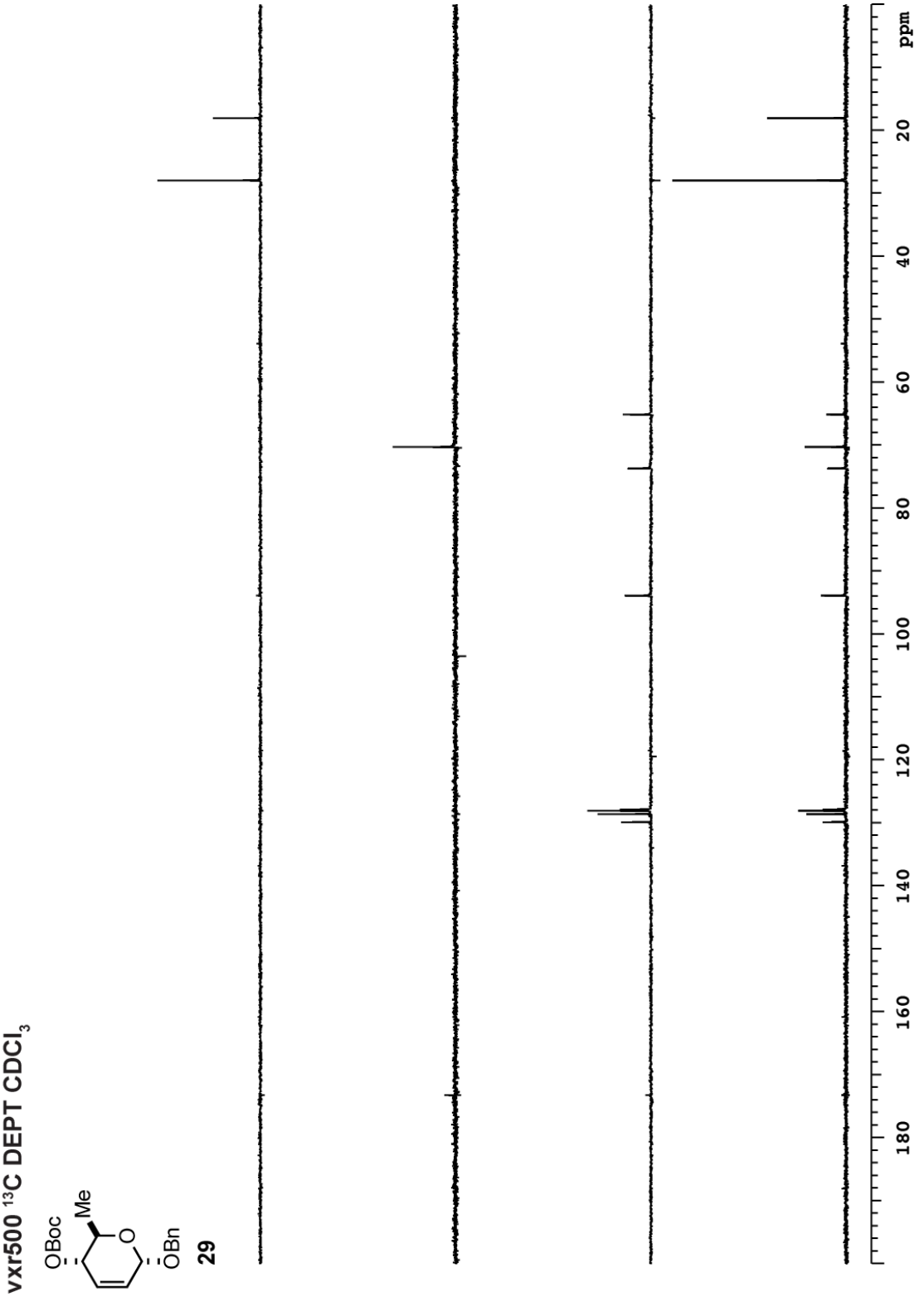
vxr500 13C DEPT CDCl3
OBoc
Me
O
OBn
29
180
160
140
120
100
80
60
40
20
ppm

CHAPTER 3

INTERACTIONS OF AMICETIN WITH THE 70S *THERMUS THERMOPHILUS* RIBOSOME

3.1 Background

Amicetin is a known protein synthesis inhibitor. In 1963, Brock compared the effects of various antibiotics on the growth of *Streptococcus pyogenes* group A and the synthesis of its virulence factor M protein.[1] Amicetin was found to inhibit both growth and M protein synthesis at a concentration of 10 μg/mL. It arrests microbial growth and peptide formation, while the synthesis of ribonucleic acid (RNA) and deoxyribonucleic acid (DNA) remain unaffected.[2]

A number of studies have been done to investigate amicetin's mechanism of action; however, the exact molecular mechanism is not well understood. Data from early biochemical studies, however, have narrowed down the possible mechanism of action. Early studies have shown that amicetin does not facilitate the transfer of amino acids to tRNAs. The transfer of phenylalanine to tRNA remained uninhibited even at 1 mM of antibiotic.[2] It also does not inhibit the binding of L-[^{13}C]-phenylalanyl-RNA to *E. coli* ribosomes, even at 1mM of amicetin.[2] However, it was reported to interfere with the binding of phenylalanine oligonucleotide, a CACCA-tRNA mimic, to the 50S ribosomal subunit,[3] which corresponds to amicetin inhibiting the binding of charged tRNA to the A-site prior to the peptide bond

formation in the elongation process.[4] Additionally, amicetin inhibits fMethionine release from the fMet-tRNA-ribosome complex.[5]

Since other cytosine nucleoside antibiotics are known to be peptidyl transferase inhibitors, it has been suggested that amicetin has the same mode of action. Amicetin inhibits the transfer of RNA-bound amino acid to the nascent polypeptide.[2] It also inhibits the reaction of [^{3}H]-puromycin with nascent peptides in native polysomes.[6] Polysomes are a group of ribosomes translating the same at the same time, allowing the production of multiple polypeptides simultaneously like a molecular assembly line that is typically found in bacteria.[7] Amicetin was also found to stabilize polysomes in the presence of compounds that induce polysome breakdown, such as puromycin, rifampin, or streptogramin A.[8] Peptidyl transferase inhibitors are known to stabilize polysomes while initiation inhibitors are known to induce polysome metabolism.[9]

Studies on amicetin, its derivatives, and other type 1 pyrimidine nucleoside antibiotics (Figure 3.1) provided insight into the structure-activity relationship (SAR) of amicetin's major chemical functionalities.[10] Oxamicetin is a bit more potent than amicetin but overall they have similar activity profiles. Removal of amicetin's α-methylseryl group in plicacetin resulted in a 10-fold loss in activity. The absence of amicetin's disaccharide moiety in the derivative cytimidine, resulted in a 50-fold loss of activity. Cytosamine triacetate, the amicetin derivative without the α-methylseryl-*p*-aminobenzoyl group, is 100-fold less active.[10] This study supports the early hypothesis that the presence of two basic groups in amicetin's structure is required for its binding and inhibitory property.[2]

For almost two decades, interest in amicetin has waned in favor of more potent antibiotics. Since the aforementioned SAR study in 1975, no new study on

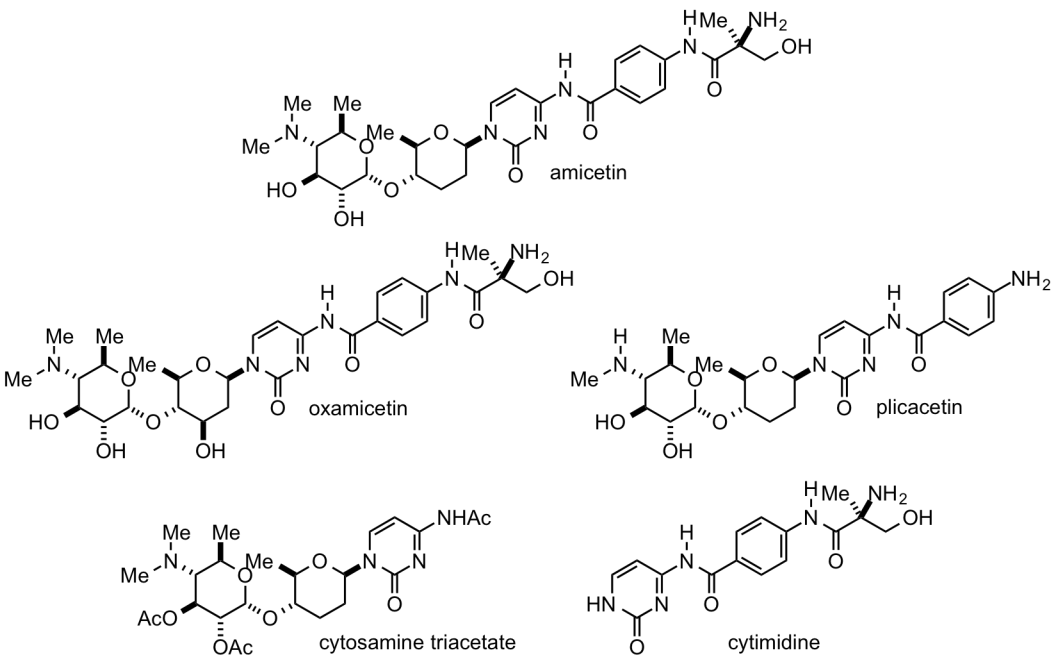

Figure 3.1 Amicetin, analogues and derivatives

amicetin was published, until 1994, when Mankin and co-workers reported a single point mutation within helix 74 in the 23S rRNA of *Halobacterium halobium* (*Hh).* Point mutation U2457C (U2438C), *Hh* (*E. coli* numbering) was found to confer resistance to amicetin (Figure 3.2).[11] This study proposed that the binding site of amicetin is close to the peptidyl transferase center and that the point mutation U2457C (U2438C) perturbs the local rRNA structure thereby disrupting the binding site of amicetin. Point mutations conferring resistance are not exclusive to binding sites, as antibiotic resistance maybe effected allosterically. Additionally, data obtained from footprinting experiments reported in this study are inconclusive.

Ramesh and co-workers conducted NMR experiments and molecular modeling studies on amicetin bound to a truncated helix 74 mimic of the 23S RNA, based on the resistance mutant found by Leviev and co-workers.[11, 12] They reported a constrained model of amicetin folding in half (Figure 3.3) where its cytosine

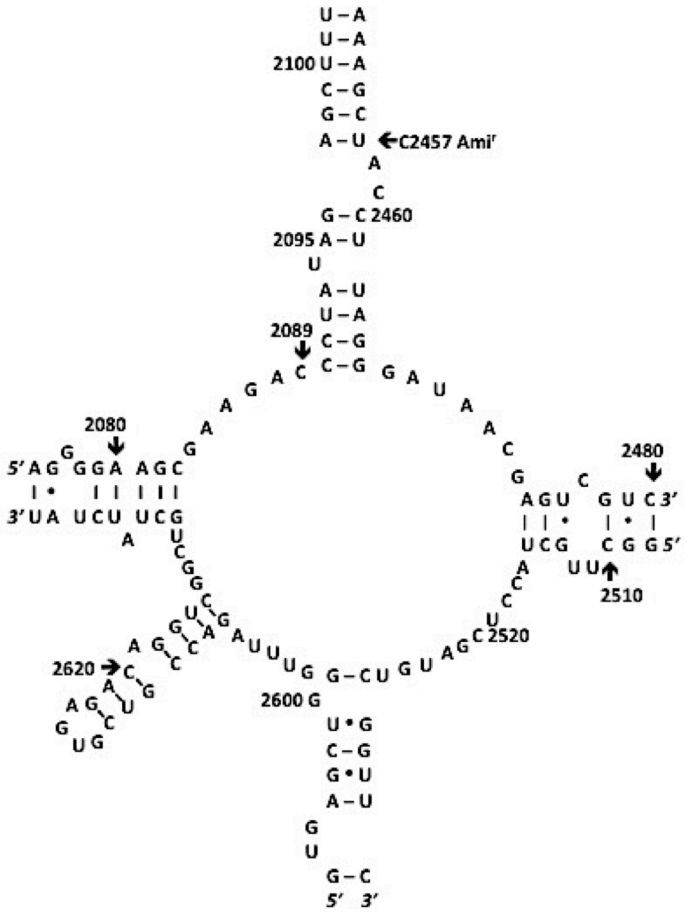

Figure 3.2 Peptidyl transferase center domain V
site of point mutation conferring amicetin resistance (*Hm* numbering)

moiety stacked and hydrogen bonded to the nucleotide U6 in the 35-mer RNA construct, corresponding to U2089 (U2094, U2068), *Tth (Hh, E. coli)* numbering. This folded conformation of amicetin was previously unseen and was drastically different from the X-ray structure of crystalline amicetin that showed a linear conformation[13] This study suggested that the highly constrained conformation is stabilized by π-stacking interactions between the aromatic ring of the *p*-aminobenzoyl moiety, the cytosine ring of amicetin, and the uracil group, in addition to hydrogen bonding between the imino proton of uracil and cytosine. Their model additionally suggests that further stabilization is achieved through an elaborate

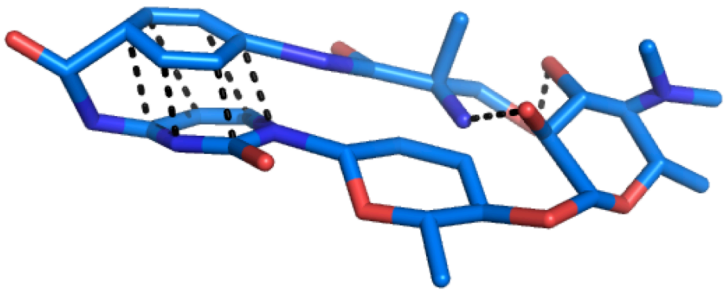

Figure 3.3 Proposed folded conformation of amicetin

intramolecular hydrogen-bonding network between the sugar and the α-methylseryl moiety of amicetin.

Reports of intramolecular π-stacking on a turn in literature are quite rare. Before Ramesh's report, this binding motif has only been seen in two other ribosomal antibiotic (Figure 3.4). The first literature precedence was reported by Ramakrishnan and co-workers in the crystal structure of ribosome-bound pactamycin.[14] The second was a computational model on a cross-linked linezolid

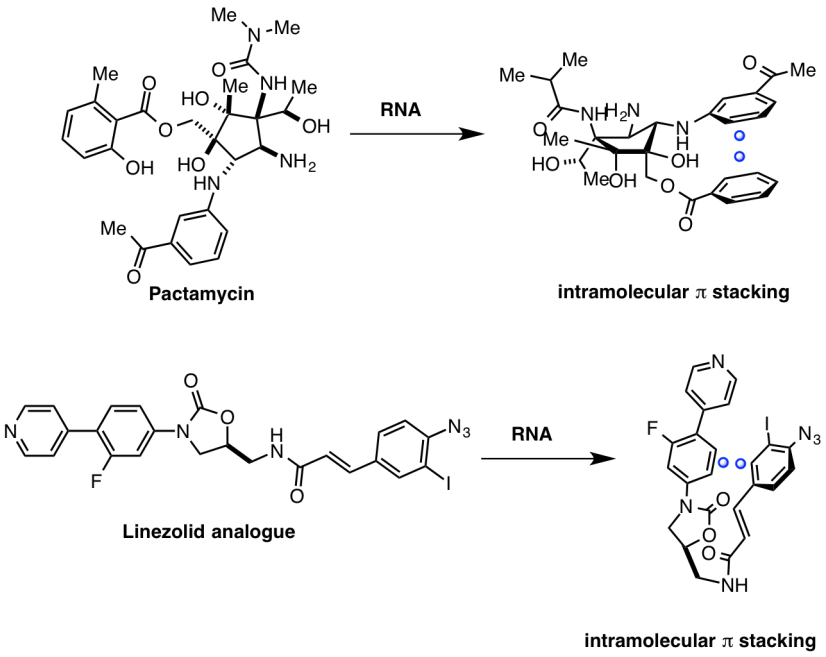

Figure 3.4 Conformation of ribosome-bound pactamycin and linezolid analogue

analogue.[15] In both examples, the molecules are not forced into an energetically unfavored conformation. This novel binding motif, while interesting, is highly suspect, especially when the high energy penalties are considered. A much more sophisticated technique in structural biology such as x-ray crystallography may be needed to elucidate the exact binding site and motif of amicetin to the ribosomal RNA.

3.2 Materials and Methods

3.2.1 Re-Isolation of Amicetin from S. vinaceusdrappus

While studies on the synthesis of amicetin and its derivatives are conducted in our laboratory, we sought to express and re-isolate amicetin from its original producing actinomycete. We sought to adapt and modify the original production and isolation procedures on a laboratory scale.[16, 17]

Streptomyces vinaceusdrappus (ATCC 25511) was grown on a sterile yeast-malt agar plate and was inoculated into sterilized growth media consisting of yeast extract, peptone, and glucose (YPG-broth). An aliquot of the YPG seed culture was transferred into the production media containing dextrose, yeast extract, soy and various salts, to express amicetin. The fermentation broth was subjected to a series of filtrations to produce the clarified production broth, which was extracted with a solution of 30% isopropanol in chloroform, about one-quarter of its volume, and was repeated thrice. The crude solid was purified using normal and reverse column chromatography. Amicetin was observed to slowly decompose *via* solvolysis, especially at higher temperatures. Crude amicetin was then carefully handled, purified and stored under dry and cold conditions. Amicetin was obtained as a white powder and was co-crystallized with *Thermus thermophilus* 70S ribosome. Detailed

description of the isolation and purification is provided in the Supplemental Information.

3.2.2 Co-Crystallization, Data Collection and Processing

X-ray Crystallography experiments were done in collaboration with Daniel Eiler of the Steitz Group at Yale University. *T. thermophilus* 70S ribosomes were purified and crystallized as previously published[18] Ribosome complexes were obtained by incubating vacant 70S ribosomes with 500 μM amicetin, 20 μM mRNA, and 20 μM fMet-tRNAfMet for 24 hours. Crystals were harvested and flash frozen in a nitrogen cryostream. Details of the crystallization and structure determination are provided in the Supplemental Information.

Data collection was performed at 100 K using synchrotron X-ray radiation at beam line 24ID-C at the Advanced Photon Source in Argonne National Laboratory (Argonne, IL) and beam line x25 at the National Synchrotron Light Source in Brookhaven National Laboratory. X-ray diffraction data was processed using X-ray Detector Software (XDS).[19] Refinements, integration and handling of scaled data were completed using Collaborative Computational Project programs.[20] Final models were built using COOT and refined using PHENIX.[21, 22] Ligand model for amicetin were built using PRODRG.[23]

3.3 Results

From the crystallographic data, the binding site of amicetin concurs with the hypothesis that it binds in the same site and in a similar manner, albeit with some differences, as another pyrimidine nucleoside antibiotic, blasticidin S.[24, 25] It also agrees with the data from previous biochemical studies indicating that it inhibits

protein synthesis by inducing a nonproductive conformation on the P-site bound tRNA, thereby arresting the peptidyl transferase reaction.

In the crystal structure of ribosome-bound amicetin (Figure 3.5), the antibiotic assumed an extended conformation, contrary to the proposed folded conformation suggested in the NMR models.[12, 26] The disaccharide portion of the molecule, amicetamine, protrudes out into helix 74 with the terminal sugar ring stacking on A2450 (A2439), *Tth (E.coli)* numbering (Figure 3.6). This affords a cation-π interaction between the dimethylamine moiety of the terminal sugar of amicetin and the purine ring of A2450 (A2439). The cytosine moiety of amicetin forms a Watson-Crick base-pair with G2262 (G2251) (Figure 3.7), mimicking the penultimate 3' cytosine, C75, of a P-site bound tRNA. In the absence of the P-site tRNA, the *p*-aminobenzoyl moiety forms π-stacking interactions with A2613 (A2602) (Figure 3.7). The terminal hydroxyl group of the α-methylseryl moiety hydrogen bonds with the R18 of ribosomal protein L16 (Figure 3.7).

3.4 Discussion

3.4.1 Proposed Mechanism of Action and Similarity to Blasticidin S

The binding location and conformation of amicetin bound to the 70S ribosome corresponds with previously reported biochemical studies. Our data agrees with the primary hypothesis that amicetin binds to the PTC of the ribosome and with preliminary observations that it inhibits peptidyl transferase reaction in a similar manner as other pyrimidine nucleoside antibiotics such as blasticidin S.[2-11]

As was discussed earlier, blasticidin S was one of the first antibiotics to have its binding site on the 50S ribosomal subunit of *Haloarcula marismortui (Hm)*

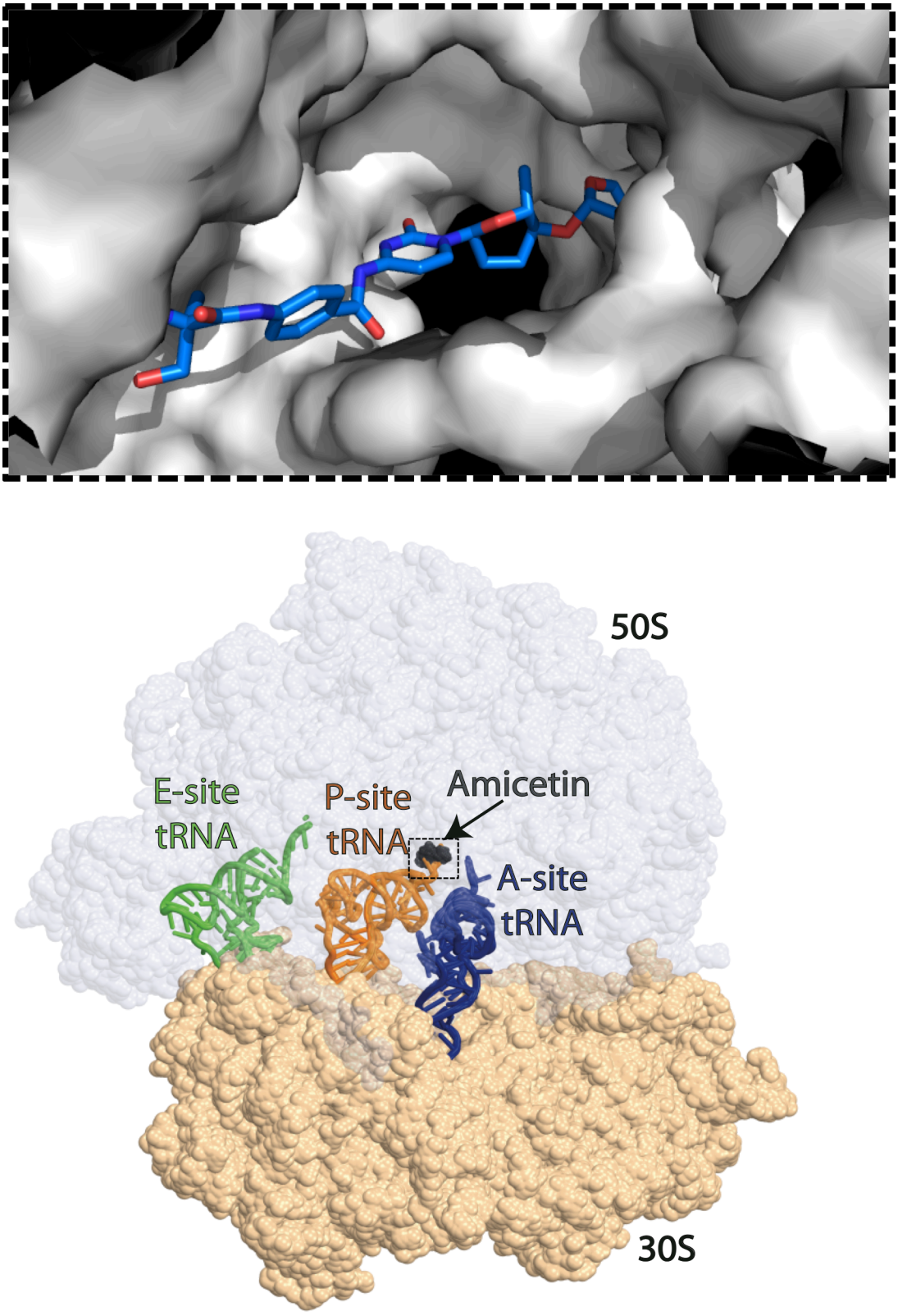

Figure 3.5 Crystal structure of amicetin bound to 70S *T. thermophilus* ribosome

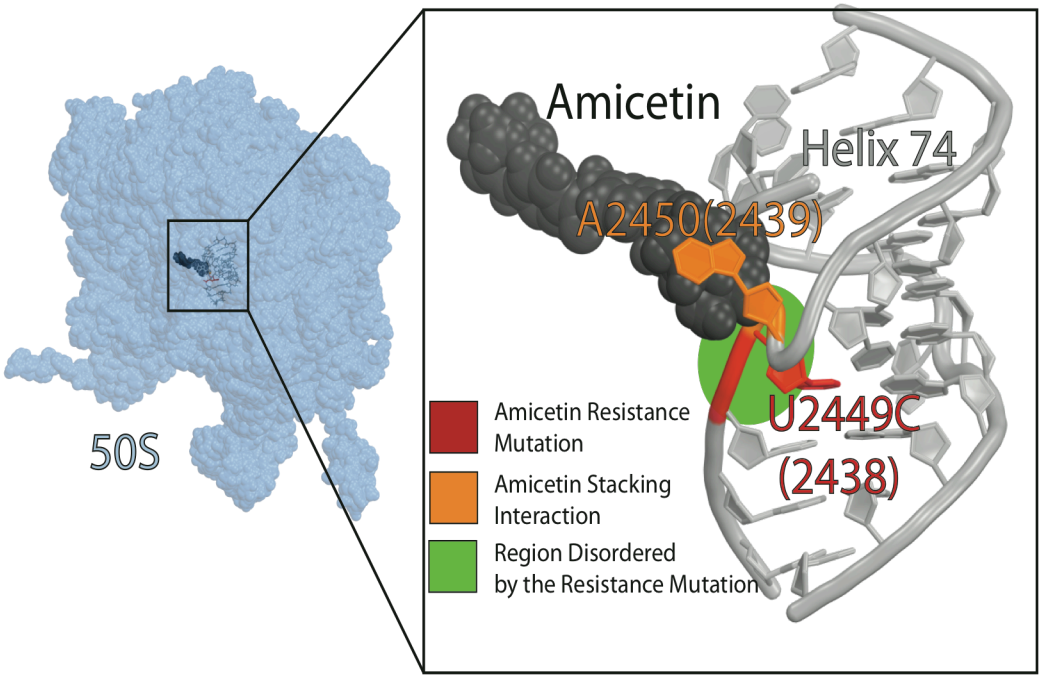

Figure 3.6 Amicetin and helix 74

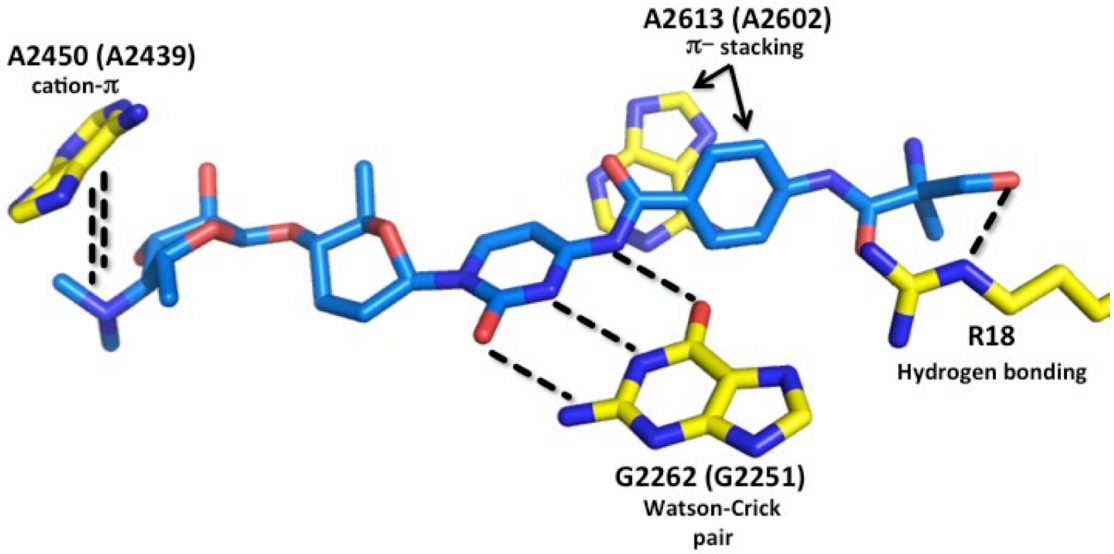

Figure 3.7 Important intermolecular contacts of amicetin within its binding site

determined by X-ray crystallography.[27] The major site mimicked the penultimate cytosine of a P-site tRNA and formed an interaction between its guanidine tail and the nucleotide base corresponding to A2449 (A2438).[28] The cytosine moiety of the minor binding site stacks with the cytosine moiety of the major site. This report suggested that blasticidin competes with tRNA binding.[27] A more recent crystal structure of the 70S ribosome in complex with blasticidin S and a P-site tRNA reveals that blasticidin S, rather than competing with the tRNA for binding to the P-site, it distorts the CCA end of the tRNA by pushing C75 out of its stacking interaction, rendering the tRNA in a nonproductive conformation on the ribosome (Figure 3.8). Similar to blasticidin S, our data shows (Figure 3.9). that amicetin traps the 3' end of a P-site tRNA in the 50S ribosomal subunit by displacing a P-site tRNA's penultimate cytosine, intercalating nucleotides C74 and A76, and forming a Watson-Crick pair with G2262 (G2251) in place of C75 at the 3' end of the P-site tRNA. This induced nonproductive conformation inhibits the peptidyl transferase reaction.

In addition, amicetin and blasticidin S form similar cation-π interactions with A2450 (A2439) and amicetin's the dimethylamino moiety, as with the guanidine tail of blasticidin S (Figure 3.10). Both basic centers are stacked on the aromatic ring of this particular adenosine and appear to be pertinent to the binding and activity of the antibiotics. Any structural change to the guanidine moiety, or its deletion from the molecule results in decreased or lost of activity.[29] The importance of this interaction in amicetin is illustrated by the effect of the resistance mutation U2449C (U2438C), *Tth (E.coli)* numbering, on the local rRNA structure.[11, 30] Changing uracil into cytosine would destabilize the Watson-Crick base pair between U2449 (U2438) and A2092 (A2071) present in the wild type ribosome. This would

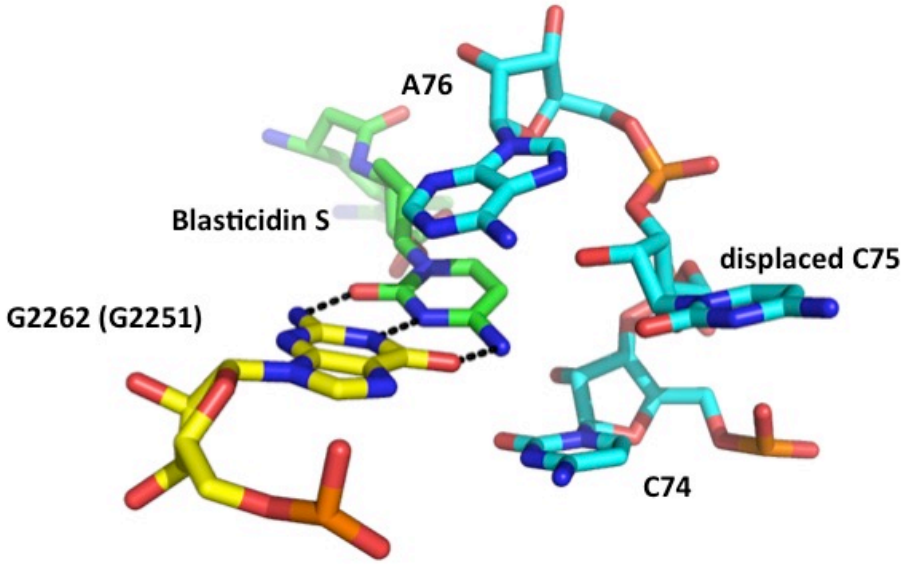

Figure 3.8 Distortion of the P-site tRNA conformation by blasticidin S in 70S *T. thermophilus* ribosome

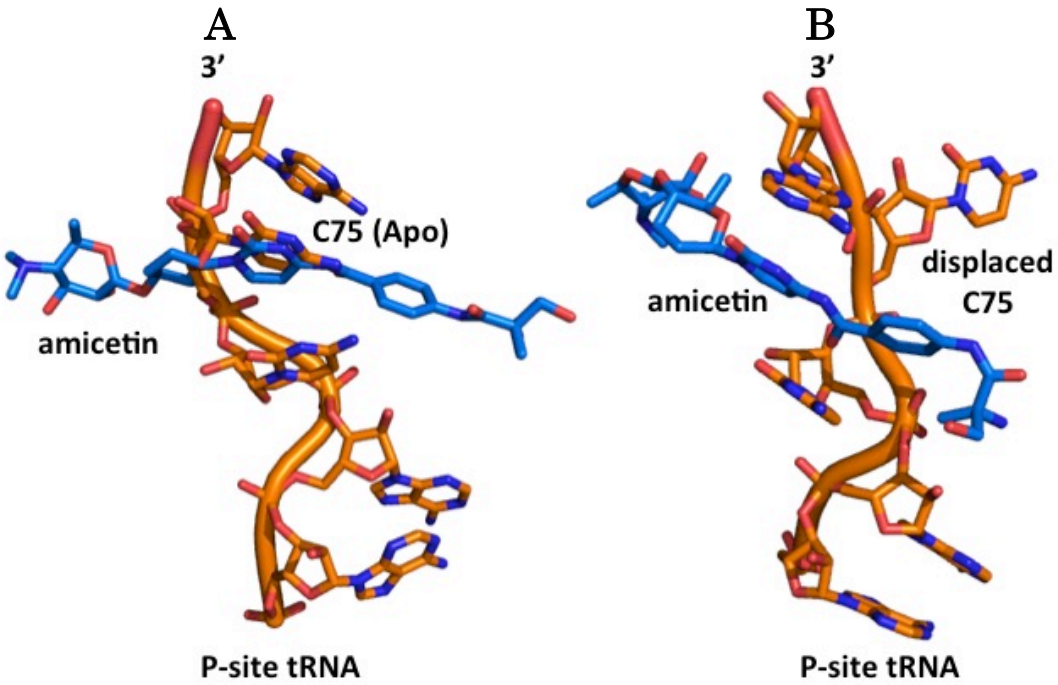

Figure 3.9 Distortion of the P-site tRNA conformation by amicetin in 70S *T. thermophilus* ribosome
A) Amicetin's cytosine overlaps with C75 of the P-site tRNA in the Apo ribosome; B) amicetin traps the 3' end of a P-site tRNA in a nonproductive conformation by pushing out C75

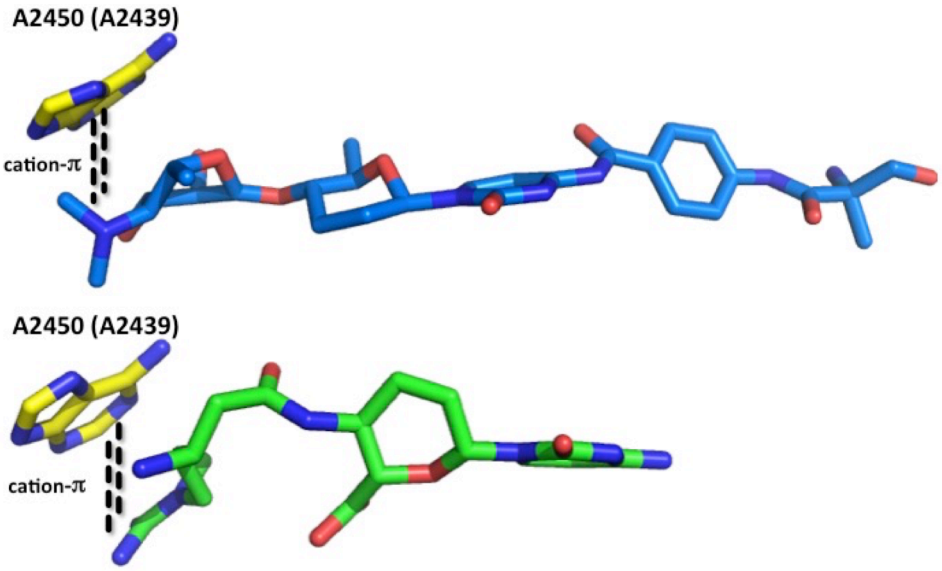

Figure 3.10 Cation-π interactions with A2450 (A2439)
Amicetin (blue), blasticidin S (green)

interfere with amicetin binding, since the mutation would likely affect the position of the backbone of U2449 (U2438) and the unpaired A2450 (A2439), disrupting the cation-π interaction with the dimethylamino group of the terminal sugar.

The crystal structure presented here is consistent with observations from available biochemical studies on amicetin. Trapping the P-site tRNA in a non-productive conformation inhibits peptidyl transferase on puromycin reactions and polyphenylalanine synthesis.[2, 6] This also provides an explanation on amicetin's ability to stabilize native polysomes.[8] Upon completion of the peptide chain at the termination codon, the ribosome dissociates from the mRNA, becoming a termination ribosome, which readily disassembles into individual ribosomal subunit, which can then re-assemble into polysomes, completing the ribosome cycle (Figure 3.11).[31] Peptidyl transferase inhibitors halt the translation process, causing the congestion of ribosomes along the mRNA. This translational "traffic jam" prevents the reading of the termination codon and the subsequent disassembly of

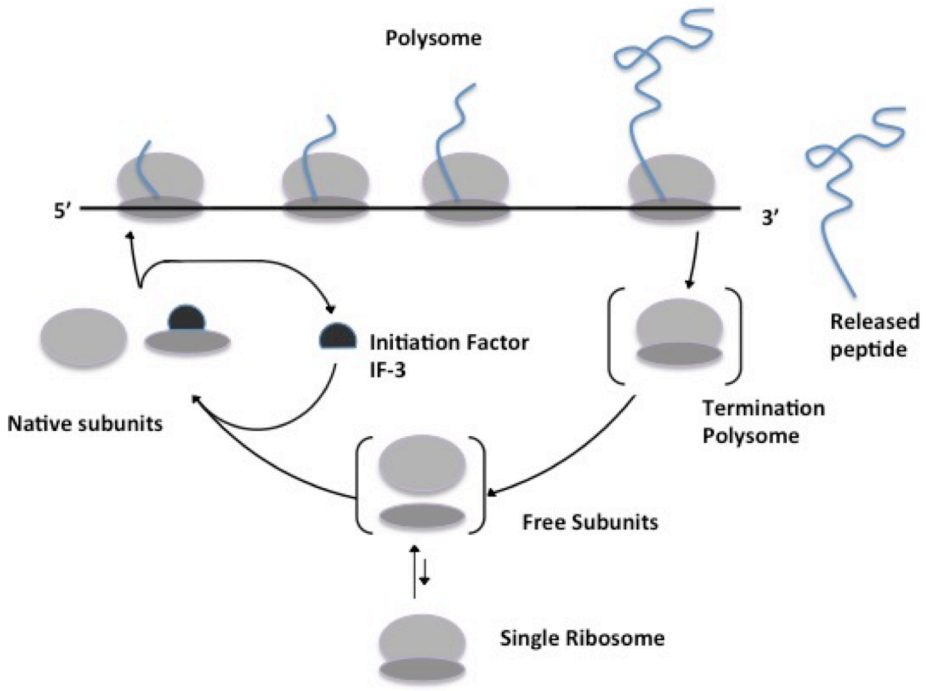

Figure 3.11 The Ribosome Cycle

the polysome, supporting amicetin's proposed mechanism of action-the inhibition of peptide bond formation.

Our data also supports amicetin's inability to inhibit pre-initiation processes like amino acid activation and early elongation steps like L-[^{13}C]-phenylalanyl-RNA binding to the ribosomes.[2] Amicetin, as shown here, interacts with residues in the P loop region, which is at least 100 100 Å away from residues of implicated in initiation processes.[14, 32] Although amicetin was also reported to interfere with the binding of C-A-C-C-A tRNA mimics to isolated 50S ribosomal subunit, it is likely due to a lack of a codon-anticodon interaction between full length tRNAs and the 50S subunit, that is present in the context of the 70S ribosomes.

Amicetin was also previously reported to inhibit fMethionine release from fMet-tRNA-ribosome complex.[5] This property of amicetin has not been revisited

since its publication in 1970. Inhibition of fMethionine release mediated by release factor RF1 has recently been reported for blasticidin S.[25] Svridstiky and co-workers proposed that the inhibition of peptide release by blasticidin may be due to steric interference of the distorted CCA 3' end of the P-site tRNA with the GGQ-containing region of release factors. A similar distortion of the P-site tRNA was also observed in our crystal structure of amicetin-tRNA-ribosome complex, and may have inhibited the RF1-mediated fMethionine release.

Amicetin's π-stacking interaction with A2613 (A2602) may be a contributing factor in inhibiting fMethionine release. Universally conserved A2613 (A2602) have been implicated in peptide release.[33, 34] *In vitro* experiments on reconstituted *Thermus aquaticus* 50S ribosome subunits and affinity-tag purified *E. coli* ribosomes have shown that A2613 (A2602) of 23S rRNA may be one of the critical residues for peptide release. Release factors trigger peptide release by reorienting A2613 (A2602) in the PTC. A2613 (A2602) subsequently coordinates with the GGQ motif of release factor proteins and activates a water molecule for peptidyl-tRNA hydrolysis.[33] Superposition of our amicetin-70S structure with previously published RF2-70S complex[35] shows that amicetin's cytosine ring occupies the same space as A2613 (A2602) in the RF2-70S complex (Figure 3.12). Upon binding of amicetin with the ribosome, A2613 (A2602) is displaced from its interaction with the GGQ motif. We speculate that the displacement of A2613 (A2602) inhibits fMethionine release.

3.4.2 Differences Between Amicetin and Blasticidin S

Amicetin's general structure is quite similar to blasticidin S. It does, however, have an additional basic center in the form of an α-methylseryl-p-amino-

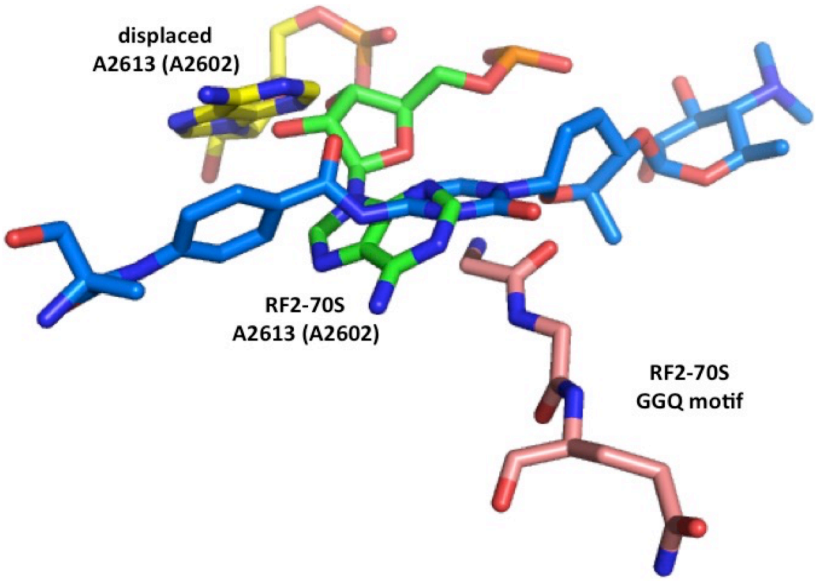

Figure 3.12 Superimposed amicetin-70S ribosome and RF2-70S

benzoyl group attached to the cytosine moiety. This affords amicetin other important contacts with the ribosome that are not available to blasticidin S. The *p*-aminobenzoyl moiety of amicetin forms π-stacking interactions with A2613(A2602). This particular interaction is interesting due to its highly dynamic nature (Figure 3.13). In the presence blasticidin S, A2613 (A2602) is slightly shifted from from its position in the Apo conformation. On the other hand, in the amicetin-70S structure, A2613 (A2602) is repositioned almost 90° relative to its conformation in the Apo 70S ribosome. When this amicetin-70S complex is overlaid with the structure of the 70S ribosome with programmed A-site, P-site and E-site tRNAs, A2613 (A2602) overlaps with C74 of the P-site tRNA.[36]

3.4.3 Differences with the Solution State NMR Studies

Our crystal structures are in conflict with the conclusions and observations reported in the solution state NMR studies on amicetin, the helix 74 mimic and the

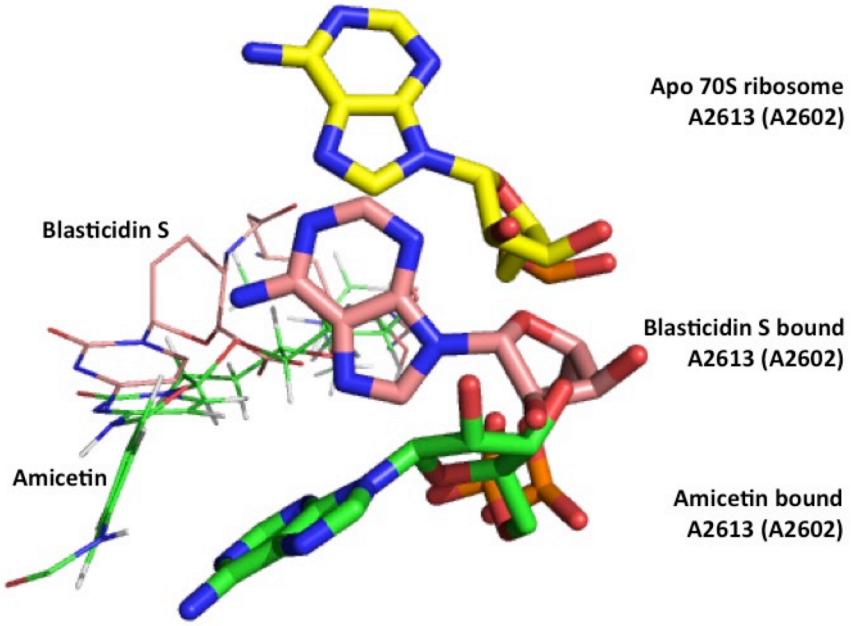

Figure 3.13 Movement of A2613 (A2602)

amicetin-helix 74 mimic complex (Figure 3.14).[12, 26, 37] We suspect that the previous reports' method in studying a system that is as complex and dynamic as the ribosome's interaction with molecules such as antibiotics were oversimplified. While NMR can provide useful structural information, using a 29-35mer RNA mimics to stand in as helix 74 of the 23S RNA was a reductionist approach to this complicated problem. We presume that truncated RNAs are not a practical model for studying interactions of antibiotics with ribosome.

First, the base interactions observed in helix 74 mimics (Figure 3.14), employed in the aforementioned studies were quite different from those observed in published ribosome crystal structures.[36, 38, 39] In the isolated model of the helix 74 mimic, noncanonical interactions are formed between U6 and U30, as well as between A9 and A27, however, in the complete ribosome, these noncanonical interactions are absent. Normally, U2089 (U2068) forms a trans Watson-

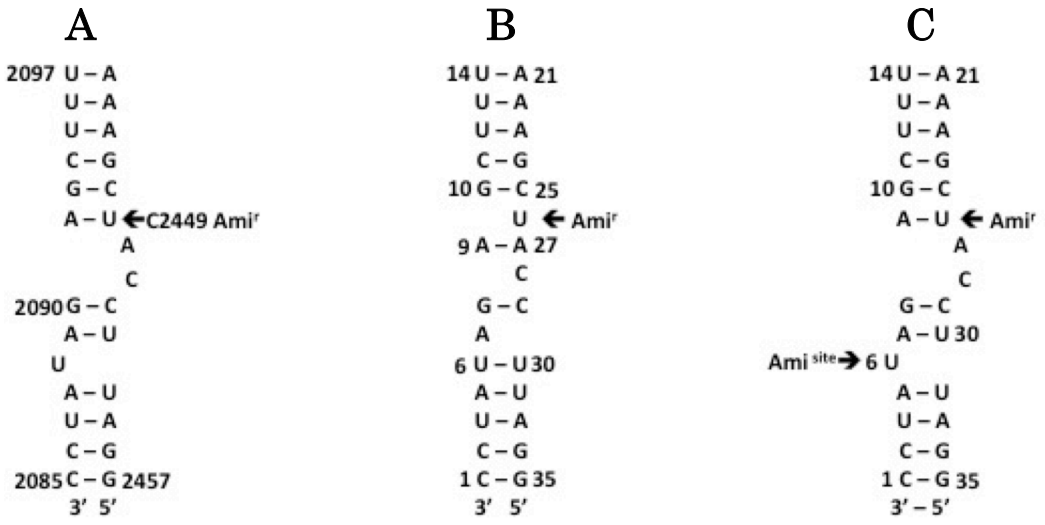

Figure 3.14 RNA mimics employed in NMR studies on amicetin
A) Secondary structure and the corresponding *Tth* numbering of the 35mer section of Helix 74; B) secondary structure of the solution state NMR structure of the 35mer Helix 74 mimic; C) putative binding site of amicetin from the solution state NMR study

Crick/Hoogsteen base pair with A2441 (A2430).[38, 39] In an attempt to focus on the interactions with the speculative binding site from the resistance mutations studies, using a truncated rRNA mimic could have resulted in the formation of these artificial conformations.

Secondly, for amicetin to afford the folded conformation as proposed by Ramesh, the amide bond between the pyrimidine ring and the aromatic ring has to assume a *cis* amide geometry, which is less favored than the *trans* conformation by an energy difference of 5 kcal/mol. By assuming a *cis* amide geometry, it has to overcome an energy barrier of 15 kcal/mol. Overall, that adds up to a total of 20 kcal/mol energy penalty. Their model suggested the folded conformation of amicetin is compensated with energy gained from both intra and intermolecular interactions, specifically with the nucleotide that corresponded to U2089 (U2068) *via* π-stacking interactions and hydrogen bonding. In our crystal structure (Figure 3.15), U2089

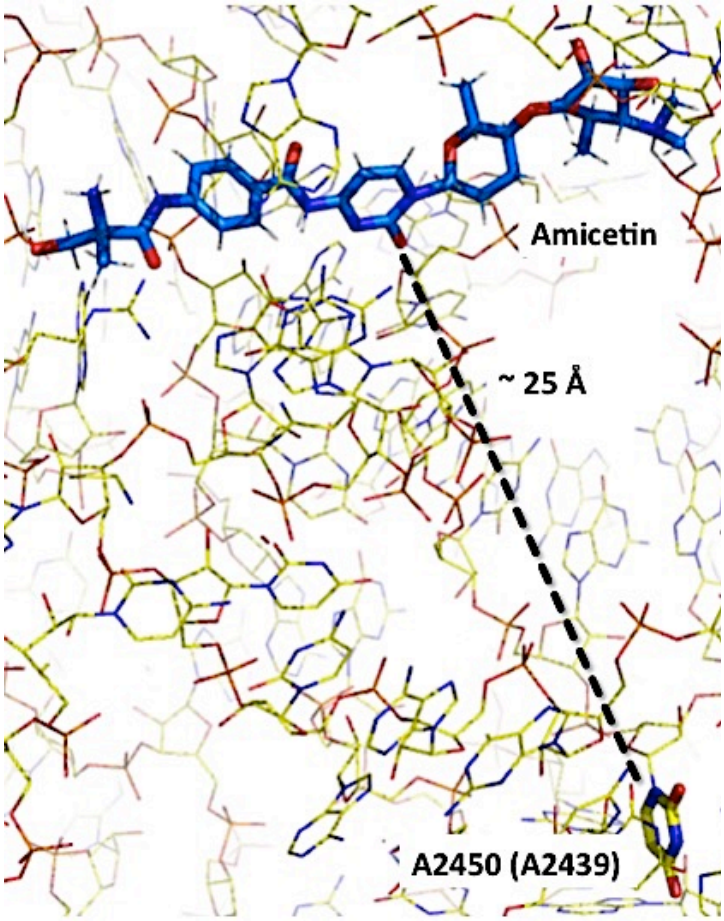

Figure 3.15 Amicetin and U2089 (U2094)

(U2068) is at least 25 Å away from the binding site It is highly improbable for U2089 (U2068) to undergo such drastic rearrangement and repositioning in the densely packed complete 50S ribosomal subunit or 70S ribosome. Furthermore, electron density from our data shows no such a rearrangement.

3.5 Conclusion

The crystal structure of the antibiotic amicetin in complex with mRNA and tRNA on the 70S ribosome from *T. thermophilus* is presented, demonstrating the possible molecular mechanism by which amicetin prevents translation. Amicetin

inhibits peptidyl transferase reaction by trapping the CCA 3' end of a tRNA into the P-site of the ribosome. Like blasticidin S, amicetin could possibly also inhibit peptide termination through its displacement of A2612 (A2602), an important nucleotide implicated in peptide release through its interaction with the GGQ motif of class 1 release factors. Our data agrees with most available biochemical data on amicetin except for a series of recently published NMR experiments. Mimics of helix 74 are outside the functional context of the ribosome and results in an artificial environment that is distinct from that of the native and complete 70S ribosome, thereby incapable of providing a relevant system to study amicetin's binding properties.

3.6 References

1. Brock, T. D. Effect of antibiotics and inhibitors on M protein synthesis. *J. Bacteriol.* **1963**, *85*, 527-531.

2. Coutsogeorgopoulos, C. Aminoacylnucleoside inhibitors of protein synthesis. the effect of amino acyl ribonucleic acid on the inhibition. *Biochemistry* **1967**, *6*, 1704-1711.

3. Pestka, S. Studies on the formation of transfer ribonucleic acid-ribosome complex, XI. Antibiotic effects on phenylalanyl-oligonucleotide binding to ribosomes. *Proc. Nat. Acad. Sci.* **1969**, *64*, 709-714.

4. Pestka, S. Studies on transfer ribonucleic acid-ribosome complexes, X. phenylalanyl-oligonucleotide binding to ribosomes and the mechanism of chloramphenicol action. *Biochem. Biophys. Res. Comm.* 1969, *36*, 589-595.

5. Tompkins, R. K.; Scolnick, E. M.; Caskey, C. T. Peptide chain termination, VII. The ribosomal release factor requirements for peptide release. *Proc. Nat. Acad. Sci.* **1970**, *65*, 702-708.

6. Pestka, S. Studies on transfer ribonucleic acid-ribosome complexes: XIX. Effect of antibiotics on peptidyl puromycin synthesis on polyribosomes from *Escherichia coli*. *J. Biol. Chem.* **1972**, *247*, 4669-4678.

7. Warner, J. R.; Knopf, P. M.; Rich, A. A multiple ribosomal structure. *Proc. Nat. Acad. Sci.* **1963**, *49*, 122-129.

8. Ennis, H. L. Polysome metabolism in *Escherichia coli*: amicetin, an antibiotic that stabilizes polysomes. *Antimicrob. Agents Chemother.* **1972** *1*, 204-209.

9. Ennis, H. L. Polysome metabolism in *Escherichia coli*: effect of antibiotics on polysome stability. *Antimicrob. Agents Chemother.* **1972**, *1*, 197-203.

10. Lichtenthaler, F. W.; Cerna, J.; Rychlik, I. The effect of oxamicetin and some amicetin analogs on ribosomal peptidyl transferase. *FEBS Lett.* **1975**, *53*, 184-187.

11. Leviev, I. G.; Rodriguez-Fonseca, C.; Phan. H.; Garrett, R. A.; Heilek, G.; Noller, H. F.; Mankin, A. S. A conserved secondary structural motif in 23 S rRNA defines the site of interaction of amicetin, a universal inhibitor of peptide bond formation. *EMBO J.* **1994**, *13*, 1682-1686.

12. Donarski, J.; Shammas, C.; Banks, R.; Ramesh, V. NMR and molecular modeling studies of the binding of amicetin antibiotic to conserved secondary structural motifs of 23S ribosomal RNAs. *J. Antibiot.* **2006**, *59*, 177-183.

13. Smith, J. L.; Sundaralingam, M. The structure of the antibiotic amicetin consisting of nucleobase, disaccharide and amino-acid moieties. *Acta. Crystallogr. B* **198**1, *37*, 1095-1101.

14. Broderson, D. E.; Clemons, W. M. Jr.; Carter, A. P.; Morgan-Warren, R. J.; Wimberly, B. T.; Ramakrishnan, V.; The structural basis for the action of the antibiotics tetracycline, pactamycin, and hygromycin B on the 30S ribosomal subunit. *Cell* **2000**, *104*, 1142-1154.

15. Leach, K. L.; Swaney, S. M.; Colca, J. R.; McDonald, W. G.; Blinn, J. R.; Thomasco, L. M.; Gadwood, R. C.; Shinabarger, D.; Xiong, L.; Mankin, A. S. The site of action of oxazolidinone antibiotics in living bacteria and in human mitochondria. *Mol. Cell* **2007**, *26*, 393-402.

16. Hinman, J. W.; Caron, E. L.; DeBoer, C. The isolation and purification of amicetin. *J. Am. Chem. Soc.* **1953**, *75*, 5864-5866.

17. De Boer, C.; Hinman, J. W. Amicetin and its production. U. S. Patent 238,012 July 23,1951.

18. Polikanov, Y. S.; Blaha, G. M.; Steitz, T. A. How hibernation factors RMF, HPF, and YfiA turn off protein synthesis. *Science* **2012**, *336*, 915-918.

19. Kabsch, W. Xds. Acta Crystallog., Sect. D: *Biol. Crystallogr.* **2010**, 66, 125-132.

20. Winn, M. D.; Ballard, C. C.; Cowtan, K. D.; Dodson, E. J.; Emsley, P.; Evans, P. R.; Keegan, R. M.; Krissinel, E. B.; Leslie, A. G. W.; McCoy, A. J.; McNicholas, S. J.; Murshudov, G. N.; Pannu, N. S.; Potterton, E. A.; Powell, H. R.; Read, R. J.; Vagin, A.; Wilson, K. S. Overview of the CCP4 suite and current developments. *Acta Crystallogr., Sect. D: Biol. Crystallogr.* **2011**, *67*, 235-242.

21. Emsley, P.; Lohkamp, B.; Scott, W. G.; Cowtan, K. D. Features and development of COOT. **2010**, *66*, 486-501.

22. Adams, P. D.; Afonine, P. V.; Bunkóczi, G.; Chen, V. B.; Davis, I. W.; Echols, N.; Headd, J. J.; Hung, L. W.; Kapral, G. J.; Grosse-Kunstleve, R. W.; McCoy, A. J.; Moriarty, N. J.; Oeffner, R.; Read, R. J.; Richardson, D. C.; Richardson, J. S. Terwilliger, T . C.; Zwarta, P. H. PHENIX: a comprehensive Python-based system for macromolecular structure solution. *Acta Crystallogr. Sect. D: Biol. Crystallogr.* **2010**, *66*, 213-221.

23. Schuttelkopf, A. W.; van Aalten, D. M. PRODRG: a tool for high-throughput crystallography of protein-ligand complexes. *Acta Crystallogr. Sect. D: Biol. Crystallogr.* 2004, *60*, 1355-1363.

24. Hansen, J. L.; Moore, P. B.; Steitz, T. A. Structures of five antibiotics bound at the peptidyl transferase center of the large ribosomal subunit. *J. Mol. Bol.* **2003**, *330*, 1061-1075.

25. Svidritskiy, E.; Ling, C.; Ermolenko, D. N.; Korostelev, A. A. Blasticidin S inhibits translation by trapping deformed tRNA on the ribosome. *Proc. Nat. Acad. Sci.* **2013**, *110*, 12283-12288.

26. Shammas, C.; Donarski, J. A.; Ramesh, V. NMR Structure of the peptidyl

transferase RNA inhibitor antibiotic amicetin. *Magn. Reson. Chem.* **2007**, *45*, 133-141.

27. Hansen, J. L.; Moore, P. B.; Steitz, T. A. Structures of five antibiotics bound at the peptidyl transferase center of the large ribosomal subunit. *J. Mol. Bol.* **2003**, *330*, 1061-1075.

28. This corresponds to U2474 in the *Haloarcula marismurti* ribosome

29. Yamaguchi, H.; Tanaka, T. Inhibition of protein synthesis by blasticidin S. II. Studies on the site of action in *E. coli* polypeptide synthesizing systems. *J. Biochem.* **1966**, 632-642

30. The point mutation corresponds to U2457 in the *Haloarcula marismurti* ribosome

31. Kaemper, R. The Ribosome Cycle. Cold Spring Harbor Monograph Archive, North America, 04, Jan. 1974. Available at: https://cshmonographs.org/index.php/monographs/article/view/3982/3199. Date accessed: 12 Mar. 2015.

32. Polaceck N.; Mankin, A. S. The ribosomal peptidyl transferase center: structure, function, evolution, inhibition. *Crit. Rev. Biochem. Mol. Biol.* **2005**, *40,* 285-311.

33. Polacek, N., Gomez, M.G., Ito, K., Nakamura, Y., and Mankin, A.S. 2003. The critical role of the universally conserved A2602 of 23S ribosomal RNA in the release of the nascent peptide during translation termination. Mol Cell 11:103-112.

34. Youngman, E.M., Brunelle, J.L., Kochaniak, A.B., and Green, R. 2004. The active site of the ribosome is composed of two layers of conserved nucleotides with distinct roles in peptide bond formation and peptide release. Cell 117:589-599.

35. Jin, H.; Kelley, A. C.; Loakes, D.; Ramakrishnan, V. Structure of the 70S ribosome bound to release factor 2 and a substrate analog provides insights into catalysis of peptide release. *Proc. Nat. Acad. Sci.* **2010**, *107*, 8593-8598.

36. Selmer, M.; Dunham, C. M.;. Murphy IV, F. V.; Weixlbaumer,A.; Petry, S.; Kelley, A. C.; Weir, J. R.; Ramakrishnan, V. Structure of the 70S ribosome complexed with mRNA and tRNA. *Science*, **2006**, 313, 1935-1942.

37. King, J.; Shammas, C.; Nareen, M.; Lelli, M.; Ramesh, V. NMR characterisation of a highly conserved secondary structural RNA motif of Halobacterium halobium 23S rRNA. *Org. Biomol. Chem.* 2013, 11, 3382-3392.

38. Ban, N.; Nissen, P.; Hansen, J.; Moore, P. B.; Steitz, T. A. The complete atomic structure of the large ribosomal subunit at 2.4 A resolution. *Science* **2000**, *289*, 905-920.

39. de Loubresse, N. G.; Prokhorova, I.; Holtkamp, W.; Rodnina, M. V.; Yusupova, G.; Yusupov, M. Structural basis for the inhibition of the eukaryotic ribosome *Nature* **2014**, *513*, 517-521.

3.7 Supplemental Information

3.7.1 General Experimental Procedure

Streptomyces vinaceusdrappus (ATCC 25511) was purchased from American Type Culture Collection (ATCC) was maintained and propagated per ATCC instructions. Materials for culture growth and propagation were purchased from BD Difco™ and Fischer Scientific® and used as received. Optical density (OD_{600}) was measured using Biomate 3 (Thermo™).

Normal phase flash chromatography was performed on Merck silica gel Kieselgel 60 (230-400 mesh) from EM Science with the indicated HPLC grade solvent. Fractions were monitored by TLC and visualized by a dual short wave/long wave UV lamp. Reverse phase chromatography was performed on packed C-18 columns using CombiFlash Rf™ (TELEDYNE ISCO) with the indicated HPLC grade solvent.

Melting point was determined using Mel-Temp® Capillary Melting Point Apparatus. Infrared Spectra was obtained using Nicolet 380-FT IR Spectrometer fitted with a Smart Orbit sample system. Optical rotations were obtained at ambient temperature on a Perkin Elmer Model 343 polarimeter (Na_D line)using microcell with 1 decimeter path length. Mass spectra were obtained at the University of Utah CIF on a Micromass Quattro II (ESI/APCI) for LRMS or an LCT XE premier (ESI/APCI-TOF) for HRMS. ^{1}H NMR spectra were recorded on Varian Unity-300 and cold probe Inova-500 MHz spectrometers. The chemical shifts (δ) of proton resonances are reported relative to CD_3OD,\ using the following format: [1, 2]

---

[1] Gottlieb, H. E.; Kotlyar, V.; Nudelman, A. *J. Org. Chem.* **1997**, *62*, 7512-7515.

chemical shift [multiplicity (s = singlet, d = doublet, t = triplet, q = quartet, m = multiplet, app = apparent, br = broad), coupling constant(s) (*J* in Hz), integral]. ^{13}C NMR spectra were recorded at 150 MHz. Chemical shifts of carbon resonances are reported relative to the deuterated solvent peak.

3.7.2 Production of Amicetin

Fermentation and production of amicetin from *Streptomyces vinaceusdrappus* (ATCC 25511) was done as**previously described.**[3] The culture of *S. vinaceusdrappus* (ATCC 25511) was maintained at 36 °C on a sterile yeast-malt extract-glucose agar (4% w/v glucose, 4% w/v yeast extract, 10% w/v malt extract, 2% w/v $CaCO_3$, and 12% w/v agar, dissolved in distilled and deionized water; pH 7.2; autoclaved at 120 ˚C for 15 min). After four days, the mycelia grown on the agar plate were inoculated in a 500-mL Erlenmeyer flask containing 100 mL of sterile yeast-peptone-glucose seed medium (10% w/v yeast extract, 20% w/v peptone, 20% w/v glucose, dissolved in distilled deionized water; pH 7.0; autoclaved at 120 ˚C for 15 min). The flasks were shaken (200 rpm) at 28 ˚C for 2 days. The seed culture (25 mL, OD_{600} of 1.6) was transferred into 2000-mL Erlenmeyer flasks, each containing 500 mL of the production media (25% w/v glucose, 2.5% w/v yeast extract, 7% w/v soybean flour, 5% w/v Na_2SO_4, 8% w/v $CaCO_3$, 4% w/v KCl, 0.4% w/v KH_2PO_4; pH 7.55; autoclaved 120 ˚C for 20 min). The inoculated production media was shaken (200 rpm) and incubated at 28 °C for 5 days.

---

[2] Hoye, T.R.; Hansen, P.R.; Vyvyan, J. R. *J. Org. Chem.* **1994**, *59*, 4096-4103.

[3] De Boer, C.; Hinman, J. W. U. S. Patent 238,012 July 23,1951.

3.7.3 Isolation and Purification of Amicetin

The production media was vacuum twice filtered to remove the mycelia using Whatman filter paper grade 1 and a third time with Whatman filter paper grade 3, yielding a brown-colored filtrate. Without pH adjustment, the clarified filtrate was extracted thrice with one-fourth its volume using 30% v/v *i*PrOH/$CHCl_3$. The extracts were combined and concentrated under reduced pressure yielding a 300 mg of brown solid of crude amicetin. The crude solid was taken up in methanol and adsorbed into 1 g of celite, and dried under reduced reduced pressure. This process was repeated thrice to ensure optimal transfer of the crude material to the adsorbing agent. The crude material was then purified by normal phase flash chromatography *via* gradient elution of 5% v/v MeOH/$CHCl_3$ to 30% MeOH/$CHCl_3$. Semi-clean amicetin was obtained from the 20-30% MeOH/$CHCl_3$ fractions. The collected fractions were concentrated under reduced pressure and were re-adsorbed in celite, as previously described. Re-adsorbed amicetin was subjected to further purification by reverse phase chromatography *via* gradient elution of 5% v/v H_2O/CH_3CN to 50% H_2O/CH_3CN. The collected fractions were concentrated under reduced pressure to yield an off-white solid, which was triturated with ether to yield pure amicetin as a white powder (30 mg) as a white solid. *Rf*= 0.33 (30% MeOH/$CHCl_3$). ^{1}H NMR (300 MHz, $CDCl_3$) δ 8.18 (d, *J* = 7.6 Hz, 1H), 7.98 (d, *J* = 8.5 Hz, 2H), 7.82 (d, *J* = 8.6 Hz, 2H), 5.78 (d, *J* = 7.6 Hz, 1H), 4.90 (d, masked by H_2O, 1H), 3.96-3.73 (m, 4H), 3.43-3.41(m, 3H), 2.47 (s, 6H), 2.40 (bs, 1H), 2.15 (m, 2H), 1.66 (dd, *J* = 9.3, 9.3, 2H), 1.37 (d, *J* = 6.0 Hz, 3H), 1.31, (s, 1H), 1.25 (d, *J* = 6.3 Hz, 3H) ppm. ^{13}C NMR (125 MHz, $CDCl_3$) δ 177.8, 164.8, 157.3, 146.2, 143.9, 130.3, 129.6, 120.5, 98.8, 96.1, 84.6, 78.4, 75.0, 74.6, 71.8, 70.2, 69.1, 67.3, 66.9, 64.7, 60.9, 42.3, 31.0, 27.7, 25.2, 22.7, 19.6, 19.1, 15.4 ppm. IR (neat) 3290, 1700, 1685 cm^{-1}. LRMS (ESI) 619.9 *m/z* (M+1).

3.7.4 ^{1}H NMR and ^{13}C NMR Spectra

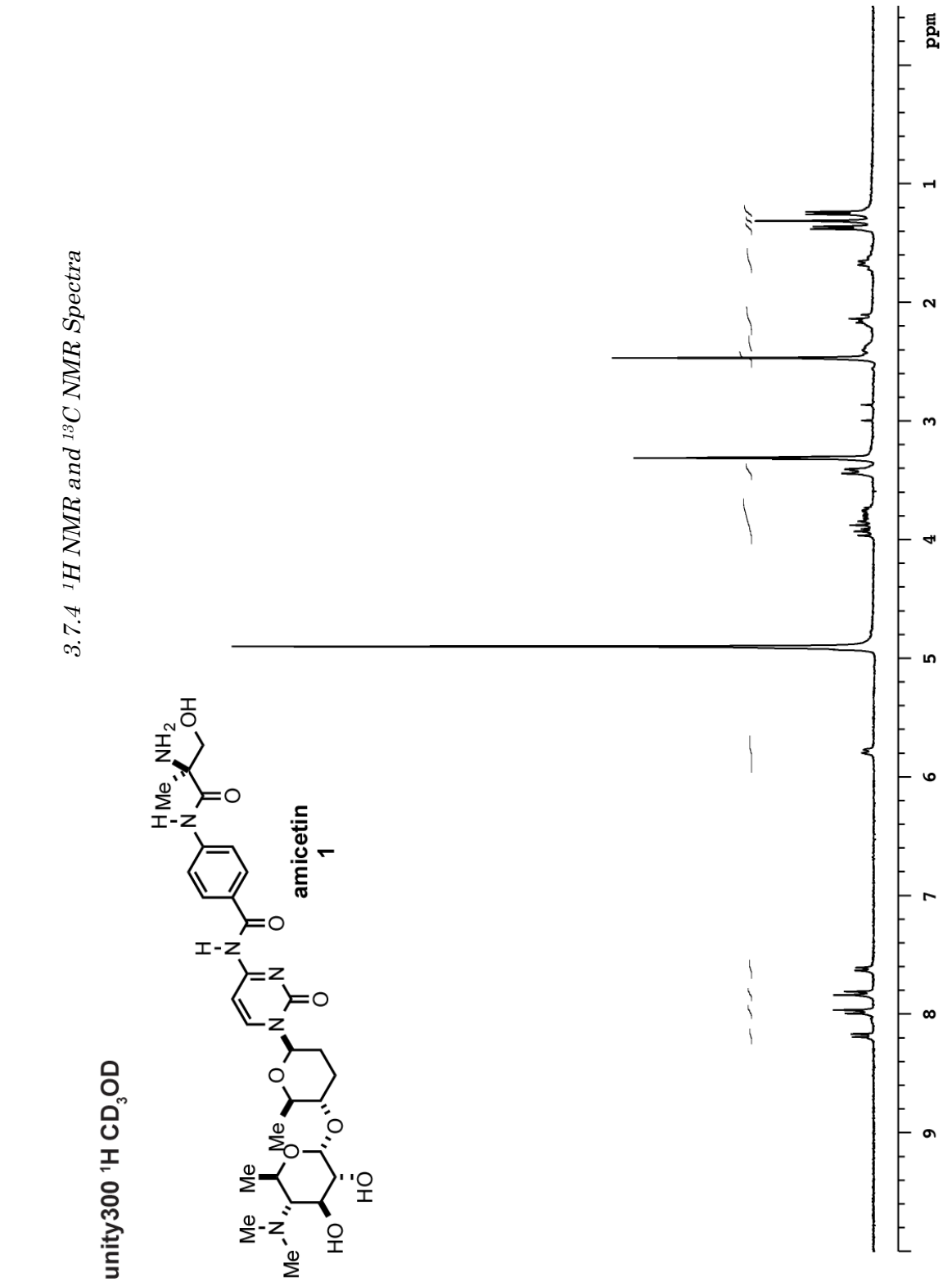

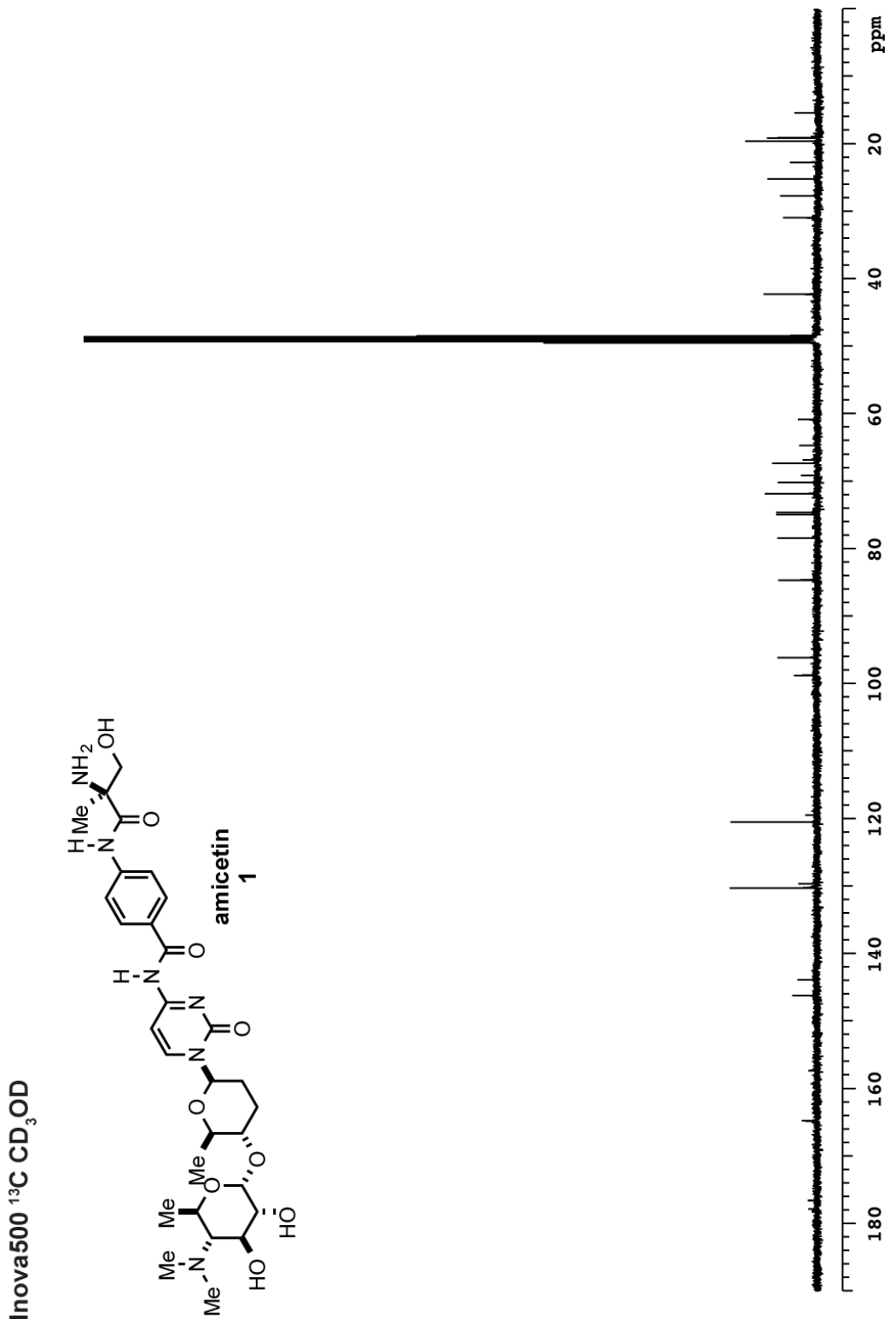
Inova500 13C CD3OD
amicetin
1
ppm
180
160
140
120
100
80
60
40
20

3.7.5 Complex Formation and Crystallization

70S *T. thermophilus* ribosomes were purified and crystallized as previously described.[4] Purified 70S ribosomes were diluted with a buffer solution [5 mM Hepes (pH 7.5), 50 mM KCl, 10 mM NH_4Cl, and 10 mM $Mg(OAc)_2$] to a final concentration of 10 mg/mL. 70S ribosomes crystals werer grown at 19°C *via* sitting-drop vapor diffusion by mixing 3 μL of the ribosome sample with 3.5-4.5 μL of the crystallization solution [2.9% PEG 20K, 9% methyl-2,4-pentanediol (MPD), 175 mM L-arginine, and 100 mM Tris–HCl (pH 7.6)]. Concentration of MPD was increased to 40% in stabilize the crystals, upon addition of 500 μM amicetin. 70s ribosomes were also co-crystallized with mRNA (20 μM) and fMet-$tRNA^{fMet}$ (20 μM). The crystals were flash frozen in a nitrogen cryostream at 80 K after 24 hours of equilibration.

---

[4] Polikanov, Y. S.; Blaha, G. M.; Steitz, T. A. *Science* **2012**, *336*, 915-918.

CHAPTER 4

BIOLOGICAL EVALUATION OF AMICETIN ANALOGUES

4.1 Background

The persisting global problem of tuberculosis (TB) and the inadequacy of the current drug treatments have led to our recent interest in developing new TB therapies. As previously discussed, we sought to employ amicetin (Figure 4.1),[1, 2] an underutilized pyrimidine nucleoside antibiotic as a possible drug lead; using its structural features to design analogues that are active against *Mycobacterium tuberculosis* and noncytotoxic to mammalian cells. Our efforts were also guided by other aminoacyl nucleoside antibiotics and TAN 1057 (Figure 4.1), a dihydropyrimidinone antibiotic.[3]

A review by Fox proposed that aminoacyl nucleosides capable of inhibiting protein synthesis have an accessible amino acid moiety (Figure 4.1, blue) attached to a carrier nucleoside (Figure 4.1, red), and another basic center at the end of the molecule (Figure 4.1, green).[4] These functional groups were thought to afford the efficient binding of the molecules to the ribosomes, providing their biological activity and inhibitory properties against protein synthesis. In addition to this, Lichtenthaler proposed that the spatial rearrangement and the distance created by the molecular spacer or linker between the nucleobase and the amino acid (Figure 4.1, black) is essential for maintaining inhibitory function.[5]

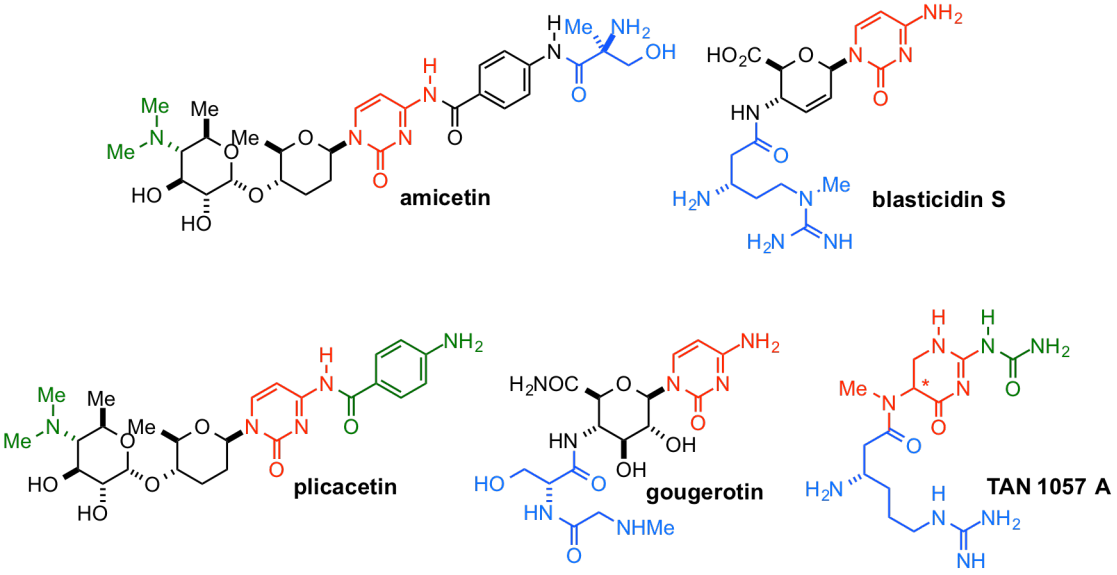

Figure 4.1 Common structural motif of pyrimidine nucleoside antibiotics

In contrast, TAN 1057, a ribosomal antibiotic that neither has a sugar moiety nor a formal nitrogenous base is known to be active against Methicillin-resistant *Staphylococcus aureus* (MRSA) and inhibits protein synthesis.[3] TAN 1057, however, has a dihydropyrimidinone that acts as a cytosine-mimic, as well as two basic centers (urea and ß-homoarginine).[15]

Considering TAN 1057's simplified structure relative to other pyrimidine nucleoside antibiotics, we speculate that amicetin analogues with simpler scaffolds can also exhibit the desired biological activity as long as the general pharmacophore is preserved. We sought to develop simplified amicetin with the general pharmacophore: a cytosine base, a linker, a cationic tail, and another cationic cap region (Figure 4.2).

Our approach to analogue design preserves the cytimidine portion of amicetin, which contain both the required nucleobase, cytosine, and the aminoacyl cap region. This allows for a focused SAR study on the disaccharide of amicetin.

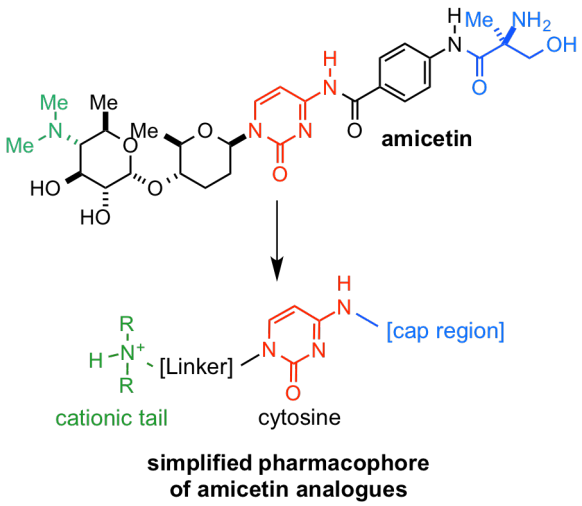

Figure 4.2 General design of amicetin analogues

We chose to replace the disaccharide with nonhydrolyzable linkers to explore possible variations of cationic tails, as well as variations of spacer length and flexibility. Substituting the sugar moiety also simplifies the synthesis of potential analogues. Drawing inspiration from the common structural features observed in pyrimidine nucleoside antibiotics and TAN 1057, we began to design and synthesize our analogues prior to solving the crystal structure of ribosome-bound amicetin.

4.2 Materials and Methods

4.2.1 Biological Evaluation of Amicetin Analogues

Amicetin analogues were prepared by Hariprassada Reddy Kannareddy of the Looper Research Laboratory. Compounds were assayed against *M. tuberculosis* H37Ra and mammalian CEM-TART leukemia cells using an MTT Assay.[6, 7] The antimicrobial spectrum of the analogues were determined against *B. subtilis*, *E. coli*, *A. baumanii*, and *C. albicans*. Protein synthesis inhibition was measured by luciferase readout using the Promega™ *E. coli* S30 Extract System. Assays were

done in triplicate. Data were processed using GraphPad™ Prism 6. Detailed procedures are provided in the Supplemental Information.

4.2.2 Co-Crystallization, Data Collection and Processing

X-Ray Crystallograpy Experiments were done in collaboration with the Steitz Group at Yale University. *T. thermophilus* 70S ribosomes were purified and crystallized as previously published.[8] Ribosome complexes were obtained by incubating vacant 70S ribosomes with analogue **1** (1 mM) and analogue 5 (3 mM) for 24 hours. Crystals were harvested and flash frozen in a nitrogen cryostream. Details of the crystallization are provided in the Supplemental Information.

Data collection was performed at 100 K using synchrotron X-ray radiation at beam line 24ID-C at the Advanced Photon Source in Argonne National Laboratory (Argonne, IL) and beam line x25 at the National Synchrotron Light Source in Brookhaven National Laboratory. X-ray diffraction data was processed using X-ray Detector Software (XDS).[9] Refinements, integration and handling of scaled data were completed using Collaborative Computational Project programs.[10] Final models were built using COOT and refined using PHENIX.[11, 12] Ligand model for amicetin were built using PRODRG.[13]

4.3 Results

4.3.1 Biological Properties of Amicetin Analogues

Our preliminary screening has produced six analogues (Figure 4.3) that exhibited antimycobacterial activity, measured as half maximal inhibitory concentration (IC_{50}), in the low micromolar concentrations (Figure 4.4, Table 4.1). Analogue 3 is the most active with an IC_{50} of 0.98 μM against *M. tuberculosis* H37Ra

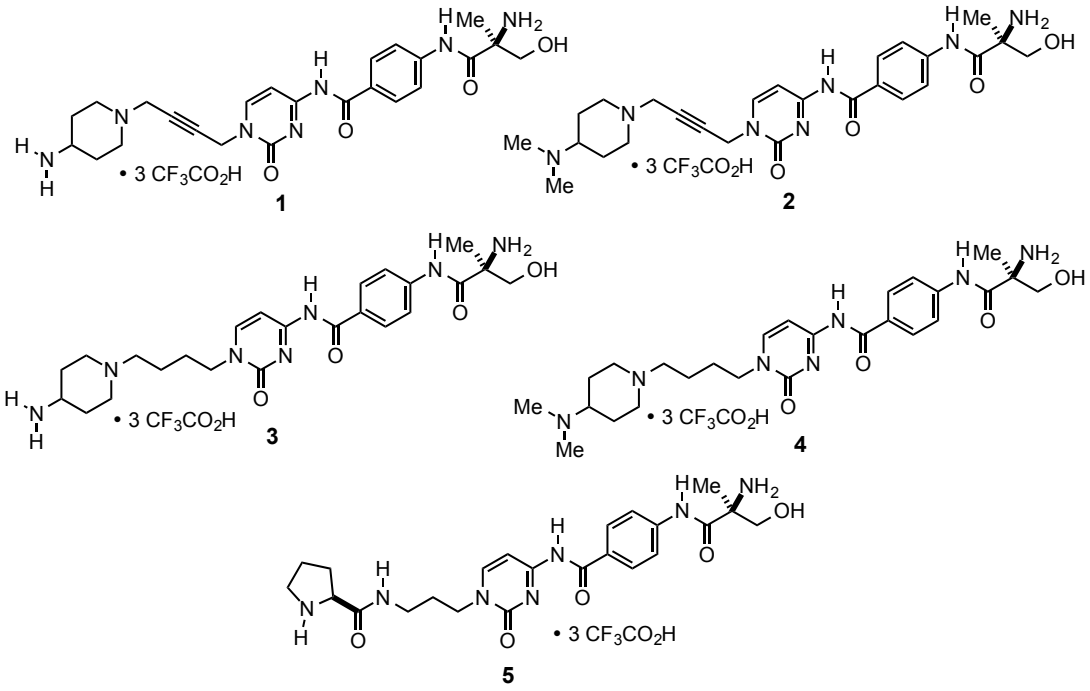

Figure 4.3 Amicetin analogues with antimycobacterial activity

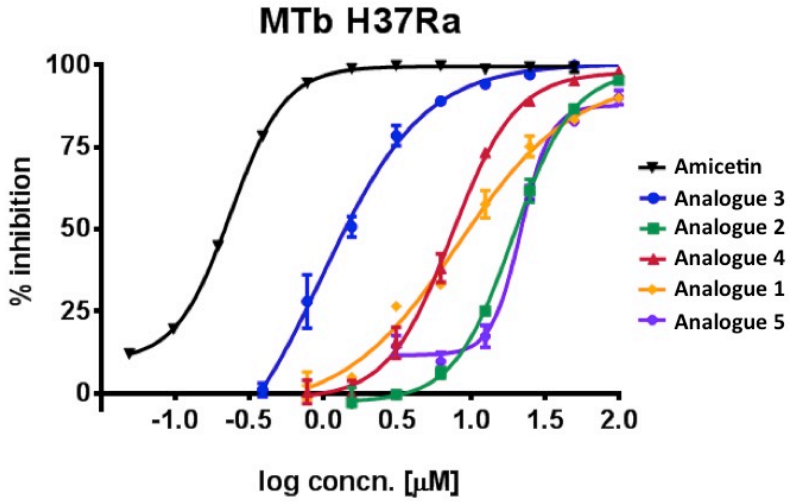

Figure 4.4 Growth inhibition curves of amicetin analogues

Table 4.1 Summary of biological activity of amicetin analogues

Compound	*M. tuberculosis* H37Ra IC_{50} (μM)	Protein Synthesis % Inhibition at 50 μM	CEM-TART IC_{50} (μM)
amicetin	0.24	100	4.5
1	8.2	77	> 100
2	19	61	> 100
3	0.98	99	> 100
4	7.4	94	> 100
5	22	42	> 100

(ATCC 25177). All six analogues exhibited inhibition of protein synthesis directly proportional to their respective antimycobacterial activity (Table 4.1). The most potent analogue, compound **3**, inhibited protein synthesis with an IC_{50} of 3.8 μM.

These compounds exhibited limited cytotoxicity (Table 4.1) against CEM-TART leukemia cells (AIDS Research and Reference Reagent Program, NIAID, NIH), IC_{50} >100 μM. All compounds tested, including the active analogues, exhibited a narrow spectrum of antimicrobial activity, and are inactive against *B. subtilis* (ATCC 6633), *E. coli* (ATCC 25922), *A. baumanii* (ATCC 19606), and *C. albicans*. (ATCC 90028).

4.3.2 Crystal Structures of Amicetin Analogues Bound to 70S T. thermophilus Ribosomes

Structures of analogues **1** and **5** bound to the 70S ribosomal subunit of *Thermus thermophilus (Tth)* occupy the same binding pocket of amicetin in the peptidyl transferase center of the 70S *T. thermophilus* ribosome as amicetin (Figure 4.5). Amicetin, analogue **1** and analogue **5** share a similar extended conformation with slight variations while the configuration of analogue **5** in the binding site deviates significantly from the other two, especially with respect to the

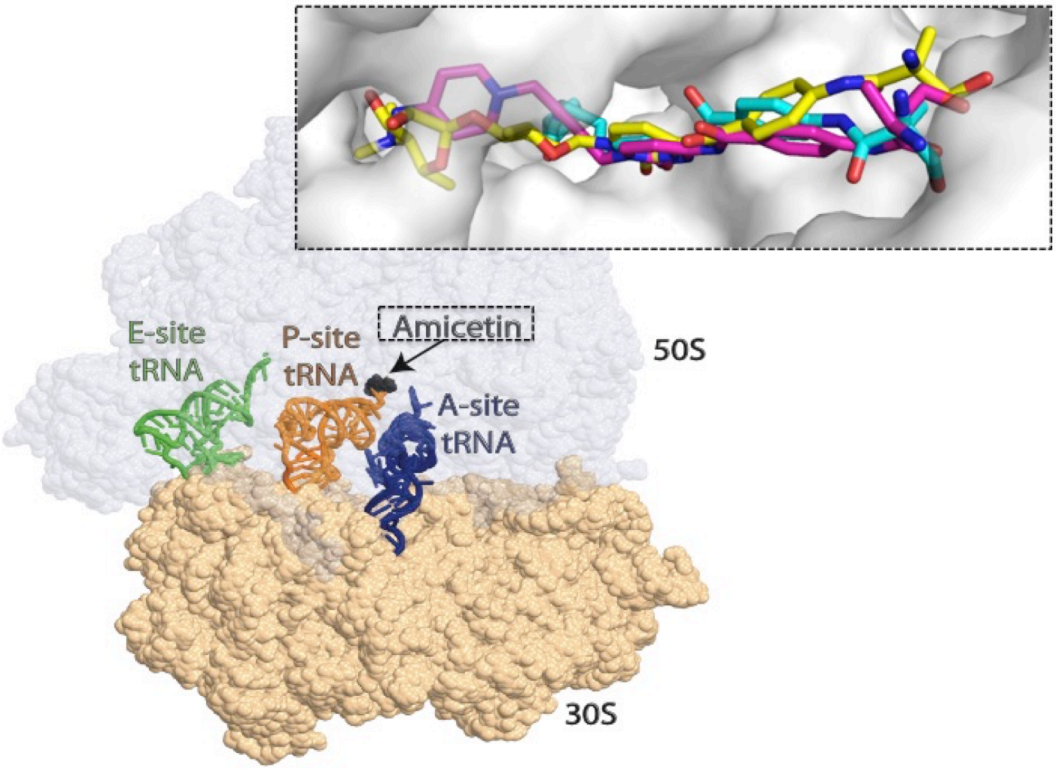

Figure 4.5 Shared binding site of amicetin (yellow) and analogues 1 (magenta) and 5 (cyan).

latter's propylprolinyl group (Figure 4.6). Unlike the respective aminohexopyranose and aminopiperidyl moieties of amicetin and analogue **1**, which the propylprolinyl tail of analogue **5** swerves into a crevice away from the exit tunnel. The basic groups of amicetin and analogue **1** sits on top of the exit tunnel, while the prolinyl of analogue **1** docks into a different crevice.

Analogue **1**, which is more potent, has a closer binding motif to amicetin than analogue **5**, and has all the ribosomal interactions reported on amicetin (Figure 4.7, Figure 4.8). Both analogues form the Watson-Crick GC pair through their cytosine, π-stacking interaction through their *p*-aminobenzoyl, and hydrogen bonding through their aminoacyl. Unlike analogue **1**, analogue **5** does not form cation-π intercations with the ribosome through its cationic tail.

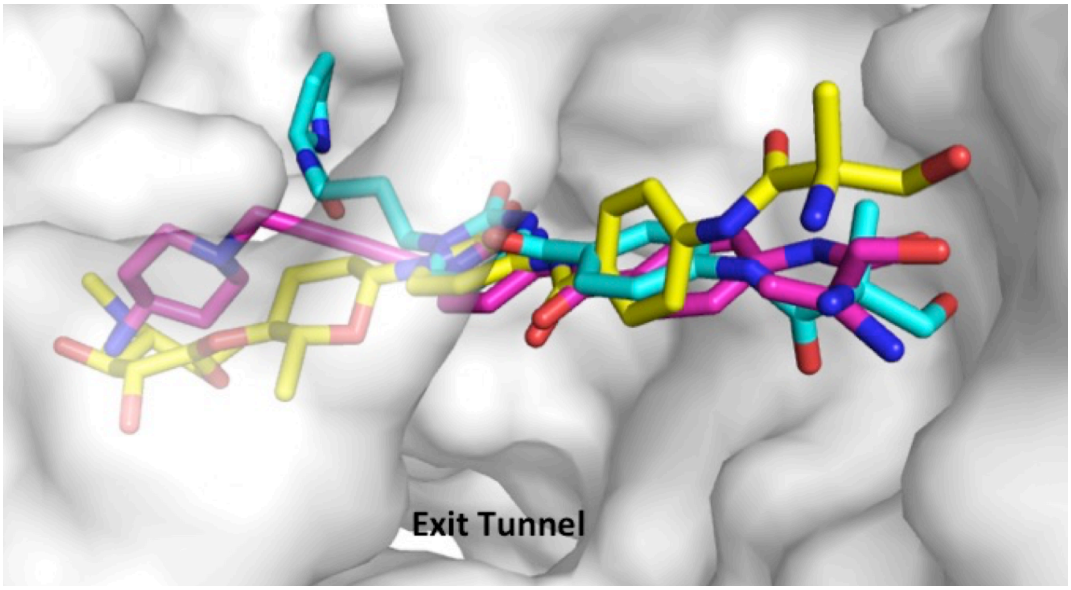

Figure 4.6 Overlapped binding conformations of amicetin: amicetin (yellow), analogue **1 (magenta), and 5 (cyan)**

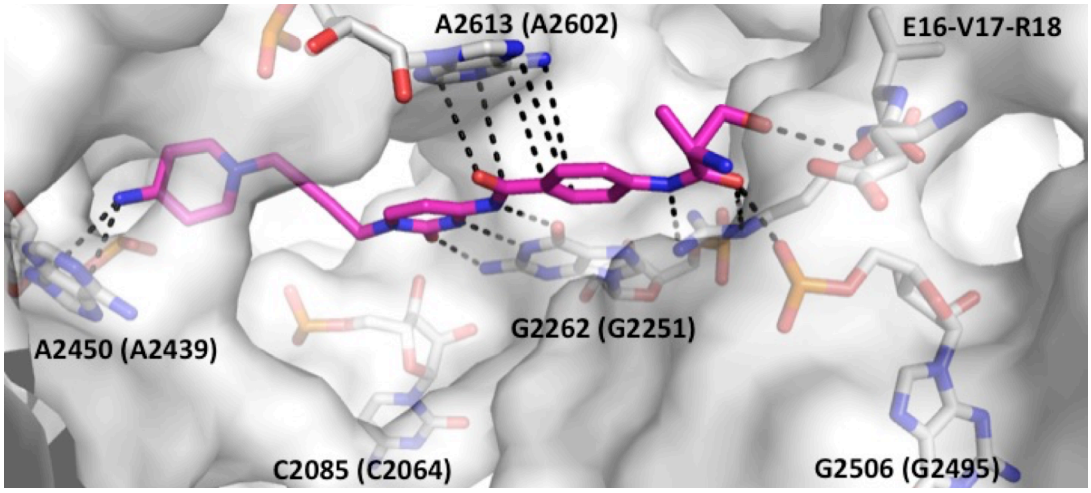

Figure 4.7 Key interactions of analogue 1 with the 70S *T. Thermophilus* ribosome

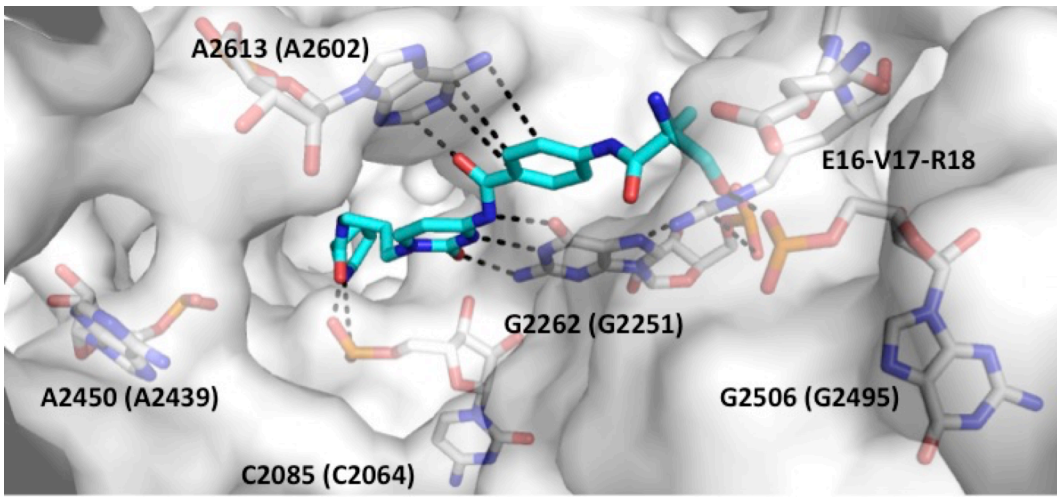

Figure 4.8 Key interactions of analogue 5 with the 70S *T. Thermophilus* ribosome

4.4 Discussion

4.4.1 Structure Activity Relationship of Amicetin Analogues with Respect to Antimycobacterial Activity

To test our hypothesis, 20 amicetin analogues in addition to cytimidine and amicetin (Figure 4.9) were assayed against *M. tuberculosis* H37Ra. Based on the following set of compounds an apparent structure activity relationship can be inferred. In line with our hypothesis, both basic centers are needed for activity, as shown by cytimidine, and analogues **6** to **12** being devoid of activity. Although analogue **8** technically has two basic centers, it appears to be at least 3 atoms short when laid side by side with blasticidin S, not to mention its molecular spacer is an alkynyl chain which has very little freedom of motion which could affect its binding affinity.

As previously discussed, Lichtenthaler proposed that the spatial rearrangement and the distance created by the molecular spacer between the nucleobase and the amino acid is essential for maintaining inhibitory function.[5]

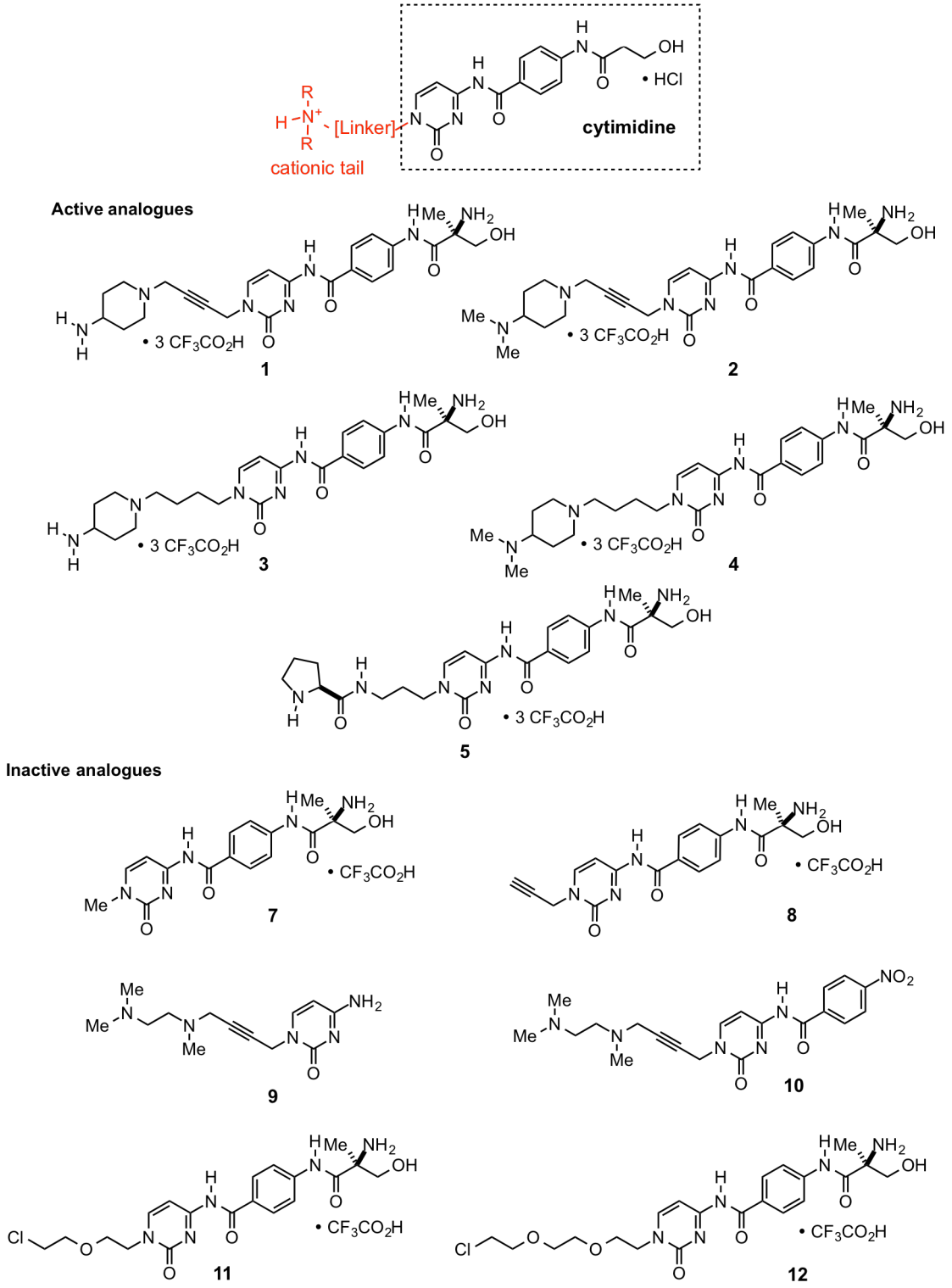

Figure 4.9 Amicetin analogues

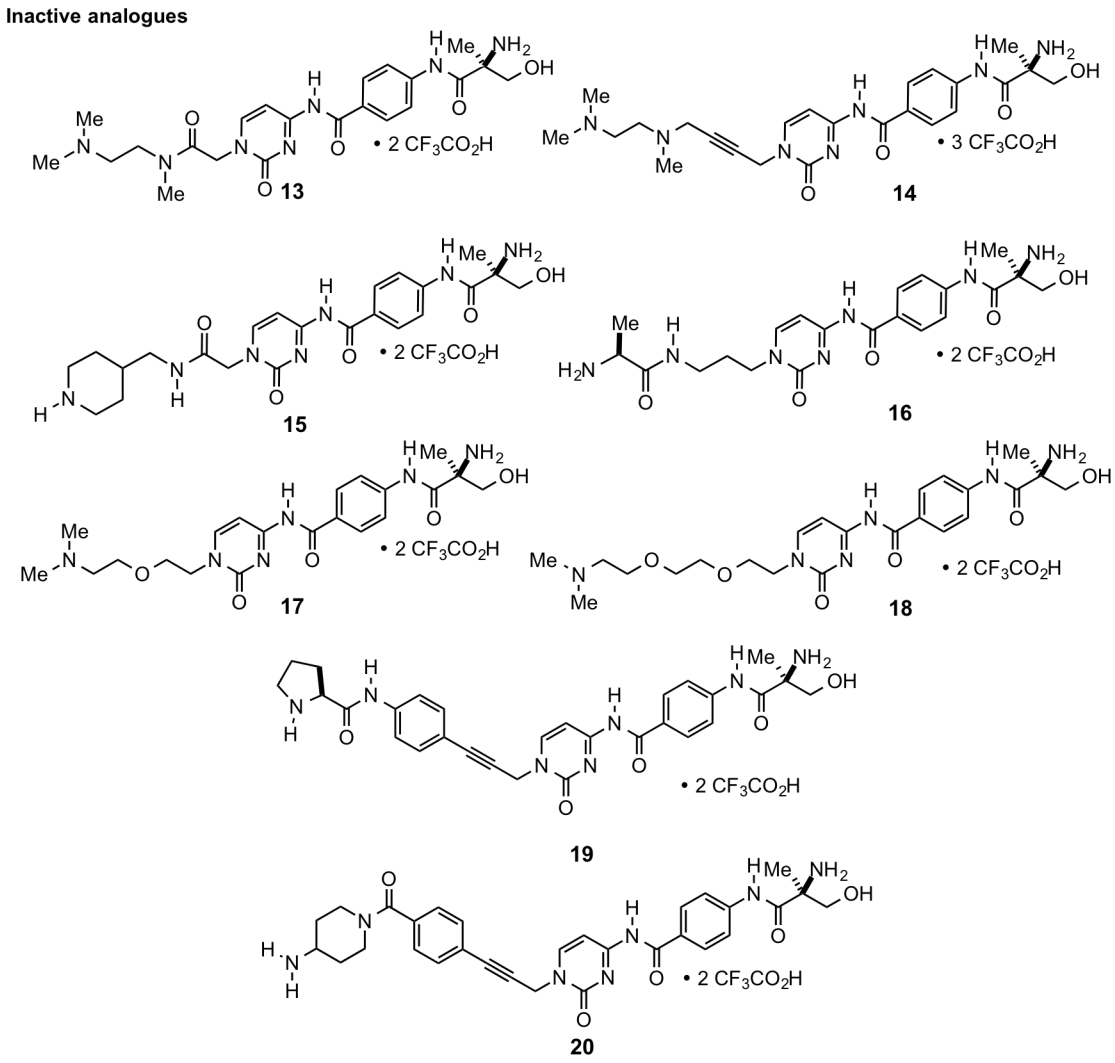

Figure 4.9 (continued…)

In spite of having an aminoacyl group, a cytosine, and a second basic center, analogues **13** to **20** are all devoid of any antimycobacterial activity, which essentially supports this hypothesis. The right molecular spacer is needed for efficient binding and activity. We presume that the molecular spacers of these compounds are too short (analogues **13** to **17**) or too long (analogues **18** to **20**) to properly mimic the conformation of the dimethylamino group of amicetin. The overall architecture of the spacers and cationic tails also affects antimycobacterial

activity. Methyl groups, carboxyl groups and phenyl rings in analogues **13** to **15** and analogues **18** to **20** are not tolerated, which may be due to a specific and tight binding pocket (*vide infra*). Antimycobacterial activity appears to be favored by having the combination of a more flexible alkyl group and a terminal primary amine. The most active of the compounds, analogue **3** (IC_{50} of 0.98 μM), contains *n*-butyl as its linker and 4-aminopiperidyl as its cationic tail. A less flexible linker such as 2-butynyl in analogue **1**, or a tertiary amine **such as** analogue **4**, leads to a ten-fold decrease in activity with analogue **1** and **4** having IC_{50} values of 8.2 μM and 7.4 μM respectively. The least active of the synthesized compounds were analogues **2** and **5**, with IC_{50} values of 19 and 22 μM, respectively. The drastic loss of activity displayed by analogue **2** further illustrates that the right molecular spacer and basic group is needed for antimycobacterial activity. Analogue **2** has a rigid alkynyl group and 3° amine, the combination of which lowered its activity 20-fold, relative to analogue **1** and 80-fold, relative to amicetin. Analogue **5** has a flexible but shorter *n*-propyl group and a 2° amine which afforded a lower antimycobacterial property.

We suspect and have confirmed via co-crystallization with 70S ribosomes that these active analogues share a similar binding conformation and binding site with amicetin (*vide infra*). The appropriate length and flexibility of molecular spacers allows these molecules to adopt a conformation analogous to amicetin (Figure 4.10). However, the absence of any activity on compounds **16** and **18**, which are close analogues to active compounds **5** and **4**, respectively, somehow contradicts this supposition. Analogue **18** has a flexible triethylene glycol (TEG) linker in place of the 1-*n*-butyl-(4-(*N,N'*-dimethyl)piperidyl group in 4, while analogue **16** has a threonine moiety in place of the proline group in **5**. One could expect the TEG analogue and threonine analogue to exhibit antimycobacterial activity similar to

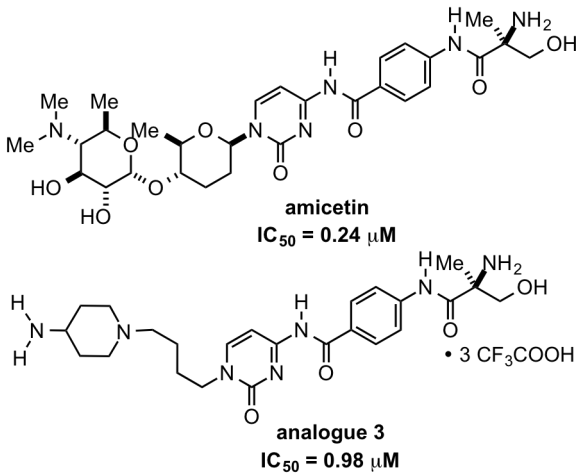

Figure 4.10 Aligned structures of amicetin and analogue 3

analogue **4** and **5**, respectively, by simply examining the aligned structures of these molecules (Figure 4.11). However, data from our MTT assay show otherwise. Either the TEG side chain was unable to generate a stable binding conformation for analogue **18**, or other factors, such as permeability, may be affecting its activity. In addition, it is unclear why proline in analogue **5** is more favored than threonine in analogue **16**. The differences in activity may be due to differences in the binding affinity of these molecules to a very specific binding pocket.

At this point, we cannot rule out other possible factors (i.e., cell wall permeability and efflux mechanisms) influencing the inefficacy of three quarters of analogues presented here. Nevertheless, we have observed a general structure activity relationship among our analogues that agrees with our proposed simplified pharmacophore. In addition to the required nucleobase, the two basic centers at both ends of the molecule are needed for activity. Appropriate length and flexibility of the molecular spacer appears to be essential for proper positioning of the cationic tail, and therefore important for antimycobacterial activity. For the cationic tail, primary amine groups are more favored than their amine counterparts, presumably

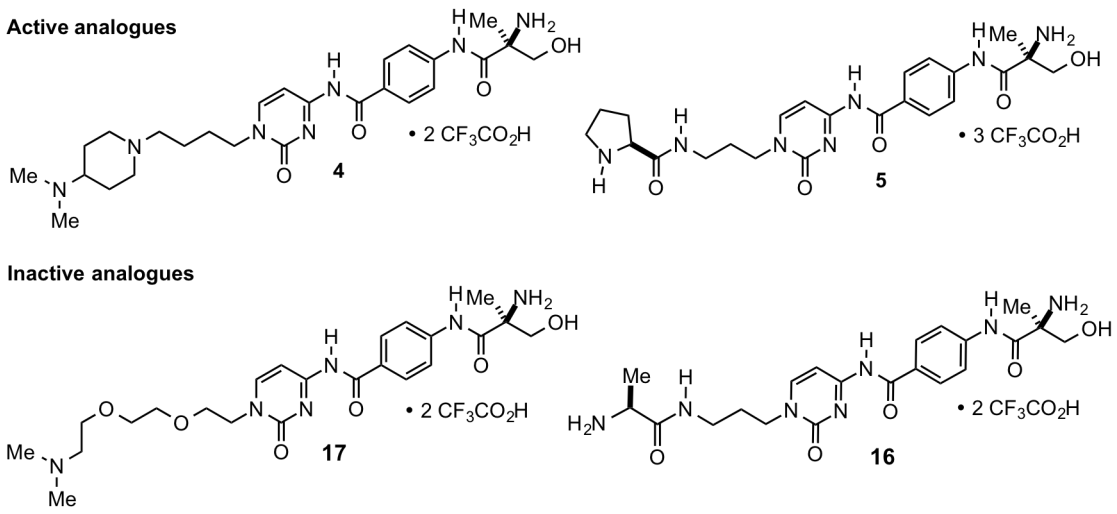

Figure 4.11 Aligned structures of amicetin analogues 4, 5, 16, and 17

due their ability to form stronger hydrogen bonding or cationic interactions.

4.4.2 Amicetin Analogues as Protein Synthesis Inhibitors

Members of the aminoacyl nucleoside class of antibiotics are known to be protein synthesis inhibitors.[14] To elucidate the mechanism of action of our compounds, we tested our analogues for protein synthesis inhibition using a cell-free translation assay. We used an *in vitro* prokaryotic protein expression system, which employs S30 *E. coli* extracts, the plasmid pBESTluc™ DNA containing the eukaryotic firefly luciferase gene, *luc*, as well as the necessary proteins for both transcription and translation of luciferase (Figure 4.12). Luciferase is the enzyme that produces bioluminescence in fireflies through the oxidation of luciferin to oxyluciferin. The light produced is easily measured using a luminometer, and is directly proportional to the amount firefly luciferase protein synthesized. Thus, light output is an indication of the level of protein synthesis. For the purposes of prelimnary investigation the assay was carried out using 50 μM of amicetin analogues.

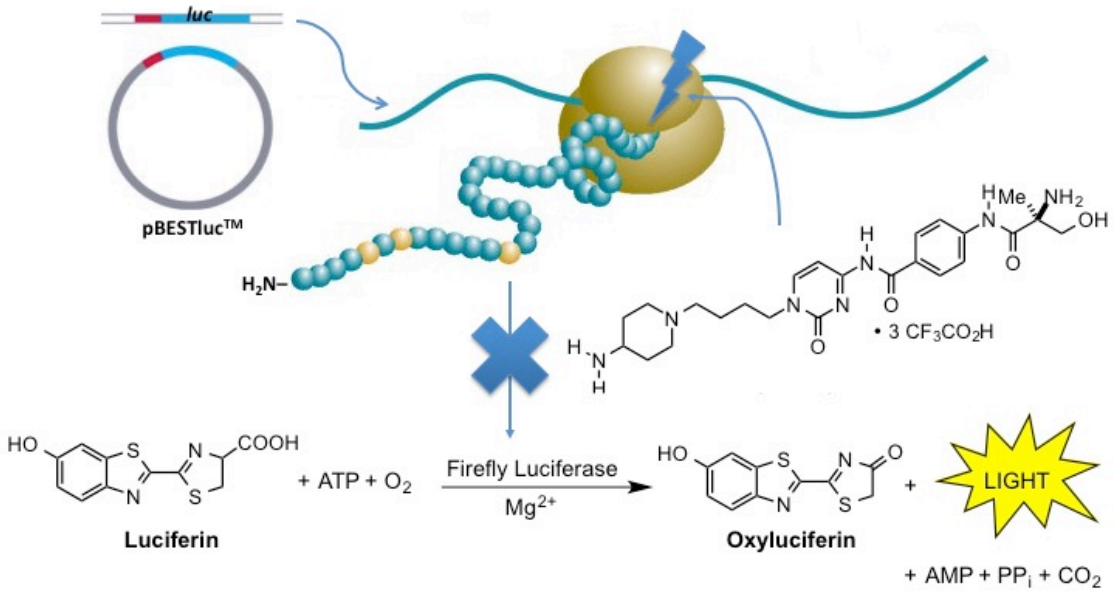

Figure 4.12 Inhibition of luciferase translation

The inhibitory properties observed in this assay correlate well with anti-mycobacterial activity and SAR of these compounds (Figure 4.13). Analogue **3** was found to be the best inhibitor, exhibiting 99% inhibition of protein synthesis, followed by analogue 4 at 94% inhibition. Analogue **1** gave modest inhibition at 77%, while analogue **2** and **5** were the weakest inhibitors at 61% and 42%. A full inhibition curve was measured for analogue **4** and amicetin (Figure 4.14). The IC_{50} of analogue **3** for protein synthesis inhibition was 3.8 μM, while the IC_{50} of amicetin was 1.6 μM. The trend we have observed supports our assumption that molecules achieve their antimycobacterial properties by inhibiting translation. The significance and correlation of these observations with respect to their interaction with the bacterial ribosomes will be further discussed in the following sections.

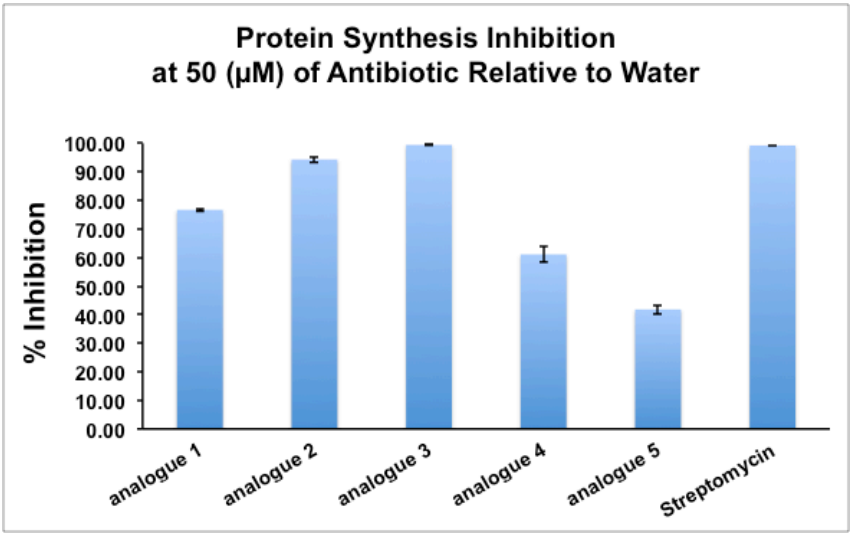

Figure 4.13 Protein synthesis inhibition of amicetin analogues

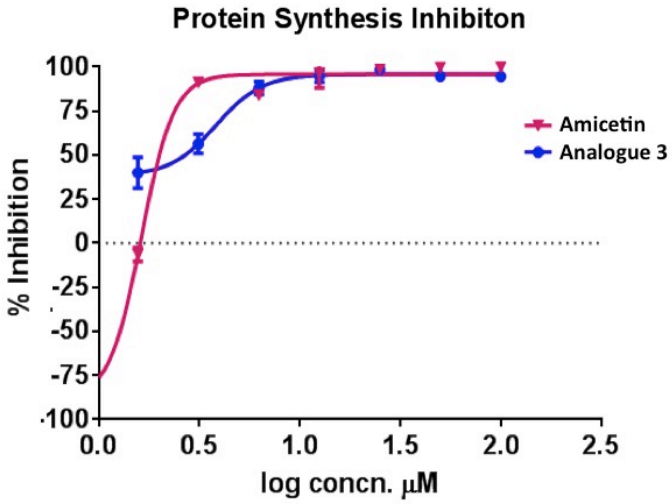

Figure 4.14 Protein synthesis inhibition curves of amicetin and analogue 3

4.4.3 Narrow Antimicrobial Spectrum of Amicetin Analogues

None of the amicetin analogues exhibited any activity against other test microorganisms. Our compounds are inactive against gram-positive *B. subtilis*, gram-negative *E. coli* and *A. baumanii*, and opportunistic fungi *C. albicans*. All compounds tested negative for any activity even at 100 μM of antibiotic. The narrow spectrum of activity observed among the analogues was expected, since our parent molecule, amicetin, is selectively effective against mycobacteria and gram-positive species such as *S. aureus* and *B. subtilis,* but is essentially ineffective against gram-negative species.[15] However, both amicetin and our active analogues were found to inhibit translation in cell-free *E. coli* ribosome. This suggests that other factors such as poor drug uptake due to cell wall permeability may be cause for the observed resistance in our analogues. On the other hand, amicetin is known to be active against *B. subtilis*, resistance of our analogues to this species was not expected. It is possible, however, that the specific strain we used for the assay is intrinsically resistant since amicetin-resistant *B. subtilis* strains have been identified.[16]

The selective antimicrobial activity of our compounds is particularly interesting since the use of narrow spectrum antibiotics is generally favored in clinical practice. Potentially, the use of amicetin analogues in the treatment of TB, which requires a long and intensive regimen of antibiotics, will circumvent resistance selection in nontargeted pathogens.

4.4.4 Selective Cytotoxicity of Amicetin Analogues

One important characteristic of a good antimicrobial agent is selective toxicity- that is the growth of the infecting organism is inhibited while the cells of the host remains largely unaffected.[17] We tested the compounds from our library

against CEM-TART leukemia cell to determine if our antimycobacterial agents are selective for *M. tuberculosis* over mammalian cells (Table 4.2). All compounds showed no appreciable cytotoxicity against CEM-TART leukemia cell lineage[18] even at a maximum concentration of 100 μM. Amicetin is less cytotoxic to mammalian cells compared with other antibiotics of its class. We were hoping to improve selectivity with our compounds. With respect to IC_{50} values, we have found all analogues, but most especially analogue **4,** to be more selective than amicetin. Amicetin's selectivity index ratio with respect to mammalian cells and mycobacteria is about 19. Selectivity is greatly improved by analogue **4** whose selectivity index ratio is greater than 100.

4.4 .5 Structures of Analogue 1 and 5 Bound to the 70S T. thermophilus Ribosomes

Based on similar inhibitory patterns and nonsynergistic inhibitory responses, members of the pyrimidine nucleoside class of antibiotics were believed to be competing for identical sites within the peptidyl transferase center (PTC) of the ribosome.[19] We postulate that our analogues possibly bind to the PTC of the blasticidin S.[20, 21] To investigate this, analogues **1** and **5** were co-crystallized with

Table 4.2 Comparison of cytotoxicity data vs. antimycobacterial activity

Compound	% Growth Inhibition of CEM-TART at 100 μM	CEM-TART IC_{50}	*Mtb* H37Ra IC_{50}
amicetin	100	4.5	0.24
1	24	> 100 μM	8.2
2	27	> 100 μM	19
3	18	> 100 μM	0.98
4	26	> 100 μM	7.4
5	31	> 100 μM	22

the 70S subunit of the ribosome of *Thermus thermophilus (Tth)*. Analogues **1** and **5** occupy the same binding site and similar conformation as amicetin (Figure 4.6, *vide infra)*. Analogue **1** closely resemble the binding conformation of amicetin compared to **5** (Figure 4.6, Figure 4.7A and Figure 4.7B *vide infra*). It forms a Watson-Crick base pair between the cytosine moiety and the guanine base of G2262 (G2251), *Tth*, *(E. coli)* numbering. The carboxyl group of α-methylserine forms a hydrogen bond with the guanidine of R18 (L16 ribosomal protein). In addition, the hydroxyl group of α-methylserine also forms a hydrogen bond with the carboxyl of E16 and with the phosphate group of G2506 (G2495). The adenine base of A2613 (A2602) π-stacks with *p*-aminobenzoyl of amicetin. The aminosugar moiety forms a cation-π interaction with the nucleobase of A2450 (A2439).

The binding conformation of analogue **5** differs from the two with respect to the some key interactions. The π-stacking interaction between *p*-aminobenzoyl of analogue **5** and A2613 (A2602) appear to be more skewed than analogue **1**. Analogue 5 also does not have the same hydrogen bond network; only its hydroxyl group from its α-methylserine forms polar contacts with the phosphate of G2506 (G2495). In addition, the cation-π interaction with A2450 (A2439) is absent in analogue **5**. Hydrogen bonding between the prolinyl group and the phosphate of C2085 (C2064) replaces this cation-π interaction. -

Our crystal structure supports the observed trend in biological activity (anti-mycobacterial property and inhibition of protein synthesis observed among the analogues. The absence of these key interactions could explain the inactivity of our analogues. Having only one basic center could eliminate either the hydrogen bonding interaction with the E16-V17-R18 sequence of the L16 ribosomal protein or the cation-π interaction with A2450 (A2439). The same inference could be made for

analogues that have molecular spacers of inappropriate length. The absence of the cation-π interaction in analogue **5** likely resulted in its weaker binding to the 70S ribosome and much lower activity compared to the other active analogues.

The strength of the binding energy appears to be important for better activity and is reflected in our SAR. Stronger cation-π interaction is afforded by having a primary amine than by having a tertiary amine. While the exact values for our substituents are not reported, a possible explanation can be derived from the electronic interactions and binding energies of ammonium cations and benzene.

The gas phase binding energy between a benzene ring and an ammonium ion decreases with each succeeding methylation (Table 4.3).[22] From this, one can predict that the binding energy of 4-aminopiperidyl group with the adenine of A2450 (A2439) would be stronger than the dimethyl analogue. The binding energy of cation-π interaction also depends on distance and conformation of the ion and the π-system; between adenine group and a protonated primary amine the value could be anywhere from 9 to 16 kcal/mol.[23] Amicetin is four times more active than analogue **1** despite having a 3° amine for its cationic tail presumably because its aminosugar moiety overlaps better with A2450 (A2439) than the aminopiperidyl group of **1** (Figure 4.15). Additionally, having a more flexible molecular spacer (alkyl vs. alkynyl) between the cytosine group and the cationic tail allows the molecule to adopt a conformation that affords stronger cation-π interactions.

Table 4.3 Experimental binding energies of cation-π interactions

Molecule-Ion	Binding Energy (kcal/mol)
C_6H_6–NH_4^+	19.3
C_6H_6–$MeNH_3^+$	18.8
C_6H_6–Me_3NH^+	15.9
C_6H_6–MeN_4^+	9.4

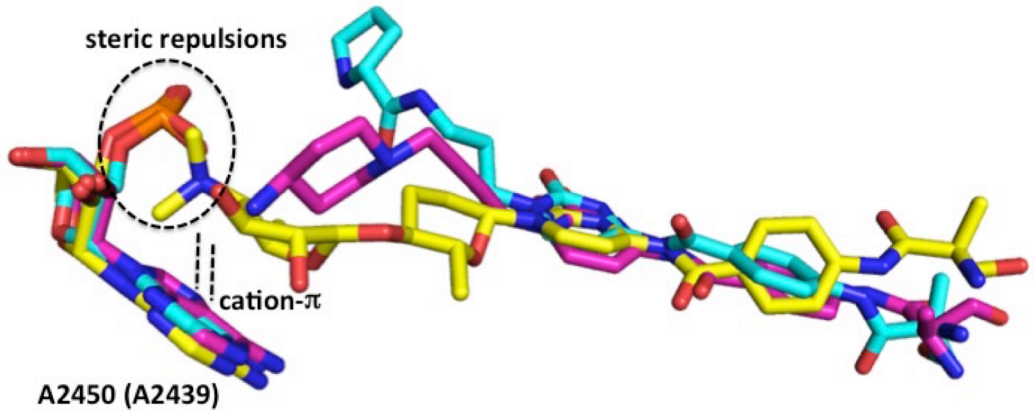

Figure 4.15 Comparison of cation-π interactions of amicetin (yellow), analogue 1 (magenta), and analogue 5 (cyan)

While electronic arguments could explain the observed SAR afforded by cation-π interactions, we cannot rule out the possible contribution of steric interactions in the observed SAR. Our crystal structure shows a rather tight binding pocket for amicetin and its analogues, specifically in the A2450 (A2439) region. In this case, having a bulky methyl group (i.e., amicetin, analogue 2, and analogue 4) in place of hydrogens (i.e., bamicetin, analogue 1, and analogue 3) in the amino end of the moleculer results in steric repulsions with the phosphate backbone of A2450 (A2439), affording a lower binding affinity presumably eventually resulting in lower antimycobacterial activity.

The strength of π-stacking interaction between *p*-aminobenzoyl moiety and A2613 (A2602) (Figure 4.16) maybe important for activity. Energies of π-stacking interactions could range from 1.6 to 2.4 kcal/mol, and are largely dependent on the electrostatics and orientation of the aromatic ring.[24, 25] The aromatic ring in amicetin overlaps with A2613 in an off-center, face-parallel manner. The stacking appears to be more skewed in analogue **1** and analogue **5**. The differences in stacking orientation could also contribute to the trend in activity observed. Better overlap

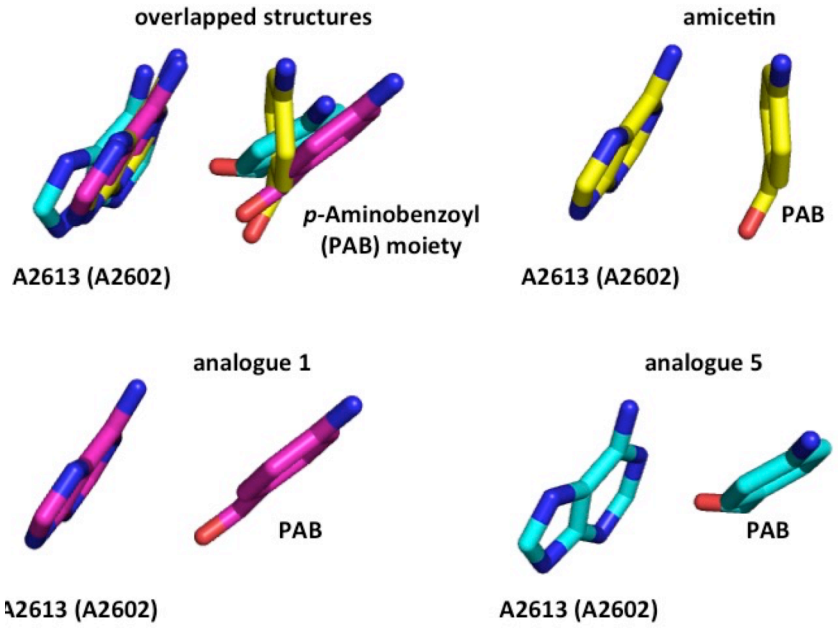

Figure 4.16 Comparison of π-stacking interactions of amicetin (yellow), analogue 1 (magenta), and analogue 5 (cyan)

between the aromatic rings contributes to a better binding interaction between the antibiotic and the ribosome, leading to better activity.

The hydrogen bonding network formed between the α-methylserine moiety and residues of L16 in amicetin and in analogue **1** and **5** may also explain the decrease in overall antimycobacterial activity with respect to amicetin. Literature precendence have established the importance of the α-methylserine moiety.[26] Inhibition of translation is decreased by 10-fold in the absence of the aminoacyl group. Our crystal structures show that hydrogen bonding interactions in amicetin are more extensive compared to the other two (Figure 4.7A and Figure 4.7B, *vide infra*) and thus could result in an overall higher binding affinity to the ribosome, and better biological activity.

Aside from antimycobacterial activity and inhibition of protein synthesis, our analogues displayed selective cytotoxicity against mycobacteria over mammalian

cells. The observed selectivity is particularly interesting, considering that the binding site of our analogues, the peptidyl transferase center, is highly conserved in prokaryotes and eukaryotes. Without discounting other mechanisms of inherent resistance (i.e., efflux pumps and cell wall permeability) present in eukaryotes, specially mammalian cells, we presume that the key interactions of our analogues with the prokaryotic ribosome is not observed in the eukaryotic system. When the crystal structures of the ribosome-bound analogues were superimposed with the crystal structure of empty 80S *S. cerevisiae* ribosomes, *S. cerevisiae* (*E. coli*) numbering (Figure 4.17),[27] it appears that certain interactions are not favored in the tight binding pocket of the yeast ribosome. Steric repulsion between the cytosine moiety of amicetin and its analogues with G2620 (G2252) is observed in the superimposed structures. (Figure 4.18). In addition, misalignment of the cytosine moiety with G2619 (G2251), preventing it to form a proper GC pair (Figure 4.19).

The α-methylserine moiety also appears to be bumping into the QQG sequence of L ribosomal protein, and the phosphate of A2864 (A2596) (Figure 4.20). In addition to this, A2808 (A2439) is located further away by at least 1 Å preventing strong binding contacts (Figure 4.21). A2971 (A2602) is also positioned several angstroms away to form any stable π-stacking intercations (Figure 4.22). We also compared its conformation with the Apo-70S *T. thermophilus* ribosomes, due to the fact that its assume different conformations and orientations in every crystalline complex. A2971 (A2602) orientation in both yeast and Apo-70S *T. thermophilus* ribosomes are very different from the orientation in our crystal structures (Figure 4.23). Based solely on our crystallographic data, it is hard to conclude on how this very dynamic residue affects the selective activity of our antibitiotics.

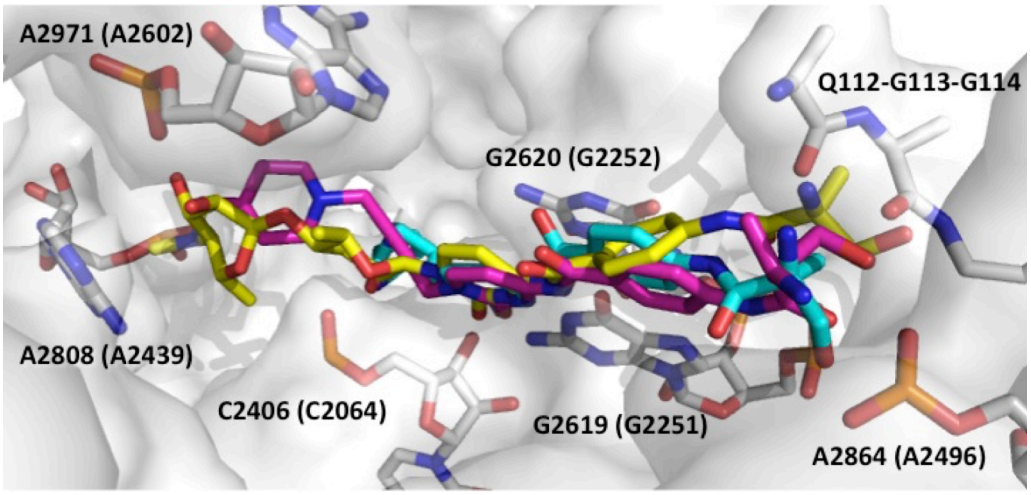

Figure 4.17 Superimposed structures of amicetin (yellow), analogue 1 (magenta), and analogue 5 (cyan) with 80S *S. cerevisiae* ribosome

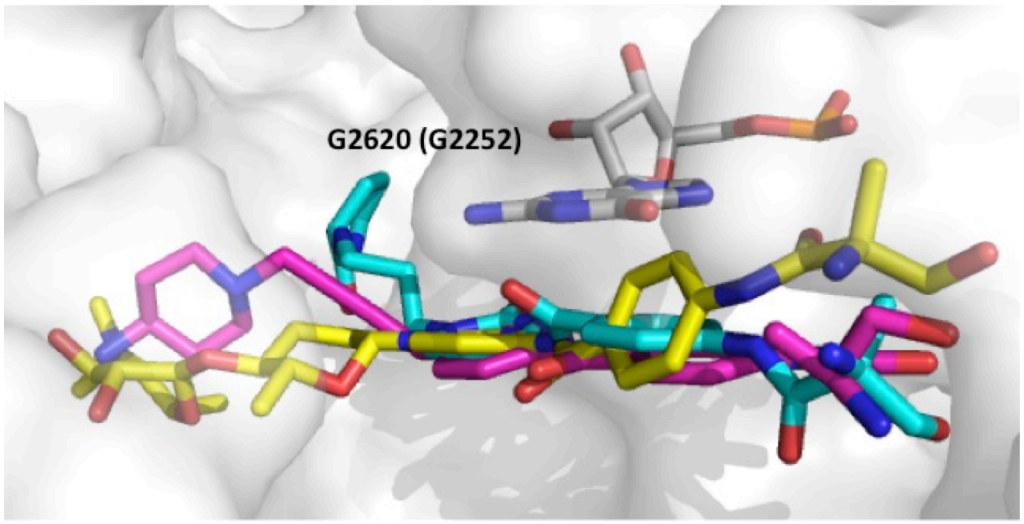

Figure 4.18 Steric replulsion with G2620 (G2252) in superimposed structures of amicetin (yellow), analogue **1** (magenta), and analogue **5** (cyan) with 80S *S. cerevisiae* ribosome

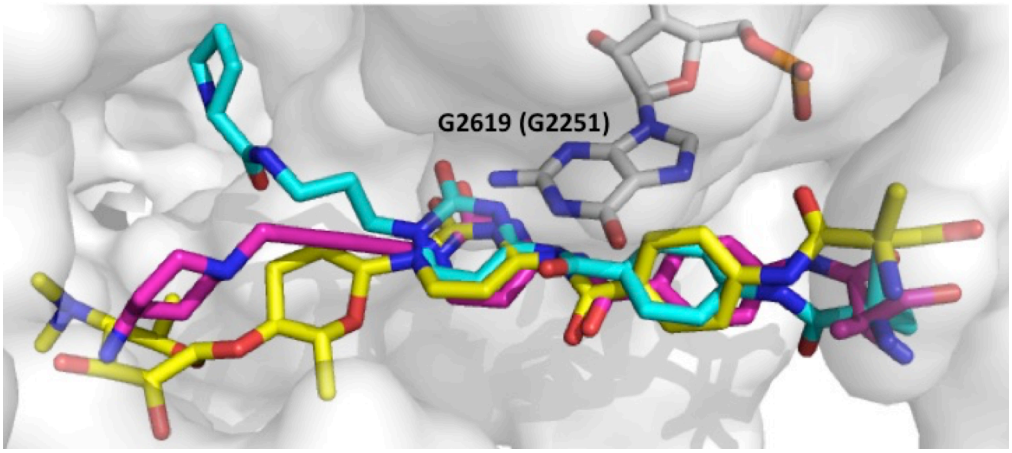

Figure 4.19 Misalignment observed in the GC pair in superimposed structures of amicetin (yellow), analogue 1 (magenta), and analogue 5 (cyan) with 80S *S. cerevisiae* ribosome

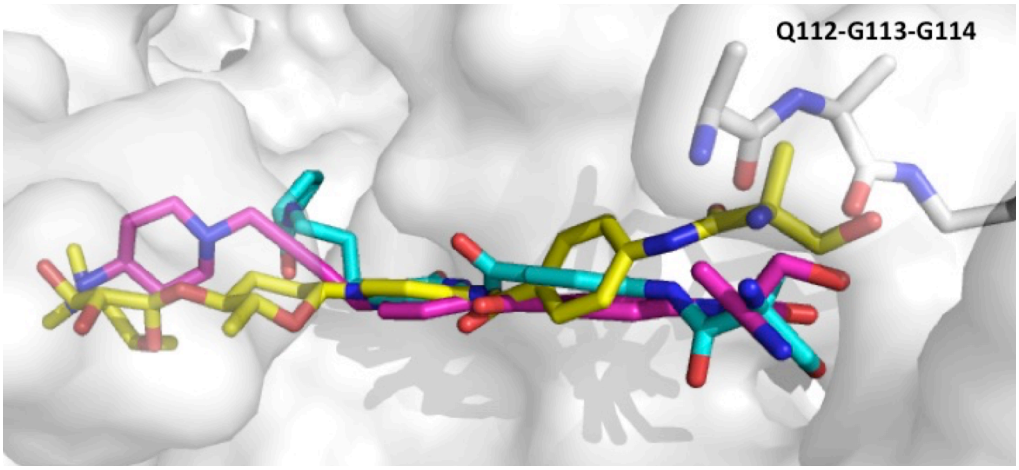

Figure 4.20 Steric replulsion with residues Q112-G113-G114 in superimposed structures of amicetin (yellow), analogue 1 (magenta), and analogue 5 (cyan) with 80S *S. cerevisiae* ribosome

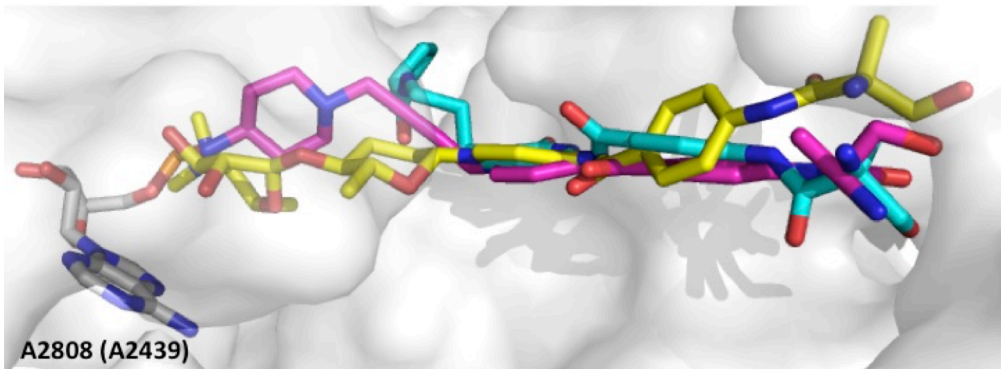

Figure 4.21 Absence of cation-π interactions with A2808 (A2439) in superimposed structures of amicetin (yellow), analogue 1 (magenta), and analogue 5 (cyan) with 80S *S. cerevisiae* ribosome

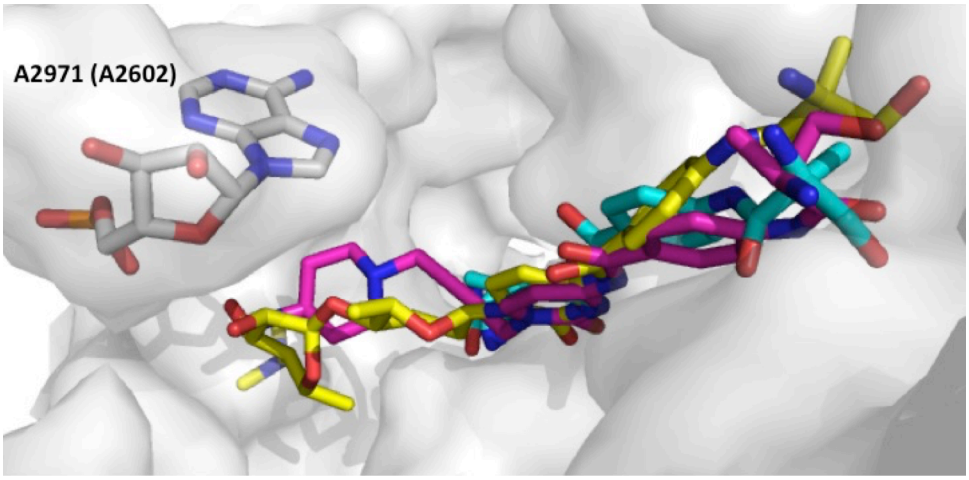

Figure 4.22 Absence of π-stacking interactions with A2971 (A2602) in superimposed structures of amicetin (yellow), analogue 1 (magenta), and analogue 5 (cyan) with 80S *S. cerevisiae* ribosome

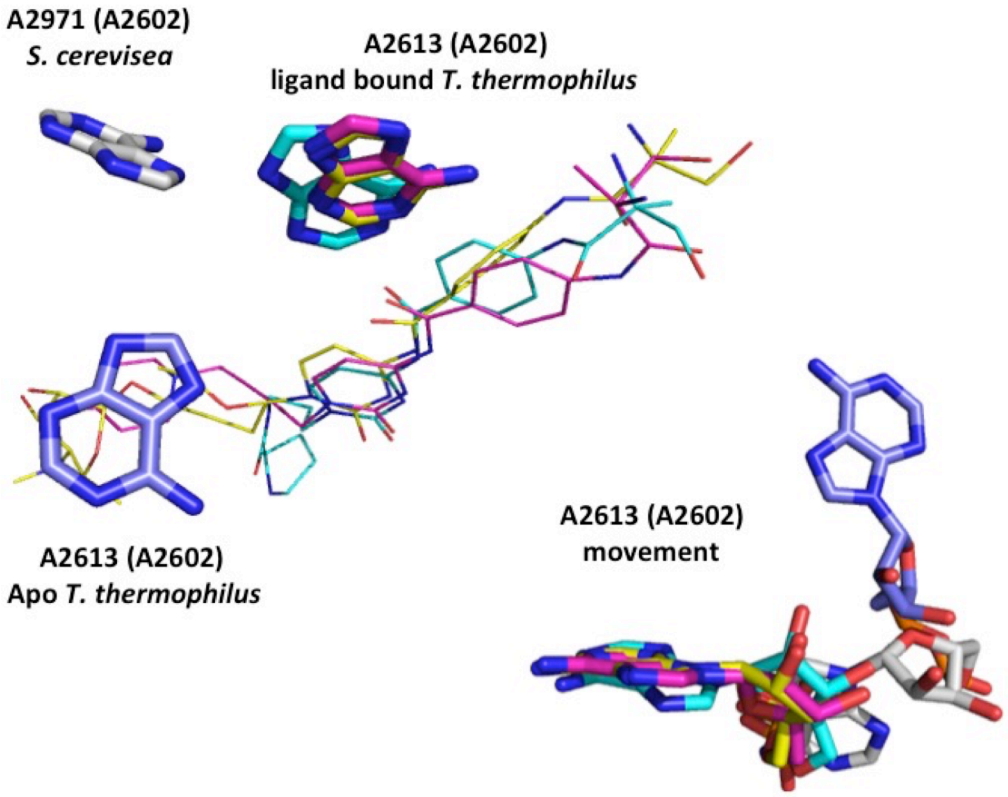

Figure 4.23 Comparison of A2971 (A2602) in superimposed structures of amicetin (yellow), analogue 1 (magenta), and analogue 5 (cyan) with 80S *S. cerevisiae* ribosome (light gray) against Apo 70S *T. thermophilus* ribosome (purple)

4.5 Conclusion

We have identified amicetin analogues exhibiting antimycobacterial activity against *M. tuberculosis* H37Ra and limited cytotoxicity against mammalian cells CEM-TART leukemia cell lineage. Analogues were found to inhibit protein synthesis. Crystal structures of ribosome-bound amicetin and representative analogues provide insight into their structure activity relationships and biological activity. This report presented our initial efforts in the discovery of amicetin anti-tubercular agents. Continued efforts are on going towards the synthesis and in depth biological evaluation of new compounds.

4.6 References

1. DeBoer, C.; Caron, E. L.; Hinman, J. W. Amicetin, a new *Streptomyces* antibiotic. *J. Am. Chem. Soc.* **1953,** *75*, 499-500.

2. Hinman, J. W.; Caron, E. L.; DeBoer, C. The isolation and purification of amicetin. *J. Am. Chem. Soc.* **1953**, *75*, 5864-5866.

3. Funabashi, Y.; Tsubotani, S.; Koyama, K.; Katayama, N.; Harada, S. A new anti-MRSA dipeptide, TAN-1057 A. *Tetrahedron* **1993**, *49*, 13-28.

4. Fox, J. J. Watanabe, K.A.; Bloch, A. Nucleoside antibiotics. *Prog. Nucleic Acid Res. Mol. Biol.* **1966**, *5*, 251-313.

5. Lichtenthaler, F. W.; Trummlitz, G. Structural basis for the inhibition of protein synthesis by the aminoacyl-aminohexosyl-cytosine group of antibiotics. *FEBS Lett.* **1974**, *38*, 237-242.

6. Koch, M.; Bugni, T. S.; Pond, C. D.; Sondossi, M.; Dindi, M.; Piskaut, P.; Ireland, C. M.; Barrows, L. R. Antimycobacterial activity of *Exocarpos latifolius* is due to exocarpic acid. *Planta Med.* **2009**,*75*, 1326-1330.

7. Noro, J. C.; Barrows, L. R.; Gideon, O. G.; Ireland, C. M.; Koch, M.; Matainaho, T.;Piskaut, P.; Pond, C. D.; Bugni, T. S. Tetrahdroxysqualene from *Rhus taitensis* shows antimycobacterial activity against *Mycobacterium tuberculosis. J. Nat. Prod.* **2008**, *71*, 1623-1624

8. Polikanov, Y. S.; Blaha, G. M.; Steitz, T. A. How hibernation factors RMF, HPF, and YfiA turn off protein synthesis. *Science* **2012**, *336*, 915-918.

9. Kabsch, W. Xds. Acta *Crystallog., Sect. D: Biol. Crystallogr.* 2010, *66*, 125-132.

10. Winn, M. D.*;* Ballard, C. C.; Cowtan, K. D.; Dodson, E. J.; Emsley, P.; Evans, P. R.; Keegan, R. M.; Krissinel, E. B.; Leslie, A. G. W.; McCoy, A. J.; McNicholas, S. J.; Murshudov, G. N.; Pannu, N. S.; Potterton, E. A.; Powell, H. R.; Read, R. J.; Vagin, A.; Wilson, K. S. Overview of the CCP4 suite and current developments. *Acta Crystallogr., Sect. D: Biol. Crystallogr.* **2011**, *67*, 235-242.

11. Emsley, P.; Lohkamp, B.; Scott, W. G.; Cowtan, K. D. Features and development of COOT. **2010**, *66*, 486-501.

12. Adams, P. D.; Afonine, P. V.; Bunkóczi, G.; Chen, V. B.; Davis, I. W.; Echols, N.; Headd, J. J.; Hung, L. W.; Kapral, G. J.; Grosse-Kunstleve, R. W.; McCoy, A. J.; Moriarty, N. J.; Oeffner, R.; Read, R. J.; Richardson, D. C.; Richardson, J. S. Terwilliger, T . C.; Zwarta, P. H. PHENIX: a comprehensive Python-based system for macromolecular structure solution. *Acta Crystallogr. Sect. D: Biol. Crystallogr.* **2010**, *66*, 213-221.

13. Schuttelkopf, A. W.; van Aalten, D. M. PRODRG: a tool for high-throughput

crystallography of protein-ligand complexes. *Acta Crystallogr. Sect. D: Biol. Crystallogr.* 2004, *60*, 1355-1363.

14. Coutsogeorgopoulos, C. Aminoacylnucleoside inhibitors of protein synthesis. the effect of amino acyl ribonucleic acid on the inhibition. *Biochemistry* **1967**, *6*, 1704-1711.

15. DeBoer, C.; Caron, E. L.; Hinman, J. W. Amicetin, a new *Streptomyces* antibiotic. *J. Am. Chem. Soc.* **1953**, *75*, 499-500.

16. Duvall, E. J.; Mongkolsuk, S.; Kim, U. J.; Lovett, P. S.; Henkin, T. M.; Chambliss, G. H. Induction of the chloramphenicol acetyltransferase gene cat-86 through the action of the ribosomal antibiotic amicetin: involvement of a *Bacillus subtilis* ribosomal component in *cat* induction. *J. Bacteriol.* **1985**, *161*, 665-672.

17. Scholar, E. M.; Pratt, W. B. The antimicrobial drugs. Oxford University Press USA: 2000; p. 3.

18. Chen, H.; Boyle, J. T.; Malim, M. H.; Cullen, B. R.; Lyerly, H. K. Derivation of a biologically contained replication system for human immunodeficiency virus type 1. *Proc. Nat. Acad. Sci.* **1992, *89***, 7678-7682.

19. Pestka, S. Studies on transfer ribonucleic acid-ribosome complexes: XIX. Effect of antibiotics on peptidyl puromycin synthesis on polyribosomes from *Escherichia coli*. *J. Biol. Chem.* **1972**, *247*, 4669-4678.

20. Hansen, J. L.; Moore, P. B.; Steitz, T. A. Structures of five antibiotics bound at the peptidyl transferase center of the large ribosomal subunit. *J. Mol. Bol.* **2003**, *330*, 1061-1075.

21. Svidritskiy, E.; Ling, C.; Ermolenko, D. N.; Korostelev, A. A. Blasticidin S inhibits translation by trapping deformed tRNA on the ribosome. *Proc. Nat. Acad. Sci.* **2013**, *110*, 12283-12288.

22. Ma, J. C.; Dougherty, D. A. The cation-π interaction. *Chem. Rev.* **1997**, *97*, 1303-1324.

23. Mao, L.; Wang, Y.; Liu, Y.; Hu, X. Molecular determinants for ATP-binding in proteins: a data mining and quantum chemical analysis. *J. Mol. Biol.* **2004**, *336*, 787-807.

24. Martinez, C. R.; Iverson, B. L. Rethinking the term "pi-stacking". *Chem. Sci.* **2012**, *3*, 2191.

25. Copeland, K. L.; Pellock, S. J.; Cox, J. R.; Cafiero, M. L.; Tschumper G. S. Examination of tyrosine/adenine stacking interactions in protein complexes. *J. Phys. Chem. B* **2013**, *117,* 14001-14008.

26. Lichtenthaler, F. W.; Cerna, J.; Rychlik, I. The effect of oxamicetin and some

amicetin analogs on ribosomal peptidyl transferase. *FEBS Lett.* **1975**, *53*, 184-187.

27. Ben-Shem, A.; de Loubresse, N. G.; Melnikov, S.; Jenner, L.; Yusupova, G.; Yusupov, M. The structure of the eukaryotic ribosome at 3.0 Å resolution. *Science* **2011**, *334*, 1524-1529.

4.7 Supplemental Information

4.7.1 General Experimental Procedures

Test organisms were obtained from the American Type Culture Collection (ATCC). Each organism was grown in their respective broth media according to Clinical Laboratory Standards Institute (CLSI) methods and published procedures.[1, 2] Chemicals and other growth supplies were purchased from commercial sources (Sigma Aldrich and Fischer Scientific). Library screening and assays were performed in 96-well plates. Absorbance measurements were measured on a Multiskan FC plate reader (Fisher Scientific, Waltham, MA). Luminescence measurements were performed on a Microbeta Trilux Liquid Scintilation and Luminescence Counter.

4.7.2 M. tuberculosis Susceptibility Testing

Mycobacterium tuberculosis H37Ra (ATCC 25177) was grown in 7H9 medium with ADC supplement (Remel, Lenexa, KS). Colorimetric 3-(4,5-dimethylthiazol-2-yl)-2,5-diphenyltetrazolium bromide (MTT) assay was employed to measure the growth inhibition of *M. tuberculosis* H37Ra (ATCC 25177) following a modified procedure from published methods.[2, 3] Test compounds were dissolved in DMSO to produce stock solutions at 2 mM concentration; effective working concentration of 100 μM. Two-fold serial dilution plates of each compound were

---

[1] Ferraro, M. J.; Craig, W. A.; Dudley, M. N.; Eliopoulos, G. M.; Hecht, D. W.; Hindler, J.; Reller, L. B.; Shelodon, A. T.; Swenson, J. M.; Tenover, F. C.; Testa, R. T.; Weinstein, M. P.; Wikler, M. A. 5th edition. Wayne: NCCLS; 2000.

[2] Koch, M.; Bugni, T. S.; Pond, C. D.; Sondossi, M.; Dindi, M.; Piskaut, P.; Ireland, C. M.; Barrows, L. R. *Planta Med.* **2009**, *75*, 1326-1330.

[3] Foongladda. S.; Roengsanthia, D.; Arjrattanakool, W.; Chuchottaworn, C.; Chaiprasert, A.; Franzblau, S. G. *Int. J. Tuberc. Lung Dis.* **2002**, *6*, 1118-1122.

prepared for growth inhibition curves; effective working concentration from 100 µM to 390 nM. 200 µL of ADC enriched 7H9 medium containing *M. tuberculosis* cultures were dispensed at approximately 10,00,000 cells per well. Each plate contains 4 wells of noninoculated media as no-growth control, 4 wells of DMSO as growth control, and 8 wells of rifampicin as positive control. One µL of test compound (in DMSO) was added to the rest of the plate in triplicate. Final well volume was 200 µL. The test plate was incubated for four days at 37 °C, after which, 11 µL of sterile MTT (5 mg/ mL in PBS) was added and was further incubated overnight. Insoluble purple formazan product formed from the metabolism of MTT by viable *M. tuberculosis* was then solubilized by the addition of 50 µL of a solubilization solution (5 % SDS w/v, 50 % DMF v/v, 45 % H_2O v/v). Cell viability was measured as the absorbance at 570 nm (A_{570}). All data were corrected against no-growth control wells. Percentage inhibition was calculated as the fraction of the average absorbance of the test wells over the corrected average absorbance of the growth (DMSO) control wells, subtracted from unity and multiplied by 100. Standard deviation was computed for error analysis. Growth inhibition curves were fitted and half-maximal inhibitory concentrations (IC_{50}) were obtained by nonlinear regression analysis using GraphPad™ Prism 6.

4.7.3 MTT Assay Growth Inhibition Curves Against M. tuberculosis H37Ra

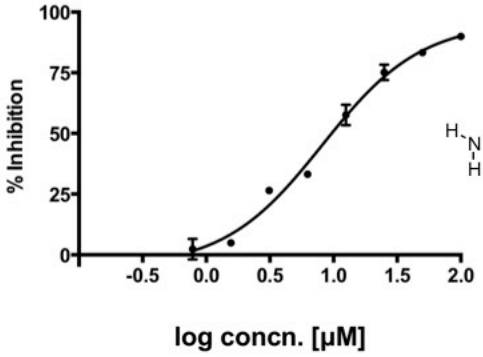

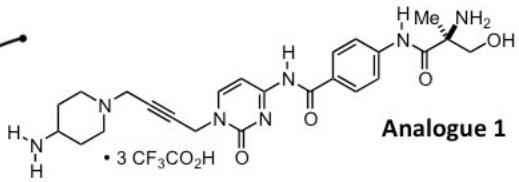

IC_{50}= 8.690 ± 1.22 μM, R^2= 0.9916

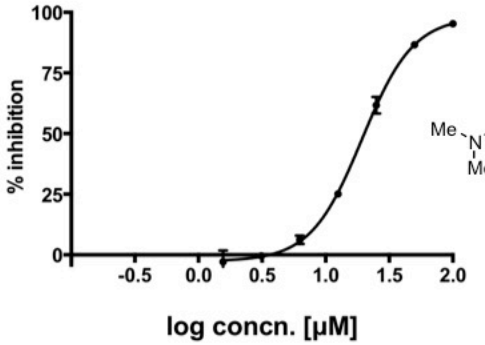

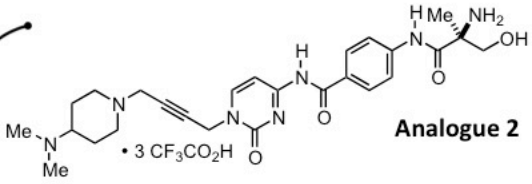

IC_{50}= 19.33 ± 1.01 μM, R^2= 0.9999

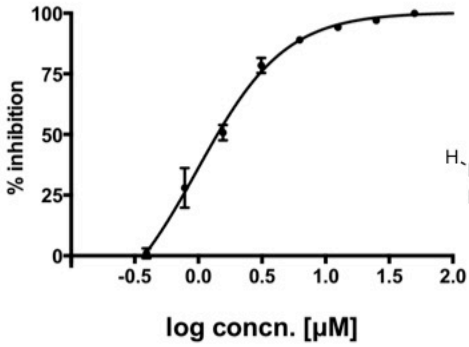

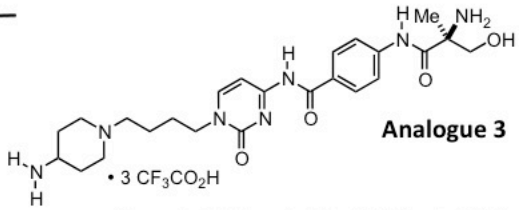

IC_{50}= 0.9811 ± 1.19 μM, R^2= 0.9977

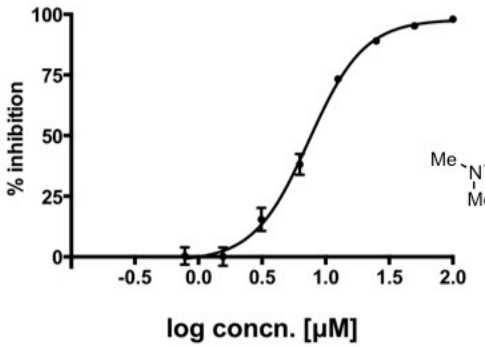

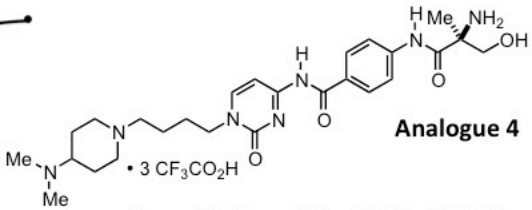

IC_{50}= 7.397 ± 1.04 μM, R^2= 0.9987

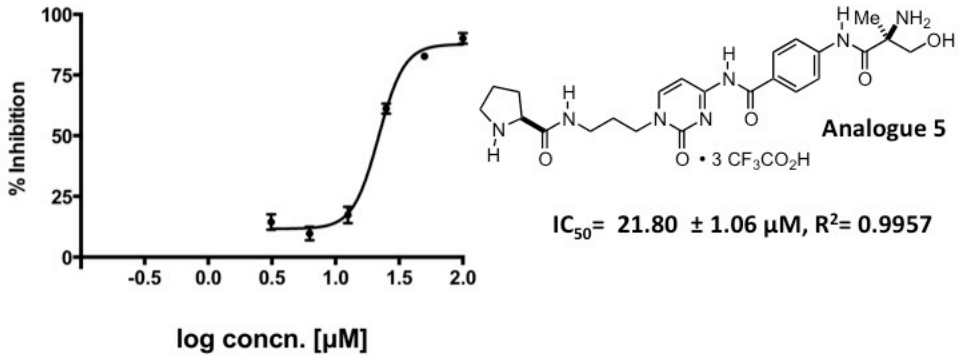

4.7.4 Antimicrobial Spectrum

Each test organism was inoculated and grown in their respective broth media: Mueller-Hinton II media (Difco BD, Franklin Lakes, NJ) for *Escherichia coli* (ATCC 25922); MOPS buffered RPMI-1640 (NCCLS 2007) for *Acinetobacter baumannii* (ATCC 19606), *Bacillus subtilis* (ATCC 6633), and *Candida albicans* (ATCC 90028).[1] Each plate contains 4 wells of uninoculated media as no-growth control, 4 wells of DMSO as growth control, and 8 wells of purchased (Sigma Aldrich), organism-appropriate antibiotic as positive control: kanamycin (*E. coli*), gentamycin (*B. subtilis*), and itraconazole (*A. baumannii* and *C. albicans*). The remaining wells received 1 μL of the test compound from the same dilution plate prepared for the TB assay. For the *B. subtilis* plate 11 μL of sterile MTT (5 mg/mL in PBS) was added. Final well volume is 200 μL. Plates were incubated overnight at 37°C. Minimum inhibitory concentration (MIC), the lowest concentration of test compound in which complete growth suppression was noted, was determined for all test organisms except for *B. subtilis*, whose data was processed similarly as *M. tuberculosis* H37Ra.

4.7.5 Cytotoxicity Assay

In vitro cytotoxicity assay was performed as previously described.[4] CEM-TART cells (AIDS Research and Reference Reagent Program, NIAID, NIH) were grown and maintained in culture media consisting of RPMI (Hyclone), 20% FBS (Hyclone), and CellGro antibiotics/mycotics (Mediatech, Manassess, VA). CEM-TART cells were dispensed at approximately 20,000 cells per well. Each plate contains 8 wells of noninoculated media as no-growth well, 8 wells of doxorubicin as positive control, and 8 wells of DMSO growth well as negative control. Test compounds (1.0 μL), from the same dilution plate prepared for the TB assay, were assayed in triplicate. Plates were incubated in a waterjacked incubator with 5% CO_2 at 37°C for 3 days. After incubation, 11 μL of 5 mg/mL MTT was added. The plate was further incubated for 2-3 hours. The plates were shaken for 5 minutes on a microplate shaker and the medium was aspirated. 150 μL DMSO was added to the formazan precipitate. Cell viability was measured as A_{570}. Percent inhibition was determined similarly as *M. tuberculosis* H37Ra.

4.7.6 Protein Synthesis Inhibition Assay

Analogues **1** to **5** were assayed for inhibition of prokaryotic translation using the commercially available *E. coli* S30 system (Promega). Protein production was monitored *via* a luciferase readout. Reactions were performed as described by the manufacturer. Stock solutions of test compounds were prepared by dissolving the analogues in DMSO to a final concentration of 2.5 mM for the preliminary screening;

---

[4] Noro, J. C.; Barrows, L. R.; Gideon, O. G.; Ireland, C. M.; Koch, M.; Matainaho, T.;Piskaut, P.; Pond, C. D.; Bugni, T. S. *J. Nat. Prod.* **2008**, *71*, 1623-1624

effective working concentration of 50 μM. Similarly, analogue **3** and amicetin were diluted to 5.0 mM and two-fold serial dilutions were made for a dose-response curve; effective working concentration from 100 μM to 781 nM. Nuclease-free water and streptomycin (10 mg/mL) were used as blank and positive control, respectively. Reactions were performed in triplicates. *In vitro* transcription/translation reactions were assembled by mixing 20 μL of S30 Premix, 15 μL of S30 extract, 5.0 μL of complex amino acids, 1.0 μL of pBESTluc plasmid, 8.0 μL of nuclease-free water, and 1.0 μL of test compound. Reactions were incubated at 37 °C for 60 min. The reactions were stopped by placing the microcentrifuges on ice for 5 min. Subsequently, 100 μL of Steady-Glo Reagent (Promega) was added to wells containing 5.0 μL of translation reaction and 95 μL distilled water. Luminescence readings obtained on Luminescence measurements were performed on a Microbeta Trilux Liquid Scintilation and Luminescence plate reader. Percentage inhibition, dose-response curve and IC_{50} data were obtained as described in the TB assay

4.7.7 Complex Formation and Crystallization

70S *T. thermophilus* ribosomes were purified and crystallized as previously described.[5] Purified 70S ribosomes were diluted with a buffer solution [5 mM Hepes (pH 7.5), 50 mM KCl, 10 mM NH_4Cl, and 10 mM $Mg(OAc)_2$] to a final concentration of 10 mg/mL. 70S ribosomes crystals werer grown at 19°C *via* sitting-drop vapor diffusion by mixing 3 μL of the ribosome sample with 3.5-4.5 μL of the crystallization solution [2.9% PEG 20K, 9% methyl-2,4-pentanediol (MPD), 175 mM L-arginine, and 100 mM Tris–HCl (pH 7.6)]. YfiA protein (59 μM) was added to stabilize the head of

[5] Polikanov, Y. S.; Blaha, G. M.; Steitz, T. A. *Science* **2012**, *336*, 915-918.

the 30S ribosomal subunit. Concentration of MPD was increased to 40% in stabilize the crystals, upon addition of analogue **1** (1 mM) and analogue **5** (3 mM). The crystals were flash frozen in a nitrogen cryostream at 80 K after 24 hours of equilibration.